

AIS 2023

**18th International Symposium on
Applied Informatics and Related Areas**

PROCEEDINGS

Obuda University

PROCEEDINGS of
18th International Symposium on
Applied Informatics and Related Areas

Editors:

Ildikó Petőné Csuka

Gyula Simon

Obuda University
November 16, 2023
Székesfehérvár, Hungary
ISBN 978-963-449-334-1

CONTENTS

Oral Session I. - Industrial and Embedded Systems	1
Csaba Bráda and László Sajó-Bohus: Unique properties of a new Al/Sn Metallic Glasses obtained by melt spinning	2
Viktor Vass and György Györök: Life Cycle Cost Analysis of Karl Fischer water determinaton for moisture sensitive materials for electric vehicles and pharmaceutical use	9
Zoltán Farkas and György Györök: Improve electric boat safety and usability with telematics	13
Ákos Jánvári and Károly Széll: Robots in Construction How is Construction Industry Doing in Automation?	18
 Oral Session II. - Applied Informatics	 22
Gaye Ediboglu Bartos and Serel Akyol: Deep Learning for Image Authentication: A Comparative Study on Real and AI-Generated Image Classification	23
Péter Udvardy: LEGO robotics as education tool	28
Todor Stoilov, Krasimira Stoilova, Éva Hajnal and Márta Seebauer: Information Support for Healthy Dietry	32
 Oral Session III. - Geodesy and Geoinformatics	 38
Gábor Molnar and Benedek Marcell Kovács: Fusion of smartphone sensors to enhance positioning accuracy	39
Attila Varga: Gross-error filtering of the tie points based on geometrical similarity in stereo image pair orientation	45
Tamás Jancsó and Attila Varga: Calculation of the volume of a corn field based on UAV images	49
 Poster Session I. – Applied Informatics	 54
Bertalan Beszédes and Bence Márta: Network-Indepentent Building Automation System	55
Dániel Kovács, Éva Hajnal and Todor Stoilov: Observation and Analysis of Wildlife Behaviour in Agricultural Areas	59
Éva Hajnal, Gergely László, Marcell Vámosi, Nikolett Szarka and Ján Erdélyi: Comparative Analysis of Fast VR Tour Creation Methods	64
Albina Kadyroldina, Assel Kussaiyn-Murat, Darya Alontseva, Alexander Krasavin and Maral Tolykbayeva: Surface restoration based on scanning data	68
Albina Kadyroldina, Assel Kussaiyn-Murat, Darya Alontseva, Alexander Krasavin and Arailym Orazova: A novel method for the identification of flat curves	73

Zoltán Szilágyi, Csaba Hajdu and Patrik Bajári: Identification of position by means of shape recognition in mixed reality systems	80
Poster Session II. - Geodesy and Geoinformatics	85
János Király, Kinga Teszárs and János Katona: The Role of Building Information Modeling in Facility Management	86
Malgorzata Verone Wojtaszek, Gabor Molnar, Balazsik Valeria, Andrea Podor, Gabor Nagy, Janos Katona, Erick Noboa, Bence Adam, Gyorgy Eigner and Gyorgy Gyorok: Water Resources in Efficient Networks (WREN) project overview and presentation of the research results carried out during the first year	90
Tamás Jancsó, Károly Széll, Gergely Vakulya, József Borbély, János Katona and Gábor Nagy: Common aspects of 3D modeling and vision solutions in robotics and geoinformatics	99
Regina Hanna Balaton, Gergely László and Zoltán Tóth: Processing 3D panoramic photos into point cloud modell	105
Levente Dimén, Clement Negrut and Alina Cristina Nuță: Safety Aspects of the Urban Green Cadaster	110
Balázs Böröcz: Estimation of the location of bee pastures in Hungary based on SENTINEL satellite images	115
Xinling Wang, Xiaojing Li and Zhe Chang: The Present and Future of Satellite Gravimetry: Advancements, Applications, and Prospects	119
Poster Session III. – Enterprise and Economics	124
Anita Lengyel, József Németh and Monika Pogatsnik: Process and quality development of an automotive production cell	125
Richárd Veres: What is a Startup Ecosystem About?	130
Ildikó Petőné Csuka and Csilla Czeglédi: Entrepreneurial spirit among young people	135
Zoltán Trenka and Csaba Bráda: Investigating the financing of secondary vocational education	141
Poster Session IV. – Information Systems in Education.....	148
Nikoletta Tolner, Andras David and Monika Pogatsnik: Challenges in Higher Education in Light of Teaching the Digital Technology	149
Csaba Majnár, Ferenc Gábor Rádli and Gaye Ediboglu Bartos: Augmented Reality in High School Literature: Enhancing Engagement and Evaluation	155
Nikoletta Tolner, Judit Módné Takács, József Halász, Tímea Bekk, Éva Takács, András Dávid, Csaba Bráda, Ildikó Petőné Csuka and Monika Pogatsnik: Well-being among students in dual and traditional education	159
Tímea Bekk, Éva Takács, Péter Tarsoly and Monika Pogatsnik: Motivational opportunities in higher education from a teacher's perspective	164
László Gugolya: Introduction of Industrial Robotic Arms in Education Using Dobot Magician	168
László Gugolya: Pepper in the library	173

ORAL SESSION I.
Industrial and Embedded Systems

Unique properties of a new Al/Sn Metallic Glasses obtained by drop cooling

Bráda Csaba
Óbuda U. Alba Regia Technical Faculty,
Székesfehérvár 8000, Hungary
Email: brada.csaba@uni-obuda.hu

Sajo-Bohus L.
Universidad Simon Bolivar. Valle de
Sartenejas 89000. Caracas,
Venezuela. Email: lsajo@usb.ve

Abstract. Poorly documented Al/Sn - noncrystalline - atomic conglomeration such as observed in bimetallic glasses (bMGs) is studied. The conglomerate is obtained by inducing a Al/Sn non crystalline structure, which can be produced by a rapid cooling process called quenching. We designed and built a device that ensures the desired large-scale cooling rate, thereby creating the Al/Sn atomic conglomeration necessary for the test. The testing bMGs is made to determine Al/Sn metallic glass specific properties in dependence on the purity of the material, cooling rate and other processing factors. It is believed that the combination of aluminium and tin can result in new metallic glass compositions where Al/Sn combination of strength, hardness, corrosion resistance and other properties offer advantages over its crystalline counterparts. This study is part of an effort to explore new bMGs compositions, processing techniques and glassforming ability of Al/Sn metallic alloy materials for future applications in aerospace electronics and medical devices.

Keywords: bimetallic glass, Al/Sn, non-crystal structure, glass-forming ability

I. INTRODUCTION

Bimetallic glasses, often referred to as metallic glass (improperly amorphous metal), is a unique type of material that combines properties of both metals and glass. Unlike conventional crystalline metals, which have a highly ordered atomic structure, metallic glasses have a disordered, non-crystalline atomic arrangement similar to that of glass. The mentioned alloy is a unique type of material that combines properties of both metals and glass, [8]. Tin (Sn) is a common solder due to its low melting point, good wetting properties, and compatibility with aluminium (Al) and metals commonly used in electronics. Proper bonding between Sn and Al is crucial for reliable connections and the overall performance of electronic devices. Aluminium (Al) –Tin (Sn) alloys are potential lead free bearing materials, widely used in automobile and marine applications due to their embedability properties i.e. the ability to absorb the foreign particles present in the lubricant to avoid scoring and wear, [12]. As an excellent structural and functional material, the transition alloy

metallic interface is of considerable importance, e.g. in quantum electronics, particularly in the context of superconducting and quantum device technologies, due to its role in enabling Josephson knots [5], superconducting qubits, quantum sensing devices, and quantum simulation platforms. Related technologies are key to the actual development of quantum computers, quantum sensors, and the advancement of quantum information science as a whole. Recently, the development of a superheated superconducting alloy metal-metal composite for granules has been used as a nuclear detector material for cold dark matter and neutrino studies [2]. Since metallic glasses interest is growing for their unique thermoplastic processing ability and excellent properties (ultra-high strength, wear and corrosion resistance, surface functionality, and soft magnetism) In this study we devised a new composite bimetal two step procedure; the first being the production of the two constituent materials as metallic glass; the second is the production and testing of laminated glass metal

II. MATERIALS AND METHOD

A. General aspects

Semimetal has a slight overlap between the conduction and valence bands; this characteristics for aluminium and tin, suggested its classification in the semimetals group. The classification justified for Al/Sn by the lack of a band gap and for having a negligible density of states at the Fermi level. A typical property in contrast of metals in that the conduction band is partially filled, [6]. In figure 1 a schematic representation shows the semimetal band structure in comparison to a semiconductor.

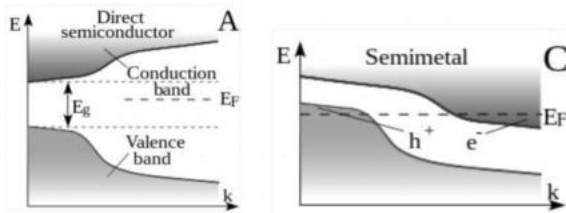


Fig. 1. schematic band structure to illustrate semimetals classification: As the right picture shows the structure has no band gap and a negligible density of states at the Fermi level, [6].

The selection on the materials used have been made on the supposition that due to the potential difference i.e. Sn (0.14 eV) and Al (1.69 eV) a photovoltaic phenomenon is expected.

Al/Sn semimetallic glass, define a material that lack a regular or a crystalline atomic structure, in opposition of that found in conventional metals. The disordered atomic arrangement in matter, similar to that of glass, shows unique properties. They typically have lower densities than crystalline metals, which can be advantageous for lightweight applications. For instance high strength and hardness, which can make them suitable for applications requiring wear resistance. Good corrosion resistance is essential for applications in harsh environments. High elastic limit allow to withstand significant deformation without permanent damage. Unique magnetic properties such as high magnetic permeability and low coercivity, making them useful in transformer cores and other magnetic applications. Good electrical conductivity favour them for electrical and electronic applications. They tend to fracture suddenly and without warning when subjected to excessive stress i.e. lack of plastic deformation before failure. Many metallic glasses have good corrosion resistance not forming grain boundaries, so no sites are formed for corrosion initiation in crystalline metals. Some alloys based on aluminium and tin have relatively good electrical conductivity. Due to their low coefficient of thermal expansion are less prone to volumetric changes with temperature variations. Soft magnetic properties, such as high magnetic permeability and low core loss, making them useful in transformers and magnetic sensors. Metallic glass have been tested also for superconductivity characteristics however so far no evidence or reports of metallic glasses made from aluminium and tin exhibiting superconducting properties at extremely low temperatures.

B. Semimetals available on the market

The exact properties of Al/Sn bMGs alloy would depend on the specific proportions of aluminium and tin and any additional elements or alloying materials used in its composition. Commercially available extrusion

aluminium alloy 6061 has the following atomic composition: Iron (Fe), 0.0 - 0.70 ; Magnesium (Mg), 0.80 - 1.20 ; Silicon (Si), 0.40 - 0.80 ; Copper (Cu), 0.15–0.40. The most popular combinations used commercially is 60% tin, 39% lead, and 1% alloys, [1]. The commercial available tin has two different composition: that employed in small technical work (Sn; 99%+Ag; 0.3% +Cu; 0.7%) and that employed for industrial product (Sn+Ag+Cu in percentage respectively 96.5%; 3%; 0.5%). Both of these materials in the form of metallic glasses, are studied to explore their potential applications and optimize their performance for the mentioned specific uses.

The compound ability to form glassy alloys is the consequence of a high configurational entropy in the liquid state, a situation that favour bypass crystallization. It is expected that heat mixing between the Al an Sn could enhance glass-forming ability. This means that the elements prefer not to mix in the solid state; for instance the mixing can hinder the formation of crystalline phases and that could be suppressed under critical cooling rate. When cooling occurred rapidly high viscosity at the liquidus temperature makes it more likely to form a glassy structure. The thermodynamic stability of the crystalline phases, if any, impede to form a bMGs. Nucleation and crystal growth during cooling could be reduced since minor elements act as good glass-forming agents. The composition range over which the alloy can form a glass is also of importance as once the glassy matter is formed, its stability at the desired operating temperature should not spontaneously crystallize during its intended application. While they are strong, they tend to fracture suddenly and without warning when subjected to excessive stress, due to the lack of plastic deformation, before failure. Nevertheless the metallic glass withstand large amounts of stress without permanently deforming or breaking, showing low deformation under applied loads.

III. EXPERIMENTAL SET-UP

Al/Sn-bMGs here are produced employing the experimental set-up based on the conceptual diagram given in figure 2.

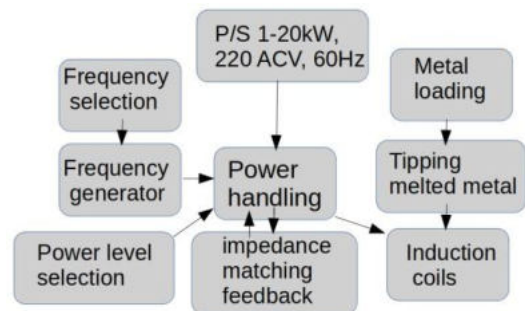


Fig. 2. Conceptual block diagram of the heat generation control and the glass metal production principle.

The block diagram provide a sintetized scheme for the Al/Sn sample rapid heating through the excited coil; the latter is reported in figure 3.

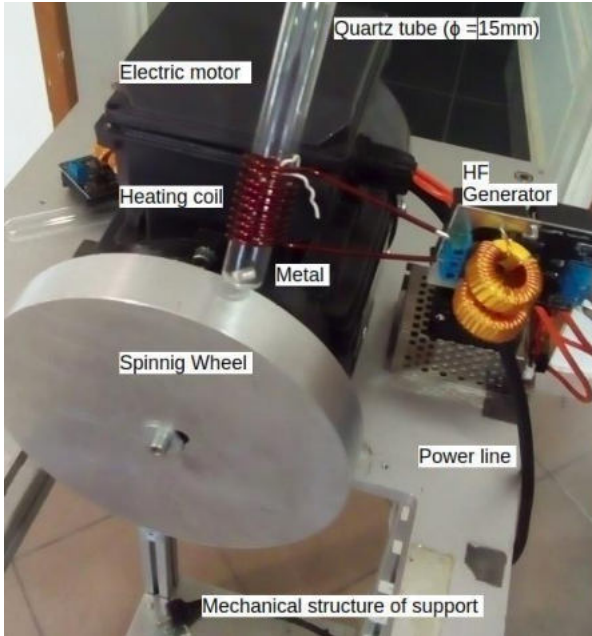


Fig.3. Picture of the power supply and the heating coil in that the bimetal is liquefied in a quartz tube. The cooling technique is obtained during the molten matter hitting the aluminium disc surface during which experiment a high rate cooling. The produced strip is released from the disc surface during wheel spinning.

The bMG sample, hitting the disc, experiments a rapid solidification trough the so called splat cooling technique or quenching. During the extremely fast cooling rate, typically on the order of millions of degrees Celsius per second, the formation of crystalline structures is prevented with the consequences mentioned. In this case atoms do not have enough time to organize themselves into a regular crystalline pattern so that the atoms bound into a disordered atomic arrays, giving the material its unique properties. The bMGs are produced by the equipment shown schematically in fig.3 and described as follows:

1. Melting the Metal: Purpose built induction furnace is employed for melting the Al/SnbMGs
2. Ejection and Rapid Cooling: Once the bimetal is in a liquid state inside a heat resistance quartz glass test tube, it is rapidly ejected onto a cold substrate to obtain a rapid solidification. The

substrate on that solidification occurred, is usually a rotating aluminium metal disc with a 20 cm diameter (at 12 hundred rpm). The distance between the nozzle orifice (at the bottom of the quartz tube) and the spinning disc surface surface is 5mm.

3. Formation of thin ribbons: the quenched bimetal provide the formation of thin ribbons 300 micrometers with thickness of few hundred microns. The thickness is set by the aluminium disc diameter and rpm-value.
4. Collection: The glassy ribbons are collected and analysed to determine its properties and therefore its suitability for a selected applications.

IV. EXPECTED PROPERTIES

Glass bimetal alloys, including those composed of aluminium and tin, can exhibit a wide range of mechanical properties depending on their composition and processing methods. Here are some considerations for improving the mechanical properties of glass bimetal aluminium-tin alloys:

- i.- Experimenting with different compositions we achieve a balance between strength, ductility, and other desired properties.
- ii.- Trace elements in commercialized Al-Sn can enhance the mechanical properties and stability of the glass bimetal structure.
- iii.- Quenching rate lead to more uniform and desirable glass metal structures, improving strength and hardness.
- iv.- Annealing improve the mechanical properties since can relieve internal stresses and enhance ductility.
- v.- Thinner glass metal may exhibit better mechanical properties compared to thicker ones. Thinner samples induce better structure.
- vi. Smaller grain sizes in the amorphous structure can enhance mechanical properties such as hardness and wear resistance.

Mechanical testing such as tensile testing, hardness testing, and impact testing to assess the mechanical properties accurately.

Experimental Optimization: advanced materials characterization techniques, such as X-ray diffraction and electron microscopy, provide information on alloy's structure.

V. RESULTS

Typical result expected for Al/Sn(40%) glass metal alloy are given in Table 1; following range of physical properties to point toward its distinctive properties :
 Table 1. Properties of bimetallic glass studied.

Physical Characteristics	Note	Range of values	Sources [14]
Structure	Metallic glass	Properties	[8]
Hardness	High	average hardness 24 ± 1.6 GPa	[13]
Elastic Limit	High	Elastic modulus: 71,0 GPa.	[17]
Strength	High	160 MPa; yield point: 75 MPa; relative extension: 10 %; Poisson's ratio: 0,33;	[16]
Brittle Behavior compressive strength	quite brittle	4.5 - 6 GPa	[15]
Density	Lowultra dense	5.5 GPa at 850 K	[21]
Corrosion Resistance	Good		[18]
Electrical Conductivity	High	$1.63 \pm 0.02 \times 10^{-7} \mu\Omega$	[19]
Thermal Expansion Coefficient	Low	Constant $\sim 8.24 \times 10^{-3} /K$	[11]
High magnetic permeability	low core loss	soft-magnetic properties	[10]
Superconduc-tivity	Not found yet		[22]

Other propeties	Ageing		[20]
-----------------	--------	--	------

Sn employed in the industry has the following properties: liquidus tem. 220 °C, solidus 217 °C . For the Al-alloys: density: 2,880 g.cm⁻³; liquidus temperature: 660 degrees Celsius; solidus temperature: 557 °C.; melting point: from 650 to 730 °C; temperature spills: from 650 to 705 °C; [3], [4]. Metal glassy temperature for a given set of alloys can be deduced from the following graphic given by Cao et al., [7]:

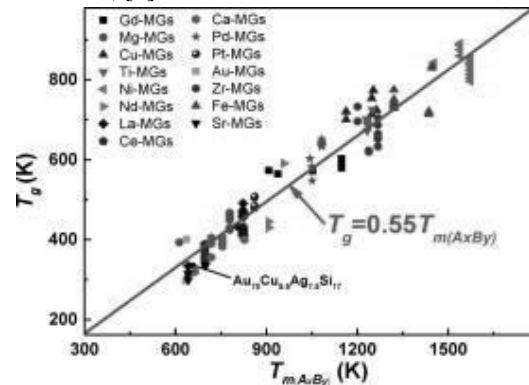


Fig. 4. Metallic glassy temperature Tg for various alloys from Cao et al., op.cit.

The next series of pictures show the metallic glass surface produced by drop cooling only.

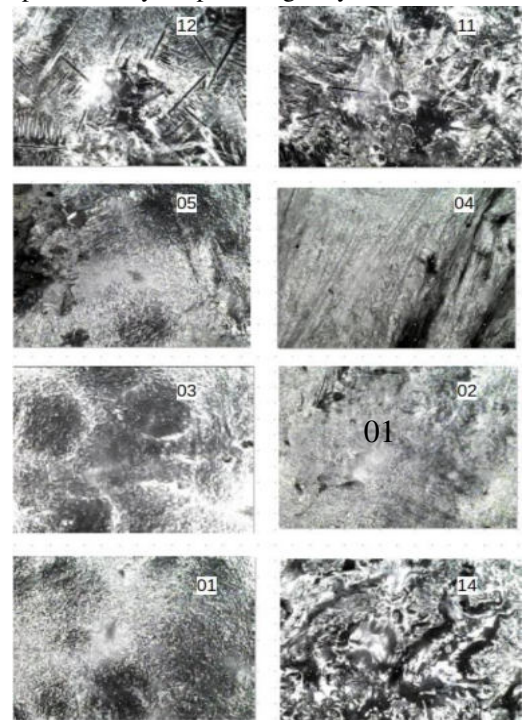


Fig. 5. Al/Sn alloy metallic glass surface microphotographs. Particularly the original images, numbers 02 and 03. clearly shows the dendritic crystallization. Pictures 04 and 05. show typical images of amorphous alloy. The others are given for analogy.

For comparison of a surface corresponding to a normal solder joint is given in figure 6, as an evidence of crystallization obtained when it cools in open air.

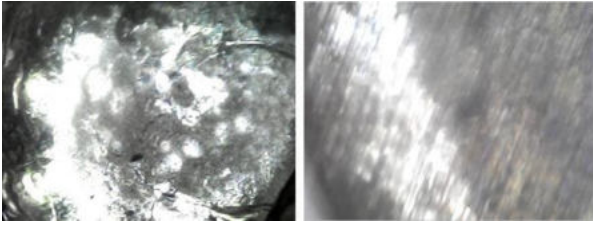


Fig. 6. For convenience and visual comparison we give two surfaces corresponding to a normal solder joint resulting from low cooling rate in open air, [op.cit].

An additional picture in figure 7, is given to show the dendritic crystallization shape that take place in bulk tin



Fig. 7. Surface of bulk tin that to shows typical dendritic crystallization structure obtained at a relatively low cooling rate, [9].

Figure 8 is given to show surficial structure difference between multi-MG and bi-MG.

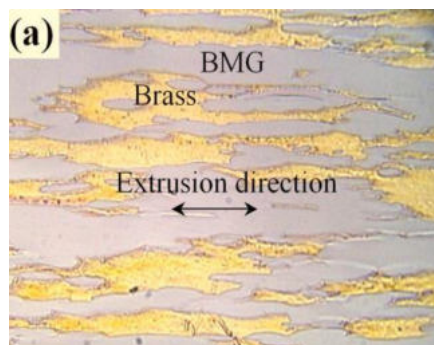


Fig. 8. Optical microphotograph of Ni (59%); Zr (20%); Ti (16%); Si (2%) Sn (3%) composite brass metallic glass surface (longitudinal section); that has an electrical conductivity of $1.63 \pm 0.02 \times 10^{-7} \mu\Omega$, 2.5 times higher in comparison to brass Cu (80%)+Zn (20%), [19].

Properties of bMG can vary significantly depending on their composition and processing methods, the specific temperature (T_g). T_g value can be deduced from Cao et al., op.cit.

VI. DISCUSSION AND CONCLUSION

Glass Al/Sn bimetal has been produced from liquid phase fast quenching process that lead to mechanical

property; these differ from the crystallized metal structure. The bMG process improve the Sn compound strength by 25%, but at the same time occur at the expense of e.g. ductility. Drop cooling, in opposition of splash cooling, resulted in our case as an effective method for producing bimetallic glasses. We confirmed that the cooling rate is the most essential parameter for the sample production since properties of glassy metals vary significantly. In general term the absence of a crystalline structure gives metallic glasses some interesting properties and advantages over crystalline metals. Al/Sn bMGs exhibit to some degree excellent properties such as ultra-high strength and excellent wear and corrosion resistance. Glass metal technology leads to fundamental changes in the properties of individual metals. The basic properties of tin (Sn) and aluminium (Al) are known as metals for industrial use, as well as their alloys. Expected mechanical properties are: tensile strength: 160 MPa; yield point: 75 MPa; relative extension < 10 %; hardness 45 NV; Poisson's ratio 0,33; elastic modulus: 71,0 GPa. In the course of our research, we are looking for answers to the question of:

Achieving a balance between different properties depends on the specific application requirements. In this study it can be appreciated that a systematic approach is required to develop a glassy aluminium-tin alloys to fulfil a particular application. Additionally, research in materials science and engineering continues to evolve, so staying updated with the latest advancements in alloy development is beneficial.

i.- Al/Sn alloy glass metal - mechanical, magnetic and electrical properties, that could be useful for industrial applications can be produced ii.- Al – Sn thin-film glass metal materials could be produced as thin ribbons.

It is assumed that based on the electrochemical potential of the raw materials, the unique magnetic properties of the new types of glass metals created from them may converge towards the properties of superconducting materials, and their optoelectric properties may make these materials suitable for the manufacture of solar cells. Characterization of the Al/Sn metallic glass is under scrutiny.

In spite of limited understanding on the relationship between their atomic structure and mechanical properties as a function of their structural state, the technique with drop cooling, is adequate for bMG production. Since it is a novel materials with unique properties could spread advantageously in various "high tech" industries. The use of artificial intelligence predict 20,000 samples of different metallic glass alloys and so far it may be considered an open field for basic research. Authors are planning to further study both the structure characterization and properties of metallic glasses.

References

- [1]. Aalco. Aluminium Alloy - Commercial Alloy - 6061 - T6 Extrusions. <https://www.aalco.co.uk › datasheets › Aluminium-All.> (2023.10.05. 11.00)
- [2]. Abplanalp M., C. Berger, G. Czapek, U. Diggelmann, M. Furlan, A. Gabutti, S. Janos, U. Moser, R. Pozzi, K. Pretzl, K. Schmiemann (1994). Detection of nuclear recoils in prototype dark matter detectors, made from Al, Sn and Zn Superheated Superconducting Granules. Preprint Bern BUHE-94-05. Submitted to Phys. Rev. D, August 1994. Available at: [arXiv:condmat/9411072v1](https://arxiv.org/abs/condmat/9411072v1) 17 Nov 1994.
- [3]. ASM 1996. Aluminum and Aluminum Alloys, ASM International, 1996
- [4]. Gilbert J. Kaufman, Elwin L. Rooy (2004.) Aluminum Alloy Castings: ASM Properties Processes And Applications
- [5]. Berdiyrov, G.R., Milošević, M.V., Kusmartsev, F. et al. Josephson (2018). Vortex loops in nanostructured Josephson junctions. *Sci Rep* 8, 2733 <https://doi.org/10.1038/s41598-018-21015-7>
- [6]. Burns, G. (1985). *Solid State Physics*. Academic Press, Inc. pp. 339–40, at: <https://en.wikipedia.org/wiki/Semimetal>.
- [7]. Cao, C.R., Ding, D.W., Zhao, D.Q., Axinte, E., Bai, H.Y. and Wang, W.H., (2014). Correlation between glass transition temperature and melting temperature in metallic glasses. *Materials & Design*, 60, 576 – 579. <https://doi.org/10.1016/j.matdes.2014.04.021>
- [8]. Greer, A.I., (2001). *Metallic Glasses*, Editors: K.H. Jürgen Buschow, Robert W. Cahn, Merton C. Flemings,
- [9]. Ilschner B, Edward J. Kramer, Subhash Mahajan, Patrick Veyssi re. (2001), (*Encyclopedia of Materials: Science and Technology*, Elsevier, 5529-5537. <https://doi.org/10.1016/B0-08043152-6/00967-0>.
- [10]. Jiang Y, Jia S, Chen S, Li X, Wang L, Han X., (2022). Theoretical Prediction and Experimental Validation of the Glass-Forming Ability and Magnetic Properties of Fe-Si-B Metallic Glasses from Atomic Structures. *Materials* doi: 10.3390/ma15093149.
- [11]. Kato, H., H.-S. Chen and A. Inoue, (2008). Relationship between thermal expansion coefficient and glass transition temperature in metallic glasses. *Scripta Materialia*, 58, 12, 11061109. <https://doi.org/10.1016/j.scriptamat.2008.02.006>
- [12]. Kumar Patel S, Kumar Swain B, Behera A, Sanjeeb Mohapatra S. (2020.) A Revolution in Material Science. *Metallic Glasses*. IntechOpen <http://dx.doi.org/10.5772/intechopen.90165>
- [13]. Madge, S.V., Caron, A., Gralla, R., Wilde, G. and Mishra, S.K. (2014). Novel W-based metallic glass with high hardness and wear resistance. *Intermetallics*. 47-6, 10,. <https://doi.org/10.1016/j.intermet.2013.12.003>
- [14]. Trexler M. M., Thadhani, N.N. (2010). Mechanical properties of bulk metallic glasses. *Progress in Materials Science*. 55, 8,, 759-839. <https://doi.org/10.1016/j.pmatsci.2010.04.002>
- [15]. Qu, RT, Volkert, C.A., Zhang, Z.F., Liu, F.R. et al. (2023), Yield strength of “brittle” metallic glass. *J. Materials Science & Technology*, Pages 247-254.
- [16]. Qu, R.T., Liu Z.Q. and Zang Z.F.(2015). Yield strength and yield strain of metallic glasses and their correlations with glass transition temperature. *J. Alloys and Compounds*, 637, 44-54.
- [17]. Tian, L., Cheng, YQ., Shan, ZW. et al. (2012). Approaching the ideal elastic limit of metallic glasses. *Nat Commun* 3, 609 <https://doi.org/10.1038/ncomms1619>
- [18]. Vahid et al., (2021). Electrochemical and Corrosion Behavior of Metallic Glasses. <https://doi.org/10.3390/books978-3-03943-723-8>
- [19]. Wang K., Fujita T., Chen M. W., Nieh T.G., Okada H., Koyama K., Zhang W., Inoue A. (2007). Electrical conductivity of a bulk metallic glass composite. *Applied Physics Letters*, 91, 15, 154101. doi: 10.1063/1.2795800.
- [20]. Yao, Y., Du, Q., Cao, Y. et al. (2023). Natural aging of metallic glasses. *Sci. China Mater.* 66, 793–800 <http://doi.org/10.1007/s40843-022-2164-8>

- [21]. Yamada, R., Shibasaki, Y., Abe, Y. et al. (2019).
Unveiling a new type of ultradense anomalous
metallic glass with improved strength and
ductility through a high-pressure heat treatment.
NPG Asia Mater 11, 72
<https://doi.org/10.1038/s41427-019-0175-1>
- [22] Johnson, W. (1980). Superconductivity In
Metallic Glasses. Journal de Physique
Colloques, 41 (C8), pp.C8-731-C8-741.
[10.1051/jphyscol:19808183](https://doi.org/10.1051/jphyscol:19808183)

Life Cycle Cost Analysis of Karl Fischer water determination for moisture sensitive materials for electric vehicles and pharmaceutical use

Viktor Vass
Óbuda University
Doctoral School of Materials Sciences
and Technologies
Budapest, Hungary
vass.viktor@phd.uni-obuda.hu

György Györök
Óbuda University
Doctoral School of Materials Sciences
and Technologies
Budapest, Hungary
gyorok.gyorgy@amk.uni-obuda.hu

Abstract—When using materials that are sensitive to moisture and water, unwanted side reactions can result in the formation of by-products, toxic substances, reduced yields and even occupational accidents. In the pharmaceutical industry and in the production of Li-ion batteries, humidity, moisture and water control of raw materials and intermediate products are of particular importance. One suitable method is Karl Fischer titration. In this work, a life cycle cost analysis of Karl Fischer water determination is presented.

Keywords— *life cycles assessment, life cycle cost, LCA, LCC, Li-ion batteries, APIs, Karl Fischer titration, water, moisture*

I. INTRODUCTION

Water is also a solvent, a reactant and a reagent, covering 71% of the Earth's surface, in solid form as ice, in liquid form as water, in gaseous form as vapour. There are many materials, production processes and methods that are sensitive to the presence or absence of water in a particular state, or that can be combined with certain substances or effects to produce undesirable processes, such as mould in residential buildings, unworkable pasta with insufficient moisture, drought and drying, sawdust splashing, accelerated degradation due to microflora or instability, for example in the case of pharmaceuticals.

In many areas of industry and research and development, the provision of adequate water content is of utmost importance [1, 2]. In this article, we focus on water and moisture sensitive materials, and analyse the water content and moisture determination methods for their processing from a life cycle cost perspective.

Life cycle analysis is an environmental management toolkit for evaluating the environmental impact of process steps from the raw material life cycle and production life cycle to waste and recycling (Fig. 1.). It is based on the ISO 14040 and ISO 14044 standards [3, 4]. The evaluation can be performed manually or by software, and there are several evaluation methods to choose from, CML and ReCiPe methods [5, 6, 7] being particularly suitable for the evaluation of chemical-intensive processes and procedures.

Life-cycle cost analysis can be used to estimate the net present value of the costs incurred in a given life-cycle phase, using USD/1000 measurements/year as the unit of measurement. Life cycle cost analysis, together with life cycle analysis, is part of sustainable development and helps to develop a circular economy approach.

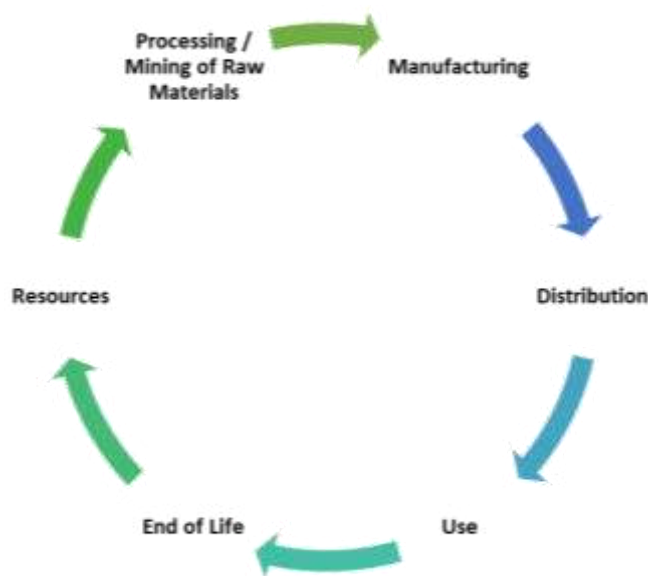


Fig. 1. Life Cycle

Determination of water and moisture content

There are several methods available, depending on the expected water content, the accuracy of the measurement, whether the material is heat sensitive, the type of instrumentation available or applicable to the production site and environment, the frequency of measurement, whether it can be automated if necessary, and whether any permits or special qualifications are required.

For high water contents, e.g. soil samples, non-heat-sensitive precipitates, a rapid moisture determination may be used, for hygroscopic materials vacuum drying, or a lyophilisation procedure for heat-sensitive materials, biological samples, and then calculation of water content based on mass measurement. X-ray and IR instruments are used to determine the water content of insensitive anhydrous materials.

Chemical measurements include gas evolution reactions and Karl Fisher titration, the latter being used to measure water contents from 1 ppm to 100 % efficiently.

Karl Fischer water determination

The principle of water determination is based on the oxidation of elemental iodine. The measuring solution typically consists of sulphur dioxide, iodine and organic base absorbed in methanol, and the end-point detection can be by fading of the solution colour or by an indicator electrode.

Particularly low water content or extremely moisture sensitive substances are usually tested by coulometric titration, where the solution contains potassium iodide rather than elemental iodine, which is released at the anode and reacts with the water content of the sample to produce the amount of charge required to generate elemental iodine, which gives the amount of water in the sample.

In coulometric measurements, the water content of the sample is between 1 ppm and 5 %, while in volumetric measurements the water content is above 100 ppm.

A simplified reaction equation of the reaction that takes place, where RN is the nitrogen-containing organic base, e.g. pyridine or imidazole, where alkylsulphate salt and hydrogen iodide compound formed.



The general composition of the reagents is described in the table below (Table I.). It can be clearly seen that in coulometric reagents for the measurement of substances with low water content (less than 5 %), in addition to methanol, the halogenated organic compound chloroform is also present as a solvent in significant quantities, but this reagent usually does not contain diethanolamine.

TABLE I. COMPOSITION OF KARL FISCHER REAGENTS

Method	Volumetric Titration Reagent		Coulometric Titration Reagent	
	Component	composition, weight %	Component	composition, weight %
Solvent	Methanol	40	Methanol	40
			Chloroform	31
Organic Base (pH Buffer)	Imidazole	12	Imidazole	12
	Diethanolamine	8		
Reagent	Sulfur dioxide	10	Sulfur dioxide	7
Iodine Reagent	Iodine, elemental	10	Potassium iodide	10

Use in the pharmaceutical industry

Moisture-sensitive substances such as metal hydrides lithium aluminium hydride, amides such as sodium amide, Grignard reagents used in the production of active substances such as the analgesic tramadol, the anti-inflammatory, antipyretic and analgesic naproxen and ibuprofen [8]. Numerous examples include the active substance remdesivir [9] used in the Covid-pandemic [10]. The water sensitivity of Grignard reagents is known, in the C-glycosylation reaction [11], or the reaction of degradable boron trichloride at -40 °C or triethylamine at -78 °C with the reaction mixture, simply because of the sub-zero temperatures, no water can be present in the system to avoid damaging the reactors.

For stability and shelf-life, a specific moisture content is required for many pharmaceutical substances such as

theophylline [11] used for asthma or levothyroxine [12] used in hypothyroidism.

Inappropriate conditions, excessive moisture or water content can destroy an entire batch, cause unwanted side reactions, lead to the formation of toxic substances or result in a mixture that is difficult to purify and may have low yields.

The importance of moisture content for lithium-ion batteries

During the production of lithium-ion battery cells, there are several critical points where the moisture content is as tightly controlled as possible and kept sufficiently low to prevent side reactions such as the formation of highly toxic and corrosive hydrogen fluoride [13] gas (a major concern from a health and safety point of view), and the reduction of the active ingredient content of NCM due to the action of water and air: lithium hydroxide formation and subsequent carbonation [14, 15], in-use failure and loss of cell capacity and life expectancy [16].

Strict quality control throughout the entire manufacturing process is important [14].

Manufacturing processes involve several drying steps, where the humidity of the manufacturing environment is set to freezing between -30 and -40 °C, while the water content of materials, such as the separator film, which has a ceramic coating that can absorb more moisture due to its porous surface, must be constantly monitored. For lithium-ion battery production, the Karl Fischer water determination [17] is ideal, very low water content is required, therefore a coulometric method is recommended.

Life Cycle Costs

The life-cycle cost of water determination in US dollars (USD) per 1000 measurements per year is illustrated in Fig. 2. For the calculation, the initial cost and installation cost as well as the termination cost were calculated for 10 years, while the other factors were calculated for 1 year. In the case of coulometric titration, it can be seen that the cost factors are higher, due to the cost of the reagent and its hazardousness, since it contains halogenated organic material, and the cost of waste disposal.

We used the prices and change rates valid in Hungary on 20th of August.

The calculations are based on 10 years of equipment runtime.

The initial cost includes the measuring system and all the basic equipment needed, such as reagents, standards. Installation costs are related to the infrastructure required for the operation of the measuring system, the measuring site and its surrounding environment, commissioning and service costs. Energy costs are the cost of the electricity used in the operation.

Operating costs include the cost of reagents, electrodes, waste containers, filters, which are constantly consumed. Service and maintenance costs are the periodic and routine (due to breakdown) material and service charges. Environmental costs are the costs of waste treatment.

Is it the cost of quality?

At the current market price, 1 tonne of NCM costs 40.000 USD, the total cost of coulometric measurements per 1000 measurements is only 15.690 USD, which means that only considering the cost of this raw material, excluding the initial costs of performing the measurements, we can prevent the production of defective semi-finished and finished products from the resulting NCM, not counting the costs of handling and transporting the resulting production waste.

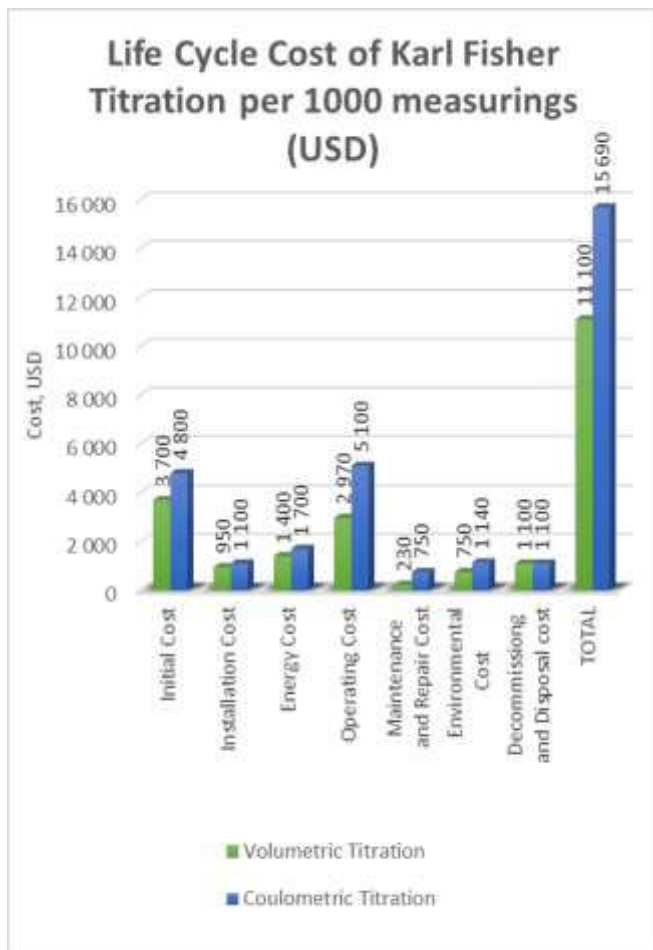


Fig. 2. Life Cycle Costs

To give an example from the pharmaceutical industry, if ibuprofen is priced at USD 25/kg, again excluding the additional cost of side effects and waste, the selling price of 630 kg of high quality ibuprofen is equivalent to the annual cost (Fig. 3.).

Karl Fisher measurement is essential to keep production costs low. Waste treatment costs due to side reactions, waste transport, waste disposal are a significant burden for companies. By strictly controlling the processes, strictly respecting the limits, professionally carrying out the measurements and their evaluation with due care, the costs can be controlled and the quality of the semi-finished and finished products can be guaranteed to the users.

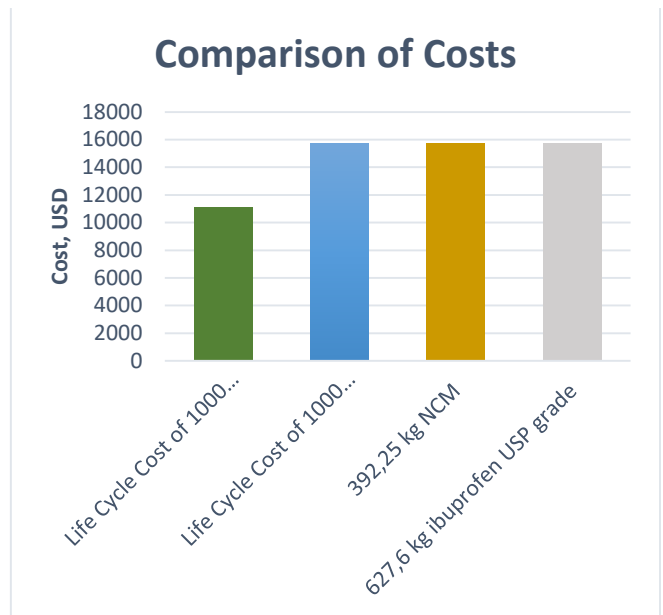


Fig. 3. Comparison of Costs

To give an example from the pharmaceutical industry, if ibuprofen is priced at USD 25/kg, again excluding the additional cost of side effects and waste, the selling price of 630 kg of high quality ibuprofen is equivalent to the annual cost.

II. CONCLUSIONS

The determination of water content is very important to reduce scrap costs, prevent accidents and side reactions and ensure the desired quality. Stability and durability are also very important. In the pharmaceutical industry and for Li-ion battery cells, the specifications for moisture and water content and humidity must be strictly observed. In Hungary, using prices and exchange rates valid on 20 August 2023, the life cycle cost of 1000 measurements is comparable to about 400 kg of NCM or 600 kg of ibuprofen using the coulometric measurement system, excluding the waste disposal costs due to side reactions. Apart from the initial cost, even for very small batches it is worth maintaining the measuring system.

III. SUMMARY

Data without sufficient resolution will give an incorrect life-cycle result. Appropriate geography is also important, and the energy mix can vary significantly. Some materials are not currently available in any life cycle inventory database, and can be further developed either from their own data or by estimation. Once the purpose of the study has been defined, it can be decided which impact assessment method will be optimal.

REFERENCES

- [1] M. Karlovits, D. Gregor-Svetic „Durability of Cellulose and Synthetic Papers Exposed to Various Methods of Accelerated Ageing” Acta Polytech. Hung., vol. 9, no. 6, pp. 81-100, 2012
- [2] N. I. Akçay, B. Nagy, S. Tuzmen „Reaction Systems for Modeling and Validation of Biological Signaling Pathways: G1/S Checkpoint of the Cell Cycle” Acta Polytech. Hung., vol. 18, no. 6, pp. 7-23, 2021
- [3] ISO 14040:2006 Environmental management. Life cycle assessment. Principles and framework, <https://www.iso.org/standard/37456.html> (hyperlink verified on 20th of August 2023) CML 2016 aug. <https://www.universiteitleiden.nl/en/research/research->

- output/science/cml-ia-characterisation-factors (hyperlink verified on 15th of July 2023)
- [4] ISO 14044:2006 Environmental management. Life cycle assessment. Requirements and guidelines, <https://www.iso.org/standard/38498.html> (hyperlink verified on 20th of August 2023)
- [5] M. J. Goedkoop, R. Heijungs, M. Huijbregts, A. de Schryver, J. Struijs, R. van Zelm "ReCiPe 2008, A life cycle impact assessment method which comprises harmonised category indicators at the midpoint and the endpoint level" First edition Report I: Characterisation; 6 January 2009, <http://www.lcia-recipe.net> (hyperlink verified on 20th of August 2023)
- [6] M. A. J. Huijbregts, Z. J. N. Steinmann, P. M. F. Elshout, G. Stam, F. Verones, M. Vieira, M. Zijp, A. Hollander, R. van Zelm "ReCiPe2016: a harmonised life cycle impact assessment method at midpoint and endpoint level" *Int. J. Life. Cycle Assess.*, vol. 22, pp. 138-147, 2017
- [7] CML 2016 aug. <https://www.universiteitleiden.nl/en/research/research-output/science/cml-ia-characterisation-factors> (hyperlink verified on 20th of August 2023)
- [8] A. Kadama, M. Nguyen, M. Kopach, P. Richardson, F. Gallou, Z.-K. Wan and W. Zhang "Comparative performance evaluation and systematic screening of solvents in a range of Grignard reactions" *Green Chem.*, vol. 15, pp. 1880-1888, 2013
- [9] E. Szendro, Z. Lakner "The Long-Range Macroeconomic Effects of Sars-Covid-19 Pandemic in Hungary: a Conceptual Framework and Methodology - Focusing Approach" *Acta Polytech. Hung.*, vol. 20, no. 9, pp. 7-22, 2023
- [10] D. F. Vargas, E. L. Larghi, T. S. Kaufman "Evolution of the Synthesis of Remdesivir. Classical Approaches and Most Recent Advances" *ACS Omega*, vol. 6, no. 30, pp. 19356-19363
- [11] M. R. Dhondale, P. Thakor, A. G. Nambiar, M. Singh, A. K. Agrawal, N. R. Shastri, D. Kumar "Co-Crystallization Approach to Enhance the Stability of Moisture-Sensitive Drugs" *Pharmaceutics*, vol. 15, no. 189, 2023
- [12] J.W. Collier, R. B. Shah; A. Gupta, V. Sayeed, M. J. Habib, M. A. Khan "Influence of formulation and processing factors on stability of levothyroxine sodium pentahydrate" *Aaps Pharmscitech* vol. 11, pp. 818-825, 2011
- [13] A. V. Plakhotnyk, L. Ernst, R. Schmutzler "Hydrolysis in the system LiPF₆-propylene carbonate-dimethyl carbonate-H₂O" *J. Fluor. Chem.*, vol. 126, pp. 27-31, 2005
- [14] M. Kosfeld, B. Westphal, A. Kwade "Moisture behavior of lithium-ion battery components along the production process" *J. Energy Storage*, vol. 57, 106174, 2023
- [15] J. Sicklinger, M. Metzger, H. Beyer, D. Pritzl, H.A. Gasteiger "Ambient Storage Derived Surface Contamination of NCM811 and NCM111: Performance Implications and Mitigation Strategies" *J. Electrochem. Soc.* vol. 166, pp. 2322-2355, 2019
- [16] M. Stich, N. Pandey, A. Bund: Drying and moisture resorption behaviour of various electrode materials and separators for lithium-ion batteries, *J. Power Sources*, pp. 84-91, 2017
- [17] M. Kosfeld, B. Westphal, A. Kwade "Correct water content measuring of lithium-ion battery components and the impact of calendaring via Karl-Fischer titration" *J. Energy Storage*, vol. 51, 104398, 2022

Improve electric boat safety and usability with telematics

1st Zoltán Farkas
Óbuda University

Doctoral School on Safety and Security Sciences
Bécsi Str. 96/b, 1034 Budapest, Hungary
Email: farkas.zoltan2@uni-obuda.hu

2nd György Györök
Óbuda University

Alba Regia Technical Faculty
Budai Str. 45, 8000 Székesfehérvár, Hungary
Email: gyorok.gyorgy@amk.uni-obuda.hu

Abstract—Telematic systems are becoming increasingly common in automotive and industrial applications. The marine industry is also following these trends. They can be used to measure and transmit selected parameters of a system to a remote server. This allows authorized personnels to know the status of the system. Further information about the system can be obtained by analyzing the collected data together. They can be used to predict possible malfunctions or emergencies. Lithium-ion batteries in recreational boats are increasing due to their favorable energy density. However used in inappropriate conditions can cause serious hazards. Continuous monitoring of the proper key parameters can increase the vehicle's safety. This paper presents a solution to avoid malfunctions, remote control the vehicle, and signal an emergency.

I. INTRODUCTION

Electric propulsion has long been used in recreational boating, primarily powered by lead-acid batteries. The use of lithium chemistry batteries is becoming more common due to their favorable characteristics. Boatbuilders prefer them because of their energy density, which allows them to build boats with longer range or higher speed. In addition, the price of lithium batteries is becoming more affordable, largely due to the electric car revolution [1]. At the same time, higher energy density means higher risk. Overloading these batteries or using them in inappropriate conditions is a huge safety risk. An overloaded lithium battery is capable of thermal runaway and can catch fire. The extinguishing of a lithium battery fire is a challenging task for firefighters [2], [3].

Sales of electric boats are far below those of electric cars, so the boats will be equipped with a propulsion system already available on the market from a specialized company. Developing a unique solution for a specific type of boat would not be profitable or would increase the boat's selling price. After installation, it is crucial to synchronize the components and establish suitable limits to guarantee safe operation. Pairing components can be challenging. However, utilizing an embedded system can simplify this task and enable control tasks that standalone devices are unable to achieve. One example of such parameters is the highest battery temperature deemed safe by the manufacturer. When the battery reaches this temperature, it should be disconnected from the loads or the power to the loads should be limited.

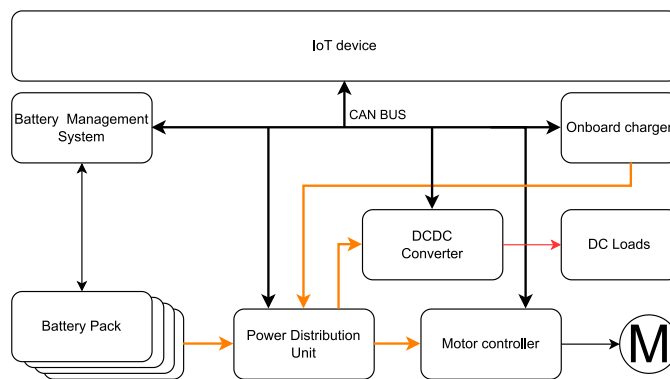


Fig. 1. Schematic of a common EV drive

Electric boats can remain connected to shore power in ports for weeks without their owners utilizing or inspecting them. For this reason, IoT-based solutions are also increasing in this segment, allowing the various units of the vessel to be monitored and controlled remotely. Beverage coolers and air conditioners can be remotely activated and deactivated. This saves energy when the boat is not in use. The devices can be activated remotely using a mobile application before the trip. The propulsion system and onboard sensors can be easily monitored and their data transmitted to a remote server, providing similar benefits to other available conveniences. When designing the system, cyber security aspects must also be taken into account [4], [5].

Fig. 1 shows a diagram of a standard electric powertrain. The electric powertrain components communicate through the CAN bus. An embedded system allows for the collection, processing, and secure transfer of all available powertrain parameters to a central server via a cellular network. The remote server can perform continuous data analysis using telemetry systems, in addition to the onboard electronics. These systems can collaborate on tasks and function in a hybrid mode. This allows for management of the vehicle's driving system as necessary, including real-time performance optimization to avoid possible malfunctions.

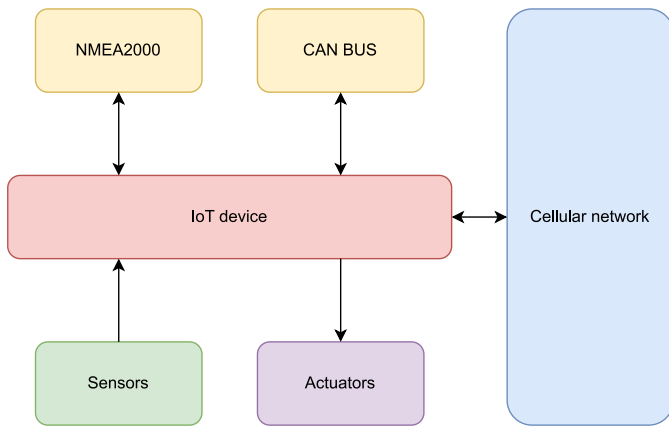


Fig. 2. External peripherals of the embedded processor

II. PROPOSED SOLUTION

A. Hardware

Fig. 2 the external peripherals for the proposed embedded computer. It is advisable to select a processor that can support an operating system commonly used in embedded environments. This will facilitate the utilization of advanced encryption protocols and remote updates. The device gathers information from the CAN and NMEA2000 communication buses. NMEA2000 is electrically identical to the CAN bus and is based on it. Its main aim is to streamline communication of information between a boat's instruments such as sensors, displays, and actuators.

While it is feasible to use alternative protocols for obtaining sensor information, it is advisable to choose ones with sufficient electromagnetic interference immunity. One can employ analog or digital inputs, as well as noise-tolerant communication buses such as RS-485. It may be beneficial to record water temperature and temperature of various compartments and equipment, while also installing smoke and flame detectors.

The system should be powered by the same low-voltage, typically lead-acid battery that powers the BMS. This battery is charged by a DCDC device, which takes power from the lithium battery. It can also be charged by a dedicated charger connected to shore power.

B. Software

1) *On-board computer program*: The on-board computer collects the data from the specified sources. The collected data is transmitted to the server via a cellular module using the MQTT protocol. The system can manage the operation of the vehicle. It can adjust drive parameters such as the maximum current that can be drawn from the batteries. Using digital outputs, it can switch devices on/off, such as pumps or contactors. It must be able to perform all basic functions without network coverage. MQTT is bidirectional, so it listens to the server commands such as modifying the vehicle parameters or doing a predefined task.

2) *Server program*: The server operates an MQTT broker that allows boats to connect and publish their current status. A server-side script subscribes to the topics published by the boats and collects their data which it saves in a database. Another script continuously analyzes the stored data and sends commands to the boats' on-board computers when needed. The database is connected to a web server that visualizes the relevant data for authorized users.

C. MQTT

as stated in the standard

MQTT is a Client Server publish/subscribe messaging transport protocol. It is lightweight, open, simple, and designed to be easy to implement. These characteristics make it ideal for use in many situations, including constrained environments such as for communication in Machine to Machine (M2M) and Internet of Things (IoT) contexts where a small code footprint is required and/or network bandwidth is at a premium [7].

The connection between the IoT devices and the MQTT broker using certificates with mutual authentication [8]. This means that both the server and client side have a certificate and identify themselves with their public/private key pair. This protocol is commonly referred to as mutual transport layer security or mTLS. The mechanism for the handshake is shown in Fig. 3. It aligns with the Zero Trust approach which by default does not trust any device [6]. Fig. 4 shows the network map of the system. Multiple boats can connect to the server using the MQTT protocol. MQTT enables numerous clients to subscribe and listen to a specific topic, resulting in multiple clients being notified by a single command [9]. On the server side, there is also an MQTT client connected to the broker which can store the data sent by the boats in the database.

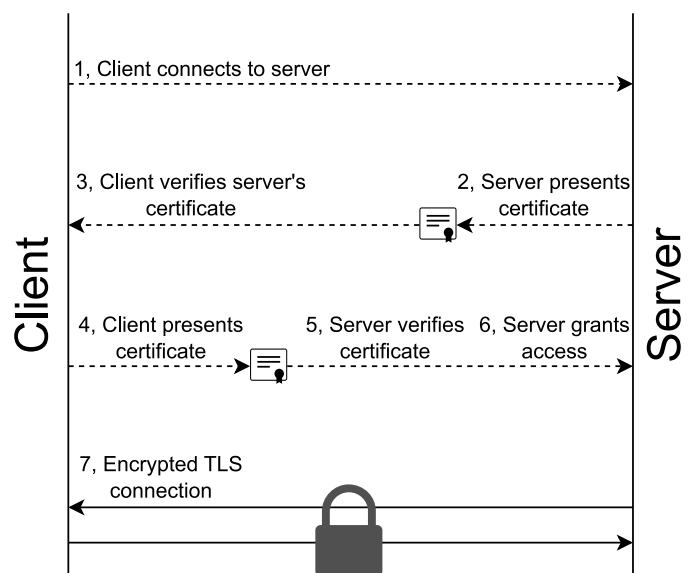


Fig. 3. mTLS handshake [6]

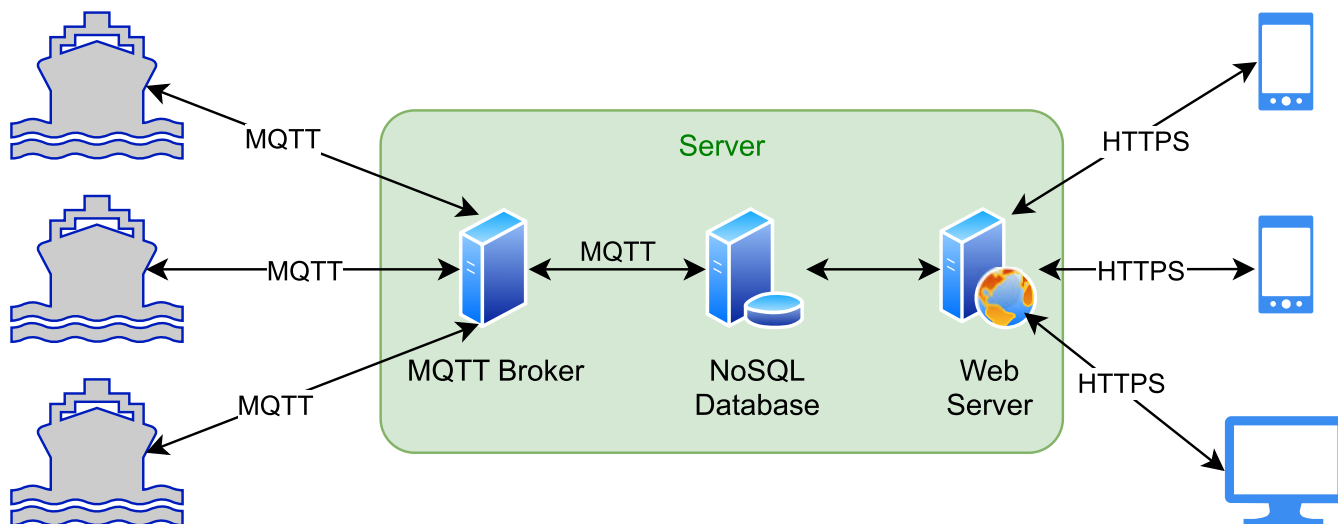


Fig. 4. Network map of the proposed system

D. Lack of cellular network coverage

If data transmission fails, the onboard electronics must store the data in a local non-volatile memory. The stored data can be synchronized when the network is available again. The data must have a timestamp to ensure that the outcome after synchronization is identical to what it would have been if the network had been continually available. The storage should have a predetermined size limit, and upon reaching this limit, new messages will automatically overwrite the oldest messages.

E. Over the air updates

The software of the onboard computer must be regularly updated to fix any flaws and security vulnerabilities whilst also adding new features. The server can send with software packages via the MQTT connection. Once the client has validated the software package, it can install it [10]. When performing updates, it is important to take extra precautions, as interruptions may occur, such as power loss. If an update attempt is interrupted, the system must still be able to continue running. One approach is to use redundant images. While the current software is operating on one image, the update can be downloaded onto the other. Once verified, the embedded system can then boot from the new image. If a modern operating system is being used on the embedded system, the update process can be simplified. It is crucial to prioritize cyber security by verifying the origin and integrity of the software package.

F. Access to the data

The stored data can be accessed by several types of devices for authorized users. Authentication is available through login using the encrypted HTTPS protocol. Depending on the level of privileges, different types of data are available to the specific user. Boat owners have access to relevant data via their mobile application, such as the charge status of their

vessel. They can use the system to request technical support or report malfunctions. The service technician can access fault messages, powertrain data, service records, etc. to assist in the troubleshooting process. This could also enhance usability and serviceability.

G. Informing methods of recipients

Notifications, alerts, and emergency calls can be sent through various channels. A pop-up message on the boat's display is enough to notify of a warning battery during use. When the boat is docked in the harbor, a notification via the phone application can help inform its owner when charging is completed. It may be necessary to indicate a clear emergency through multiple channels. As all remote notification methods require mobile network coverage, the embedded system may also need to have the capability to control the boat's lights and horn to signal the emergency to the outside world [11].

III. APPLICATION AREAS

A. Safety features

Because a cellular module is connected to the embedded system, it can not only transmit data, but also make emergency calls and send messages. The recipient can be a pre-set phone number or the emergency services. An automatic emergency call device implemented this way increases safety and the chances of getting out of an emergency with as little loss as possible. For example, if a fire breaks out on the vessel while it is parked in the port, the staff and emergency services can be quickly informed of the fire.

1) *Detection thermal runaway*: The most expensive and dangerous component of electric vehicles using lithium chemistry is the battery. In extreme cases, a catastrophic thermal runaway can occur, endangering the vehicle's occupants and the environment. In the case of boats, the emergency is further compounded by the fact that it is impossible to simply get out of the vehicle in open water. For this reason, every effort must

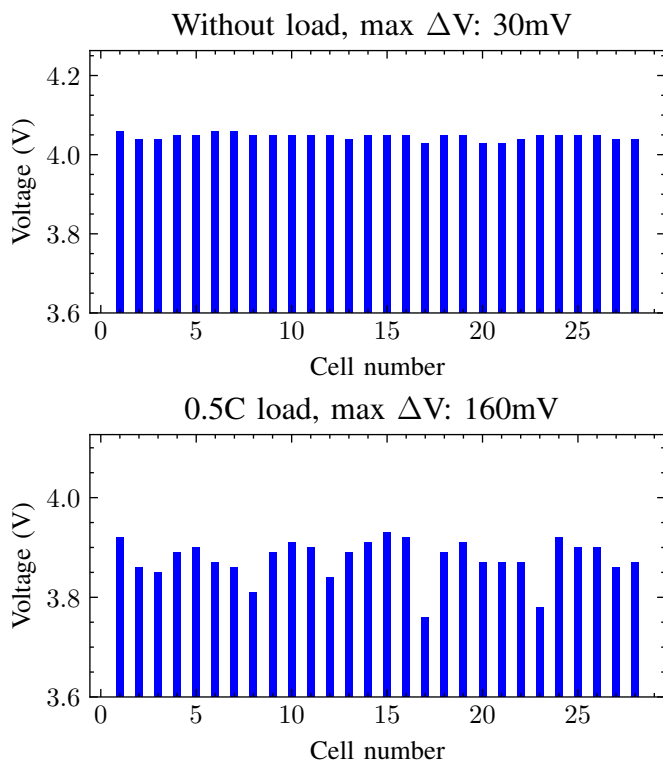


Fig. 5. Voltage of EV battery cells observed at a 0.5C load. The first graph displays the voltage measurements taken prior to the load, while the second graph shows the voltage measurements taken after the load was applied.

be made to prevent this type of fatal failure from occurring. If it does occur, it should be detected at an early stage to allow as much time as possible to leave the vehicle. Thermal runaway can result from either overcharging or over-discharging the battery. Monitoring and avoiding these failure modes is the responsibility of the battery management system. However, a faulty cell or some external impact such as a collision can cause a deformation that triggers a chain reaction that the battery management system cannot control because the failure is in the battery cell [12]. For this reason, it is worthwhile to create a system that can detect such a severe failure.

Thermal runaway in batteries can be detected by observing certain characteristics, such as cell temperature and voltage. Additionally, the use of suitable gas and smoke sensors can also detect this phenomenon [13], [14].

2) *Fire detection*: Heat, smoke, gas, flame sensors can be used to detect a fire on the vessel. These sensors are strategically placed throughout the vessel to continuously monitor the environment for any signs of smoke, abnormal heat, flammable gases, or open flames [15]. The importance of early detection cannot be overstated. Starting the extinguishing operation as soon as possible is crucial as ignition of a battery pack can intensify the emergency situation, potentially leading to a more hazardous scenario.

B. Monitoring of powertrain parameters

By observing the drive train, several faults can be predicted. Such detections can work well if historical values of the observed characteristics are available. In the described system these values are stored in the database. The change in the values can predict an event that could lead to a failure. Imagine, for example, an increasingly polluted cooling circuit. The deposition of contaminants continuously degrades the efficiency of the cooling system. Until eventually it reaches a level where the cooling efficiency deteriorates to the point where the cooling circuit elements have to be reduced to avoid overheating. If the battery overheats, the power of the connected loads must be reduced. Additional information about the vehicle can be revealed by observing certain events, such as a fault code or activation of a protection mechanism. The server can run a script that monitors both the current and historical status of the boat. Knowing this data, an expert system can find an optimum to determine the maximum output power of the motor. Suppose there is a maximum motor current MQTT topic that the server script can read and write. If it differs from the currently set value, it can change the value. The onboard electronics program will detect this change and update the motor controller with new value via CAN bus.

C. Modify instruments configuration

The onboard computer has interfaces to the CAN and NMEA2000 bus. The system can then update the configuration on all connected devices supporting it. This provides a cost-effective way to reconfigure a specific parameter on either a single vessel or an entire fleet.

D. Weakest cell identification

The presence of a significant voltage difference at high load levels may be an indication that the cells are at different levels of degradation. [16]. Fig. 5 shows the cell voltages before and after the load was turned on.

IV. CONCLUSIONS

The use of the proposed system can increase the safety of the vehicle by continuously monitoring the battery status and providing an alarm when a critical failure occurs. Such an automatic signal can help save time for vehicle occupants and emergency responders. The result can be a reduction in the impact of an emergency. Continuous monitoring of the defined characteristics helps to understand the processes taking place in the vehicle. Hidden faults can be detected or the correct functioning of the system can be verified. Such information can facilitate the troubleshooting process and simplify the work of the service technician.

From the manufacturer's perspective, collecting real-world data can help to better understand the system being optimized. This data is valuable in organizing service work and can guide future improvements.

The owner can be provided with useful and clear information to improve the usability and user experience of the boat.

REFERENCES

- [1] J. Van Mierlo, M. Bercibar, M. E. Baghdadi, C. De Cauwer, M. Messagie, T. Coosemans, V. A. Jacobs, and O. Hegazy, "Beyond the State of the Art of Electric Vehicles: A Fact-Based Paper of the current and Prospective Electric Vehicle Technologies," *World Electric Vehicle Journal*, vol. 12, no. 1, p. 20, 2 2021. [Online]. Available: <https://doi.org/10.3390/wevj12010020>
- [2] P. V. Chombo and Y. Laounal, "A review of safety strategies of a Li-ion battery," *Journal of Power Sources*, vol. 478, p. 228649, 12 2020. [Online]. Available: <https://doi.org/10.1016/j.jpowsour.2020.228649>
- [3] L. B. Diaz, X. He, Z. Hu, F. Restuccia, M. Marinescu, J. V. Barreras, Y. Patel, G. J. Offer, and G. Rein, "Review—Meta-Review of Fire Safety of Lithium-Ion Batteries: Industry Challenges and research Contributions," *Journal of The Electrochemical Society*, vol. 167, no. 9, p. 090559, 1 2020. [Online]. Available: <https://doi.org/10.1149/1945-7111/aba8b9>
- [4] M. Čerģeĭ and J. Hudec, "Cyber-Security Threats Origins and their Analysis," *Acta Polytechnica Hungarica*, vol. 20, no. 9, pp. 23–41, 1 2023. [Online]. Available: <https://doi.org/10.12700/aph.20.9.2023.9.2>
- [5] M. Stanojević, D. Čapko, I. Lendák, S. Stoja, and B. Jelacic, "Fighting Insider Threats, with Zero-Trust in Microservice-based, Smart Grid OT Systems," *Acta Polytechnica Hungarica*, vol. 20, no. 6, pp. 229–248, 1 2023. [Online]. Available: <https://doi.org/10.12700/aph.20.6.2023.6.13>
- [6] "What is mutual TLS (mTLS)?" [Online]. Available: <https://www.cloudflare.com/learning/access-management/what-is-mutual-tls/> (accessed Sep. 01, 2023)
- [7] *MQTT*, OASIS Std. 5.0, 2019.
- [8] D. Díaz-Sánchez, A. Marín-López, F. Almenárez, P. Arias-Cabarcos, and R. S. Sherratt, "TLS/PKI challenges and certificate pinning techniques for IoT and M2M secure communications," *IEEE Communications Surveys and Tutorials*, vol. 21, no. 4, pp. 3502–3531, 1 2019. [Online]. Available: <https://doi.org/10.1109/comst.2019.2914453>
- [9] B. Mishra and A. Kertész, "The Use of MQTT in M2M and IoT Systems: A survey," *IEEE Access*, vol. 8, pp. 201 071–201 086, 1 2020. [Online]. Available: <https://doi.org/10.1109/access.2020.3035849>
- [10] H. Chien and N.-Z. Wang, "A novel MQTT 5.0-Based Over-the-Air updating architecture facilitating stronger security," *Electronics*, vol. 11, no. 23, p. 3899, 11 2022. [Online]. Available: <https://doi.org/10.3390/electronics11233899>
- [11] A. S. Bale, V. Narayanaswamy, V. Y. Shanthakumar, P. B. Shyla, S. Balakrishna, V. S. Nagaraja, S. B. Menasinakai, M. K. Hitesh, and E. Esarapu, *Recent advancement in emergency vehicle communication system using IoT*, 10 2022. [Online]. Available: <https://doi.org/10.1201/9781003217404-7>
- [12] S. Mallick and D. Gayen, "Thermal behaviour and thermal runaway propagation in lithium-ion battery systems – A critical review," *Journal of Energy Storage*, vol. 62, p. 106894, 6 2023. [Online]. Available: <https://doi.org/10.1016/j.est.2023.106894>
- [13] K. Bhaskar, A. Kumar, J. Bunce, J. Pressman, N. Burkell, and C. D. Rahn, "Data-Driven thermal anomaly detection in large battery packs," *Batteries*, vol. 9, no. 2, p. 70, 1 2023. [Online]. Available: <https://doi.org/10.3390/batteries9020070>
- [14] Z. Liao, Z. Shen, K. Li, G. Zhang, and T. Habetler, "A survey of methods for monitoring and detecting thermal runaway of lithium-ion batteries," *Journal of Power Sources*, vol. 436, p. 226879, 10 2019. [Online]. Available: <https://doi.org/10.1016/j.jpowsour.2019.226879>
- [15] D. Kaliyev, O. Shvets, and G. Györök, "Computer Vision-based Fire Detection using Enhanced Chromatic Segmentation and Optical Flow Model," *Acta Polytechnica Hungarica*, vol. 20, no. 6, pp. 27–45, 1 2023. [Online]. Available: <https://doi.org/10.12700/aph.20.6.2023.6.2>
- [16] D. Istardi and I. Z. Putra, "The Weakest Cell Identification in Li-Ion battery packs using Discharging Technique Performance," *2018 International Conference on Applied Engineering (ICAE)*, pp. pp. 1–4, 10 2018. [Online]. Available: <https://doi.org/10.1109/incae.2018.8579414>

Robots in Construction

How is Construction Industry Doing in Automation?

Ákos Jánvári
Alba Regia Technical Faculty
Óbuda University
Székesfehérvár, Hungary
akos.janvari@abci.hu

Dr. Károly Széll
Alba Regia Technical Faculty
Óbuda University
Székesfehérvár, Hungary
szell.karoly@amk.uni-
obuda.hu
ORCID: 0000-0001-7499-5643

Abstract— As energy and materials are getting more expensive, efficiency and productivity are becoming the most important factors in Engineering. Construction Industry is historically rooted in manual labor a traditional practices, but the need of transformation is clear and new technologies are being introduced. From improved efficiency and enhanced safety to precision and sustainability, robots are offering new possibilities for the whole sector. In this study we are preparing an overview about the most interesting developments focusing on robotics.

Keywords—BIM, autonomous robotics, mobile robotics, collaboration, construction

I. INTRODUCTION

The Construction Industry (CI) is still a challenging field for robotics but more and more innovation are introduced to improve efficiency and safety. [1] Digitalization can help us to control cost, safety and project timeline with simulating entire project lifecycle, understanding the risks and issues before we are facing with it. The whole approach is changing as design is getting more important – and it helps introducing more robotic applications as the biggest challenge of the robots was always the uncontrolled circumstances. If we can turn it into controlled and predictable environment we will win the possibility to use more automated solutions growing productivity, sustainability and reducing waste.

II. PROBLEM DESCRIPTION

What are the biggest challenges we face? Today we live in an era of soaring energy, building materials and labor prices. One of the most important aspects has become efficiency. In the case of construction projects of almost any scale, it can be said that the sustainability of the planned budget fundamentally depends on the planning – whether every detail has been planned and how we manage to stick to the plans during construction. To address these challenges, the construction industry is responding with significant changes – prefabricated elements, reinforced concrete structures, lightweight construction methods are spreading among construction methods, while digital solutions are also beginning to appear in work organization. How the industry is changing? What could be the future?

III. DIGITALIZATION

Digitalization is getting more important is Construction Industry. Growing productivity is not possible if we have no

data, so nowadays from design via logistics to construction tons of data is collected and used for planning and control. Building Information Modeling (BIM) is a new way of visualizing the construction project creating a real simulation of the whole project by understanding the processes and risks [2]. Successful implementation of BIM requires digitalization from the beginning – you have to create an intelligent 3D model of the construction and during the entire project you have to update statuses and simulation [3], [4].

BIM is revolutionizing the way how a Construction project is planned. As the main goal of BIM is to keep all communication within stakeholders and vendors on the same platform it requires a detailed 3D-design model with all the construction processes analyzed & defined. During the project this will be the common input for all activity planning. From robotic perspective it is offering a huge possibility as the repetitive tasks and high precision activities are the most relevant for introducing automated solutions.

This new environment is supporting the usage of robotic solutions as with the more available data it is possible to go down to low-level tasks planning which is a must for robot involvement [5].

BIM is also very much interested in status reporting – and automated applications are the best for such purposes.

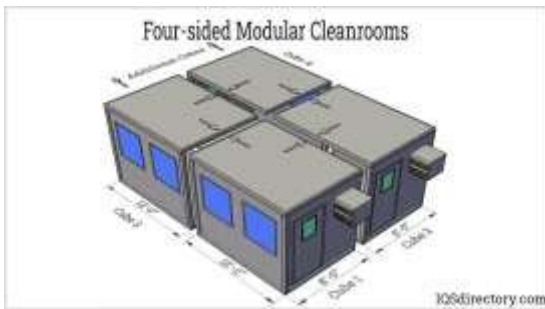
IV. BUILDING STRUCTURES

Basically, developments are taking place in 3 main directions regarding the basic concept:

- using prefabricated elements
- 3D printed buildings
- automated masonry solutions

A. Prefabricated elements

Onsite construction is struggling with many ad-hoc problems to solve. To avoid that many technological steps can be provided off-site under controlled circumstances. During production of prefabricated elements many existing robotic technologies can be easily used with proper design. In such condition robotic systems can deal with many predefined tasks.



1. Figure Prefabricated modular blocks

Prefabricated elements are usually manufactured through well-automatized production lines to improve efficiency, quality and overall control on the process [6].

Significant advantage of this technology is the reduced overall schedule of the construction as right after the approved design, parallel to the construction site preparation and foundation the prefabricated elements can be manufactured and prepared for the transportation.

Using prefabricated elements (see figure 1.) – especially when the elements are re-used in more constructions – can significantly reduce cost with appropriate design and offers more sustainability through reduced waste and using less polluting materials compared to traditional building technologies.

Although the technology offers more flexibility during the design there is less space for customization during the production. As the production requires lots of storage space it has a significant upfront cost.

B. 3D printed technology

Practically simultaneously with the advent of 3D printing, thinking started about how the technology could be applied to the construction of smaller or larger buildings. Developments in the area are continuous, the design of the completed buildings, the formation of the layers and their thickness are improving year by year. In practice, the technology has reached the point where wall structures can be printed from concrete, adobe and local building materials within a few days, and their utility value is completely acceptable with reasonable compromises. However, the disadvantage of the technology is that in its current form the size of the structure to be constructed is limited in size, primarily in height (see figure 2.).



2. Figure 3D printed house by COBOD

Key participant in this sector is COBOD (<https://cobod.com/>).

C. Masonry robots

Over the past 8-10 years, more and more experimental workshops, typically in cooperation with technical universities, have reached a level where they can test their designs in practice – mostly to gain experience.

1) SAM 100

The first truly spectacular and full-fledged (that is, not only stacking bricks, but also applying binders) copies, moving along an installed track, are designed specifically for the implementation of repetitive tasks in the masonry process. Their introduction illustrates how much better robots perform in large-scale, repetitive, precise tasks.

Well-known representative of these robots is the SAM 100 system (see figure 3.) designed by Construction Robotics (<https://www.construction-robotics.com/sam-2/>).

This system is much faster in bricklaying than any professional – estimated laying 5x more bricks in a shift-, but with the limitation that this system can build only a single straight wall and require a constant 3-4 workers to be present during its service. [7]



3. Figure Construction Robotics' SAM 100 in service

2) Hadrian X

About 10 years ago, an Australian-based development team, Fastbrick Robotics [8], came up with a completely new concept: they built a robotic arm long enough to reach every point in a house (see figure 4.)! In the case of the robot arm, extremely long distances required new technology in damping, because without it, the robot arm wobbled terribly under load. In 2016, the Hadrian 105 robot was used to build the first wall structure without human intervention, and based on this experience, Hadrian X was born, the only commercially available robot that can be used for independent construction today.



4. Figure Hadrian X in service

The concept of the system is very interesting: we are talking about a robot mounted on a conventional truck that can go practically anywhere. The robot itself is actually a huge, multi-joint, telescopic robotic arm built in the truck, which provides highly accurate positioning over long distances thanks to various balance mechanics. Thanks to the very long arm, it can easily overcome distances and heights on traditional construction sites, thus providing serious assistance in the construction of masonry structures.

The design of the building, of course, requires "brick", so Hadrian X is able to carry out the construction process with minimal losses with the help of the built-in cutting mechanism.

The disadvantage of the original robot arm is that due to the stabilization and load on the robot arm, it works with special lightweight construction elements designed for this purpose. To remedy this problem, they have entered into a cooperation with Wienerberger AG, a manufacturer of building materials, which helps to further develop the concept. The system has a great future ahead of it, and I think it is one of the most promising developments among the experimental technologies available for residential construction.

3) *KM Robotics*

In addition to the Hadrian X collaboration, Wienerberger is also developing a mobile robot platform in cooperation with the Technical University of Prague and the Czech startup KM Robotics [9], which will provide solutions primarily for indoor construction tasks and will actually combine the features of initial track-based robot structures and mobile robots by providing a mobile platform capable of independent movement and translational movement (see figure 5.).



5. Figure KM Robotics mobile brick laying robot application []

The solution is robust enough to work with actual standard materials, but due to its stability the height of the structures is limited.

4) *Human-robot collaboration – MULE*

Using an automated masonry solution require complex preparation from design to setting up the system. Construction Robotics therefore introduces MULE (Material Unit Lift Enhancer), a lift-assist equipment built to handle and move heavy material on construction sites (see figure 6.). MULE is improving safety beside helping to keep worker healthy. [10][11]



6. Figure Human-robot collaboration (MULE) [10]

D. *Robot support*

Wide range of robots can be used for supporting the CI.

In the following we will highlight some interesting projects where robots are supporting different activities on the field.

Common in these solutions is that all these robot solutions contain a mobile robotic platform which is communicating with a static station so the actual position is identified. Of course the positioning is supported also with SLAM to identify the close-range environment also.

1) *Construction monitoring by robot*

When using BIM it is important to get appropriate information about the current status. Using mobile robots (see figure 7.) environment scanning solutions can help building 3D models of the construction site, control conditions, document different statuses and identify possible failures or dangers. [12] [13]



7. Figure Mobile robot scanning a construction site [12]

The solution let user to build up a 4D twin of the construction site.

2) *Special-task robots*

Mobile robot platform can be used to support various task - from drilling to painting there are many useful solutions available on the market, helping to manage wide areas, high distances, repetitive work.

The basic concept is the same (see figure 8. for a typical representation):

- having a mobile robot platform to move the robot in the construction site as fast and accurate as possible
- and some kind of robotic arm with the actuator to offer the service

These application are normally running in semi-automated mode as the operator can insert new tasks or redefine existing ones.



8. Figure HILTI Jaibot drilling mobile robot in operation [14]

Most of these applications have a common preparation step when using some external tools, like laser scanner with SLAM the system need to be initiated.

3) Layout printing mobile robot

Mobile robots with printing capability can print the designed layout on the surface (see figure 9.) so on-site workers are able to work precise without using plans and measurement tools, but still kept on the common platform.

Of course the mobile robot platform need a high-precision position information within the site as it is determining the accuracy of the printed plans.



9. Figure Mobile robot printing the layout design

V. ROBOT COOPERATION

As we have seen all the above solutions are still about using a single robot on the field. We have many different tasks supported by robots preferably in semi-automated way, but robot cooperation in particular AI is still waiting for introduction in CI.

VI. CONCLUSION

Construction Industry is improving fast in digitalization. Many new developments are introduced for support for wide range of activities, but these solutions are mainly for independent use - integrated environment for different robots is still challenging. Industrial real-time integration standard for controlling robot cooperation is still limited beside the lack of precise onsite, real-time positioning.

Trend is clear and the long-term future is the low-level designed robot cooperation, but the short-term future is much more about human-robot collaboration and using human-controlled robots in on-site construction.

VII. ACKNOWLEDGEMENT

The authors wish to thank the support to the Arconic Foundation and the Howmet Aerospace Foundation.

VIII. REFERENCES

- [1] J. Manuel Davila Delgado, L. Oyedele, A. Ajayi, L. Akanbi, O. Akinade, M. Bilal, H. Owlabi, "Robotics and automated systems in construction: Understanding industry-specific challenges for adoption" in *Building Engineering* volume 26, November 2019
- [2] L. Wang, Y. He, Y. Han, "Research on Power Engineering Construction Management Based on BIM Technology" in *International Conference on Robots & Intelligent System (ICRIS)*, 2018
- [3] W. Anane, I. Iordanova, C. Ouellet-Plamondon, "BIM-driven computational design for robotic manufacturing in off-site construction: an integrated Design-to-Manufacturing (DtM) approach" in *Automation in Construction* volume 150, June 2023
- [4] M. Sanches Moura, C. Rizzo, D. Serrano, "BIM-based Localization and Mapping for Mobile Robots in Construction" in *International Conference on Autonomous Robot Systems and Competitions (ICARSC)*, 2021
- [5] A. Zhu, P. Pauwels, B. De Vries, "Smart component-oriented method of construction robot coordination for prefabricated housing" in *Automation in Construction* volume 129, September 2021
- [6] <https://www.iqsdirectory.com/articles/modular-building/prefabricated-building.html> (page visited October 2023)
- [7] Peter Kenter, "Bricklaying robot readied for construction market" in *Daily Commercial News / Technology*, 27 March 2015,
- [8] <https://www.fbr.com.au/view/hadrian-x> (page visited October 2023)
- [9] <https://www.wienerberger.com/en/stories/2021/20211117-robotics-czech-republic.html> (page visited October 2023)
- [10] <https://www.construction-robotics.com/mule/> (page visited October 2023)
- [11] M. Zhang, R. Xu, H. Wu, J. Pan, X. Luo, "Human-robot collaboration for on-site construction" in *Automation in Construction* volume 150, June 2023
- [12] <https://blog.allplan.com/en/construction-monitoring-by-robots> (page visited October 2023)
- [13] S. Park, S. Yoon, S. Ju, J. Heo, "BIM-based scan planning for scanning with a quadruped walking robot" in *Automation in Construction* volume 152, August 2023
- [14] <https://aec-business.com/hiltis-robot-breaks-records-on-a-yit-construction-site/> (page visited October 2023)

ORAL SESSION II.
Applied Informatics

Deep Learning for Image Authentication: A Comparative Study on Real and AI-Generated Image Classification

Gaye Ediboglu Bartos
Alba Regia Technical Faculty
Obuda University
Szekesfehervar, Hungary
gaye.ediboglu@uni-obuda.hu

Serel Akyol
Faculty of Engineering and Natural
Sciences
Kütahya Health Sciences University
Kütahya, Turkey
serel.akyol@ksbu.edu.tr

Abstract— The rapid advancement of AI-based image generation techniques has led to the increasing need for methods to distinguish between real and AI-generated images. In response, this study applies two popular deep learning algorithms namely Residual Networks (ResNets) and Variational Autoencoders (VAEs) to recognize AI-generated synthetic images. The algorithms adopted in the study approach the problem differently: ResNets aim to distinguish between real and fake images by analyzing high-level features and structural patterns within the images, while VAEs approach the problem as an anomaly detection task. The performance of the abovementioned algorithms is assessed using the CIFAKE image dataset containing 120000 images (60,000 synthetically generated images and 60,000 real images). The experimental results indicated that ResNets outperform VAEs in accurately classifying real and AI-generated images. VAEs, approaching image classification from an anomaly detection point of view, yielded insufficient performance in the case of the CIFAKE dataset. The findings underscore that the model selection, training objective, dataset attributes, and the specific task are all significant factors influencing a model's performance.

Keywords— *deep learning, image authentication, real image, ai-generated image, fake image, synthetic image, ResNet, Residual Network, VEs, variational autoencoder, anomaly detection, feature extraction, image classification.*

I. INTRODUCTION

The rapid evolution of artificial intelligence (AI) has led to an era where AI-generated images have become increasingly difficult to distinguish from authentic photographs. As the boundaries between real and AI generated synthetic content blur, it is crucial to develop effective methods for discerning between images created by AI algorithms (such as Generative Adversarial Networks [1] or Diffusion Models [2]) and those originating from the real world. Common applications of synthetic images include generating synthetic handwriting [3][4] and photorealistic faces [5]. With an effort to overcome the abovementioned challenge, this research seeks to employ two powerful deep learning architectures: Residual Networks (ResNet) and Variational Autoencoders (VAEs) [6][7]. Our objective is to develop and evaluate separate classification models based on ResNet and VAEs for discriminating between authentic real-world images and AI generated ones. CIFAKE image database consisting of 60000 real and 60000 fake images is used in training and evaluation of the models giving [8].

Detecting whether an image is a real image or an AI-generated one is a challenging task. To address this challenge, various approaches can be employed, including discriminator

networks, anomaly detection, and feature extraction. Discriminator Networks are used as a part of generative models together with a generative network. The discriminator is responsible for distinguishing the real data from the data created by the generator. Therefore, discriminator networks such as in GANs can be used to detect fake images. Another approach to this challenge is to treat the synthetic images as anomalies based on how different they are from real images and use anomaly detection algorithms such as autoencoders and Variational Autoencoders (VAEs). Another common approach is to use a pre-trained deep convolutional neural network (CNN) [9] such as VGG, ResNet, or Inception to extract features from the images and then classify them according to the distinct features. Besides the abovementioned methods, combination of predictions from multiple models might improve performance. In this study, two separate algorithms were employed namely ResNet using feature extraction and VAEs using anomaly detection approach to classify real and fake images from the CIFAKE database. It is also worth mentioning that certain modifications on both architectures were also deployed to find the most suitable model for the target input.

ResNet, renowned for its prowess in image classification tasks, has been chosen as one of the primary models. Its capability to capture intricate visual features and patterns has made it a standard choice for various computer vision tasks. This study explores the potential of ResNet in addressing the critical challenge of distinguishing AI-generated images from real-world photographs, capitalizing on its discriminative abilities.

Conversely, VAEs, primarily designed for generative tasks, offer unique potential for detecting anomalies in image data. By encoding and decoding images, VAEs can reconstruct input data, making them valuable for anomaly detection. In our research, we harness the anomaly-detection capabilities of VAEs to create a distinct classification model. The objective is to assess whether VAEs can excel at identifying AI-generated images by detecting deviations from learned real-world data distributions. It should be noted that VAEs usually demand more computational power during training compared to models like ResNet for image classification due to their generative nature. The following section provides an overview of relevant research in the field.

II. RELATED WORK

The classification of real and AI-generated images, along with the detection of fake images, has become a crucial

research area in recent years. The rapid growth of generative models resulted in the creation of realistic content such as images and text. In response to the advancements in fake content generation, techniques to detect such content have also emerged. In terms of AI generated image detection, most of the research focuses on the detection of deepfakes which are synthetic images of human faces. However, this research does not only focus on detection of fake human faces but also any other image containing skyline, animals, vehicles etc. thus it appears to be a more challenging task than detection of deepfake images. The challenge derives from the fact that animals and vehicles have a wide variety of shapes, sizes, and appearances, making it challenging to create a comprehensive detection model that can identify all possible variations accurately. Detection of fake human faces as a task is simpler because facial structures have certain consistent features and symmetry, allowing for the development of more reliable algorithms that can pinpoint inconsistencies associated with deepfake manipulations. In this section, the focus will be the research conducted on detecting AI generated rather than deepfake images. In the next section, the database and the adopted CNN architectures are explained in detail.

In 2021, Goebel et. al proposed a method to detect, attribute and localize GAN generated/manipulated images [10]. The proposed model was then evaluated using 2.76 million images (1.69 real images and 1.07 million fake images from 5 different GAN databases). The performance of the proposed method was compared with eight other CNN architectures such as ResNet, VGG16 [11] and InceptionV3[12] and it yielded promising results in detecting GAN generated images. In 2023, Dogoulis et. al. published a study to address the challenge of generalization for fake image detection in the cross-concept scenario caused by training the model on samples of random AI-generated images [13]. Their proposal includes a probabilistic method to evaluate the quality of generated images and training image detectors with those higher-quality images instead of randomly picked ones. The results indicate that using more realistic images to train the detector can significantly improve the generalization ability.

Xi et. al. proposed an ai-generated image detection method consisting of a dual-stream network comprised of a residual stream and a content stream [14] in 2023. To be able to test the capabilities of the proposed model, the authors created two databases consisting of AI-generated images using text to image AI generators. The performance of the proposed classifier was compared with seven other popular classifiers such as ResNet and CGNet [15]. The performance of the proposed fake image detector outperformed all seven classifiers on both the generated database and excelled when applied to mainstream computer graphics detection datasets. Zhu et al. put forward the GenImage database consisting of over 1 million pairs of AI-generated fake images and collected real image generated by the state-of-the-art diffusion models and GANs in 2023 [16]. The database does not focus on a specific class of AI generated images, it includes general images from 1000 image classes. In their study, in order to evaluate the GenImage dataset, different CNN architectures and image transformers were used.

In the subsequent sections, we demonstrate the methodologies, hardware and software employed, the datasets utilized, and the experimental results obtained through the application of ResNet and VAEs in image

classification. Furthermore, we will conduct a comparative analysis to clarify the variations in performance between the two models.

III. EXPERIMENTS

In this section, we present the experimental setup, procedures conducted to assess the efficacy of deep learning models namely Variational Autoencoders (VAEs) and Residual Networks (ResNet) for image authentication. Our objective was to investigate and compare the models' performance in distinguishing real images from AI-generated images using the CIFAKE dataset.

The following sections put forward the details on the hardware and software used for the experiments, the dataset used, the modifications on partitioning of the dataset and image loading phase and finally the changes made on the deep learning models consequently.

A. Experimental Hardware and Software

The neural networks used for detecting AI-generated images were constructed using Python and key deep learning libraries such as TensorFlow and PyTorch [18][19]. All TensorFlow and PyTorch random seeds were initialized to ensure result reproducibility. The Variational Autoencoder (VAEs) and ResNet models were implemented using the resources provided by Google Colab within the Jupyter Notebook environment [20]. However, we encountered difficulties due to the substantial size of the input dataset, which consisted of 120,000 images. The challenge arose from the necessity to load and preprocess (resize) this extensive dataset before training. Consequently, we had to revise our initial approach to loading and processing images, incorporating optimizations to handle the large dataset efficiently.

The VAEs model was trained leveraging the GPU allocated by Google Colab, as was the ResNet model. All image data was processed at a resolution of 64x64 pixels. Google Colab provided the necessary environment and GPU resources for efficient computation and analysis of the models.

B. The Dataset

In this study, the CIFAKE image dataset is used to train and test the methods used for classification. CIFAKE dataset is a balanced dataset and includes 120000 images from two different classes namely real images (60000 instances) and AI-generated synthetic images (60000 instances) [8]. The real images are from the CIFAR-10[17] dataset and the synthetic images are generated using Latent Diffusion Model [2]. The generated images belong to the class of general images, they are not on a specific content such as human face or art. Samples belonging to real images category are shown in the Fig. 1 and samples from the synthetic image category are represented in Fig. 2 below. The partitioning of the dataset into training and test set is provided in the next section.



Fig. 1 Examples of AI-generated images from the dataset [8]



Fig. 2 Examples of real images from the dataset [8]

C. Modifications on the Image Loading and Partitioning Phase:

In this section the partitioning of the dataset and the changes on the image loading and resizing are provided. As previously highlighted, we encountered significant challenges stemming from the extensive size of our input dataset and the constraints posed by limited computational resources for image processing. Consequently, we devised specific modifications to mitigate this issue. This section provides an in-depth discussion of the challenges we faced, along with the solutions we implemented.

In the earlier attempts, all 120000 images from CIFAKE dataset were loaded and resized one by one without using explicit batch processing. The images were loaded and processed individually inside the for loops that iterated over the image files in the directories. However, it was exhausting for the system therefore to reduce the load on the GPU and optimize the code for handling many images, a few optimizations were implemented namely batch loading and parallel processing. Batch loading helps us to load the images in batches instead of loading all images at once. This process helps in managing memory more efficiently. At the same time, using parallel processing helps us load images concurrently thus speeding up the image loading process.

Since the experiments were carried out in the Google Collaboratory using python programming language, the “ThreadPoolExecutor” class is utilized to create a pool of threads that execute the function that loads the images concurrently, loading images in parallel for each batch instead of the for loop in the original code. This parallelism helps speed up the image loading process by utilizing multiple threads. Each thread processes a batch of images independently, improving overall efficiency. Another change to weigh down the code was made by using a more efficient image loading library. The “opencv” library for loading images was applied instead of the initial “PIL” library to try and improve the performance.

After several experiments, we further optimized the code by reducing the batch size. At first, a batch size of 32 was implemented, however, experiments showed that batch size 16 worked the best for our needs.

Additionally, the partitioning ratio was also determined at this step. Since ResNet model took less time to train, in order to determine the best partitioning was decided using ResNet with 50 epochs and the batch size of 64. The table below shows that the partitioning of 75% training set and 25% test set provided the highest classification accuracy. Therefore, the abovementioned partition is used to train and test the models in the next section. The next section puts forward the changes made to the models in details.

TABLE 1 PERFORMANCE OF DIFFERENT PARTITIONING OF DATASET

Size of Training Set (%)	Size of Test Set (%)	Accuracy
70%	30%	0.85
75%	25%	0.89
80%	20%	0.94

D. Modifications on Algorithms:

In this study two deep learning algorithms were adopted for the image authentication purpose namely VAEs and ResNet. The model architectures of the algorithms can be seen in Fig. 3 and Fig. 4 below [6][7].

Fine-tuning a VAEs involves making modifications to the architecture, loss function, or training process to better suit a specific task or dataset. In our study, due to the limited computational power, the fine tuning applied on VAEs was changing the batch size and number of epochs. We varied the batch size between 16 and 128 to assess the trade-off between computational efficiency and gradient accuracy. Additionally, experiments with different numbers of epochs were carried out. The number of epochs ranged from 40 to 80, to understand the model's convergence behavior and generalization.

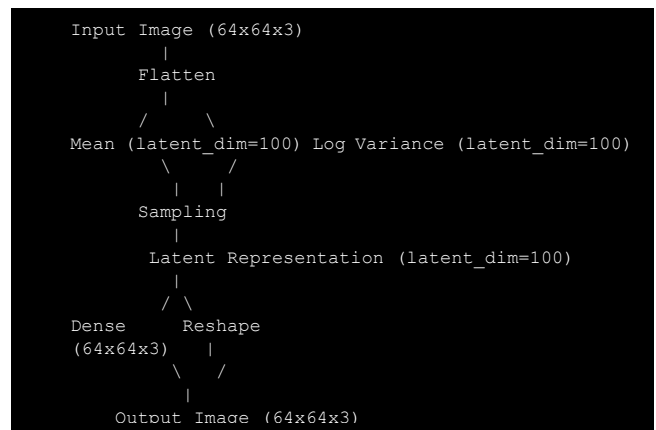


Fig. 3 Variational Auto Encoder Architecture

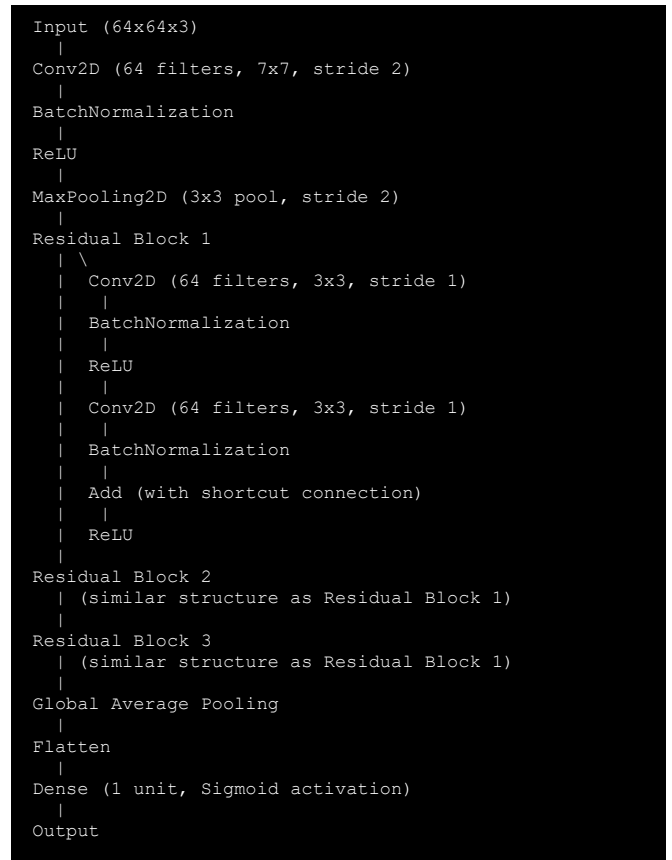


Fig. 4 Residual Network Architecture

Common fine tuning performed on ResNet includes using a pre-trained ResNet Model, modification of the last classification layer and fine tuning hyperparameters such as learning rates and batch sizes. Similar to the changes on VAE, we tuned the batch size, exploring values from 16 to 128, to balance computation efficiency and gradient accuracy. In addition to those, the number of training epochs varied from 40 to 80, seeking an optimal convergence point and avoiding overfitting.

IV. RESULTS

In this section, we present the results of our comparative study on image authentication using VAEs and ResNet. We conducted experiments to evaluate the performance of these models on classifying real and AI-generated images using a dataset specifically curated for this research, namely the CIFAKE dataset. The performance metrics were calculated using “sklearn.metrics” module and they include precision, recall, f1 score, accuracy as well as weighted average and macro average of those metrics.

We first fine-tuned both the VAEs and ResNet models using different batch sizes and number of epochs. As anticipated, VAEs needed a lot more computational power during training compared to ResNet for image classification due to their generative nature. In contrast, models like ResNet do not have the added complexity of generative tasks thus resulting in less computational requirements during training. Training VAEs model on CIFAKE took at least 0.5 times more time than training ResNet model at almost every experiment using the same hardware. The table below shows the accuracy of both models using different hyperparameters.

In terms of the number of epochs tested were 40, 50, 60,70 and 80. However by watching the learning curve and performance metrics closely, it could be seen that 50 epochs were ideal for our domain. The classification accuracy did not change in a noteworthy way after 50 epochs. Additionally, after 40 epochs the validation loss reached a plateau state and the decrease in the training loss was insignificant. Therefore, for the future experiments and epoch number 50 was set. As can be seen in the table below, the batch size of 64 resulted in the highest accuracy in both models.

	precision	recall	f1-score
0	0.96	0.91	0.93
1	0.92	0.96	0.94
accuracy			0.94
macro avg	0.94	0.94	0.94
weighted avg	0.94	0.94	0.94

Fig. 5 Performance Parameters of the best performing ResNet

TABLE 2 EXPERIMENTAL RESULTS

Batch Size	Accuracy ResNet	Accuracy VAEs
16	0.92	0.69
32	0.91	0.69
64	0.94	0.71
128	0.93	0.68

An attempt to further improve the classification performance of the VAEs was made by carrying out an additional experiment. The experiment included changing the loss function from 'binary_crossentropy' to 'mean_squared_error' and changing the learning rate parameter (0.001). Additionally, an early stopping was also adopted to prevent overfitting. However, the classification accuracy remained at 68.5% after the changes.

The results of our experiments demonstrated that ResNet achieved superior classification performance compared to VAEs in distinguishing real images from AI-generated images. ResNet achieved a maximum accuracy of 94% while VAEs achieved an accuracy of maximum 71%. The detailed performance metrics of the experiment yielding in the best performance can be in the Fig. 5 below. The difference in accuracy and efficiency suggests that ResNet, with its powerful feature extraction capabilities, is more effective for image authentication tasks on the CIFAKE dataset. Generative models such as VAEs and GANS take longer to train yet the VAEs in this domain yielded a lot lower performance. It is also important to note that the hyperparameter modifications have an impact on performance of both models. Fine-tuning these parameters improved the classification accuracy for both VAEs and ResNet, reinforcing the importance of hyperparameter tuning for optimizing model performance.

As mentioned earlier, VAEs are originally generative models however they can be used to classify real and synthetic images by trying to detect the anomalies within fake images. However, in the case of the CIFAKE dataset, the VAE model adopted had a significantly lower performance compared to the other model. The cause of it may be their generative and unsupervised learning nature, not having the same level of discriminative capacity as ResNet. Another reason for the poor performance may be its shallow architecture compared to the deep model of ResNet.

In summary, it is worth pointing out that the choice of model, training objective, dataset characteristics, and the task at hand all play crucial roles in determining the performance of a model. Overall, our findings highlight the efficacy of deep learning models, particularly ResNet, for image authentication tasks, emphasizing the necessity of tailoring hyperparameters to achieve optimal results.

V. CONCLUSION

This study put forward a comparative study on how to classify real and AI-generated images using deep learning. We employed two powerful deep learning architectures, Variational Autoencoders (VAEs) and Residual Networks (ResNet) and performed a comparative analysis using the CIFAKE dataset. VAEs are generative models, and they simulate real images and identify anomalies in AI-generated ones. ResNet are discriminative models, and they excel in feature extraction and are vital for distinguishing real from fake images. Both models used in the experiments were then optimized by changing batch sizes and training with different number of epochs.

Our experiments were facilitated within the Google Colab environment, providing us with the necessary computational resources, including GPU support. This allowed us to efficiently train and evaluate our models on a significant dataset. However, as mentioned earlier, the default GPUs provided by Google Colab were insufficient in several cases

during our experiments. We encountered challenges due to the sheer size of the dataset, necessitating adaptations in our approach to image loading and processing. These modifications were crucial in optimizing the training process and overcoming resource limitations.

The results of our study revealed intriguing insights into the capabilities of VAEs and ResNet in the domain of image authentication. ResNet model exhibited commendable performance, showcasing the potential of deep learning in distinguishing real images from their AI-generated counterparts. However, the classification performance of VAEs was far from ideal and due to their generative nature, VAEs demanded more computational resources to operate optimally. These findings emphasize that it is crucial to pick the optimal approach for specific image classification tasks.

In conclusion, this study contributes to the evolving field of image authentication by providing insights into the efficacy of deep learning models approaching the same problem differently (generative model and discriminative model). The insights gained from this study also underscore the need for careful consideration in selecting an appropriate architecture based on specific application requirements. Nevertheless, there exist promising avenues for future exploration and enhancement of this study. One way could be to extend the scope of fine-tuning the algorithms to improve the performance. However, it should be noted that, such task would require substantial computational resources beyond what Google Colab could provide in our case.

VI. REFERENCES

- [1] I. Goodfellow et al., “Generative adversarial networks,” *Commun. ACM*, vol. 63, no. 11, pp. 139–144, 2020.
- [2] R. Rombach, A. Blattmann, D. Lorenz, P. Esser, and B. Ommer, “High-Resolution Image Synthesis with Latent Diffusion Models,” *Proc. IEEE Comput. Soc. Conf. Comput. Vis. Pattern Recognit.*, vol. 2022–June, pp. 10674–10685, 2022.
- [3] T. Luhman and E. Luhman, “Diffusion models for Handwriting Generation,” pp. 1–17, 2020.
- [4] G. Ediboğlu Bartos, Y. Hoscan, A. Kauer, and É. Hajnal, “A Multilingual Handwritten Character Dataset: T-H-E Dataset,” *Acta Polytech. Hungarica J. Appl. Sci.*, vol. 17, no. 9, 2020.
- [5] M. Kim, F. Liu, A. Jain, and X. Liu, “DCFace: Synthetic Face Generation with Dual Condition Diffusion Model,” pp. 12715–12725, 2023.
- [6] K. He, X. Zhang, S. Ren, and J. Sun, “Deep residual learning for image recognition,” *Proc. IEEE Comput. Soc. Conf. Comput. Vis. Pattern Recognit.*, vol. 2016–Decem, pp. 770–778, 2016.
- [7] D. P. Kingma and M. Welling, “An introduction to variational autoencoders,” *Foundations and Trends in Machine Learning*, vol. 12, no. 4, pp. 307–392, 2019.
- [8] J. J. Bird and A. Lotfi, “CIFAKE: Image Classification and Explainable Identification of AI-Generated Synthetic Images,” 2023.
- [9] Y. LeCun, Y. Bengio, and G. Hinton, “Deep learning,” *Nat. Methods*, vol. 13, no. 1, p. 35, 2015.
- [10] M. Goebel, L. Nataraj, T. Nanjundaswamy, T. M. Mohammed, S. Chandrasekaran, and B. S. Manjunath, “Detection, attribution and localization of GAN generated images,” *IS T Int. Symp. Electron. Imaging Sci. Technol.*, vol. 2021, no. 4, 2021.
- [11] K. Simonyan and A. Zisserman, “Very Deep Convolutional Networks for Large-Scale Image Recognition,” in *International Conference on Learning Representations*, 2015, pp. 1–14.
- [12] C. Szegedy, V. Vanhoucke, S. Ioffe, J. Shlens, and Z. Wojna, “Rethinking the Inception Architecture for Computer Vision,” *Proc. IEEE Comput. Soc. Conf. Comput. Vis. Pattern Recognit.*, vol. 2016–Decem, pp. 2818–2826, 2016.
- [13] P. Dogoulis, G. Kordopatis-Zilos, I. Kompatsiaris, and S. Papadopoulos, Improving Synthetically Generated Image Detection in Cross-Concept Settings, vol. 1, no. 1. Association for Computing Machinery, 2023.
- [14] Z. Xi, W. Huang, K. Wei, W. Luo, and P. Zheng, “AI-Generated Image Detection using a Cross-Attention Enhanced Dual-Stream Network,” 2023.
- [15] Y. Yao, Z. Zhang, X. Ni, Z. Shen, L. Chen, and D. Xu, “CGNet: Detecting computer-generated images based on transfer learning with attention module,” *Signal Process. Image Commun.*, vol. 105, no. March, p. 116692, 2022.
- [16] M. Zhu et al., “GenImage: A Million-Scale Benchmark for Detecting AI-Generated Image,” 2023.
- [17] A. Krizhevsky, “Learning Multiple Layers of Features from Tiny Images,” 2009.
- [18] TensorFlow. 2023. “An Open-Source Machine Learning Framework for Everyone.” <https://www.tensorflow.org/>.
- [19] PyTorch. 2023. “An Open-Source Deep Learning Platform That Provides a Seamless Path from Research Prototyping to Production Deployment.” <https://pytorch.org/>.
- [20] Google. 2017. “What Is Colaboratory.” <https://colab.research.google.com/notebooks/intro.ipynb#recent=true>.
- [21] Goodfellow, Ian, Yoshua Bengio, and Aaron Courville. 2016. *Deep Learning*. MIT Press. <https://www.deeplearningbook.org/>.

LEGO robotics as educational tool

Péter Udvardy
 Alba Regia Technical Faculty
 Institute of Science and Software Technology
 Obuda University
 Szekesfehervar, Hungary
 udvardy.peter@amk.uni-obuda.hu

Abstract— LEGO robotics seems to be a good tool for educational purposes as it helps problem solving skills, enhance teamwork and increase creativity of students at different ages. Many years of experiences shows that from the primary school up to the University MSc level the same approach, but different difficulty level and complexity gives a good result in the learning process. The implementation of LEGO robotics sets in education helps not only knowledge sharing but the interest and motivation toward STEM and engineering.

Keywords— LEGO, robotics, education, STEM

I. LEGO ROBOTICS SINCE THE BEGINNINGS

LEGO factory produces construction toys since 1932 started with wooden toys and since 1947 plastic bricks were produced, too. Generally speaking, LEGO sets are for playing but there are special sets which are for educational purposes.

LEGO Mindstorms sets were released in 1998 and serve as a robotic educational tool for building and programming purposes. The robotic sets are based on the programmable brick developed at MIT’s laboratories which is the core of the LEGO robots with inputs, outputs and power capacity. The robotic sets were changed from time to time, but the core brick remained the same with minor changes. [1]

For nearly twenty years, LEGO has been producing building sets that include not only hardware but also software, in which the built model can be programmed and controlled. The first such set appeared in the late nineties and was called LEGO Mindstorms RCX (Robotic Command eXplorers). The brain of the set was the brick, which connected to the computers via an IR port. The brick contained 3 output and 3 input ports to which sensors and motors were connected. [2]

The LEGO Mindstorms NXT was released in 2006 and became a success not only as a programmable toy but in education as well. The set was available in two different versions, the retail version and the educational set which came out with optional LabVIEW software. The core of the robotic set remained the same, the ‘brick’ takes four separate inputs and control three different motors. The connection between the brick and the peripherals was via RJ12 cables (similar to RJ11 phone cable). The brick has a monochrome LCD display unit and works with a 32-bit ARM7TDMI core Atmel AT91SAM7S256 microcontroller with 256 KB of flash memory and 64 KB of RAM. Power source is supplied with six AA 1.5V batteries in the retail version and Li-ion batteries in the educational version.

The second version of the previous set called LEGO Mindstorms NXT 2.0 was released in 2009 and contained a new color sensor and its capabilities were improved. Developer kits are available for the set, hardware, software and Bluetooth developer kits contains detailed schematics for developers and the firmware of NXT is also open source.

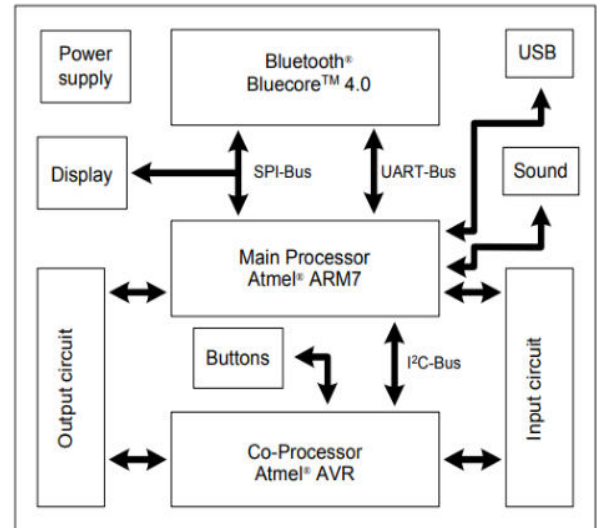


Fig. 1. Hardware block diagram of LEGO Mindstorms NXT [1]

There are three different ways for NXT programming. Simple programming possibilities are available through the monochrome 100x64 pixels LCD display. The software programming through a computer based on National Instruments LabVIEW and users can program by clicking on blocks and create connection between them or writing code lines. MATLAB is high-level programming language for computing and data analyses which can be used for LEGO Mindstorms NXT programming and controlling via serial Bluetooth connection or via USB. Free open-source NXT toolboxes are available. Simulink is a block diagram modelling and simulation environment which allows to create a controlling simulation environment for LEGO Mindstorms NXT.

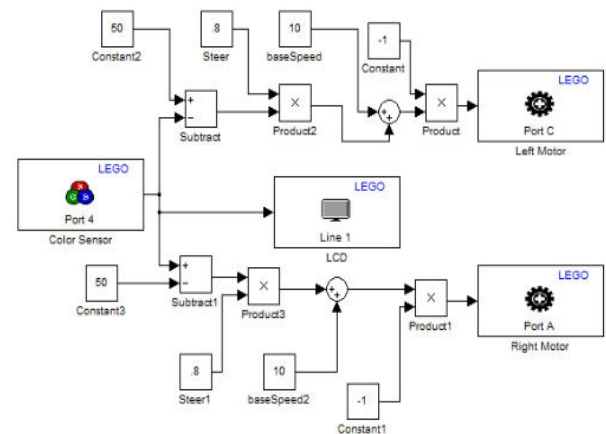


Fig. 2. Line follower EV3 robot controlled in Simulink [3]

The LEGO Mindstorms EV3 set were released in 2013 in original and in educational version. The core of the set was modified, and the ‘brick’ contains an ARM9 CPU with 16 MB of flash memory and 64 MB of RAM using Linux. The central unit contains an USB socket and an SD card slot. The sensors changed and instead of ultrasonic sensor an infrared sensor is available in the set beside the touch sensor and the color and light sensor. An infrared remote control also serves with a special beamer function which allows the robot’s infrared sensor to locate and approach the counterpart precisely. Gyro sensor is not in the set but can be bought separately.

Two different types of motors are in the set, large motors make great movements and medium motors help precise low speed motions. The main difference between the motors is not only the size but the motor axes are in different directions. There are many robots design beside the officially released robots and there are some notable one such as Rubic cube’s solving robots (i.e. CubeStormer, MindCuber).

LEGO Mindstorms NXT motors and sensors are compatible with the new LEGO Mindstorms EV3 series, the NXT brick can be programmed with EV3 software but EV3 can not be programmed with standard NXT software but there are 3rd party support for doing that. Programming the LEGO Mindstorms EV3 robot is like the previous NXT robot, on screen programming, block type programming and MicroPython programming are available. MATLAB also can be used for LEGO Mindstorms EV3 programming and controlling via USB, Bluetooth or Wi-Fi. Free open-source EV3 toolboxes are available, and Simulink also allows to create a controlling simulation environment for LEGO Mindstorms EV3.

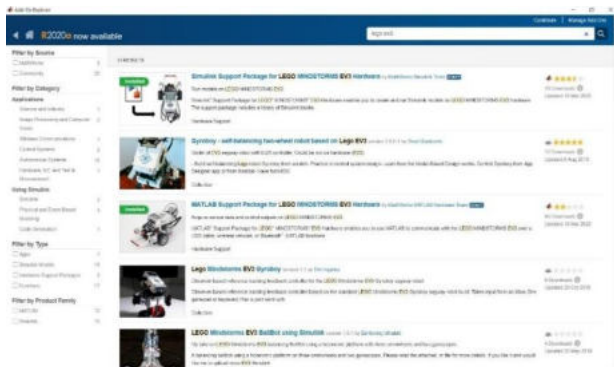


Fig. 3. LEGO Mindstorms EV3 add-ons in Matlab [2]

Mindstorms EV3 can be programmed with its own free software, the modules required for the sensors can also be downloaded from the LEGO website. The application is available for tablets/smartphones (<https://www.lego.com/hu-hu/mindstorms/apps/ev3-programmer-app>), and the software for computers (<https://www.lego.com/hu-hu/mindstorms/downloads/download-software>). Programming is icon-based and does not require any prior training. The icons must be aligned one after the other in the correct order, and then the operating parameters must be entered within each icon. The program is built by connecting the icons. In the EV3 help menu, there is a detailed description of setting the icon parameters. You can open a new project or access previous projects on the opening screen of the software. The usual elements are also available here, as well as five ‘factory’

projects, complete with description, construction guide, programming aid and demonstration. [2]

The Lego Mindstorms Inventor robotic set was launched in 2020 and have a different new approach to LEGO robotics. The set contains 949 pieces, twice as much as the former sets and the central piece of the set is the ‘Intelligent Hub’ which was shown first in Spike Prime LEGO set. The hub uses an STM32F413 microcontroller based on ARM Cortex-M4F core and has a built in six-axes gyroscope and an accelerometer. The hub can be accessed via Bluetooth or USB and has a 5x5 LED ‘display’ matrix for displaying graphics and animations. The built-in lithium-ion battery can be charged through USB connection.

Color sensor can be attached to the hub for measuring ambient light intensity and reflectance and to distinguish eight different colors. The distance sensor works as the eye of the robot by measuring and comparing distances. The four angular motors act not only as moving components of the robot but the built in rotation sensor makes the motors able to be sensors for positioning at the same time. Motors and sensors can be connected to all ports which also a new feature compared to the former releases.

The Lego Mindstorms Inventor robotic set has a dedicated software and mobile application where scratch-like drag and drop visual coding for beginners and python coding for advanced users are available. Many tutorials are reachable in the software which helps to learn programming.

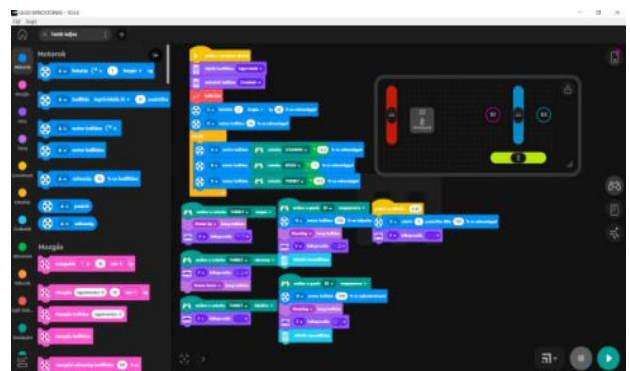


Fig. 4. LEGO Mindstorms Inventor software interface

The hub can remember multiple programs and run them autonomously or for direct controlling of the robot program streaming via Bluetooth can be the proper method where Play Station DualShock 4 controller, Microsoft Xbox controller or on-screen controllers can be applied. Test mode is not available in the software.

II. LEVELS AND APPROACHES

The LEGO Mindstorms EV3 mobile robot set contains all the elements that can be used to demonstrate the structure, main parts, and programming possibilities of robots at all levels of education. When compiling the material, the progress last from simple tasks (‘move the robot’) to more complex tasks requiring sensors and even multiple motors. [2] Experience shows that early technical and science education can result in greater engagement for robotics among students in the long term. [4] [5]

Different levels of education in elementary school needs more off-class approach in STEM teaching. Results show that

LEGO education programs enhance the motivation for mathematics and STEM related subjects between students and improve their knowledge level. [6]

For the primary and secondary school students who meet the robotics for the first time, the ‘doing by playing’ approach seems to be the most effective way to involve them in robotics and in science. The Alba Regia Technical Faculty has a long-time experience in robotics teaching for 8-18 years old student who participated in ‘Titkok Háza’ Scientific Experience Centre’s out of school extracurricular activities. The activities were carried out in 90 minutes education period.

LEGO Mindstorms EV3 sets are used for inquiry-based education for student with disabilities and the results show that students with mild or moderate disabilities enjoyed working with LEGO sets and seemed to be more effective in social skill and collaborative working areas. [7]

A LEGO Mindstorms EV3 (31313) programmable robotics set was available to perform the tasks. The purpose of the construction was to build a stable, simple basic robot that can be easily assembled at any time during education, even with minimal 'Lego' practice. Among the construction instructions on the official LEGO website, the basic structure of the TRACK3R robot seemed to be the right choice for this, since the massive basic frame can be built in 10 steps, by placing the bricks on it and only minimal additions are needed to ensure mobility.[2]

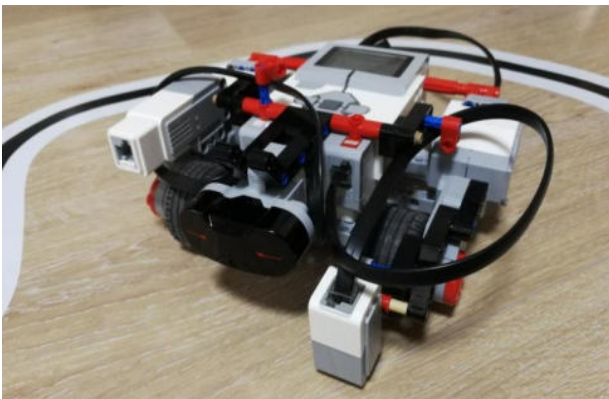


Fig. 5. The standard LEGO Mindstorms EV3 robot set

The first occasion was the introduction of the robotic set and the first movements of the robots. Building, programming, and experiencing seems to be the most fruitful way to fulfil the tasks. The LEGO Mindstorms EV3 robot was connected to the computer via Bluetooth and after the successful connection the robot properties are shown in the right corner of the software. Motor status, sensor measurements and connection type are monitored in the built-in software and the program can also started from this dialog box. The motors can act like sensors thus rotation data can also be used form programming purposes.

The next task is based on the previous experiences, but sensors also were used. For the first occasion infrared sensor were applied for obstacle avoidance purposes. This sensor can be used as a distance meter where it measures and compares proximity and makes the robot turning. There are two ways to use the sensor, in one the approach or distance is compared

with a predetermined value, while in the other case a given distance is measured.

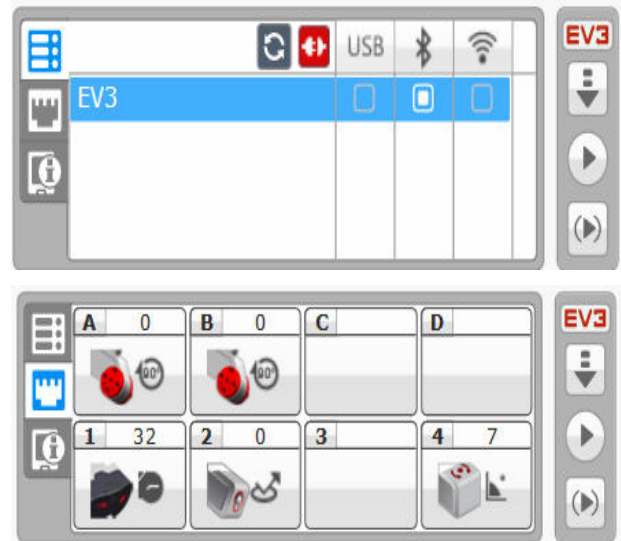


Fig. 6. Connection and port view of the EV3 set

The infrared sensor can also be used as the receiver part of the infrared transmitter (remote control) included in the kit, in which case the robot receives instructions or searches for the source of the infrared signal (beacon mode) and the degree of angular deviation from the signal source can also be set. The latter can be useful when performing more complex tasks, when, for example, the infrared remote control is part of a pallet, and the forklift uses the infrared sensor to locate the pallet and turn completely in front of it to lift it. [2]

Obstacle avoidance the infrared sensor is located at the front of the moving robot and at a certain distance the actuator intervenes and turns the robot into a different direction. On the graphical programming interface, a switch was put to the program and generally 20 centimeters of distance was set as a threshold value for turning movement.

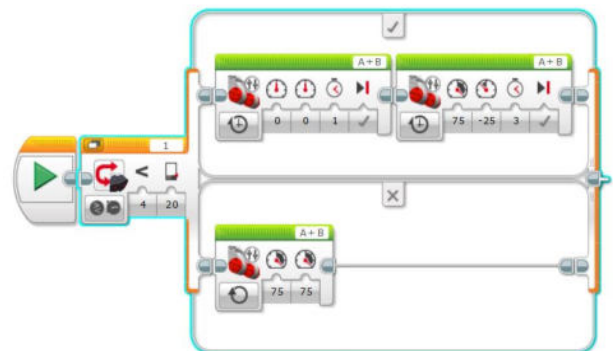


Fig. 7. Object avoidance programme

In the third task the same robot was used with different sensors for line tracking purposes. The color and ambient light sensor help to distinguish the white background from the dark line. For human beings to follow a line is an easy task as we look straight but the robot’s sensor looks downward and sees only the next 1 centimeter. Real life robots use additional sensors such as induction sensor, vision-based search, or laser scanners. The LEGO robot starts at the black line and detects the color changes during moving forward and corrects deviation from the right path which means white color

detection in practice. The robot's velocity determines the preciseness of the line following as the higher the speed the bigger the chance for leaving the right path. The execution of this task can be done from small turning corrections by using switches during programming up to mathematical operations, depending on the students' level of knowledge.



Fig. 8. Summer School for primary school students

There are many types of robotic activities carried out at Alba Regia Technical Faculty containing robotic programs. For the primary school students, a robotic summer school is held for one week where these students learn robot programming using LEGO Mindstorms EV3 sets and recently LEGO Mindstorms Inventor sets. Both LEGO is suitable for educational purposes and students have the occasion to compare these sets during the summer school.

The Bejczy Antal robotic contest is organized every year in online form via YouTube platform where the secondary school students create, build and program LEGO robots for different purposes. Ecological smart dustbin, daily clock, smart car and other special instruments were prepared, and the winners get precious prizes at the end of the school year.

For the University students a completely different approach seems to be effective. The prebuilt LEGO robotic sets can be programmed on graphical interface and by using codes. The aim of the LEGO set usage is not to open their mind toward STEM or engineering but to widen their existing knowledge and to show new ways, methods, and new possibilities for controlling the robots.

Through the LEGO Mindstorms sets based modular building and modular programming method students become active leaders of their own education in robotics and in informatics. LEGO robotics helps students to develop different solutions for the same problem and share their knowledge and skill to their community.[8]

As early as 1999, LEGO tools were used in teaching and according to those experiences, students included in the education program achieved better results in STEM education than their peers who did not use LEGO tools.[9]

For the students learning economics and management the basic programming methods and techniques are presented via LEGO robotics and the connection points to their profession are highlighted on BSc level. Moving the robot by basic programming surface, programming the line following robot and control the LEGO sets are effective methods to give an overview on robotics.

Students on MSc level have more experience with robotics including industrial robots, too. Their need for robotics is not to learn basic elements of programming and controlling robots

but to program robots that behave human-like and observe their interaction in a closed area. Multiagent robotics systems contains informatics and robotics with some artificial knowledge and the practical part of the subject is to build and to program a robot that works as a human behavior individual. [10]

III. SUMMARY

LEGO Mindstorms sets from RCX up to Inventor versions are available for primary and secondary school students and for universities for educational purposes. From the primary school level up to the higher educational level these sets seems to be a good and effective tool for robotics and programming education. In this paper the LEGO Mindstorms sets, the educational levels and approaches were introduced, and different programming tools were shown. Matlab and Simulink programming environment could be also a good solution beside the LEGO's 'native' drag-and-drop block type programming environment.

At the Óbuda University Alba Regia Technical Faculty these versatile LEGO sets are available at different educational levels. LEGO sets are in education in Bejczy Antal junior programming competition for the primary school students, Bejczy Antal LEGO programming contest for the secondary schools and Multiagent robotic systems on university level.

REFERENCES

- [1] lego.com
- [2] P. Udvardy: LEGO robotics at service of education In: Petóné Csuka Ildikó (szerk.) AIS 2022 - 17th International Symposium on Applied Informatics and Related Areas, Székesfehérvár: Óbudai Egyetem, pp 33-37 (2022)
- [3] mathworks.com
- [4] V. Chaudhary et al.: An Experience Report on Teaching Programming and Computational Thinking to Elementary Level Children Using Lego Robotics Education Kit 2016 IEEE Eighth International Conference on Technology for Education (T4E), Mumbai, 2016, pp. 38-41, doi: 10.1109/T4E.2016.016.
- [5] N. Montes et al.: A novel educational platform based on matlab/simulink/lego ev3 for teaching with robots, 2018. INTED2018 proceedings, pp. 975-980. ISSN: 2340-1079
- [6] B. Altakhayneh: The Impact of Using the LEGO Education Program on Mathematics Achievement of Different Levels of Elementary Students. European Journal of Educational Research, v9 n2 p603-610 2020
- [7] S. Disseler, G. Mirand: Students with Disabilities and LEGO Education Journal of Education and Human Development September 2017, Vol. 6, No. 3, pp. 38-52
- [8] E. Danahy et. al.: LEGO-based Robotics in Higher Education: 15 Years of Student Creativity. International Journal of Advanced Robotic Systems. 2014;11(2).
- [9] B. Erwin et al.: LEGO Engineer and RoboLab: Teaching Engineering with LabVIEW from Kindergarten to Graduate School. International Journal of Engineering Education Vol. 16, No. 3, pp. 181-192, 2000.
- [10] M. Seebauer, P. Udvardy: Collective Behavior Simulation of Mobile Robots Using Lego NXT Sets In: Orosz, Gábor (szerk.) AIS 2018 - 13th International Symposium on Applied Informatics and Related Areas Székesfehérvár, Magyarország : Óbudai Egyetem, Alba Regia Műszaki Kar (2018) pp. 122-125. , 4 p.

Information Support for Healthy Dietary

Todor Stoilov
*Institute of Information and
 Communication Technologies
 Bulgarian Academy of Sciences*
 Sofia, Bulgaria
todor.stoilov@iict.bas.bg

Éva Hajnal
*Alba Regia Technical Faculty
 Óbuda University*
 Székesfehérvár, Hungary
hajnal.eva@amk.uni-obuda.hu

Krasimira Stoilova
*Institute of Information and
 Communication Technologies
 Bulgarian Academy of Sciences*
 Sofia, Bulgaria
krasimira.stoilova@iict.bas.bg

Márta Seebauer
*Alba Regia Technical Faculty
 Óbuda University*
 Székesfehérvár, Hungary
seebauer.marta@amk.uni-obuda.hu

Abstract—The goal of this research is development of an information solution for health care related tasks. The information solution refers to the design of an optimization problem that is applied to estimate the content of foods that meets both energy and nutrient content recommended for a healthy diet. The information solution recommends an individual set of foods that corresponds to the content of products for men and women of different ages.

Keywords—information technologies, health care for nutrition, optimization of food ingredients

I. INTRODUCTION

The application of information technologies in the field of health care is growing rapidly. Health informatics is a combination of health information, data and knowledge. An overview for users of health informatics can be found in [1,13]. Applications of health informatics include protein structure prediction, genome annotation, comparative genomics, and health and drug discovery [2]. Information technology has its place in human lifestyle. Lifestyle tasks relate to improving diet, physical activity, obesity, smoking and alcohol use [3]. Information technology is applied to define healthy diets. High consumption of fat, sugar and salt, together with low consumption of fruits and vegetables, is the average cause of chronic diseases. Application of information technology tools can promote healthy eating [4,14]. A healthy diet takes into account healthy unsaturated fats, whole grains, fruits and vegetables [5]. Information technology solutions can optimally determine the content of foods for diets based mainly on health criteria.

Human nutrition is a function of food, which is a prerequisite for the successful treatment of diseases. A well-defined diet plays an important role in good health [6]. Healthy eating also affects psychology [7]. The success of the diet depends on the psychological acceptance of the recipient. This is a prerequisite for its successful implementation.

Information technology is entering the field of diet for its definition and evaluation. In [8] the artificial intelligence approach was applied to the definition of nutrition and definition of diet. An overview of the use of information technology solutions for dietetics is presented in [9]. Information technology is helping to develop new solutions for practicing dieting [10]. In [11] the potential of wireless networks, big data and artificial intelligence for application in the food industry is analyzed. Such an evaluation for mobile health applications was done in [12].

This paper does not claim to be relevant to nutrition and dieting. But we are trying to derive an information solution to recommend a healthy be selecting an appropriate food component. Healthy foods are selected according to optimization criteria and compliance with the restrictions recommended by the dietary requirements. Diet consists of defining and solving an optimization problem. Its solution is carried out in Excel environment, which is a prerequisite for using the developed information solutions due to the wide distribution of this software environment.

II. MATERIAL AND METHODS

A healthy diet depends on the content of the set of selected foods. In addition, the nutrient ratios of the food affect the inclusion of the respective food in a potential diet. For practical reasons, food costs play an important role in the inclusion of a predetermined food in the diet. These general considerations justify that the definition of the food portfolio for a diet can be formalized as an optimization problem. The solutions of this problem $\mathbf{X}=(X_1, \dots, X_n)$ will give the amount of foods $X_i, i = 1, \dots, n$, where n is the number of foods in the diet set.

The goal function of the optimization problem refers to a practical case of minimizing the diet costs. Formally, this is quantified by vector multiplication

$$\min_{\mathbf{X}} \mathbf{C}^T \mathbf{X}, \quad (1)$$

where $\mathbf{C}=(C_1, \dots, C_n)$ are the costs for each product under consideration.

Each product contains nutrients in the right ratio. For this study, the energy content of each food was taken as the nutritional component: proteins, fats and carbohydrates. The quantities of these components must meet the nutritional requirements of the particular diet. These requirements should be formalized as constraints on the optimization problem. These general considerations are applied to the derivation and implementation of an information solution for defining and solving an optimization problem for defining a diet.

III. INITIAL DATA FOR THE OPTIMIZATION PROBLEM

The data for this optimization problem is taken from available sources in the virtual environment. No specific and special data requests were used. Food types for 15 categories that are often present in people's daily food have been selected. For each food, 4 important characteristics are identified: energy content, proteins, fat and carbohydrates.

These features are taken from <http://r-media.org>. The data set collected is given in Table 1.

TABLE 1: INITIAL DATA FOR THE OPTIMIZATION PROBLEM

FOOD	PRICE, C [BGN]	CALORIES, L [CAL]	PROTEIN P [GR]	FAT F [GR]	CARBOHYDRATE H [GR]
BEAN	0.6	260	21.30	1.6	40
MILK	0.35	69	3.56	4.59	4.20
YOGURT	0.37	72.1	9.7	4.59	4.20
BUTTER	2.78	742	0	81.6	0
WHITE CHEESE	2.05	299	16.9	24.7	1.4
YELLOW CHEESE	2.42	381	25.8	23.6	1.6
PORK	1.22	219	18.8	157	0
CHICKEN	0.85	178	17.7	20.8	0
TOMATOS	0.35	18	2.86	0.39	3.63
CUCUMBERS	0.31	12	0.59	0.16	2.16
POTATOS	0.21	80	2	0.1	19
CARROTS	0.23	41	0.93	0.24	9.58
APPLE	0.34	52	0.26	0.17	13.81
ORANGE	0.28	55	1	0	11
BREAD	0.26	245	5.4	1.3	57

In addition, the prices of these 15 food products were taken from <http://foodprice.bg>, where they are monitored at the Regional and National level. Values for prices, calories, protein, fat and carbohydrates are calculated in [gr] per 100 gr of each food category.

A healthy diet requires these nutrients to be consumed in appropriate proportions. The ratios that are estimated are based on the recommendations for men, women and recommendations for protein, fat and carbohydrate matching.

Recommendations for the energy content of foods are taken from <http://spiritell.com>. A person's age has a strong influence on recommended energy levels. The levels applied in this study are summarized in Table 2.

TABLE 2: ENERGY RECOMMENDATIONS FOR FOODS

WOMEN		
AGE	31-50	+50
CALORIES	$b_1 = 2000$	$b_2 = 1800$
MEN		
AGE	31-50	+50
CALORIES	$b_3 = 2600$	$b_4 = 2400$

The healthy diet recommended by <http://zasporta.com> gives a different ratio between nutrients. A widely applied and recommended one is given in Table 3.

TABLE 3: CONTENT OF TWO APPLIED DIETS

	PROTEINS	FAT	CARBOHYDRATES
DIET	P=30%	F=30%	H=40%

These numerical data are applied as parameters to define an optimization problem that will give as a solution the amount of foods that are optimal for the selected diet with components according to Table 3.

IV. FORMAL DEFINITION OF THE OPTIMIZATION PROBLEM

The solution of the problem is denoted by $\mathbf{X}=(X_1, \dots, X_{15})$ and has 15 components corresponding to the selected set of foods given in Table 1. Since the input is normalized to 100 gr of food, the value $X_i, i = 1, \dots, 15$ will determine how much of 100 gr is produced as a solution for food i .

The goal function of the optimization problem is chosen according to (1) and has a linear form

$$\min_{X_1, \dots, X_{15}} \sum_{i=1}^{15} C_i X_i \quad (2)$$

The problem constraints should take into account the numerical requirements given in Table 2 and Table 3.

Energy requirements must accumulate to a level of calories defined in Table 2 and denoted by $b_j, j = 1, \dots, 4$. The optimization problem must be solved for each category of men and women according to their age. Formally, this constraint has the form

$$\sum_{i=1}^{15} L_i X_i = b_j, \quad (3)$$

where b_j takes the value from Table 2 for each optimization problem.

The constraints that should formalize the requirements of Table 3 are defined differently, since the values in Table 3 refer to the nutritional components, but they are not explicitly involved in the optimization problem. The solution of the optimization problem $\mathbf{X}=(X_1, \dots, X_{15})$ gives the food weights,

not the food component weights. The protein content of the problem solution will be given by the sum

$$p = \sum_{i=1}^{15} P_i X_i \quad (4)$$

Accordingly, the content of fats and carbohydrates in the allowed diet are

$$f = \sum_{i=1}^{15} F_i X_i \quad (5)$$

and

$$h = \sum_{i=1}^{15} H_i X_i \quad (6)$$

The requirements of Table 3 insist on equality in the values of (4) and (5), since protein and fat must have the same value of 30% in the total diet. Formally, this relationship is included in the optimization problem by equation

$$\sum_{i=1}^{15} P_i X_i - \sum_{i=1}^{15} F_i X_i = 0 \quad (7)$$

Table 3 gives a higher weight of carbohydrates with a value of 40% total, where proteins are 30%. This logical constraint gives numerically the ratio h=40/30, or

$$\sum_{i=1}^{15} 1.33H_i X_i - \sum_{i=1}^{15} P_i X_i = 0 \quad (8)$$

The optimization problem can take on additional constraints that come from practical considerations. In this study, the restrictions has been added that the total weight of the diet solution cannot be more than 2 kg, giving 20 sets of 100 grams. Formally, this restriction is analytic

$$\sum_{i=1}^{15} X_i = 20 \quad (9)$$

Another practical consideration is added by giving upper and lower food limits

$$0 \leq X_i \leq 4 \quad (10)$$

which means that no more than 400 g should be included from one meal. The chosen values in (9) and (10) can be modified for personal application of the optimization problem. Formally, the optimization problem contains an goal function (2) and a set of constraints with relations (3), (7), (8), (9) and (10). For a clear presentation, the analytical form of the optimization problem is as follows

$$\min_{X_1, \dots, X_{15}} \sum_{i=1}^{15} C_i X_i \quad (11)$$

$$\sum_i^{15} L_i X_i \leq b_j$$

$$\sum_{i=1}^{15} P_i X_i - \sum_{i=1}^{15} F_i X_i = 0$$

$$\sum_{i=1}^{15} 1.33H_i X_i - \sum_{i=1}^{15} P_i X_i = 0$$

$$\sum_{i=1}^{15} X_i = 20, \quad 0 \leq X_i \leq 4, i = 1, \dots, 15$$

The solution of problem (11) is illustrated in the EXCEL environment.

V. SOLUTION OF THE OPTIMIZATION PROBLEM IN THE EXCEL ENVIRONMENT

The initial data for the optimization problem are placed in positions as follows:

- the cost vector **C** takes cells B3 to P3 ;
- the calorie vector **L** is on cells B4 to P4;
- the protein concentration vector **P** is on cells B5 to P5;
- the fat concentration vector **F** is on cells B6 to P6;
- the carbohydrate concentration vector is on cells B7 to P7, Fig. 1.

Fig. 1. Basic programmingsheet of the optimization problem

The vector **X** for the solutions to the optimization problem is listed in cells B9 through P9.

The goal function (2) is calculated in cell B11 by the function =SUMPRODUCT(B3:P3;B9:P9). The latter evaluates the vector product of vectors **C** and **X**.

Cell B12 contains the vector product of calories **L** and **X** for the right side of constraint (3) using the function =SUMPRODUCT(B4:P4;B9:P9). Cell D12 gives the caloric values for men or women as defined in Table 2.

Cell B13 contains the vector multiplication for the protein contained in the diet (4) by the function =SUMPRODUCT(B5:P5;B9:P9). The corresponding fat concentration (5) is evaluated in cell D13 using the function =SUMPRODUCT(B6:P6;B9:P9). These two values are used for the definition of constraint (7).

Cell B14 evaluates the vector product 1.33**H**^T**X** using the function =1.33SUMPRODUCT(B5:P5;B9:P9). This estimate is needed for the left component of constraint (8). The right-hand component of (8) gives the vector product **P**^T**X** with the function =SUMPRODUCT(B7:P7;B9:P9).

Cell B15 contains the sum of constraint (9) from the =SUM(B9:P9) function.

The optimization problem is solved using the SOLVER function. This function needs additional programming to interface with the main screen in Fig.1. This is illustrated in Fig.2.

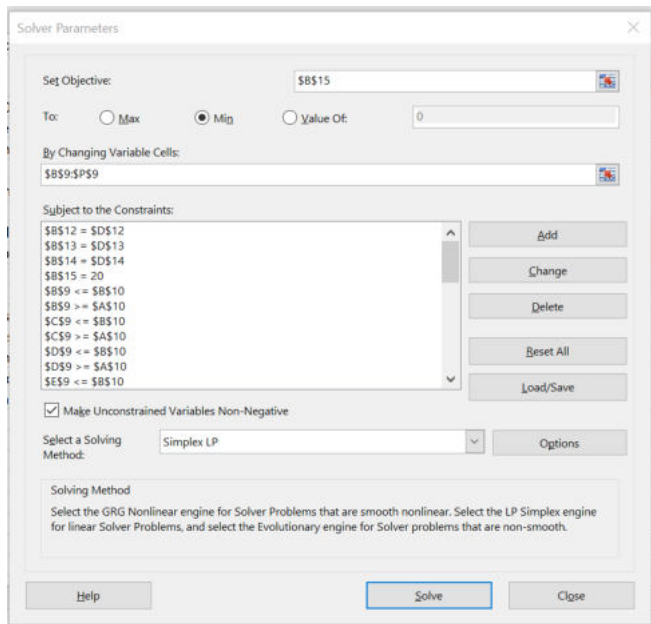


Fig. 2. Programming in SOLVER

The goal function of the optimization problem is evaluated in cell B15 and recorded as the *Set of Objectives* field. The SOLVER must find the minimum of the goal function. The solution set **X** is given in the box *By Changing Variable Cells* with B9:P9.

The constraint field contains the relations (3) and (7) through (10).

The ratio (3) for the caloric content is realized by the equality $B12=D12$.

Equation (7) insists on equalities between protein and fat concentrations and is realized by the equality $B13=D13$.

The ratio (8) is similarly realized by the equality $B14=D14$.

Relation (9) is implemented by requiring cell B15 to be equal to 20, $B15=20$.

The set of upper and lower bounds for the component of solutions $X_i, i = 1, \dots, 15$ is entered for each X_i . The lower bound value is taken from cell A10. In this case zero is selected. The upper bound is taken from cell B10, which is currently set to 4. For illustration, the value X_1 , which is in cell B9, must respect the constraints

$$B9 \leq B10 \text{ and } B9 \geq A10.$$

The upper and lower limits can change according to the type of diet chosen.

The optimization problem (11) is linear programming and the chosen *Solving method* is Simplex LP.

The problem is solved repeatedly with different energy requirement data from Table 2 for the male and female cases. The obtained results are preferably presented in graphical form.

VI. EXPERIMENTS AND RESULTS

The case of a diet for men determines that their caloric content for a day changes depending on age. For men aged 31 to 50, the calorie requirements are 2600 cal., but for age 50+ this value decreases to 2500 cal. according to Table 2. The solution to the optimization problem is given in Fig.3.

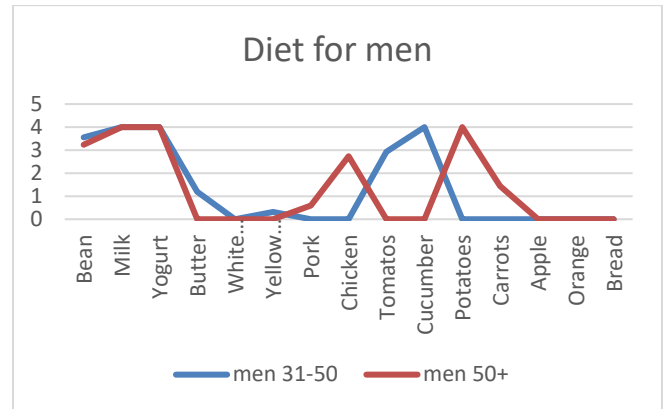


Fig. 3. Comparison of the diet for men

The graphical comparison shows that for younger ages the diet should contain more vegetables such as tomatoes and cucumbers.

The case of comparisons for women is illustrated in Fig.4.

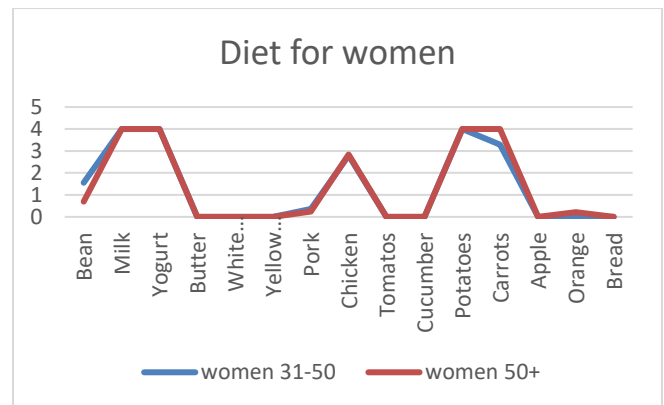


Fig. 4. Comparison of the diet for women

The results in this case are significantly different. It can be concluded that age does not affect the choice of foods for the diet. Both graphics for ages 31-50 and 50+ are pretty much the same.

The solutions of the optimization problems are compared for equal ages for both men and women. Figure 5 graphically illustrates the content of the diet for men and women for the aged 31-50 years. It is easy found that for younger aged men, the requirements are to consume more vegetables for the tomato and cucumber categories. The difference in women is that their diet increased with potatoes and carrots.

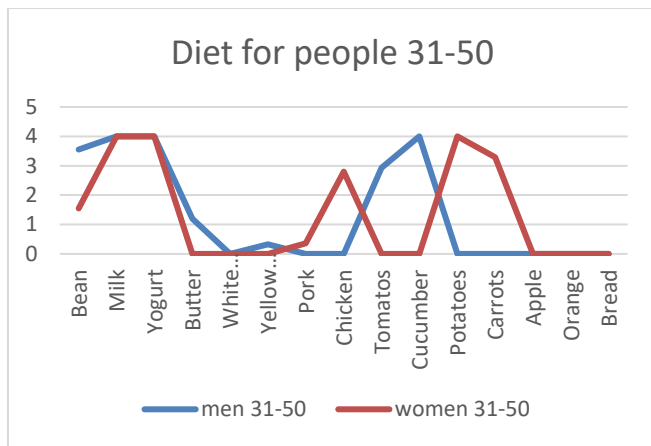


Fig.5 Comparison of diet for men and women aged 31-50 years

The same comparison is made for both men and women over the age of 50 in Fig.6. The results obtained give almost the same content of food for this age category.

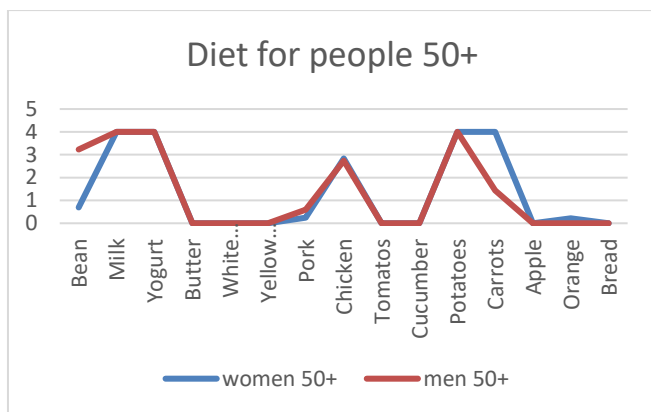


Fig.6 Diet comparison for men and women aged 50+

Finally, a comparison of the costs of diets for men and women in the two age categories is given in Fig.7. As a result, it is evident that the diet for men is more expensive compared to women.

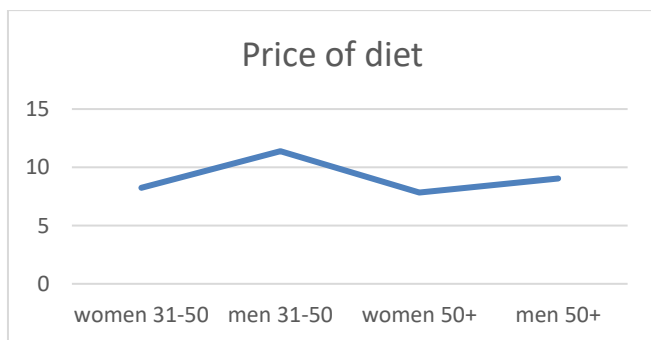


Fig.7 A comparison of the costs of diets for men and women

VII. CONCLUSIONS

This study introduces an optimization approach to determine diets by selecting a set of foods that can satisfy both energy needs and nutrient content. The advantage of using the

optimization approach is that the solutions obtained give both the type of foods for the diet and their amounts to be applied. This is an advantage for the combination of “which food with “how much” to use.

The paper illustrates a solution to formalize the optimization problem in widely distributed Excel software environment. This is a prerequisite for the potential application of the obtained model for other types of diets. The parameters of the optimization problem can be easily modified to meet additional or new requirements for the healthy diet process.

A potential extension of the optimization problem is to complicate it by generating a weekly or longer time horizon for the diet. The current horizon was chosen to be one day short. This is a simplistic assumption that can be complicated. A possible solution is by changing the available foods inputs to the optimization problem for each individual day of the diet.

Another possible solution is to expand the set of foods with many relatively closed types of foods and, after finding an optimization solution, extract the corresponding foods as input data for the next optimization solution. Thus, on different days, the set of foods as optimal solutions will be different. These are potential future opportunities to expand and further develop the optimization approach applied to healthy living.

ACKNOWLEDGMENT

This research is partly supported by project BG05M2OP001-2.016-0023 titled “Creation of a multi-educational environment for the development of personnel with integral competencies in the field of biomedicine and health care”.

REFERENCES

- [1] G. Demiris. Consumer Health Informatics: Past, Present, and Future of a Rapidly Evolving Domain, 2016, Yearbook of Medical Informatics 25(Suppl. 1) DOI: 10.15265/IYS-2016-s005 https://www.researchgate.net/publication/303391950_Consumer_Health_Informatics_Past_Present_and_Future_of_a_Rapidly_Evolving_Domain
- [2] M. Vinayak, P. Sudip, and J. Rachna. Bioinformatics for Healthcare Applications, 2019, pp. 204-207. 10.1109/AICAI.2019.8701277. https://www.researchgate.net/publication/332762073_Bioinformatics_for_Healthcare_Applications
- [3] A. Ashkan, D. Babalola, M. Mclean, Z. Yu, W. Ma, C. Y. Chen, M. Arabi, and D. Mozaffarian. “Information Technology and Lifestyle: A Systematic Evaluation of Internet and Mobile Interventions for Improving Diet, Physical Activity, Obesity, Tobacco, and Alcohol Use.” Journal of the American Heart Association: Cardiovascular and Cerebrovascular Disease, 2016, 5 (9): e003058. doi:10.1161/JAHA.115.003058. <http://dx.doi.org/10.1161/JAHA.115.003058>. <https://dash.harvard.edu/bitstream/handle/1/29408362/5079005.pdf>
- [4] J. Kaur, M. Kaur, V. Chakrapani, J. Webster, J. A. Santos, and R. Kumar. Effectiveness of information technology-enabled 'SMART Eating' health promotion intervention: A cluster randomized controlled trial. PLoS One. 2020 Jan 10;15(1): e0225892. doi: 10.1371/journal.pone.0225892. PMID: 31923189; PMCID: PMC6953835. <https://www.ncbi.nlm.nih.gov/pmc/articles/PMC6953835/>
- [5] P. Skerrett, and W. Willett. “Essentials of Healthy Eating: A Guide.” Journal of midwifery & women's health. Vol. 55, pp. 492-501, 2010, 10.1016/j.jmwh.2010.06.019. https://www.researchgate.net/publication/47543852_Essentials_of_Healthy_Eating_A_Guide

- [6] L. De, and T. De. Healthy food for healthy life. *Journal of Global Biosciences*. Vol.8., N9, pp. 6453-6468, 2019. https://www.researchgate.net/publication/336231128_HEALTHY_FOOD_FOR_HEALTHY_LIFE
- [7] D. Ridder, F. Kroese, C. Evers, M. Adriaanse, and M. Gillebaart, "Healthy diet: Health impact, prevalence, correlates, and interventions." *Psychology & Health*, Vol. 32, pp. 1-35, 2017. 10.1080/08870446.2017.1316849. https://www.researchgate.net/publication/316530587_Healthy_diet_Health_impact_prevalence_correlates_and_interventions
- [8] I. Ülker, and F. Ayyıldız. (2021). "Artificial Intelligence Applications in Nutrition and Dietetics." *Journal of Intelligent Systems with Applications* pp. 125-127, 2021. 10.54856/jiswa.202112175. https://www.researchgate.net/publication/357352908_Artificial_Intelligence_Applications_in_Nutrition_and_Dietetics
- [9] J. Ngo, A. Engelen, M. Molag, J. Roesle, P. García-Segovia, and L. Serra-Majem, "A review of the use of information and communication technologies for dietary assessment." *British Journal of Nutrition*, vol. 101(S2), pp. S102-S112, 2009. doi:10.1017/S0007114509990638 <https://www.cambridge.org/core/journals/british-journal-of-nutrition/article/review-of-the-use-of-information-and-communication-technologies-for-dietary-assessment/7BAA1713607E59E256804072D1645CDF>
- [10] L. Brennan, and B. McNulty. "New technology in nutrition research and practice." *Proceedings of the Nutrition Society*, vol.76(3), pp. 173-174, 2017. doi:10.1017/S0029665117001021 <https://www.cambridge.org/core/journals/proceedings-of-the-nutrition-society/article/new-technology-in-nutrition-research-and-practice/610C5AC07A933B58807A7873F5FF1C9E>
- [11] V. Raja, S. Krishnamoorthy, J.A. Moses, and C. Anandharamakrishnan. *ICT applications for the food industry*, Editor(s): Rajeev Bhat, Future Foods, Academic Press, 2022, pp. 613-626, ISBN 9780323910019, <https://doi.org/10.1016/B978-0-323-91001-9.00001-3>.
- [12] B. N. Limketkai, K. Mauldin, N. Manitus, L. Jalilian, and B. R. Salonen. The Age of Artificial Intelligence: Use of Digital Technology in Clinical Nutrition. *Curr Surg Rep* 9, 20, 2021. <https://doi.org/10.1007/s40137-021-00297-3>
- [13] M. Garai-Fodor and A. Popovics, "Changes in Food Consumption Patterns in Hungary, with Special Regard to Hungarian Food," *Acta Polytech. Hungarica*, vol. 19, no. 8, pp. 187–204, 2022.
- [14] M. Seebauer „Expert System for Optimization of Food Consumption in Intelligent Home” 9th IEEE International Symposium on Applied Machine Intelligence and Informatics, SAMI 2011, January 26-29, 2011, Smolenice, Slovakia - Piscataway (NJ),: IEEE, (2011) pp. 255-258. ISBN: 9781424474301

ORAL SESSION III.
Geodesy and Geoinformatics

Fusion of smartphone sensors to enhance positioning accuracy

Gábor Molnár

*Alba Regia Technical Faculty, Institute of Geoinformatics
Óbuda University
Székesfehérvár, Hungary
molnar.gabor@amk.uni-obuda.hu*

Benedek Marcell Kovács

*Alba Regia Technical Faculty, Institute of Geoinformatics
Óbuda University
Székesfehérvár, Hungary
benedek.kovacs@stud.uni-obuda.hu*

Abstract—In this article we present a sensor fusion algorithm to combine measured GPS and MEMS sensors' data of a smartphone to enhance the accuracy of position data.

For this purpose we processed the measured GPS trajectory together with the raw accelerometer, gyroscope and magnetometer measurements.

The developed Matlab code was a realization of the Kalman filter algorithm that estimated the position parameters (coordinates and attitude angles) of the smartphone for each timestamp.

Visualizing the covariance matrices with error ellipses proved that the updated trajectory was a better estimation of the actual trajectory than the GPS measurements alone.

Index Terms—Kalman filter, GPS, MEMS sensor, Dead reckoning

I. INTRODUCTION

In this paper we present the details of the sensor fusion algorithm, that merges the data measured by the smartphone's sensors and improve the accuracy of the device's trajectory.

During the processing and evaluating of the measurement, we are interested not only in the result of the measurement, but we are also interested, how accurate our measurement is, how much mean error (standard deviation) it has.

In our work, in addition to the inaccuracy of GPS-based telephone positioning, we also received a covariance matrix describing the accuracy of the location data obtained from the joint evaluation of the measurements of the usable sensors (accelerometer, gyroscope, magnetometer) and the error ellipse that can be formed from it. Knowing them will give us an idea of the improvement in accuracy. If these measurements can be used to improve accuracy, this could open up new application possibilities for phones.

Kalman-filtering was first used in practice in the Apollo program to optimize the navigation systems of spacecraft and lunar landers. In addition to navigation, it has been used for flight control for the 1960s. [1] Later the filter was further developed and used for system modeling and the creation of algebraic systems theory. The Kalman filter has outlived its namesake, as the algorithm is still used in airplanes, spacecraft, drones and other signal processing systems.

II. DATA

Smartphones have numerous sensors, and some of them can be used for obtaining the position and the orientation of the device:

Satellite Positioning Unit (commonly referred as GPS or GNSS receiver) provides location data in the form of WGS84 ellipsoidal coordinates. Typical sampling interval is 1Hz (one position measurement per second).

Accelerometer measures the acceleration of the device with a Micro-ElectroMechanical System (MEMS) sensor. The sensor has a charged microscopic moving part, that is kept in relative position to the device by a counteracting electrical field produced by charged electrodes. If the device is in rest, the electrical field counteracts the weight of the moving part. When the device start moving, the electrical field has to increase to accelerate the moving part, to keep its relative position to the device. From the charge on electrodes the forces and accelerations are calculated. The accelerations are stored as three vector components along the axes of phone's own (local) coordinate system. It is important to remark, that a device in rest measures approximately 9.81 m/s^2 acceleration due to the Earth's gravity field.

Magnetometer (magnetic field meter) measures the magnetic flux density, which is supposed to be mostly the Earth's magnetic field. The three measured vector components represent the magnetic field in the local coordinate system of the device. This measurement is supporting information for the spatial orientation of the device.

Gyroscope inherits its name from the spinning disk instruments, that are based on the theory of the conservation of angular momentum. Unlike its predecessors, smartphone gyroscopes are MEMS sensors, that technically contain several properly placed accelerometer MEMS sensors. As the centrifugal acceleration is a function of the angular velocity, from the small spatial variation of the measured accelerations, the angular velocity of the device's rotation is calculated. The measured angular velocities are the three components of the angular velocity vector, in the aforementioned local coordinate system, in radians per second.

Barometer measures the air pressure, and from the pressure, the height above sea level is calculated internally. The calculated absolute height above sea level varies with the meteorological conditions. However as the time variation of the meteorological conditions is significantly smaller than the sampling frequency of the barometer measurements, the barometers measurement very well support the relative height

variation of the device. This fact is significant, because the GNSS receiver can measure height only with large errors. In addition to these five measuring instruments listed, there are several others in the phone, but currently only the ones already mentioned above provide relevant data for positioning.

III. MEASURED DATA

The measurements were made in Székesfehérvár on *Hosszúsétető* Street. This site proved to be an optimal measurement environment in several respects. There was little traffic on the street and the bike lane on the side of the road was marked by a painted (approximately 10 cm wide) painted strip. The measured route consisted of three almost straight sections and two 90° turns. The elevation difference was negligibly small, so the change in the altitude coordinate was supposed to be 0 meters. There only one and two storey buildings along the road with front yard, so the GPS signal was not heavily disturbed by buildings.

The measurement was carried out with a *Xiaomi Redmi Note 9* phone, and *SensorData* application was responsible for storing sensor measurement data. For data collection the smartphone was attached to the handlebars of a bike, and during the ride the yellow paint strip (that separates the traffic lane from the bike lane) was followed. As this paint strip clearly seen on the high resolution orthophoto of the measurement site (Fig. 3 and 4) the measured and the calculated trajectory can be compared to the actual path.

IV. METHODS

A. Data preprocessing

The smartphone used in this experiment did not have barometer, so there were no accurate elevation data available for the calculations. For the trajectory estimation we only used the measured GPS coordinates, accelerometer data, and gyroscope measurement, stored in three separate UTF-8 coded ASCII files.

In the case of accelerometer and gyroscope measurements, the stored time data had erroneously repeated values. For the correction of these erroneous time data a linear regression correction function was calculated, and time values were corrected with interpolation, see Fig. 1.

As the sampling frequency of the GPS instrument was significantly less than the sampling frequency of the two other sensors, all measurements were resampled to the time values of the GPS measurements, see Fig. 2.

B. The Kalman filter

The Kalman filter algorithm calculates the states of a system for discrete time moments, considering both the previous state and the control inputs, and letting measurements to influence this calculated state.

The theory of the Kalman filter originates from the least squares adjustment used for estimating parameters (unknown values), so the output of the Kalman filter is from statistical point of view is an *estimation*.

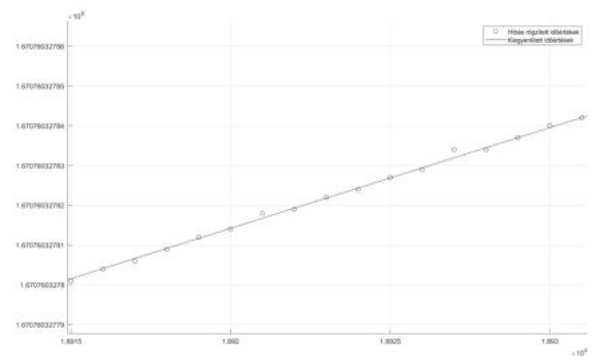


Fig. 1. Sequence number (horizontal axis) vs. time data (vertical axis). The stored time data of the accelerometer measurements have different and erroneous time increment values (circles) that were corrected using linear interpolation.

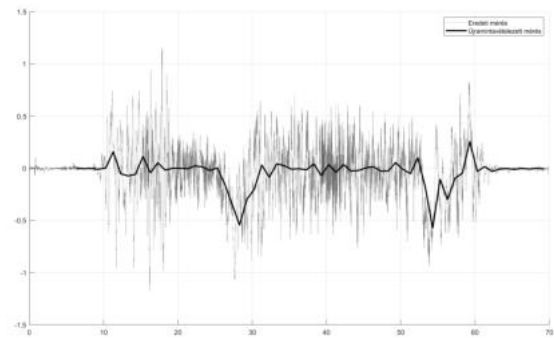


Fig. 2. Measured angular velocities around the (near-vertical) axis (dashed line) and interpolated angular velocity values for GPS recording times (solid thick line). The definite negative values at 27 and 54 seconds represent the two right-hand turns

The state of the system means a set of quantities, that (for the specific problem) properly represent the actual state of the system, e.g. coordinates, and velocities. State quantities are aligned in an array called *state vector*. The state vector for the k -th time moment is \mathbf{x}_k .

The Kalman filter consists of two main phases: **prediction** and **update**.

In the **prediction** phase, the filter calculates the state vector for k -th time moment from the state vector of the previous ($k-1$)-th moment:

$$\hat{\mathbf{x}}_{k|k-1} = \mathbf{F}_k \mathbf{x}_{k-1|k-1} + \mathbf{G}_k \mathbf{u}_k \quad (1)$$

where $\hat{\mathbf{x}}_{k|k-1}$ is the estimated state vector, \mathbf{F}_k is the state transition matrix, \mathbf{G}_k is the control-input matrix which is applied to the \mathbf{u}_k control vector.

Additionally, the estimated variance-covariance matrix of the state-transition is estimated by the formula:

$$\hat{\mathbf{P}}_{k|k-1} = \mathbf{F}_k \mathbf{P}_{k-1|k-1} \mathbf{F}_k^T + \mathbf{Q}_k \quad (2)$$

where $\mathbf{P}_{k-1|k-1}$ is the variance-covariance matrix of the state vector for $(k-1)$ -th moment, and \mathbf{Q}_k is the covariance matrix of the process noise.

In the **update** phase, we use observations, to refine the state vector of the system. In many cases, the state vector components are not directly observable, so from the predicted state vector one has to calculate such quantities, that can directly compared to the measurements.

The difference between the measured quantities and quantities calculated from the predicted states vector is as follows:

$$\tilde{\mathbf{y}}_k = \mathbf{z}_k - \mathbf{H}_k \hat{\mathbf{x}}_{k|k-1} \quad (3)$$

where $\tilde{\mathbf{y}}_k$ is the innovation (or measurement pre-fit residual) and \mathbf{z}_k contains our measurements arranged in a column vectors. The \mathbf{H}_k is the observation matrix, which maps the true state space into the observed space. Multiplying the \mathbf{H}_k by the preliminary (predicted) state vector $\hat{\mathbf{x}}_{k|k-1}$, we get a value, what we should have measured if the system would be error free.

The \mathbf{S}_k innovation covariance is calculated by

$$\mathbf{S}_k = \mathbf{H}_k \hat{\mathbf{P}}_{k|k-1} \mathbf{H}_k^T + \mathbf{R}_k \quad (4)$$

where \mathbf{R}_k is the covariance matrix of the observation noise.

To calculate the \mathbf{K}_k Kalman gain matrix, we use the previously calculated matrices:

$$\mathbf{K}_k = \hat{\mathbf{P}}_{k|k-1} \mathbf{H}_k^T \mathbf{S}_k^{-1} \quad (5)$$

The final step of the update phase is to determine the new state and its covariance. The updated state vector is

$$\mathbf{x}_{k|k} = \hat{\mathbf{x}}_{k|k-1} + \mathbf{K}_k \tilde{\mathbf{y}}_k \quad (6)$$

where we used the predicted state vector, and we modified it with the multiplication of Kalman matrix by innovation vector.

The covariance matrix of the updated state vector:

$$\mathbf{P}_{k|k} = (\mathbf{I} - \mathbf{K}_k \mathbf{H}_k) \hat{\mathbf{P}}_{k|k-1} \quad (7)$$

where \mathbf{I} is a unit matrix consisting of columns and rows equal to the number of state vector elements.

The newly obtained state can be compared with the observations:

$$\tilde{\mathbf{y}}_{k|k} = \mathbf{z}_k - \mathbf{H}_k \mathbf{x}_{k|k} \quad (8)$$

where the $\tilde{\mathbf{y}}_{k|k}$ vector is called *post-fit* residual. This value is not taken into account in further calculations.

At the end of this cycle, the steps are repeated for the next discrete time moment, the updated state vector and its covariance matrix of the previous step are used in the predict step of the new cycle.

C. Implementation of the Kalman filter

1) *State vector*: The state vector components are the essential quantities, that uniformly represent the state of a system. As the smartphone can regarded as a rigid body, its attitude (orientation), position and velocity are such quantities.

- Orientation quaternions (4 components): Unit quaternions are dimensionless quantities, that are commonly used

for formulation of attitude. Unit quaternions consist of four quantities: q_0, q_1, q_2, q_3 [2]. Other, more convenient formalism, like Euler angles are easier to comprehend and imagine, however singularities (gimbal lock) can occur during their usage. The usage of unit quaternions avoids this pitfall. From the quaternions the well known rotation matrix can be constructed, see bottom left corner of (12). This matrix is the attitude matrix, that convert any vector in the smartphone's local coordinate system to the global coordinate system (e.g. the Unified National Map Projection System of Hungary, EOV).

- Location data coordinates (3 components): Three coordinate values, measured in meters, in a global (EOV) coordinate system. Coordinate axes pointing towards the eastern, northern and local vertical at the given test site (East-North-Up, ENU system).
- Instantaneous velocity (3 component): Components of the velocity vector in global coordinates, expressed in m/s.
- Gravitational parameter (1 component): A constant 1 value, necessary to properly handle the acceleration caused by the Earth's gravity field.

Thus, the state vector consists of a total of 11 components:

$$\mathbf{x}_k = [q_0 \ q_1 \ q_2 \ q_3 \ X \ Y \ Z \ v_x \ v_y \ v_z \ 1]^T \quad (9)$$

2) *Predict Phase*: The predicted state vector is calculated using (1). For this, the actual form of the matrices \mathbf{F} (10), \mathbf{G} (12) and of control vector \mathbf{u} (11) are used.

The state-transition matrix \mathbf{F}_k , (10) determines the interdependence of components between two different temporal states. This matrix is formally constant in our case and can be written as follows:

$$\mathbf{F}_k = \begin{bmatrix} 1 & 0 & 0 & 0 & 0 & 0 & 0 & 0 & 0 & 0 & 0 \\ 0 & 1 & 0 & 0 & 0 & 0 & 0 & 0 & 0 & 0 & 0 \\ 0 & 0 & 1 & 0 & 0 & 0 & 0 & 0 & 0 & 0 & 0 \\ 0 & 0 & 0 & 1 & 0 & 0 & 0 & 0 & 0 & 0 & 0 \\ 0 & 0 & 0 & 0 & 1 & 0 & \Delta t & 0 & 0 & 0 & 0 \\ 0 & 0 & 0 & 0 & 0 & 1 & 0 & 0 & \Delta t & 0 & 0 \\ 0 & 0 & 0 & 0 & 0 & 0 & 1 & 0 & 0 & \Delta t & -g\Delta t^2 \\ 0 & 0 & 0 & 0 & 0 & 0 & 0 & 1 & 0 & 0 & 0 \\ 0 & 0 & 0 & 0 & 0 & 0 & 0 & 0 & 1 & 0 & 0 \\ 0 & 0 & 0 & 0 & 0 & 0 & 0 & 0 & 0 & 1 & -g\Delta t \\ 0 & 0 & 0 & 0 & 0 & 0 & 0 & 0 & 0 & 0 & 1 \end{bmatrix} \quad (10)$$

where Δt is the time increment in seconds between two moments of measurement time.

The control vector represents the external effects, that modify the state of the system. In the case of the smartphone, both the acceleration and the angular velocity is measured. The control vector consist of six elements:

$$\mathbf{u}_k = [a_x \ a_y \ a_z \ \omega_x \ \omega_y \ \omega_z]^T \quad (11)$$

The manner in which these measured data influence the elements of the next state vector is defined by the \mathbf{G}_k (12) matrix [3].

$$\mathbf{G}_k = \begin{bmatrix} 0 & 0 & 0 & \frac{\Delta t}{2} q_1 & \frac{\Delta t}{2} q_2 & \frac{\Delta t}{2} q_3 \\ 0 & 0 & 0 & \frac{\Delta t}{2} q_0 & \frac{\Delta t}{2} q_3 & -\frac{\Delta t}{2} q_2 \\ 0 & 0 & 0 & \frac{\Delta t}{2} q_3 & -\frac{\Delta t}{2} q_0 & -\frac{\Delta t}{2} q_1 \\ 0 & 0 & 0 & \frac{\Delta t}{2} q_2 & -\frac{\Delta t}{2} q_1 & \frac{\Delta t}{2} q_0 \\ \frac{\Delta t^2}{2}(q_0^2 + q_1^2 - q_2^2 - q_3^2) & \Delta t^2(q_1^2 q_2^2 - q_0^2 q_3^2) & \Delta t^2(q_1^2 q_3^2 + q_0^2 q_2^2) & 0 & 0 & 0 \\ \Delta t^2(q_2^2 q_1^2 + q_0^2 q_3^2) & \frac{\Delta t^2}{2}(q_0^2 - q_1^2 + q_2^2 - q_3^2) & \Delta t^2(q_2^2 q_3^2 - q_0^2 q_1^2) & 0 & 0 & 0 \\ \Delta t^2(q_3^2 q_1^2 + q_0^2 q_2^2) & \Delta t^2(q_3^2 q_2^2 + q_0^2 q_1^2) & \frac{\Delta t^2}{2}(q_0^2 - q_1^2 - q_2^2 + q_3^2) & 0 & 0 & 0 \\ \Delta t(q_0^2 + q_1^2 - q_2^2 - q_3^2) & \Delta t 2(q_1^2 q_2^2 - q_0^2 q_3^2) & \Delta t 2(q_1^2 q_3^2 + q_0^2 q_2^2) & 0 & 0 & 0 \\ \Delta t 2(q_2^2 q_1^2 + q_0^2 q_3^2) & \Delta t(q_0^2 - q_1^2 + q_2^2 - q_3^2) & \Delta t 2(q_2^2 q_3^2 - q_0^2 q_1^2) & 0 & 0 & 0 \\ \Delta t 2(q_3^2 q_1^2 + q_0^2 q_2^2) & \Delta t 2(q_3^2 q_2^2 + q_0^2 q_1^2) & \Delta t(q_0^2 - q_1^2 - q_2^2 + q_3^2) & 0 & 0 & 0 \\ 0 & 0 & 0 & 0 & 0 & 0 \end{bmatrix} \quad (12)$$

The control-input matrix \mathbf{G}_k (12) determines the influence of measurements (the control vector) on the state vector. This matrix converts the accelerations and angular velocities measured in the local coordinate frame of the device into the global coordinate system of the state vector, so the matrix elements represent rotation matrix components. As mentioned earlier, the rotation matrix elements are calculated from orientation quaternion elements. In our case the matrix consists of 6 columns and 11 rows [4] [5].

The \mathbf{Q}_k covariance matrix of the process noise used in (2) can be calculated from the variances of the control-input signal:

$$\mathbf{Q}_k = \mathbf{G}_k^T \mathbf{C}_k \mathbf{G}_k \quad (13)$$

where \mathbf{C}_k is a matrix constructed of the variances of the control-input accelerations and angular velocities :

$$\mathbf{C}_k = \begin{bmatrix} \sigma_{a_x}^2 & 0 & 0 & 0 & 0 & 0 \\ 0 & \sigma_{a_y}^2 & 0 & 0 & 0 & 0 \\ 0 & 0 & \sigma_{a_z}^2 & 0 & 0 & 0 \\ 0 & 0 & 0 & \sigma_{\omega_x}^2 & 0 & 0 \\ 0 & 0 & 0 & 0 & \sigma_{\omega_y}^2 & 0 \\ 0 & 0 & 0 & 0 & 0 & \sigma_{\omega_z}^2 \end{bmatrix} \quad (14)$$

These variances were calculated from the measured accelerations and angular velocities when the device was in rest in the first 5 seconds of the measurement.

3) *Update phase*: In the update phase, the measurements are compared with the predicted state. As in many cases, these two type of data can not be simply compared, so an \mathbf{H} matrix (15) transforms state vector component into the measurement space. In our case this matrix has three rows and 11 columns.

$$\mathbf{H}_k = \begin{bmatrix} 0 & 0 & 0 & 0 & 1 & 0 & 0 & 0 & 0 & 0 & 0 \\ 0 & 0 & 0 & 0 & 0 & 1 & 0 & 0 & 0 & 0 & 0 \\ 0 & 0 & 0 & 0 & 0 & 0 & 1 & 0 & 0 & 0 & 0 \end{bmatrix} \quad (15)$$

In our case we have only three measurements, the position coordinates measured by the GPS sensor:

$$\mathbf{z}_k = [X \quad Y \quad Z]^T \quad (16)$$

In the update phase the new state vector $\mathbf{x}_{k|k}$, and its covariance $\mathbf{P}_{k|k}$ are calculated using 3-7.



Fig. 3. Ortophoto of the experiment site, with the trajectory of measured GPS (white circles, dashed line) and the Kalman filter processed coordinates (black dots, dotted line). This site is the first turn, where the processed trajectory properly fits on the edge of the bike lane.

V. RESULT

The process presented in the previous section was repeated for each time moment of the GPS measurements (approximately for each second), so for each time moment the elements of the updated state vector were calculated.

The horizontal coordinates stored in the stated vector and the same coordinates measured by the device's GPS receiver are plotted on Fig. 5.

A detail of the route is visualized on Fig. 6. On this figure, both the measured GPS coordinates, and the calculated horizontal coordinates stored in the state vector are also plotted. For each calculated horizontal coordinate pair, the error ellipse is also plotted around the point. The error ellipses are representing a subset of (7) state vector covariance matrix (Fig 6).

Both right hand turn sections of the route are mapped on the high resolution ortophoto of the experiment site (Figs. 3 and 4). On these figures, both GPS measured coordinates and

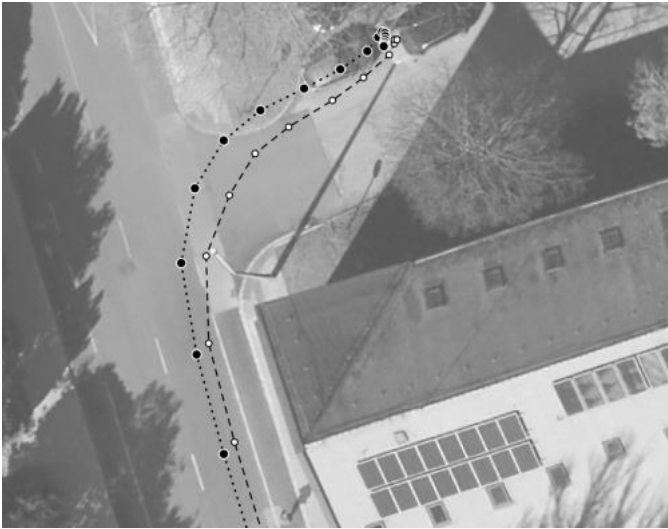


Fig. 4. Orthophoto of a detail of the experiment site, with the trajectory of measured GPS (white circles, dashed line) and the Kalman filter processed coordinates (black dots, dotted line). This site is the second turn, where the applied method could not improve the accuracy of the GPS measurements, because of the accumulated errors in orientation calculations.

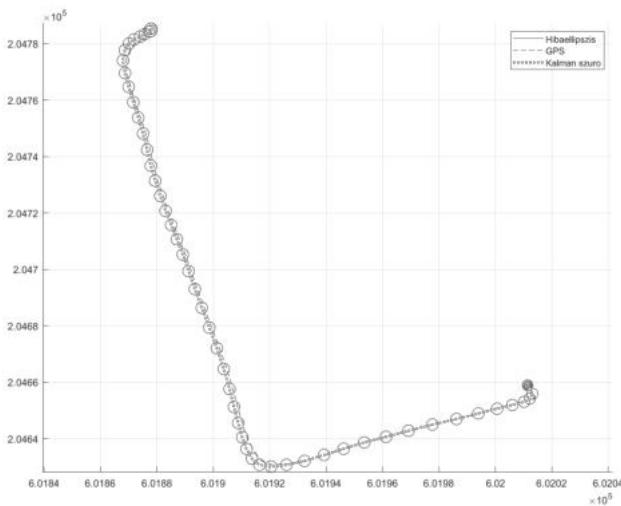


Fig. 5. Plot of horizontal coordinates of the smartphone's trajectory. The coordinates measured by GPS and the Kalman filtered coordinates slightly differ from each other. The plotted error ellipses are calculated for respective covariances of the calculated coordinates.

state vector horizontal coordinates are plotted, without error ellipses.

VI. DISCUSSION

On Fig. 5, the horizontal coordinates calculated by Kalman filter algorithm and stored in the state vector are representing the trajectory more accurately than the GPS measurements alone.

On Fig. 6 however the calculated coordinates are shifted from the measured GPS coordinates in erroneous (North-West) direction. This is the consequence of the errors in

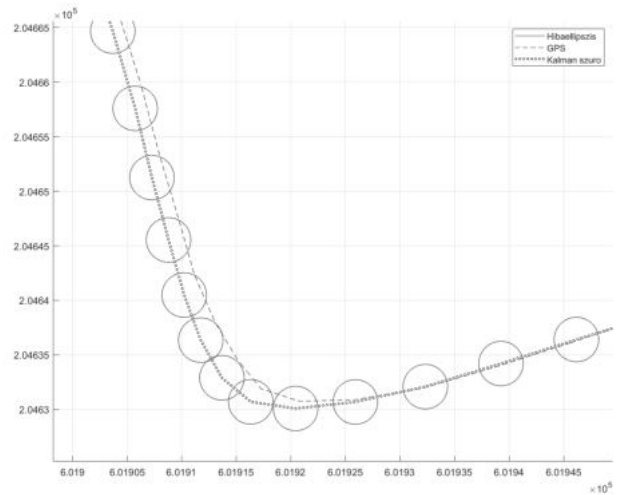


Fig. 6. Detail of the plot of smartphone's trajectory. Both measured GPS coordinates and Kalman filtered coordinates are plotted. Error ellipses of the calculated coordinates are nearly circular.

exterior orientation estimation. Small errors in angular velocity measurements has been accumulated in time integration of the prediction phase, and without using the magnetometer sensor data, there were no measurements to check or compensate this error.

An observable consequence of this phenomena, that the erroneous exterior orientation transforms the measured accelerations into wrong direction.

VII. CONCLUSION

Currently, the method works with post-processing, which means that the results are not obtained in real time.

The possible direction of continuation is the implementation of the program on the phone, where the measurements coming from the sensors could have been processed by an application in real time.

This would make it possible to have frequent location data between GPS measurements, which are more accurate than simple extrapolation of the movement measured by GPS.

REFERENCES

- [1] M. S. Grewal and A. P. Andrews, "Applications of kalman filtering in aerospace 1960 to the present [historical perspectives]," *IEEE Control Systems*, vol. 30, no. 3, pp. 69–78, Jun. 2010. DOI: 10.1109/mcs.2010.936465.
- [2] N. Liu, W. Qi, Z. Su, Q. Feng, and C. Yuan, "Research on gradient-descent extended kalman attitude estimation method for low-cost MARG," *Micromachines*, vol. 13, no. 8, p. 1283, Aug. 2022. DOI: 10.3390/mi13081283.
- [3] J. Wu, Z. Zhou, H. Fourati, and Y. Cheng, "A super fast attitude determination algorithm for consumer-level accelerometer and magnetometer," *IEEE Transactions on Consumer Electronics*, vol. 64, no. 3, pp. 375–381, Aug. 2018. DOI: 10.1109/tce.2018.2859625.

- [4] S. Sarabandi and F. Thomas, “Accurate computation of quaternions from rotation matrices,” in *Advances in Robot Kinematics 2018*, Springer International Publishing, Jun. 2018, pp. 39–46. DOI: 10.1007/978-3-319-93188-3_5.
- [5] B. K. P. Horn, “Closed-form solution of absolute orientation using unit quaternions,” *Journal of the Optical Society of America A*, vol. 4, no. 4, p. 629, Apr. 1987. DOI: 10.1364/josaa.4.000629.

Gross-error filtering of the tie points based on geometrical similarity in stereo image pair orientation

Attila Varga

Doctoral School of Applied Informatics and Applied Mathematics

Obuda University

Budapest, Hungary

vargaa@stud.uni-obuda.hu

Abstract—There are several steps in photogrammetric processing where measurements are needed. In photogrammetry, the orientation of stereopairs also requires measurement of tie points. During these measurements, errors are generated, among which particular attention must be paid to gross errors. In case of orientation based on automated image matching, the gross errors are mainly due to misalignment of the points. Such gross errors should be detected and filtered during the image matching process, in order to prevent the propagation of errors to further steps in the process.

Keywords—photogrammetry, gross error, image matching, MATLAB

I. INTRODUCTION

This paper addresses gross errors that occur during the orientation of stereopairs in automatic image matching of tie points and proposes a method to detect them. While gross error filtering in absolute orientation is extensively discussed in the literature, the detection and filtering of gross errors in the measurement of tie points during stereopair orientation is less researched. The most common gross error in automatic image alignment, which are nowadays widely used in photogrammetry, is the misidentification and mismatching of tie points. It is crucial to eliminate these errors during image matching to prevent their propagation to orientation parameters and point cloud generation. This paper investigates the potential of an error filtering procedure based on the geometric similarity of the distribution of tie points. To test this procedure, MATLAB software was used.

The need to detect and filter gross errors during image matching was inspired by a photogrammetric survey of an agricultural land. After the evaluation of photogrammetric process, the errors of resulted point cloud could be attributed to the poor quality of the tie points and ground control points (GCPs). This is due to the fact, that the texture of the images is too homogeneous, making the measurement and identification of tie points problematic. Either the processing software cannot identify points, or it incorrectly identifies tie points.

II. GROSS ERRORS IN THE PHOTOGRAMMETRY

As with all measurements, photogrammetric evaluation can be subject to gross errors. Gross errors are classified in several ways in the literature. [1] One possible classification of gross errors is the following [2]:

- *Very large gross errors* are gross errors that are mainly due to mistakes. This may be caused by misidentification of pixels or ground control points,

exchange of sequence of point numbers, or exchange of image coordinates.

- *Small gross errors*, mainly due to inaccurate orientation of pixels or incorrect measurement of ground control points.
- *Medium gross errors*, which are also due to incorrect measurement or orientation, ranging from small to large coarse errors.

In photogrammetry, measurements involve marking of common pixels, or the marking of pixels and ground control points. In photogrammetric processing, there are three steps where measurement plays a role, where measurement errors, including those caused by gross errors, could occur. These steps can be:

- *relative orientation* of stereopairs, where common tie points in the image pairs are measured,
- *absolute orientation*, utilizing measured ground control points to perform a similarity transformation between the model coordinate system and the geographic coordinate system,
- and *spatial reconstruction*, determining the spatial position of ground points corresponding to each pixel using oriented images (e.g. generating of point clouds).

In photogrammetric practice, residuals after alignment during absolute orientation provide an opportunity for gross error detection. For spatial similarity transformation, an overdetermined system of equations is iteratively solved using the method of least squares. The characteristics of least squares adjustment is that the gross errors are spread over the points. In such case, the examination of residuals (e.g. by rigorous statistical methods) can detect large gross errors, but may hide smaller gross errors.

Therefore, alternative methods should be employed to detect minor gross errors. One possibility is using the method of least squares with weight functions, or other alternative methods like the Jacobian criterion for smoothness. [3]

As illustrated above, there are several manual steps in traditional photogrammetric surveying and processing where gross errors can occur. With the increasing use of digital photogrammetry and automated photogrammetric processing software, the relevance of gross errors has diminished. However, there are still areas where manual surveying is essential. These include the measurement of ground control points, where the possibility of erroneous measurement and misidentification remains. Another significant source of

errors may be incorrect matching of identified points in the automatic orientation of stereopairs. This is because in automatic image matching, the procedures scan a smaller region around the detected points leading to incorrect identification. This paper focuses on the latter issue.

III. AUTOMATIC MEASUREMENT OF TIE POINTS

Modern photogrammetric software automatically measures tie points for the orientation of stereopairs. This capability has been facilitated by spread of digital photogrammetry and advancements in digital image processing.

The two major methods of point detection in digital image processing are area-based and object-based point detection. Of course, there are other, more complex methods, but these two methods are the most widely used in practical applications.

Area-based image matching involves examining region of pixels with high or low intensity in a digital image converted to grayscale where a search mask is used to find similar regions in the other image. [4]

Object-based image matching is also common in digital image processing. In this method, a characteristic corner point is searched by corner detector algorithm. Corner points are well-defined feature points of the image. Unlike the area (region) of the image being investigated, the corner point is invariant to shift, rotation and magnification, and is therefore less sensitive to differences between images.

One such technique is the Harris corner detector based on the intensity difference between neighboring pixels in the X and Y directions of the image plain. [5] By analyzing intensity differences in matrix form and calculating the eigenvalues of the resulting matrix, a kind of "sparsity" parameter is obtained. Where the two eigenvalues are sufficiently large, a corner point is found in the image. Having done the corner point assignment on both images of the stereopair, the next step is to find the corner points that belong together. This involves looking at the intensities of the pixels in the region around the corner points and their distribution. A descriptor is constructed for the distribution of pixel intensities and the point identification is based on a comparison of these descriptors. The descriptor for rotation is also invariant. An example of such an image matching procedure using the steps described above is SIFT (scale-invariant feature transform) method. [6]

IV. GROSS ERRORS IN AUTOMATIC IMAGE MATCHING

One of the challenges in automated photogrammetric processing is that there are parts of the image that are so homogeneous that the image matching algorithm may struggle to identify a corner point. On the other hand, when a corner point is available, the descriptors may be so similar that a mismatch occurs. The latter, if not filtered out, this mismatch can cause a gross error in orientation.

The gross errors resulting from misidentification of tie points were produced by practical measurements using the SURF image matching method, which is an improved version of the SIFT method. To do this, functions available in MATLAB's Image Processing and Computer Vision package were used, which are also available integrated into the Registrator Estimator application. There is also a possibility to set several parameters. Sensitivity of the corner detector

(effectively the threshold of the corner parameter), as well as the similarity threshold of the descriptors describing the environment of the points can be set. During image matching, the MATLAB functions return an array of detected points with their pixel coordinates, and an array of paired points with their identification numbers. In addition, the orientation parameters between the two images can be computed using the *Image registrator* function. [7]

Images used to generate the tie points were taken in an agricultural area, where the surveyed area also includes a small industrial section (the surface facilities of a natural gas well) using DJI Mavic Pro UAVs at an altitude of 120 m. These images were captured ensuring regular photogrammetric surveying flight along regular lines. The overlap between the images was 70% in every strip. (Figure 1.)

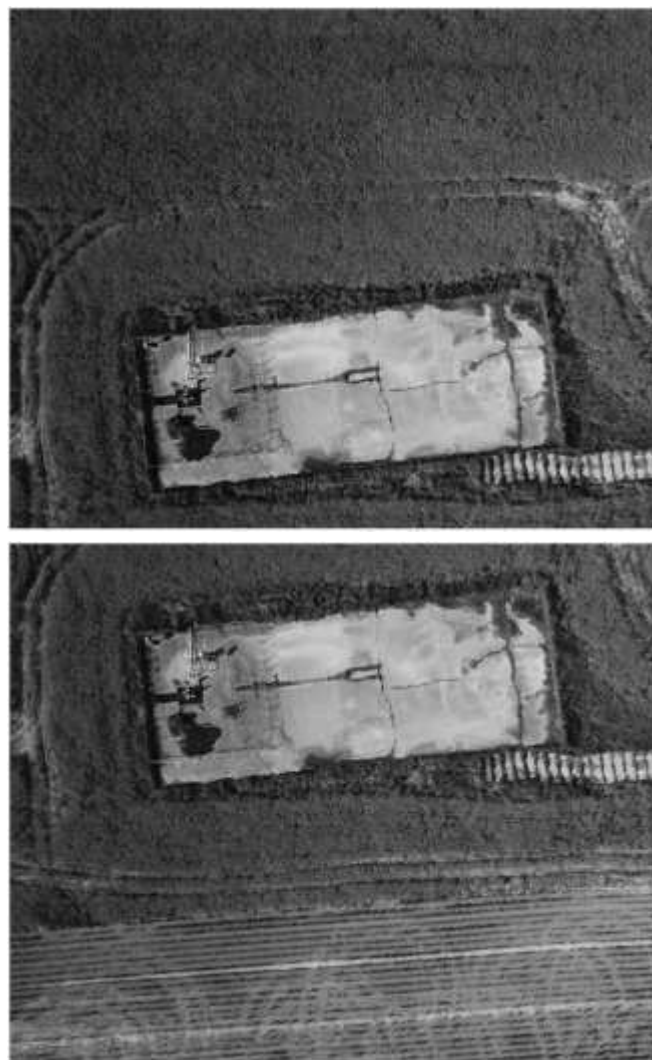


Figure 1. Two aerial photos used for automatic image registration.

The resulted images displayed gross errors after automatic image matching. The amount of these errors depends, of course, on the parameters of the image matching procedure. In our case, large gross errors can be clearly identified visually. (See Figure 3.) Since there is only an offset between the two images (and possibly an insignificant rotation), the lines connecting tie points of two the images are nearly parallel, while the lines connecting the misidentified points are crossing each other under different angles. The task is

therefore to deal with this visually perceptible error by mathematical means.

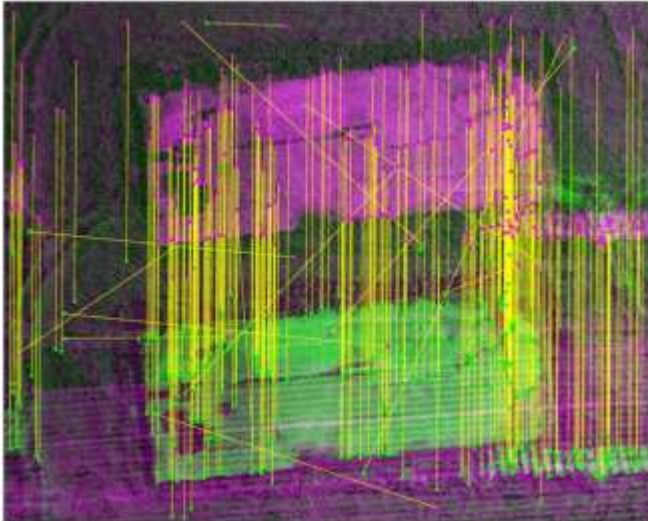


Figure 2. The stereopair is illustrated together with the identified tie points. 293 tie points were identified, among them 11 are wrong.

V. ERROR FILTERING BASED ON GEOMETRIC SIMILARITY OF POINT DISTRIBUTION

While in the absolute orientation, the gross error detection is based on the examination of residuals, produced by overdetermination of the system, the gross error filtering in the relative orientation of a stereopair requires a different approach, since it is a matter of examining the point on a pair of two-dimensional images.

The procedure is based on the assumption that the spatial distribution of identical points (i.e. the tie points) marked on different images is similar. However, to handle this mathematically, the distortion caused by the image projection has to be treated. Such distortion can be caused by a different center of projection, the relationship between the surface and the image plane in two images, but it can also be caused by changes in the flight altitude, although this may not be so significant in images with large overlap. In addition, the direction of flight may cause also changes in stereopairs, so that a rotation may occur between the plane of two images. Mathematically, these factors can be calculated by similarity transformation: offsets, rotations, scale and distortion, which need to be corrected for comparability. In addition, to examine the tie points in the same system, a reference system must be defined for the position of each point.

To ensure the above conditions, a preliminary relative orientation should be carried out. This procedure gives the relative positions of images of a stereo image pair relatively to each other. As a result, we can describe the coordinate system of one image in relation to the other one. This also means that we can eliminate distortions in the tie point distribution in every image. The centroid of the point distribution sketch, as it is used frequently in geostatistics, was chosen as fixed reference point, which is clearly characteristic for the point distribution.

In this system each tie point i is characterized by its position vector with two parameters: the vector length (l) and angle (ω) (Figure 3.).

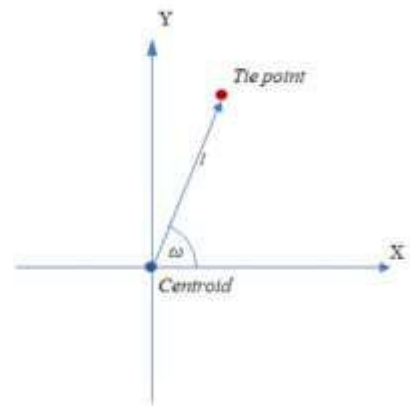


Figure 3. Parameters (polar coordinates) describing tie points: length (l) and angle (ω) of position vector.

To describe the distribution of tie points these position vectors are used. To detect and filter gross errors at the tie points, we have to analyze these system of vectors. There are two ways for analysis: calculation and comparison of vector length, and the difference of angles between position vectors. If there is a gross error at a point, then the difference of length of the position vectors, or the angle between the vectors of the related tie points could be significant. (Figure 4.)

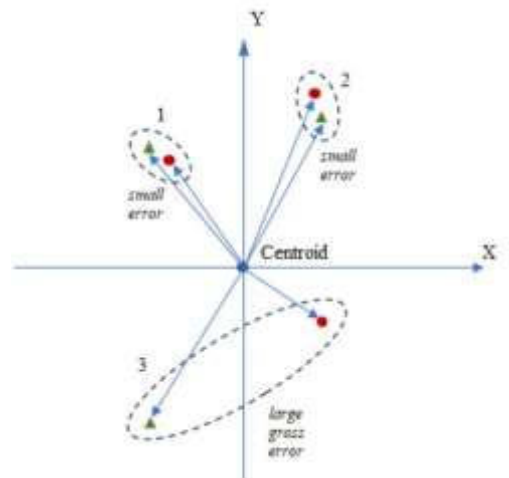


Figure 4. Position vectors as the descriptors of the tie point distribution. Corresponding ties points No. 1. and 2. have small error, tie points No. 3. has large gross error.

Given two images of a stereopair, with the tie points resulted by automatic image matching, and the tie points are also matched to each other. The filtering procedure is as follows:

1) Phase I

- A preliminary orientation is performed with randomly selected tie points on the stereo image pair. The resulting orientation parameters are used to perform image correction to compare the distribution of tie points. This is provided by the orientation elements (rotation angles) obtained during the orientation. (As a simplification, the scale factor is not considered in this case because the flight altitude was the same.) For orientation, we use randomly selected tie point.
- In both images, we calculate the centroid of the tie points. Here we move the origin of our coordinate

system to the centroid for further investigation. The two coordinate systems are rotated to overlap with the angle of rotation of the image planes obtained from the orientation parameters.

- We calculate the difference in the direction angles of the position vectors of the merging points. Large angular differences are filtered out and these points (i.e. very large gross errors) are excluded from the subsequent analysis. In case of incorrect point identification, the angular difference between the position vectors of two points is so large that we can work with thresholds up to 5-10 degrees. This is also justified by the fact that a point with gross error may be used for a preliminary orientation.
- After excluding very large gross errors, another preliminary orientation is performed. The previous step ensures that large gross errors are no longer included in the group of tie points used for orientation. With the resulting orientation data, a new image correction is performed.

2) Phase II

- In the second phase, the difference in length between position vectors is calculated, i.e. the error in points is determined in the common coordinate system.
- For the final orientation, we select the tie points with the smallest errors.

CONCLUSIONS

In the first step of the multi-step procedure, very large gross errors are excluded by examining the angular differences between the position vectors bound to tie points on the stereo image pair. In the second step, the difference in the length of the position vectors is investigated using tie points, which are already free of gross errors after a new orientation. As a last step, a final orientation is performed using tie points with the smallest errors.

The advantage of this procedure is that all the nodes are examined. Gross errors can be detected with a high degree of confidence, even if faulty tie points have been used for the preliminary orientation.

An iterative solution is also possible in the second phase. The change in the recalculated centroid position after the exclusion of the faulty point pairs should be examined. After each iteration step, we always exclude points with significant

big errors, by this way we can redefine the centroid by changing its position to a smaller and smaller extent. The change below a given threshold, the solution is considered to be final and the final orientation is performed with the centroid having the smallest error.

However, repeated orientation is computationally a time-consuming process, especially when using an iterative solution. Therefore, it would be useful to develop the procedure further using a different mathematical approach in such a way that no prior orientation is required.

Furthermore, it is envisaged that the procedure could be adapted to absolute orientation and gross error filtering prior to point cloud generation. The other way for development would be to move the procedure on fuzzy logic instead of using simple thresholds for filtering.

ACKNOWLEDGMENT

The paper was supported by the Bilateral Chinese-Hungarian Project No. 2019-2.1.11-TÉT-2020-00171 with the project title of "Investigation of the characteristics of surface shapes in rural environment based on point clouds and remote sensing data".

REFERENCES

- [1] F. S: El-Hakim, H. Ziemann: Step-by-step Strategy for Gross Error Detection, in. Photogrammetric Engineering and Remote Sensing, Vol. 50., No. 6, June 1984, pp. 713-718.
- [2] Jancsó Tamás: Nemlineáris modellek fotogrammetriai alkalmazása a geokörnyezettudományban (Photogrammetric applications of nonlinear models in geoenvironmental science), PhD thesis, Nyugat-Magyarországi Egyetem, 2006., pp. 61-91.
- [3] Jancsó Tamás: Durva hibák szűrése térbeli hasonlósági transzformációval (Filtering gross errors with spatial similarity transformation), in: Geomatikai Közlemények, XII, 2009.
- [4] Rafael C. Gonzalez: Digital Image Processing, Pearson Education, Inc., Upper Side River, 2008, ISBN 978-0-13-168728-8
- [5] C. Harris, M. Stephens: A Combined Corner and Edge Detector, in: Proceedings of the Alvey Vision Conference, Alvey Vision Club, 1988, pp. 23.1-23.6, URL: <https://www.bmva.org/bmvc/1988/avc-88-023.html>
- [6] Faraj Alhwarin: Fast and Robust Image Feature Matching Methods for Computer Vision Applications, University of Bremen, 2011, URL: <https://d-nb.info/1071842021/34>
- [7] Register Images Using Registration Estimator App, Matlab.com, URL: <https://www.mathworks.com/help/images/register-images-using-the-registration-estimator-app.html>

Calculation of the Volume of a Corn Field Based on UAV Images

Tamas Jancso
Alba Regia Technical Faculty
Institute of Geoinformatics
Obuda University
Szekesfehervar, Hungary
jancso.tamas@amk.uni-obuda.hu

Attila Varga
Doctoral School of Applied Informatics
and Applied Mathematics
Obuda University
Szekesfehervar, Hungary
vargaa@stud.uni-obuda.hu

Abstract—UAV technology provides the opportunity to carry out aerial surveys of small agricultural areas at regular intervals. With this method, it is possible to continuously monitor the growth rate of crops, and to make possible areas of erosion visible in the area. In addition, the 3D model of the area can be generated by automatic point cloud generation. The 3D models made on the basis of point clouds can be extracted from each other, so the volume of the vegetation can be calculated, on the basis of which further calculations can be made (e.g. yield estimation). This article presents the volume calculation process through a small sample project.

Keywords— UAV surveying, 3D modelling, environmental analysis, point cloud

I. INTRODUCTION

The use of UAV in damage assessment of cornfields is a frequently used method [1]. In this project, we have undertaken to calculate the volume of the corn land in addition to the damage assessment, which can help later in the crop estimation. In this project the main tasks were:

- | Taking aerial photos at three different times,
- | Block adjustment,
- | Generate point clouds,
- | Producing orthophotos,
- | Producing point cloud differences,
- | Mapping of erosion areas,
- | Calculation of volumes to determine the amount of corn.

To have exact 3D models, we needed enough number of high-precision, well-arranged ground control points (GCPs). These UAV survey parameters are summarized in Table I.

TABLE I. UAV SURVEY PARAMETERS

Date	Number of Photos	Avg. Flight Height [m]	Ground Resolution [cm]
2003.05.01.	134	304.1	3.58
2023.06.17.	199	292.9	3.08
2023.08.15.	95	287.8	3.34

We needed control points in the corners of the block.

The points must be clearly visible. Fig. 1 shows the location and the distribution of control points inside the triangulation block.

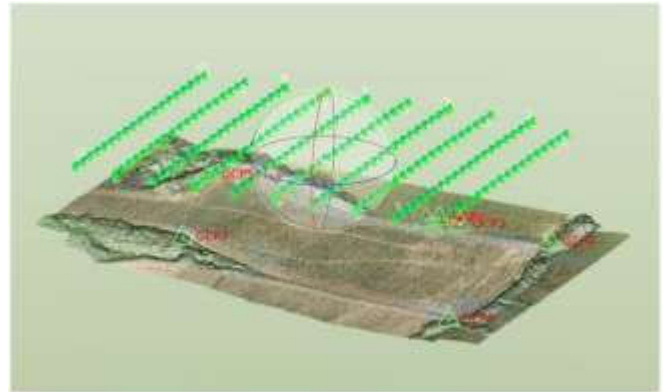


Fig. 1. Test field with control points

Every point was marked with a distinctive color as it is shown in Fig. 2.



Fig. 2. Ground control point marker

The block adjustment was carried out in Trimble UASMaster software. As a result, we got the sigma naught values for the whole block, the standard deviation of exterior orientation elements (Fig. 3), the mean standard deviations of horizontal and vertical coordinates, and the RMS (Root mean square) errors of GCP points. Table II. summarizes the gained accuracy results.

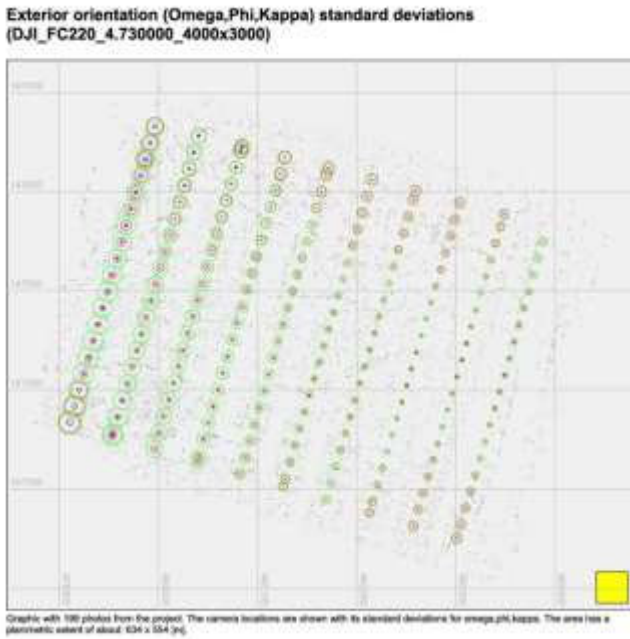


Fig. 3. Exterior orientation standard values

In Table II, we can see that the height errors became quite large compared to the field resolution of the images of around 3 cm.

TABLE II. ACCURACY VALUES

Date	Sigma naught [pixel]	Mean standard deviation of Height [m]	GCP RMS error [mm]
2003.05.01.	1.0521	0.2822	0.0040
2023.06.17.	1.1803	0.2964	0.0045
2023.08.15.	1.0828	0.4329	0.0016

There are several reasons for this larger height error. One of these factors can be the base ratio (ratio of flight height to recording base) that is too high. The usual value of this is 4 at most [3], in our case this value is around 24. This means that the intersection angle for the projection radii of the connected points is too small and far from the ideal 90 degrees. The steeper this intersection angle is, the greater the height error will be. Another reason may be that the automatic determination of the tie points is more uncertain than usual due to the nature of the surface, i.e. the surface is discontinuous and shows an irregular, undulating microtopography, such as the covering surface of the corn field in our case.

II. BUILDING OF 3D MODELS

A. Terrain model – 2023.05.01.

The first survey shows the surface without vegetation. The terrain model was created automatically using an autocorrelation process. The completed 3D model shows small ditches and protrusions, but the surface is basically continuous. There are faint signs of soil erosion in the center of the model (Fig. 4 and 5).

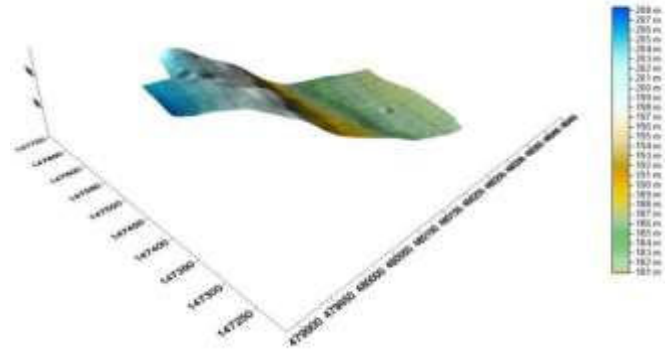


Fig. 4. Colored surface model (date: 2023.05.01.)

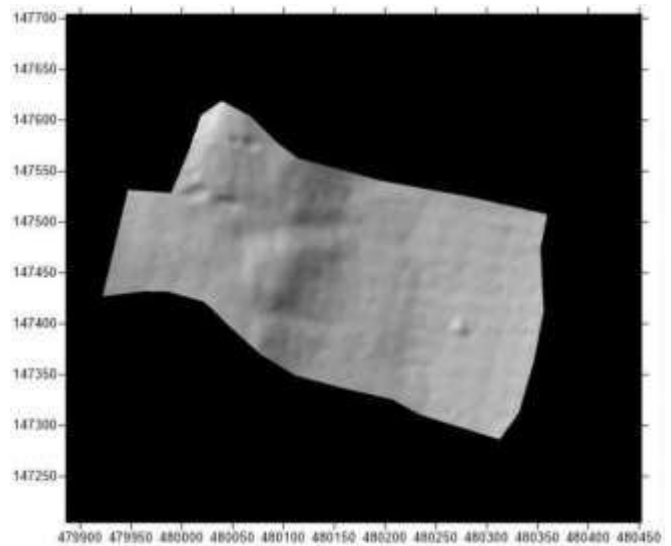


Fig. 5. Shaded relief model (date: 2023.05.01.)

B. Terrain model – 2023.06.17.

The 2nd survey took place on June 17. The completed surface model clearly shows the areas not covered by corn, as well as the traces of washes that cause soil erosion, along which the vegetation is also incomplete (Fig. 6 and 7). In this 3D model, the average height of the corn is 1m.

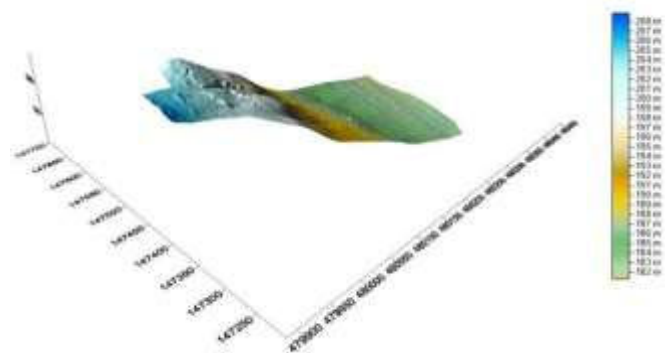


Fig. 6. Colored surface model (date: 2023.06.17.)

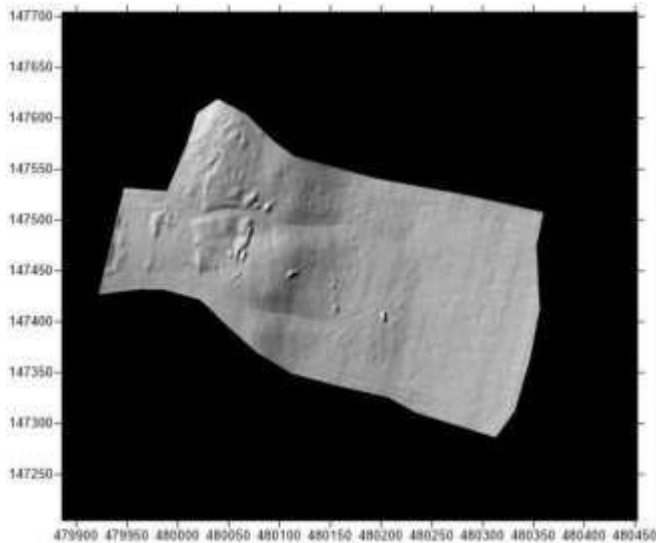


Fig. 7. Shaded relief model (date: 2023.06.17.)

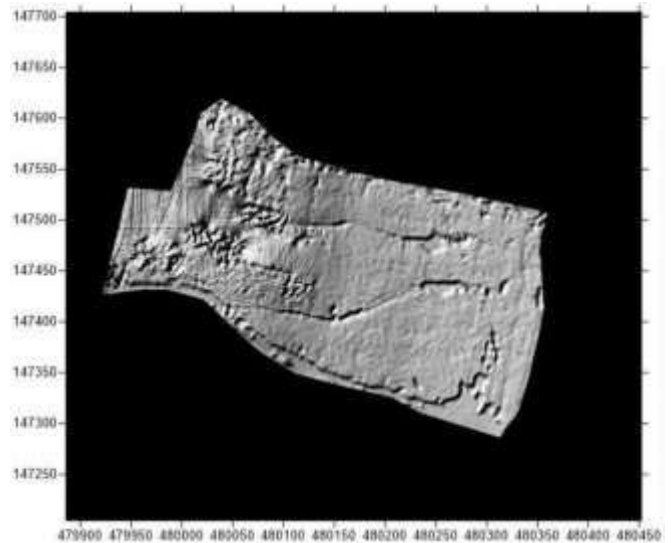


Fig. 9. Shaded relief model (date: 2023.08.15.)

C. Terrain model – 2023.08.15.

The third UAV survey took place in mid-August. These shots show the fully developed corn field. In this terrain model, the erosion-burdened plains are even more prominent. Based on the generated 3D model, the average height of the corn is 1.7m. Unfortunately, a technical error occurred during the UAV flight and a few shots were missed in a strip in the western corner of the area, so the terrain model in that area became incomplete and unreliable. This is clearly visible in Fig. 8 and 9.

For the reliability of the volume calculations, we cut out the common areas for all three times, as shown in Figure 10.

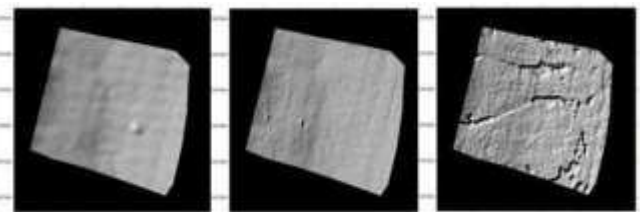


Fig. 10. Common areas (dates: 2023.05.01, 06.17 and 08.15. respectively)

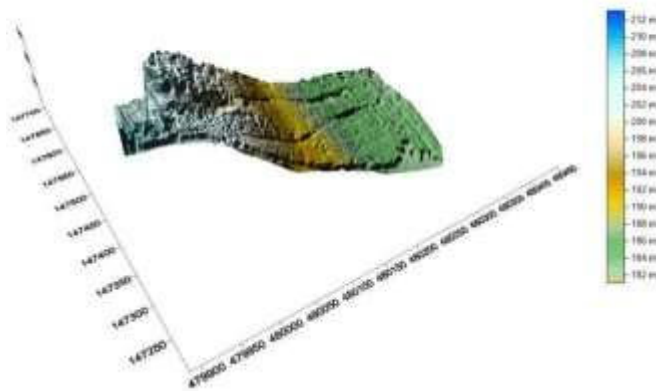


Fig. 8. Colored surface model (date: 2023.08.15.)

III. VOLUME CALCULATIONS

As the first step in the volume calculation, we created the GRID models with a cell size of 50 cm. The volumes were then calculated in two versions. In the first case, we created the difference between the May and June topography models and in the second case, we created the difference between the May and August 3D models. The volumes of these differences were calculated in the Surfer program (Fig. 11 and 12), and in the CloudCompare application (Fig. 13 and 14).

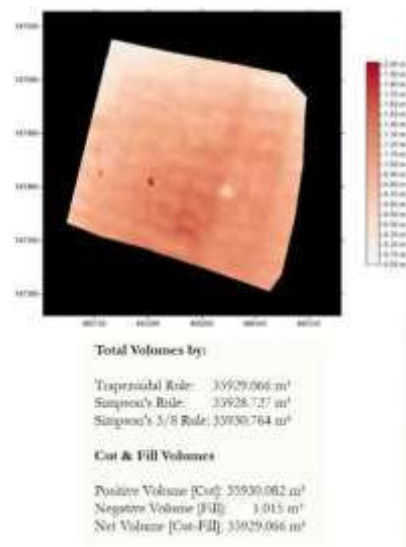


Fig. 11. Volume calculation in Surfer (dates: 2023.05.01 and 06.17)

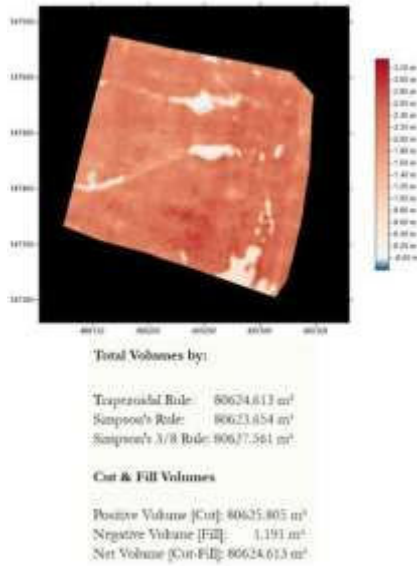


Fig. 12. Volume calculation in Surfer (dates: 2023.05.01 and 08.15)

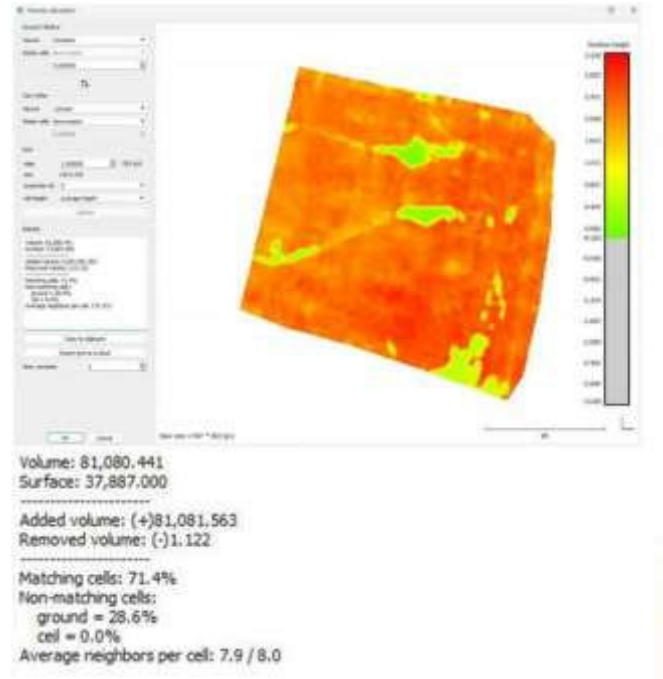


Fig. 14. Volume calculation in CloudCompare (dates: 2023.05.01 and 08.15)

Examining the difference between the two calculations, it can be seen that there is no significant difference between the volumes calculated by the two software (Fig. 15). The difference is only around 0.5%. The resulting volumes and their difference are summarized in Table III.

TABLE III. VOLUME VALUES AND DIFFERENCES

Period	NET Volume Surfer [m ³]	NET Volume CloudCompare [m ³]	Difference [m ³]
2003.06.17-05.01.	35929.066	36099.924	170.858
2023.08.15-06.17.	44695.547	44980.533	284.986
2023.08.15-05.01.	80624.613	81080.441	455.828

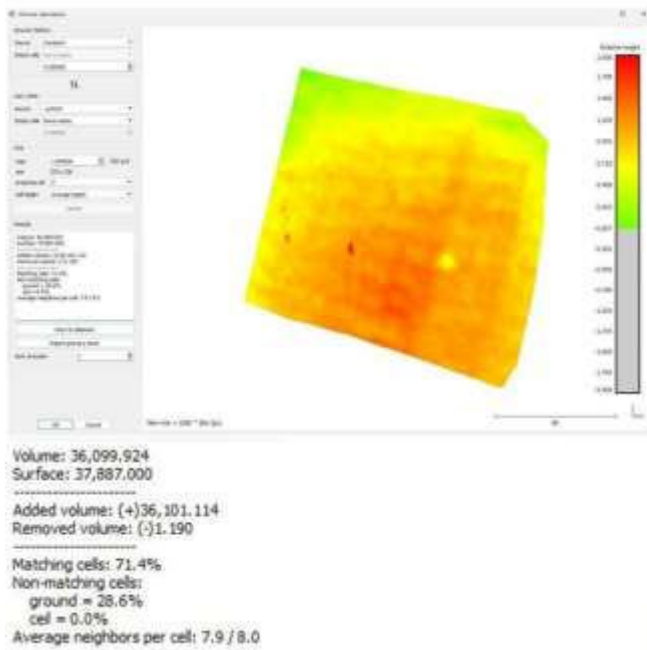


Fig. 13. Volume calculation in CloudCompare (dates: 2023.05.01 and 06.17)

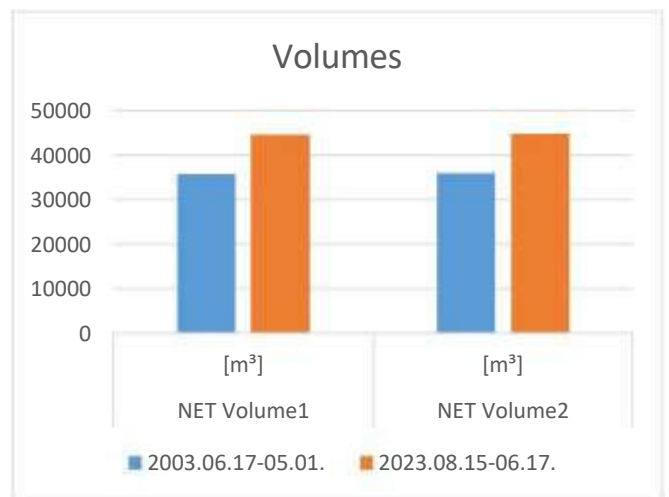


Fig. 15. Volume calculations

IV. CONCLUSIONS

Based on the experience gained during the work, we can make the following important conclusions:

- | Control points are needed in the corners of the block and preferably in the middle as well.
- | To achieve good results, the field resolution should be below 5 cm.
- | To increase the block adjustment accuracy, the camera should be calibrated.

As a continuation of the work, our plans include the calculation of the leaf surface index, the amount of the plant and the weight of the corn. For this, we need the corn phenological time series, the distances between the corn stalks and more precise height data [2], [4], [5]. To this end, we will repeat the UAV surveys in the following year, paying more attention to the placement of the ground control points, and the height accuracy considering the base ratio and a smaller distance between two consecutive pixel centers measured on the ground.

ACKNOWLEDGMENT

The paper was supported by the Bilateral Chinese-Hungarian Project No. 2019-2.1.11-TÉT-2020-00171 with the project title of “Investigation of the characteristics of surface shapes in rural environment based on point clouds and remote sensing data”.

REFERENCES

- [1] Dobosz B., Gozdowski D., Koronczok J., Žukovskis J., Wójcik-Gront E., “Evaluation of Maize Crop Damage Using UAV-Based RGB and Multispectral Imagery”, *Agriculture*, 13(8), 1627; <https://doi.org/10.3390/agriculture13081627>, 2023
- [2] Gilliot J.M., Michelin J., Hadjard D. et al., “An accurate method for predicting spatial variability of maize yield from UAV-based plant height estimation: a tool for monitoring agronomic field experiments”, *Precision Agric* 22, 897–921, <https://doi.org/10.1007/s11119-020-09764-w>, 2021.
- [3] Kraus K., “Photogrammetry - Geometry from Images and Laser Scans”, De Gruyter, ISBN 978-3-11-019007-6, 32-33 pp., 2007.
- [4] Shuai G., Martinez-Feria R. A., Zhang J., Li S., Price R., Basso B., “Capturing Maize Stand Heterogeneity Across Yield-Stability Zones Using Unmanned Aerial Vehicles (UAV)”, *Sensors*, 19(20), 4446; <https://doi.org/10.3390/s19204446>, 2019.
- [5] Yang B., Zhu W., Eyshi Rezaei E., Li J., Sun Z., Zhang J., “The Optimal Phenological Phase of Maize for Yield Prediction with High-Frequency UAV Remote Sensing”, *Remote Sensing*, 14(7), 1559; <https://doi.org/10.3390/rs14071559>, 2022.

POSTER SESSION I.
Applied Informatics

Network-Independent Building Automation System

Bertalan Beszédes
Óbuda University
Alba Regia Technical Faculty
Székesfehérvár, Hungary
beszedes.bertalan@uni-obuda.hu
<https://orcid.org/0000-0002-9350-1802>

Bence Márta
Óbuda University
Alba Regia Technical Faculty
Székesfehérvár, Hungary
martabence2000@gmail.com

Abstract— Within a multi-master environment, the Network-Independent Building Automation System (NIBAS) is structured around a hierarchical topology encompassing a management bus and a universal bus, with slave devices interconnected. This innovative system capitalizes on decentralized control algorithms, edge computing capabilities, and robust communication protocols to establish a self-reliant building automation framework. NIBAS is engineered to operate independently of traditional network infrastructures, ensuring the robustness and resilience demanded by diverse applications. By distributing intelligence across a network of sensors and actuators, NIBAS enables real-time monitoring and control of building systems, even in situations where centralized network connectivity is unavailable.

Keywords— multi-master environment, building automation, edge computing, robust topology, robust communication, real-time system, real time monitoring, decentralized algorithm

I. INTRODUCTION

One of the primary design goals for NIBAS is to achieve simplicity without compromising robustness and security for applications that require it. The basic topology of the system is intentionally designed with some overhead to ensure resilience in the face of failures, preventing them from affecting the entire system. [1-4]

In this architecture, most end devices are connected to easily implementable buses, such as those based on RS485 based communication standards or CAN protocols. These buses then interconnect with a mesh of "Managers," which play a crucial role in data management and routing between the end devices.

This hierarchical structure ensures that the failure of individual components or devices does not lead to system-wide disruptions [5-8]. It also simplifies the maintenance and scalability of the NIBAS, making it adaptable to various building automation scenarios. Additionally, the use of well-established communication standards like those built upon RS485 and CAN enhances compatibility and ease of integration into existing systems .

II. END DEVICE BUSES

The flexibility of NIBAS extends to the physical layout of the device and management buses. There is no rigid, predefined boundary dictating where these buses should start and end. Instead, this configuration can be tailored to

suit the specific needs of the user, taking into account factors such as the number of devices in the network and the physical constraints of the environment and the chosen bus technology [9-12]. The system also can be used in education for demonstrational and experimental purposes [13-15].

This adaptability allows users to optimize their NIBAS installation based on the unique requirements of their building or automation project. For instance, in a smaller-scale application with a limited number of devices, the user may choose to create shorter bus segments to simplify wiring and reduce complexity. Conversely, in a larger-scale deployment, the buses can be extended to accommodate a higher device count, ensuring efficient coverage of the entire system.

Furthermore, the physical flexibility in defining bus boundaries ensures that NIBAS can be seamlessly integrated into diverse environments, whether it's a sprawling industrial facility with extensive distances between devices or a compact residential setting with close proximity between components. This user-defined approach empowers individuals to tailor NIBAS to their specific needs, enhancing its versatility and applicability across a wide range of scenarios [16-19].

Certain end devices may be designed with redundancy in mind, offering the capability to connect to two separate end device buses. This redundancy ensures that if one bus experiences a disruption, the device can seamlessly switch to the backup bus, maintaining continuous operation. This feature is particularly valuable in critical applications where uninterrupted functionality is paramount.

Moreover, NIBAS allows for the deployment of multiple Manager devices connected to the same end device bus. This redundancy at the management level serves as a robust safeguard against manager faults. In the event that one manager encounters an issue or fails, the others can seamlessly take over the management of the connected devices and ensure the continued flow of data and control commands. This redundancy at both the end device and manager levels enhances the overall resilience and reliability of the building automation system, offering seamless error handling in a wide variety of operational scenarios.

III. TOPOLOGY IN PRACTICE

A. Management mesh

The utilization of a mesh network configuration for Manager devices within NIBAS is a strategic decision driven by several key advantages. Notably, in a mesh network, the need for complex media access control mechanisms is significantly reduced. Unlike other topologies, such as a bus or star, where precise control over media access is critical, the mesh design allows for a more simplified approach to data transmission. In essence, devices within the mesh can communicate directly with one another, eliminating the need for intricate protocols to manage access to the communication medium (see in Fig. 1.).

Furthermore, the inherent redundancy of a mesh network is a pivotal feature that enhances the overall reliability of NIBAS. Within this architecture, the presence of redundant paths for data transmission between Manager devices is a fundamental requirement. Consequently, if a single connection experiences a disruption or failure, the system autonomously reroutes data through alternative paths (see in Fig. 2.). This inherent fault tolerance ensures that a failure in one part of the network does not cascade into a system-wide failure, bolstering the robustness of a NIBAS framework.

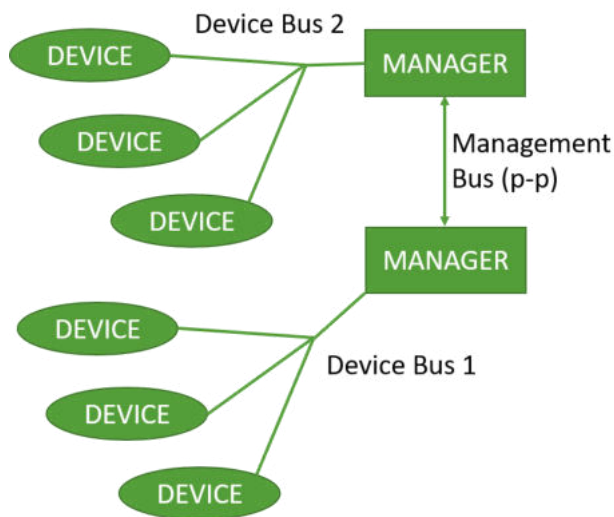


Figure 1. System topology

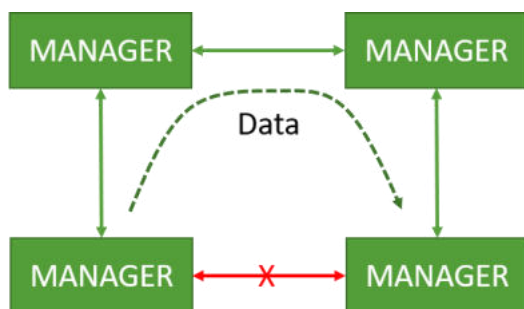


Figure 2. Error handling methodology

In summary, the mesh network topology not only simplifies data transmission by reducing the need for complex media access control but also provides a robust and fault-tolerant infrastructure. It ensures that single connection failures do not compromise the integrity of the entire NIBAS system, making it an ideal choice for building automation applications where reliability is paramount.

B. End Devices

Smart Lighting Controllers: These devices allow for intelligent control of lighting systems. They can adjust lighting levels based on occupancy, time of day, or user preferences, contributing to energy savings and enhancing user comfort.

HVAC (Heating, Ventilation, and Air Conditioning) Thermostats: HVAC thermostats equipped with NIBAS compatibility enable precise temperature control within a building. They can respond to environmental conditions and user input to optimize energy efficiency and maintain desired comfort levels.

Environmental Sensors: Sensors measuring parameters like temperature, humidity, CO₂ levels, and air quality play a crucial role in maintaining a healthy and comfortable indoor environment. NIBAS can collect and analyze data from these sensors to trigger automated responses, such as adjusting HVAC settings or activating air purification systems.

Smart Plugs: These end devices can be controlled remotely via NIBAS, allowing users to manage and monitor the power consumption of appliances and devices connected to them. They can be used for energy management and scheduling.

Occupancy Sensors: Occupancy sensors can be used to detect the presence of people in rooms or areas. NIBAS can respond by adjusting lighting, HVAC, and security settings based on occupancy patterns.

Shade and Blind Controllers: Automated window coverings can be controlled by NIBAS to optimize natural light, reduce glare, and enhance energy efficiency by adjusting shades and blinds based on external light conditions and user preferences.

An example to end devices is a multi-channel LED controller (as can be seen on Fig. 3.) that has an RS485 connection (Fig. 4.), as a proof of concept device.

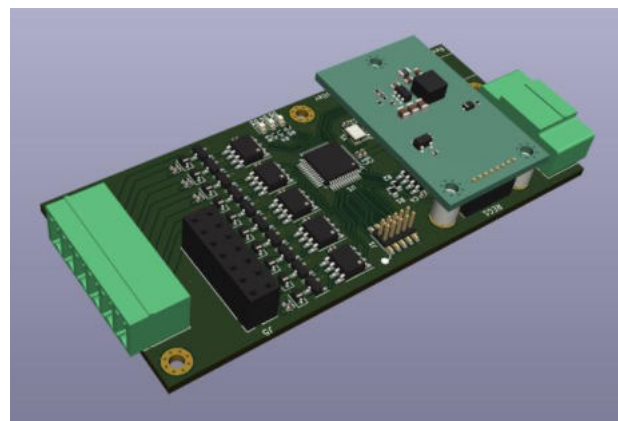


Figure 3. Prototype PCB isometric model

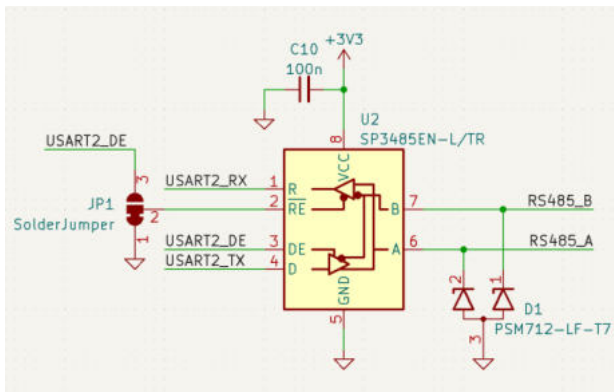


Figure 4. Communication interface design

C. Error Handling

Although the management mesh is meticulously engineered to provide redundancy and fault tolerance, it's imperative to acknowledge that even within this resilient structure, the possibility of total communication breakdown between different parts of the network must be a key consideration. While the mesh topology mitigates the risk of isolated failures affecting the entire system, it's not impervious to extreme scenarios or catastrophic events that could disrupt multiple critical connections simultaneously.

Within the local end device buses, it's important to note that communication remains uninterrupted even in the event of mesh network disruptions. Each segment of the mesh that includes a device capable of managing the remaining devices will continue to function autonomously, isolated from the rest of the network. To address potential data source cutoffs, some devices may be equipped with emergency protocols, ensuring that critical functions are maintained.

In the event of a mesh fault, users will be promptly notified of the issue through devices that display the system status. Additionally, users have the flexibility to define specific devices to execute predefined actions if a mesh failure occurs. This proactive approach empowers users to tailor the response to their specific needs and priorities, further enhancing the adaptability and resilience of the system.

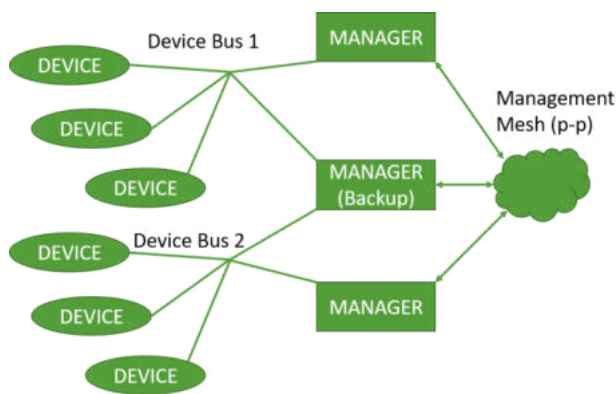


Figure 5. Multiple managers connected to the same bus for redundancy

D. Safety and security

It's important to note that security and safety devices, such as fire alarms, smoke detectors, and intrusion detection systems, are typically excluded from reliance on NIBAS. Critical applications demand a high degree of reliability and should not be dependent on the same network that handles automation and environmental control, just like the following works [20-22]. By maintaining separate, dedicated networks for security and safety, any potential issues with the automation network will not compromise the integrity and effectiveness of these crucial systems. This segregation ensures that security and safety devices operate independently, providing uninterrupted protection even in challenging scenarios.

While security and safety systems should maintain their independence, NIBAS to enhance overall building functionality and safety. For instance, in the event of an emergency, such as a fire or intrusion, security and safety systems can communicate with NIBAS to trigger specific actions, such as automatically turning on emergency lighting, shutting down HVAC systems to prevent spreading of smoke or toxic gases or disabling elevators.

IV. CONCLUSION

Through comprehensive experimental assessments, this paper underscores NIBAS's adaptability and reliability, offering significant potential for enhancing building efficiency, sustainability, and resilience in scenarios where network connectivity may be limited or compromised. This research contributes to the advancement of autonomous and resilient building systems, marking a significant stride toward network-independent solutions.

ACKNOWLEDGMENT

The authors would like to thank all the Obuda University Alba Regia Technical Faculty staff and member that provide help and assistance throughout the project completion.

REFERENCES

- [1] Bingol, O., Tasdelen, K., Keskin, Z., & Kocaturk, Y. E. (2014). Web-based smart home automation: PLC-controlled implementation. *Acta Polytechnica Hungarica*, 11(3), 51-63.
- [2] Györök, György, Baklanov, Alexander E. Beszedes, Bertalan. Extension of Nodal Voltage Method with the Thermosensing. In: Orosz, Gábor Tamás (szerk.) AIS 2017 - 12th International Symposium on Applied Informatics and Related Areas organized in the frame of Hungarian Science Festival 2017 by Óbuda University : Proceedings. Székesfehérvár, Magyarország : Óbudai Egyetem (2017) 204 p. pp. 201-204. , 4 p.
- [3] Györök, Györök, András, Dávid, Nikolett, Tolner, Bertalan, Beszedes, Dániel, Cseh. Supervision of the operation of digital circuits by Embedded Microcontroller. In: Orosz, Gábor (szerk.) AIS 2018 - 13th International Symposium on Applied Informatics and Related Areas. Székesfehérvár, Magyarország : Óbudai Egyetem, Alba Regia Műszaki Kar (2018) pp. 29-35. , 7 p.
- [4] Alexander Baklanov, Svetlana Grigoryeva, György Györök, Control of LED Lighting Equipment with Robustness Elements, *Acta Polytechnica Hungarica Acta Polytechnica Hungarica Vol. 13, No. 5, 2016. pp. 105-119.*
- [5] Mon, Y. J., Lin, C. M., & Rudas, I. J. (2012). Wireless sensor network (wsn) control for indoor temperature monitoring. *Acta Polytechnica Hungarica*, 9(6), 17-28.

- [6] A. Baklanov, S. Grigoryeva, Gy. Györök. Intelligent control of LED luminaries. 9th International Symposium on Applied Informatics and Related Areas - AIS 2014, Székesfehérvár, 2014. pp. 87-91 (ISBN:978-615-5460-21-0)
- [7] Bartos, Gaye Ediboğlu, et al. "A Multilingual Handwritten Character Dataset: THE Dataset." Acta Polytechnica Hungarica 17.9 (2020).
- [8] Meng Qingyan ; Chen Xu ; Zhang Jiahui ; Sun Yunxiao ; Li Jiaguo ; Jancsó Tamás; Sun Zhenhui Canopy Structure Attributes Extraction from LiDAR Data Based on Tree Morphology and Crown Height Proportion PHOTONIRVACHAK / JOURNAL OF THE INDIAN SOCIETY OF REMOTE SENSING (0255-660X 0974-3006): 46 9 pp 1433-1444 (2018)
- [9] Xiaojiang, Li ; Weindong, Li ; Qingyan, Meng ; Chuanrong, Zhang ; Tamas, Jancso ; Kangli, Wu Modelling building proximity to greenery in a three-dimensional perspective using multi-source remotely sensed data JOURNAL OF SPATIAL SCIENCE , 16 p. (2016)
- [10] Baklanov, A., Baklanova, O., Grigoryeva, S., Kumargazhanova, S., Sagynganova, I., Vais, Y., & Györök, G. (2020). The Development of Hybrid IP Architecture for Solving the Problems of Heating Networks (using pipeline-parallel data processing technology). Acta Polytechnica Hungarica, 17(1), 123-140.
- [11] G. Simon and L. Sujbert, "Special issue on "Recent advances in indoor localization systems and technologies"," Applied Sciences, Vol. 11, No. 9, paper 4191, May 2021.
- [12] L. Sujbert, G. Simon and G. Peceli, "An Observer-Based Adaptive Fourier Analysis," IEEE Signal Processing Magazine, Vol. 39 No. 4, pp.134-143, Oct. 2020.
- [13] Pogátsnik, Monika. Dual education: connecting education and the labor market. Opus et Educatio: Munka és Nevelés 8 : 3 pp. 304-313. , 10 p. (2021)
- [14] Pogatsnik, Monika. Measuring Problem Solving Skills of Informatics and Engineering Students. In: Szakál, Anikó (szerk.) IEEE Joint 19th International Symposium on Computational Intelligence and Informatics and 7th IEEE International Conference on Recent Achievements in Mechatronics, Automation, Computer Sciences and Robotics : CINTI-MACRo 2019
- [15] Módné, Takács Judit ; Pogátsnik, Monika. The online learning from the students' perspective. In: Szakál, Anikó (szerk.) 2021 IEEE 19th World Symposium on Applied Machine Intelligence and Informatics (SAMI). Budapest, Magyarország : IEEE Hungary Section (2021) 507 p. pp. 00027-00032. , 6 p.
- [16] Ladislav Fozo ; Rudolf Andoga ; Radovan Kovacs. Thermodynamic cycle computation of a micro turbojet engine. 2016.In: CINTI 2016. Danvers : IEEE, 2016 P. 000075-000079. ISBN 978-1-5090-3909-8
- [17] FŐZŐ, Ladislav ; ANDOGA, Rudolf ; KOVÁCS, Radovan. Experimental identification of a small turbojet engine with variable exhaust nozzle. 2015. In: CINTI 2015. Danvers : IEEE, 2015 P. 65-69. ISBN 978-1-4673-8519-0
- [18] KOMJÁTY, Maroš ; FŐZŐ, Ladislav ; ANDOGA, Rudolf. A Digital Diagnostic System for a Small Turbojet Engine 2013. In: Acta Polytechnica Hungarica. Vol. 10, no. 4 (2013), p. 45-58. ISSN 1785-8860
- [19] ANDOGA, Rudolf ; FŐZŐ, Ladislav ; MADARÁSZ, Ladislav - KAROL, Tomáš. Innovative approaches in modeling, control and diagnostics of small turbojet engines. 2013. In: Acta Polytechnica Hungarica. Vol. 10, no. 5 (2013), p. 81-99. ISSN 1785-8860
- [20] M. Kaluza, I. B. Foldes, E. Racz, M. I. K. Santala, G. D. Tsakiris, and K.-J. Witte, 'Relativistic self-focusing of fs-laser pulses and their heating effect on the preformed plasma', *IEEE Trans. Plasma Sci.*, vol. 33, no. 2, pp. 480–481, Apr. 2005, doi: 10.1109/TPS.2005.845114.
- [21] Z. Varga and E. Racz, 'Machine Learning Analysis on the Performance of Dye-Sensitized Solar Cell—Thermoelectric Generator Hybrid System', *Energies*, vol. 15, no. 19, p. 7222, Oct. 2022, doi: 10.3390/en15197222.
- [22] Udvardy, P. ; Jancso, T. ; Beszedes, B. 3D modelling by UAV survey in a church. In: Rudolf, Andoga (szerk.) New Trends in Aviation Development 2019 : The IX. International Scientific Conference. Piscataway (NJ), Amerikai Egyesült Államok : IEEE (2019) pp. 189-192. , 4 p.

Observation and Analysis of Wildlife Behaviour in Agricultural Areas

Dániel Kovács
Székesfehérvári Szc Széchenyi István
Műszaki Technikum
Székesfehérvár, Hungary
ua723ic@gmail.com

Éva Hajnal
Alba Regia Technical Faculty
Óbuda University
Székesfehérvár, Hungary
hajnal.eva@amk.uni-obuda.hu

Todor Stoilov
Institute of Information and
Communication Technologies
Bulgarian Academy of Sciences
Sofia, Bulgaria
todor.stoilov@iict.bas.bg

Abstract—Maximizing the quantity of crops is crucial in modern agriculture. Effectively preventing wildlife damage is one of the ways to optimize crop quantity in agriculture. In addition to the traditional methods of wildlife damage management, it is important to know if and in what numbers wildlife is present in the area, at what time of day and how animals move around the area. If the right information is available, current wildlife damage prevention methods can be applied at the right time and in the right place to protect an area more effectively. There are multiple methods for obtaining information. Automated monitoring systems can greatly aid in observing wildlife and analyzing their behavior, in addition to traditional field observation. In agricultural areas, up-to-date information on the state of the agricultural land can greatly facilitate wildlife damage control. The purpose of this article is to present a comparison of current monitoring systems.

Keywords—sensor network, monitoring system, wildlife, agriculture

I. INTRODUCTION

One way to produce food is to grow crops in the open air. Crop production is influenced by many external conditions. Among the external conditions, there are factors that are difficult to modify. Despite these difficulties, large quantities of food crops are still grown in open large fields. The difficulties include rainfall, topography, soil quality, and damage to wildlife. The extent and type of damage caused by wildlife can vary when analyzed over a number of years. Damage caused by wildlife is not only present in large areas of several hectares, but also in forestry, where some wild species can cause significant damage. In forestry, I would highlight those forests that are not Natura 2000 sites, but planted forests that have been established for some economic purpose. Forests established for economic purposes are usually planted with tree species that the management organization needs, so if wildlife damage occurs in this type of forest early in the planting process, it can delay the time for felling by several years. Monitoring and control of the quality and quantity of wildlife is necessary in crop production. In forests established for economic purposes, tree species are usually planted according to the needs of the management organization, but if wildlife damage occurs in this type of forest early in the planting process, this can delay the time to harvest by several years. Monitoring and control of the quality and quantity of wildlife are necessary in crop production. Wildlife damage can be mitigated in several ways. The company responsible for wildlife management conducts continuous field work through personal observation, which is a method of monitoring wildlife

populations. The use of camera systems installed on the spreaders and wild feeders is another method. This paper deals with the types of damage caused by wild animals, the control and measurement of wildlife damage, and a short conclusion about the development goals and possible strategies.

II. DAMAGE CAUSED BY WILD ANIMALS

Wild animals can cause a variety of damage. Serious damage can be caused by different species, depending on the number of individuals and the type of crops grown in an area. When there are thousands of feral rabbits per unit area in a hunting area, and negligible numbers of feral hogs because of the unsuitable habitat and living conditions for feral hogs, the feral hogs cause less damage to the crop than the feral rabbits. The extent of damage is dependent on the crop's species and developmental stage. In the case of sunflowers, damage to the crop by the wild rabbit during the emergence stage can be fatal when the crop is only two petals old, because the wild rabbit will eat the whole crop and there will be no more plants in the field. In the growing stage, sunflowers can be damaged by roe deer as well. Wild damage to sunflowers at maturity can also be caused by the Balkan pigeon, the Eurasian dove and the house pigeon, these birds pluck the sunflower seeds from the plant, damaging the sunflower field.



Figure 1. Damage caused by a wild rabbit in a sunflower field [1]

The damage caused by wild rabbits shown in Fig. 1 is an example of damage to agricultural production caused by wild animals. The production of crops can be damaged by any herbivorous animal [9]. The extent of the damage may also be dependent on the natural food it finds in its natural habitat. The extent of wildlife damage can be influenced by the size of the natural habitat when compared to the amount of a given wild animal. The extent of wildlife damage is influenced by the natural vegetation of the natural habitat and the complexity of the system it forms. The quantity of rainfall in these areas is crucial, as if there is enough precipitation, wildlife will be more likely to find food in the natural habitat [14].

The management organization always compensates for damage caused by wild animals by the company that is authorized to hunt. It is fortunate if there is communication between the hunting organization and the management organization, as preventive wildlife damage prevention can minimize any wildlife damage that may occur. There are several ways in which wildlife damage can occur. Wild animals can damage farmland not only by eating it, but also by using it as a hiding place, trampling the crop, and causing damage [19]. If there are no other woodlands in the area to shelter it, the roe deer is frequently sleeping in wheat during the day. There are many forms of wildlife damage, but we have distinguished agricultural forms of wildlife damage from forestry forms of wildlife damage.

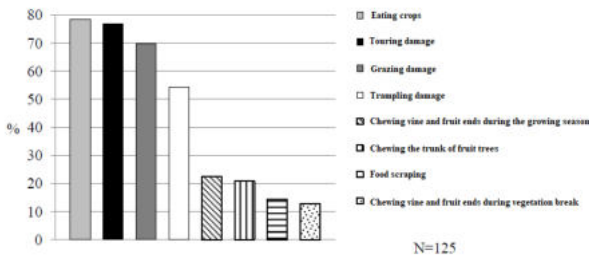


Figure 2. Agricultural wildlife damage types [2]

Fig. 2 [2] shows the types of damage to wildlife in agriculture, with significant damage been caused by the consumption of the product, because a natural need of the wild animal may depend on it for its life. In areas where wild pig populations are strong, poke damage is also crucial. The wild pig population in certain areas has been reduced by African swine fever. African swine fever has the potential to be dangerous to pigs in livestock. In agricultural damage, there is damage that the owner of a field of maize on several hectares only notices when harvesting, because the wild pig can cause such wild damage that in the maize field when the maize is ripening it will cut off whole stalks of maize so that the piglets can eat the maize. The edges of the corn field are usually where this type of damage is created to use as a shelter [16].

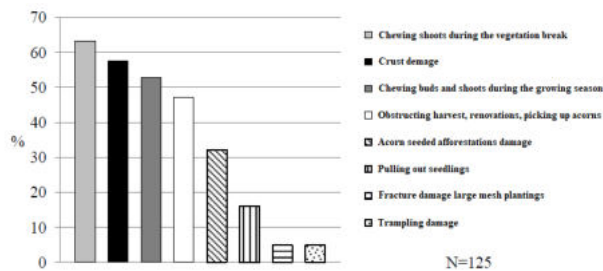


Figure 3. Types of forest damage [2]

In areas where deer and roe deer numbers are high, the impact of plant shoot chewing on wildlife is significant, as shown in Fig. 3. [12] Deer and roe deer play a significant role in bark damage because when their antlers mature they clear antlers on the trees. By cleaning their antlers on younger trees, they can completely destroy them. There is a special case of wild shoot chewing, when freshly planted saplings are damaged in the forest, because their growth can be severely hampered if the middle shoot is damaged. This type of damage can lead to the tree's quality being reduced and it becoming a bush. In Hungary, there are differences in the extent of damage caused by wild animals from county to county. Wild

damage is determined by the type of crops grown in agriculture and the size of the natural areas where animals are present. The reduction of wildlife damage could be achieved by afforesting areas that were previously natural forests, but there are few examples of this in today's world as demand for food increases. Some counties have low levels of damage caused by wildlife, because damage is preventable and any damage can be detected early, so that early intervention can be taken to avoid greater damage.

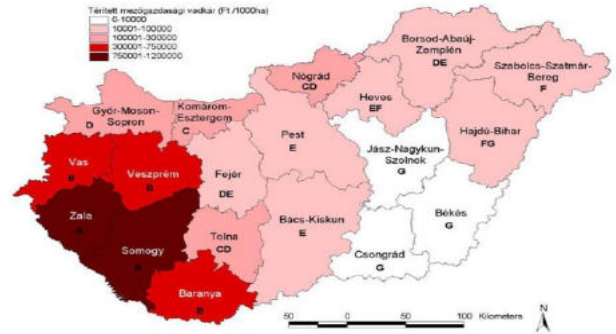


Figure 4. Amount of compensated agricultural wild damage by county [3]

Fig. 4 displays the amount of agricultural [3] wild damage that has been compensated per 1000 ha. The measurement data covers the period of 1997-2011. The issue with the reimbursed agricultural wild damage is that the organization that is entitled to hunt must pay this amount to the organization that is carrying out the agricultural activity. In successive years, the compensation rate can be highly variable. Therefore, it is difficult to predict the cost of wild damage [13]. To prevent and reduce damage, hunting organizations employ a variety of methods. If the wild damage is high, the production capacity of the area is reduced because destroyed crops do not become food. This is not beneficial to the farmer either. It is advantageous to have communication between farming and hunting organizations about what is planned to be grown in the area and when. The number of wildlife damages recorded in Zala and Somogy counties was the highest during the four-year period. In Jász Nagykun Szolnok, Csongrád, and Békés counties, the damages were the lowest. The map indicates that the distribution of damages is not uniform, as it is greatly influenced by the local conditions [8]. The natural movement of wild animals depends on the population size, which can vary from species to species. Wild animal movement can be greatly influenced by the availability of food and water in the area. The Zala and Somogy counties have a high concentration of wildlife and intensive agriculture in the region. In addition to significant agricultural production, forestry is also practiced, which is not depicted on the map. Depending on the way the forest is managed, it can also affect agricultural damage, because forest management can also use, wildlife damage prevention methods that reduce the amount of land that can be accessed by wildlife in the long term. The installation of multi-year wildlife fencing can be used as a control method to prevent damage to plants and trees from herbivorous wildlife, which can have a negative impact on tree growth. Although the method is generally effective in the area, it has the disadvantage of limiting the area in the county that wildlife can use.

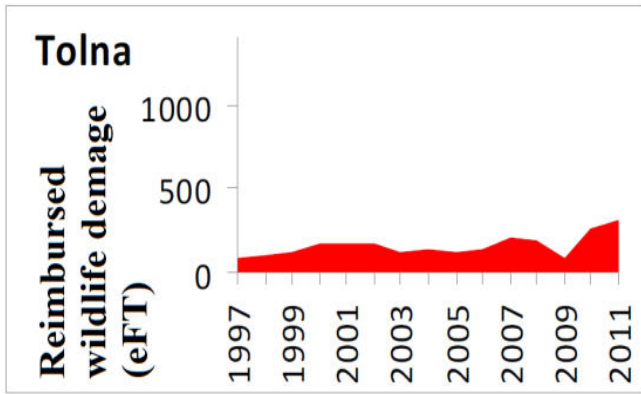


Figure 5. Wildlife damage compensation in Tolna county [3]

Fig. 5 depicts the compensation for wild damage in Tolna County, broken down by years, in thousands of HUF per 1000 ha. The HUF 500 000 threshold for wildlife damage in Tolna County was not reached in any year. The financial threshold for hunting organizations is even higher now. The financial compensation to be paid by the hunting organization can be relatively well estimated.

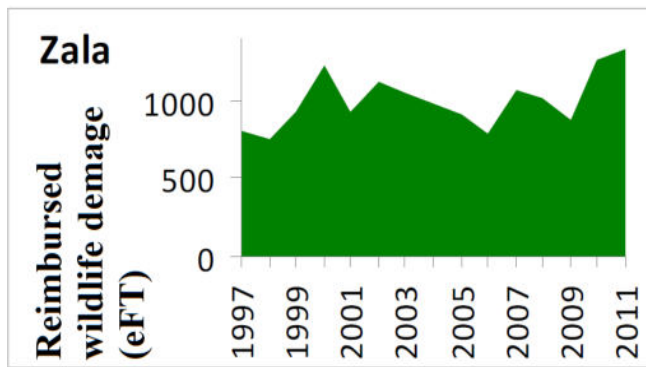


Figure 6 Compensation for wild damage in Zala county [3]

In Fig. 6, the compensation for wildlife damage in Zala County is shown in thousands of HUF per 1000 hectares, broken down by years. [7] The compensation for wildlife damage in Zala County has been several times higher or has reached 1000000 HUF. Wild management organizations in other areas of the country have a lower cost than wild management organizations in this area. In the Zala county it is more difficult to estimate the extent of damage caused by wild animals, because there are greater differences between years and it is therefore more difficult to predict the extent of damage. The threshold for HUF 500 000 per 1000 hectares is always exceeded by the years examined.

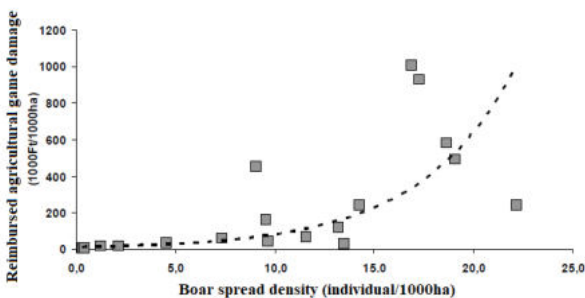


Figure 7. Wild boar presentation [3]

The relationship between boar density and game damage is shown in Fig. 7 [3]. A positive exponential relationship between wild boar and deer density and game damage was shown by Norbert Bleier in his doctoral thesis in 2014. The doctoral dissertation also included roe deer, but no such association was found in wild roe deer [3],[15].

III. CONTROL AND MEASUREMENT OF WILDLIFE DAMAGES

The damage caused by wild animals in agricultural areas can be mitigated in several ways. The method chosen is determined by the nature of the area. Effective wildlife damage control requires a thorough understanding of the characteristics of the surrounding wildlife areas [11]. Some of the methods are designed for a short period of time and are seasonal, such as having an active hunter present in a sunflower field to alert. To effectively use this method, the organization responsible for the agricultural area must agree with the organization responsible for hunting and jointly organize the protection of the area. The damage caused by wild rabbits can be mitigated through the use of this control method. Depending on the area and rainfall, the duration of this control method is usually 2-3 weeks. Another approach is to use easily deployable small game nets for the same time interval. Small game nets that can be easily deployed are useful for this type of damage when it's not feasible for hunters to be present in the area. This type of net system can be damaged by a passing presence of large games in the area, which can reduce its effectiveness. Periodically, it is necessary to check the installed netting systems for damage. It is important to organize the installation for a larger area before planting the seeds [17]. During the growth phase, agricultural crops should also be protected against wild damage, and this protection may vary depending on the type of crop. To prevent wild damage, it is crucial to know the location of the area to be protected, such as if there is a forest belt nearby. Traditional wire fencing is the simplest way to prevent wildlife damage on farmland that is adjacent to a woodland strip. The wire fence acts as a physical barrier, preventing the game from entering the cultivated agricultural land [4]. The disadvantage of a wire fence is that it is more difficult to use a large machine on the land and requires more attention from the operator. The free movement of game between fields is an issue with wire fencing. If large areas are fenced, game can cause more damage to smaller farmland by simply passing through them, and if it feeds, losses can increase gradually. Areas that border forest belts are protected by electric fencing. The electric fence is high voltage, often hundreds of kilovolts, but the current is low, so it is not fatal to the animal when it is electrocuted, but the sensation is unpleasant. This is noted by the wild and avoided for a while. The handling is similar to that of a conventional wire fence, but the battery must be checked and replaced if necessary to ensure proper game protection. In addition to physical barriers, chemical alarm devices are also available. Chemical alarm devices commonly emit an odorous substance that irritates the game and causes it to avoid the barrier. There are multiple versions of these chemical alarms. One version of this is when ordinary rags are soaked in a chemical agent. The area is protected by the placement of these rags. It is necessary to change the soaked rags periodically because the chemical agent evaporates. A chemical wildlife alarm that is pre-made is available commercially and can be placed in the area you wish to protect. The effectiveness of these methods depends on the number of times the game is used in the area. Otherwise, the

game may become habitual and this method of control may not be effective. It is recommended to use them in conjunction with other methods for preventing wildlife damage. Another method for preventing wildlife damage is using ultrasonic game alarms. A high-frequency loudspeaker that emits a disturbing sound is used to operate ultrasonic game alarm systems. Battery-operated or battery-powered devices can be powered by a solar panel that charges the battery during the day.



Figure 8 Solar panel powered ultrasonic game alarm [5]

The ultrasonic game alarm device can be seen in Figure 8. To prevent wildlife damage effectively, it is necessary to place several of these devices in the same area. To maximize the effectiveness of the system, manufacturers suggest a distance of installation between devices. During the day, the solar panel can be used to power the system and charge its battery for night operation. The game can become accustomed to the constant operation of ultrasonic game alarms, which can result in ineffective alerts. In addition to the constant mode, there are other modes that detect motion in infrared and are only active when it is detected. These devices are more difficult for game to get used to in the field. The gas cannon is also used as a method of alarming the game. The gas cannon emulates the sound of a shot made during hunting.



Figure 9. Gas cannon [1]

The gas cannon is shown in Figure 9. The gas cannon is an effective game deterrent because the sound effect can resemble the sound of a gunshot. A PB cylinder and control electronics are necessary to operate the gas cannon. The control electronics are responsible for controlling the amount of gas entering the barrel and the ignition of the gas. Several game species can be deterred by the gas cannon. If the cannon is installed in a constant location, the game can become accustomed to its presence and sound. If the gas cannon is

relocated several times, and the timer program is changed occasionally, the game will have more difficulty getting used to the presence of the gas cannon and will be more effectively deterred. Wild animals were deterred by previous methods. While animal deterrence in agricultural areas is important, it is not always sufficient. If the wildlife population in an area is overpopulated in relation to the area or is causing extensive damage to agricultural crops on a regular basis, a wildlife deterrent hunt should be ordered. To prevent wildlife damage, a hunt must be organized and the wildlife species that can be hunted during this time must be highlighted. There are also species within the huntable game species that should be protected in order to conserve and control the game species population [18]. The organization with the right to hunt can facilitate the work of the organization with the right to hunt by planting crops on the edges of the fields that facilitate the detection and evaluation of game, for example: alfalfa. The hunt in this case is a hunt from a hunting flock. Hunting flocks are usually those that can be relocated to another site for a successful wildlife damage control hunt, but this depends on the nature of the area. Wildlife damage avoidance hunting alone can reduce the amount of wildlife damage, the sound of the shots will cause different species to react in different ways over the long term. Some game species will avoid the area for a while, and some will return to the area immediately.



Figure 10. Alfalfa band on the edge of a maize field [1]

Fig. 10 shows a maize field with an alfalfa strip. This solution helps the success of the wildlife damage avoidance hunters. It is an extra burden for the farming organization, which not all farming organizations like, because it reduces the area they can devote to the crop they are targeting. The alfalfa has to be cut, which is extra work and time and fuel for the farming organization, but it also helps to control wildlife damage. Farming organizations that have suffered major wildlife damage since their business was established will take every opportunity to mitigate wildlife damage.

IV. CONCLUSION

Different kinds of damage can be caused by wild animals. The damage caused by wild animals places a financial burden on hunting organizations and causes damage to agricultural organizations. The common goal of these organizations is to decrease the amount and severity of damage caused by animals. Successful methods for preventing wildlife damage can vary. Good results can be achieved by considering ever-changing circumstances and active observation. The objective is to create an effective wildlife warning system that uses modern science to help farmers detect wild animals damaging crops and thus reduce damage. Our plan is to develop an IoT system that will perform its task with the help of machine learning algorithms. Unfortunately, we could not find any scientific description or study of such systems. Therefore, for

its task specification, we have collected types of wildlife damage and types of protection, with which information we can then tune our own system. The next step of the work will be to prepare some system designs and then to select the appropriate one according to its feasibility and cost-effectiveness. This work can be considered as a situation assessment for the further tasks.

REFERENCES

- [1] Gombos Tamás "Vadkalandok (19.rész) Vadkárelhárítás" 2023 movie Accessed: 2023.09.20:
https://www.youtube.com/watch?v=0IkWq_Xcqso
- [2] Antal Borbála, Szendrei László, csajbók József "ADATOK A VADKÁR ÉS A VADFÖLDGAZDÁLKODÁS HAZAI HELYZETÉRŐL," NAIK ERTI, Ültetvénytudományi Osztály, Püspökladány, Debreceni Egyetem, MÉK, Természetvédelmi Állattani és Vadgazdálkodási Tanszék, 3 Debreceni Egyetem, MÉK, Növénytudományi Intézet, 2016, pp 33-34, [PDF] Accessed: 2023.09.20: http://epa.niif.hu/03400/03455/00017/pdf/EPA03455_kut_atoi_nap_2016_031-034.pdf
- [3] Norbert Bleier, "A mezőgazdasági vadkár ökológiai és ökonomiai összefüggései," Szent István Egyetem, 2014.
Scott R. Craven, Scott E. Hygnstorm "DEER," University of Nebraska Lincoln, USA, 1994 1. 1. pp 29-35, University of Nebraska Lincoln NE 68583 Accessed: 2023.09.20
file:///C:/Users/CFY/OneDrive/Asztali%20g%C3%A9p/Vadk%C3%A1r%20Projekt/doxmand_vr1_ultrahangos_vadriaszto-1_1-450x254.webp
- [4] <https://www.axial.hu/cikkek/hirek/akcios-kinalatunkbol-nk52-es-gazagyu> Accessed: 2023.09.20
- [5] Bleier N., Szemethy L., Csányi, S. (2011) Skody sposobené zverou v Madarskej republike, ekologické, ekonomické a právne súvislosti. (Vadkárhelyzet Magyarországon: ökológiai, ökonomiai- és jogi vonatkozások) 75-80.p. In: Skody zverou a na zveri a moznosti ich obmedzenia. Léva (Szlovákia), 2011.02.04. (124pp.) (ISBN: 978-80-89418-12-1)
- [6] Bleier, N., Szemethy, L., Csányi S. (2008): A mezőgazdasági vadkár befolyásoló tényezők: egy összetett rendszerben működő kapcsolatok felderítése. Multifunkcionális Mezőgazdaság. Nemzetközi tudományos konferencia, Hódmezővásárhely. Agrár- és Vidékfejlesztési Szemle, 3. évf. 1. szám CD melléklete ISSN 1788-5345
- [7] Katona, K., Szemethy, L., Kiss, M., Bleier, N., Székely, J., Nyeste, M., Kovács, V., Terhes, A., Fodor, Á., Olajos, T. (2011): Climate change and sensitivity to game damage in the Hungarian even-aged forests. Forest Biodiversity in a Changing Climate: Understanding Conservation Strategies and Policies. International Conference, Freiburg, Németország, 2011. 09. 22-2011. 09. 23
- [8] Szemethy L., Biró, Zs., Katona, K., Heltai, M., Bleier, N. (2010) Mekkora területen mozog a gímszarvas? 82-87.p. In: Csányi S. és Heltai M. (szerk.) Vadbiológiai olvasókönyv: Szemelvények a vadbiológia új eredményeiről a Vadvilág Megőrzési Intézet munkatársainak ismeretterjesztő cikkei alapján. 205.pp. Mezőgazda Kiadó (ISBN:978-963-286-592-8)
- [9] Csányi S., Lehoczki, R., Bleier, N., Sonkoly, K., Schally, G. (2010) Otthon az élőhelyen. 88-99.p. In: Csányi S. és Heltai M. (szerk.) Vadbiológiai olvasókönyv: Szemelvények a vadbiológia új eredményeiről a Vadvilág Megőrzési Intézet munkatársainak ismeretterjesztő cikkei alapján. 205.pp. Mezőgazda Kiadó (ISBN:978-963-286-592-8)
- [10] Szemethy, L., Biró, Zs., Katona, K., Mátrai, K., Orosz, Sz., Bleier N. (2006): Seasonal home range shift of red deer in a forest-agriculture area, Hungary. 6th International Deer Biology Congress, Csehország, Prága
- [11] Bleier, N., Szemethy, L., Csányi, S. (2010): A nagyvadfajok állománysűrűsége és a mezőgazdasági vadkárközötti kapcsolat. Vadbiológia, 14: 1-12.p.
- [12] Katona, K., Szemethy, L., Nyeste, M., Fodor, Á., Székely, J., Bleier, N., Kovács, V., Olajos, T., Terhes, A. És Demes, T. (2007): A hazai erdők cserjeszintjének szerepe a nagyvad-erdő kapcsolatok alakulásában. Természetvédelmi Közlemények, 13: 119-126.p.
- [13] Biró, Zs., Katona, K., Bleier, N., Lehoczki, R., Újváry, D., Szilágyi, Zs., Markolt, F., Szemethy, L. (2012): A körösladányi vadaskert vaddisznó állományának hatása a védett növényekre. Természetvédelmi Közlemények, 18: 67-76.p.
- [14] Bleier, N., Lehoczki, R., Újváry, D., Szemethy, L., Csányi, S. (2012): Relationships between wild ungulate density and crop damage in Hungary. Acta Theriologica, 57:351-359.p. DOI: 10.1007/s13364-012-0082-0 (IF 2012: 0.949)
- [15] Bleier N., Mátrai K., Lehoczki R., Csányi S. (2007): Cultivated plants in roe deer summer diet in agricultural environment of Hungary. 8th Roe Deer Meeting, Velenje, Slovenia. ERICo. June 25-29, 2007. Book of Abstracts: 62. (Absztrakt)
- [16] Szemethy, L., Katona, K., Biró, Zs., Mátrai, K., Bleier, N., Terhes, A. (2007): Long term study of reddeer for a better management in Hungary. 1st International conference on Genus Cervus, Olaszország, Primiero, Trentino. Abstracts, 107.p
- [17] Katona, K., Szemethy, L., Székely, J., Bleier, N., Nyeste, M., Kovács, V., Olajos, T., Terhes, A., Mátrai, K. (2005) Egy fejtetőre állított rendszer: a gímszarvas és az erdő. III. Magyar Természetvédelmi Biológiai Konferencia, Eger

Comparative Analysis of Fast VR Tour Creation Methods

Éva Hajnal

*Alba Regia Technical Faculty
Óbuda University*
Székesfehérvár, Hungary
hajnal.eva@amk.uni-obuda.hu

Marcell Vámosi

*Alba Regia Technical Faculty
Óbuda University*
Székesfehérvár, Hungary
vam.marcell@gmail.com

Ján Erdélyi

*Department of Surveying
Slovak University of Technology in
Bratislava*
Bratislava, Slovakia
jan.erdelyi@stuba.sk

Gergely László

*Alba Regia Technical Faculty
Óbuda University*
Székesfehérvár, Hungary
laszlo.gergely@amk.uni-obuda.hu

Nikolett Szarka

*Alba Regia Technical Faculty
Óbuda University*
Székesfehérvár, Hungary
szarkanikolett20@gmail.com

Abstract— Nowadays, it's a common practice to create a VR demonstration tour, whether it's for an industrial plant virtual visit, educational material, or a real estate deal. Due to the high resource requirements, creating VR tour applications is still a challenge. Our paper examines the development possibilities of VR tour applications by demonstrating methods that can be implemented with relatively small human resources.

Keywords— VR, Virtual Reality, 360°Image, uv mapping, Unity software, VR Tour.

I. INTRODUCTION

Nowadays, VR tour applications are present everywhere [1], [2]. They can help you explore the major cities of the world, while also taking you to dangerous places or virtual travel to exotic landscapes. It is also being utilized in industrial practice, such as education and real estate. Frequently used as a research methodology in the science, e.g. remote sensing [3] One might assume that building these applications would be a simple, routine task, but it's not the case. A true VR tour, which can be applied to virtual reality devices (Head Mounted Device – HMD), requires the creation of a 3D model of the area to be presented, which must be textured with the surface image of the area or device, i.e. to create a material whose pixels can be accurately projected onto the 3D surfaces by means of a suitable function [1], [4]. Such an application can be traversed at will, using all the degrees of freedom of the 6DOF tool, and can be extended with additional interactive elements, which can provide extra information compared to the real traversal and enrich the experience of the tour. Interactive elements can include animations, text bubbles, video playback, location-based interactive text narration, avatars, etc. Such applications are being developed for robotic tasks, but are also used in health applications. Two ways or a combination of both can be used to produce these 3D models[6]. One way, which can be called the generative method, essentially works by building a 3D model of the area from 3D primitives based on measurements or plans[7]. The other generates a point cloud based on laser scanner mapping, which can be used to create a 3D mesh of the site, and then textured realistically with drawings or photographs of the area [7]. To implement these methods in practice, they often

necessitate a significant amount of memory or computational intensity. By using automatic mapping methods, human labor input can be minimized. The larger the targeted area, the higher the cost of VR implementation, and it is not directly proportional to linear size, but proportional to the volume or to the mapped area, depending on the application, so the method is limited to smaller areas [5]. To perform these tasks with an acceptable use of resources, it is common to use a pseudo 3D solution for this purpose [8], [9]. This paper aims to provide a brief overview of methods for rapid 3D surveying and rapid techniques for building VR tour applications [9]–[13]. Moreover, it will summarize their advantages and disadvantages, and present our own solution in comparison to commercially available or open source applications.

II. METHOD

Data collection for VR tour applications

The authors collected the data, taking into account the use of appropriate fast data collection methods. Fast data collection methods include the possibility of 360-degree photography combined with a laser scanner. The survey was made with a Ricoh Theta Z1 360° camera, with Matterport data recording application.

Although the method is suitable for processing without connecting points, it is advisable to use point marks on external parts and in areas where similar patterns would appear on photographs. This method is called Assisted Alignment by the software. The marks have a unique shape, which ensures identification for spatial positioning.

After visiting the area to be surveyed, these marks must be placed in such a way that they can be formed in the center of the images if possible (so that they suffer minimal distortion), i.e. at the same height as the camera. If this arrangement is not possible, we can also place them on the floor with adhesive tape so that they not move. In terms of the distance of their location, they should be approximately 4.5 meters from the recording locations and from each other.

According to experience, in the case of highly detailed areas such as production lines, the quality of the final result can be improved by placing the positions more densely.

The geometric accuracy can be further improved and the processing can also be performed with other software if the 3D positions of the recording locations are surveyed. This can be done using geodesic methods, we chose a GeoMax total station for the task.

The photographing takes 2-3 minutes per position, the preparation time for each position is roughly the same, so the survey takes about 4-5 minutes per position. Surveying a 20-meter production line takes 20-40 minutes, depending on the recording density and the complexity of the object.

In principle, the processing in the Matterport software is automatic, but experience shows that the automatic alignment function is not the most reliable for this type of application, and therefore involves significant manual work. The reason for this is that alignment errors affect every subsequent survey position, so dozens of positions often had to be placed manually, and the software was often unable to transform the data to the right place the first time.

Overall, it can be stated that, contrary to the promises, it is difficult to achieve a suitable result, at least in an industrial environment, with automatic methods or the use of Matterport, professional photogrammetry software or geodetic procedures may be required.

Rapid implementation techniques for VR tour applications

The implementation of VR tour applications based on real 3D models is a very labor and resource (storage space, computational capacity) intensive task, therefore a simplified solution is attempted, which can be placed between 2D and real 3D depending on the solution used. The solution is based on the fact that the object photographed can essentially be considered as the interior of a spherical surface. More precisely, it is a spherical slice on a roughly flat basis. The human eye can perceive two different images in stereoscopic vision, but it is only noticeable for relatively close objects. The spatial vision of distant objects is determined by their relative size and occlusion. These are the basis for how the brain arranges the virtual space. Creating a spatial experience can be achieved by projecting a 360° image onto the inside of a spherical or cylindrical surface.

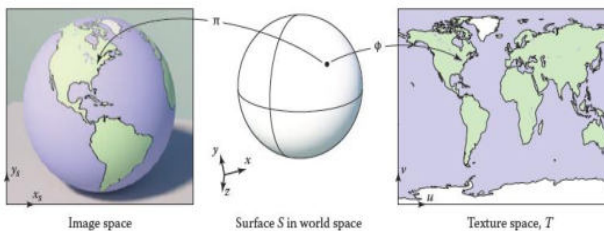


Figure 1: Base concept of UV mapping from rectangular map to a 3D shape.

The UV mapping procedure's basic principle is shown in Fig. 1. In this method function Π is used to switch between the world coordinate system and the coordinate system of the image object, and another function Φ is used to switch between the two-dimensional coordinate system of the image and the three-dimensional coordinate system of the body, or in many cases the polar coordinates of the sphere.

$$\Phi: S \rightarrow T$$

$$: (x, y, z) \mapsto (u, v). \tag{1}$$

Where S is the surface in the world space and T is the surface in the texture space, u, v are texture coordinates and x, y, z are the 3D world coordinates

To calculate the UV mapping, most software divides the 3D object surface into smaller polygons (vertices), and the calculation can be easily done based on the normal vector of each polygon (Fig. 2). There is nothing to do but to negate the normal vectors, then the projection is made onto the inside of the sphere surface and a pseudo 3D illusion is created when viewed from inside the sphere. If the projection is not distorted, then the user can rotate the head around any axis and the experience is sustained, and if the size of the displayed scene is large enough, even small displacements will not break the VR experience. For larger displacements, the 3D nature of the objects already causes the spherical projection to be distorted and the deception becomes obvious. The size of the sphere chosen is an important issue, because with a small sphere the 3D illusion can be broken very easily, while with a very large sphere the computer graphics problems of remote projection are a problem. The other option is an intermediate solution between 3D modelling and spherical projection, with a slightly more detailed survey by creating a 360 image and providing markers to measure dimensions. To create a more realistic VR image, a 3D model of the surveyed area can be calibrated and projected onto it. Linking different locations is difficult or impossible due to the markers.

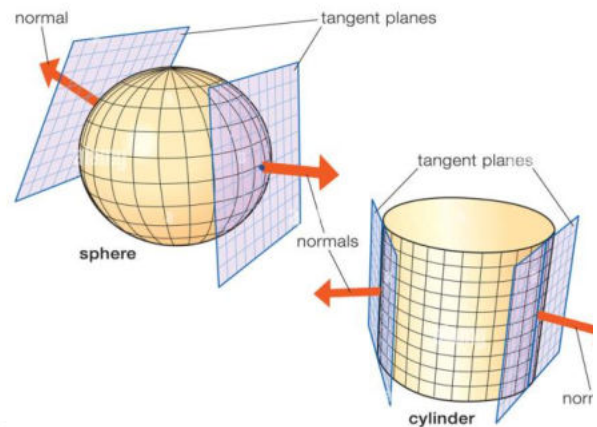


Figure 2 Mapping onto sphere and cylinder with help of the surface normals. It is projected onto the outer side, because of the direction of the surface normals. If the aim is to map onto the inner side of the objects, the direction of the surface normals should be reverted.

III. RESULTS AND DISCUSSION

The experience with the three software solutions identified is summarized in Table 1. Matterport's software is excellent because it facilitates the site survey and then the development of a 3D tour application. The application that is resulting has excellent image quality and is not distorted. The disadvantage of the system is that it is mainly comfortable to use on a computer monitor, but it is even more difficult to use on a VR HMD device, and the survey and VR tour design requires a lot of human labour and geoinformatics expertise. Good quality, simple applications can be created without storing extra information, and 360° images can be exported from the system. In order to create a VR tour application in a VR creator software, we tested VR packages that can be installed using Unity Engine. Unfortunately, both packages we tried

had fundamental problems. The Vour package is a simple VR framework in which a VR application can be developed in a user-friendly way by filling out a form in a control interface without any VR expertise[9]. The same drawback of the system is that there are no scripting options at all to speed up the work of the more experienced, making it an almost impossible task to set up a larger tour. In addition, there are a number of graphical issues with the software. One of the problems is that it does not support the HDRP graphics pipeline and as a result the image quality of the VR application is quite poor. There is a tendency for the picture to be blurred. The graphics engine renders the pixels as a distant image because the image is projected onto an infinite sphere, resulting in a loss of resolution. Because it places the user origin in a large sphere, the user's position is always in the center of the space, so for high interiors it is not possible to get a realistic height viewpoint and it gives the effect of looking down from very high up, the VR space becomes disproportionate. The editing interface of Digital Salmon's application[11] is more advanced, making it easier to edit sophisticated views. The software's spatial handling is comparable to the one mentioned earlier, and the graphical problems mentioned earlier are also present.

Our ÓE VRTour application was created to compensate for the disadvantages in Table 1, and we achieved the following outcome. The user origin is placed in a scalable sphere for imaging.

TABLE I. COMPARISON OF VR SOFTWARES

	Vour[9]	Digital Salmon[11]	Matterport [14]	ÓE VRTour
3D modell	infinite size sphere	infinite size sphere	rough 3D model of the target	parametric sized sphere
UI	user friendly non scriptable	user friendly non scriptable	user friendly non scriptable	scriptable
Extra elements (video, textblocks, voice)	+	+	-	+
Resource need for VR tour	time	time	time+ expertise	expertise
Image Quality	Poor	Poor	Excellent	Normal
Target device	HMD	HMD	Screen	HMD
VR artifacts	yes	yes	no	minimal

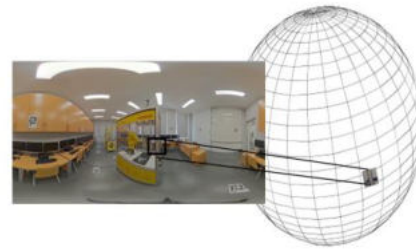


Figure 3. 360°Image of Industrial Robotics Laboratory of ÓE AMK. The image is projected onto the spherical vertex.

As the sphere is scalable, it is advisable to choose the size of the sphere to match the height of the ceiling, which in the example shown is 4m. Within this, the user origin should be adjusted to the normal human eye level. In the future this will be calibrated for different body heights, currently the software is fixed at 1.6m eye height. As shown in Fig. 3, the 360°Image is projected by the software onto the surface of the sphere. A special shader program is used to project not only the outer but also the inner surface. The vertex density (number of polygons) of the used spherical model was set to dense in a 3D modelling application, so that the texturing is more accurate. Fig. 4 shows the 360°Image has already projected onto the sphere, and you can see that the contour is quite smooth and circular due to the increased number of polygons in the mesh. The resulting VR experience can be seen from inside the sphere (Fig. 5). It can be seen that the resulting image is of good quality, proportional, roughly color correct, i.e. it can deliver the VR experience needed. Unfortunately, the image quality is still not perfect, as the graphics engine applies lossy compression during rendering to achieve a proper computational intensity for 90 fps processing, which causes a minor degradation in quality.

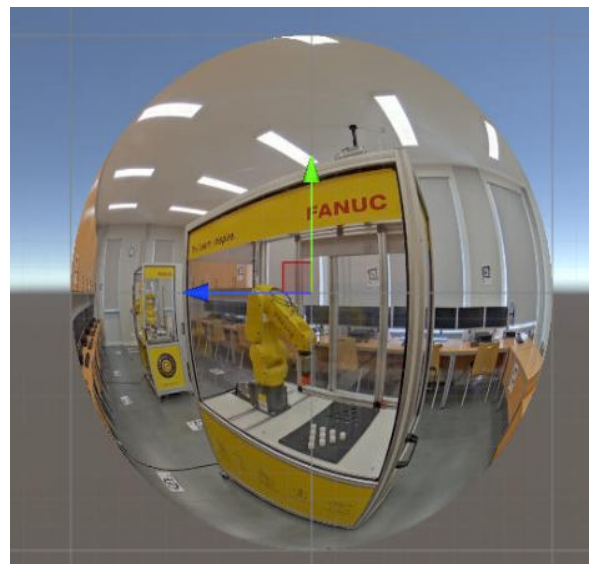


Figure 4. Image projected onto the outer surface of the sphere

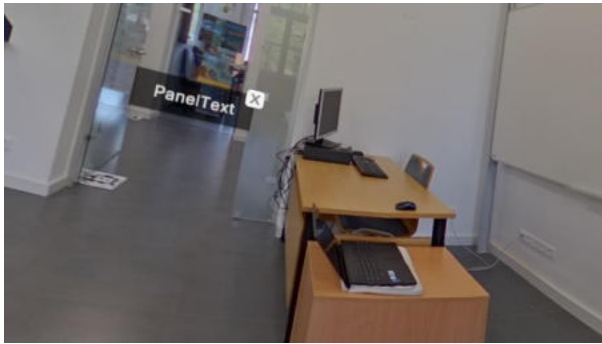


Figure 5 Image projected onto the inner surface of the sphere and the user is in the center of the sphere and the image gives real VR experience.

Commercially available software allows 3 degrees of freedom of movement, which means rotating the head around 3 axes. Our own software has slightly extended this to 6 degrees of freedom, which in practice allows 3 degrees of freedom of rotation and 3 degrees of freedom of small displacement of up to 0.5m. The distortion caused by the projection of the sphere is already present in this larger movement. A collider object that is placed inside the sphere limits displacements above 0.5 m and prevents exit from the sphere. The result of the running application is shown in Fig. 5 The application is easy to use for a person with little programming knowledge, because after importing the images, the VR tour script essentially builds the tour based on a sheet, and this sheet has to be edited and parameters added. Additional information, like a text block as depicted in the figure, can also be displayed by the application, and it can also play a video. The app is equipped with a map navigation assistant, where you can see the planned route on a map, but you can also navigate in the displayed world individually based on the map.

IV. CONCLUSION

VR tours apps have become very popular. Many of these applications can be seen on the internet and we also receive orders for them as development tasks. VR tours are being developed by many institutions to demonstrate their infrastructure. Experience has shown that there are only a few VR tour applications that are truly good quality and provide the right user experience on HMD devices. The reason for this is that the fast VR tour development methods are not meeting the modern requirements. We have analyzed the available software solutions and rapid VR development options that are relatively cost-effective. Despite the fact that this genre may seem trivial, there are no truly challenging applications in the market for its development, as it was found. Our own VR framework was created because of this reason. This publication presents the first step that is usable. Our software is superior in certain aspects to the other softwares that were tested. The quality of the image, image proportions, and user degree of freedom have been improved. Our VR application has some essential elements that can enhance its quality

compared to other software. However, it was developed for our own purposes and now some fashion functions are missing. We are optimistic that we will be able to develop our application further and create a product that can be published in the future.

ACKNOWLEDGMENT

We would like to thank the help and the effort of colleagues and students. The financial support of this paper was from Arconic 2022 grant.

REFERENCES

- [1] E. Fedkin, S. Kumargazhanova, S. Smailova, N. Denissova, and G. Györök, "Considering the Functioning of an e-learning System, Based on a Model for Assessing the Performance and Reliability of the System," *Acta Polytech. Hungarica*, vol. 19, no. 2, pp. 93–112, 2022.
- [2] E. Dobra and É. Nagyné Hajnal, "Virtual Reality Game Development with External Hand Motion Sensor," in *AIS 2022 - 17th International Symposium on Applied Informatics and Related Areas - Proceedings, 2022*, pp. 121–124. [Online]. Available: <https://m2.tmt.hu/api/publication/33263472>
- [3] Q. Meng *et al.*, "Relationships between land surface temperatures and neighboring environment in highly urbanized areas: Seasonal and scale effects analyses of Beijing, China," *Remote Sens.*, vol. 14, no. 17, p. 4340, 2022.
- [4] Z. Nagy *et al.*, "STATISTICAL VALIDATION OF A HIGH PRECISION CELL SIZE MEASUREMENT SOFTWARE," in *Annual University Scientific Conference 2021, 2021*, pp. 714–725. [Online]. Available: <https://m2.tmt.hu/api/publication/32129131>
- [5] S. Marschner and P. Shirley, *Fundamentals of Computer Graphics*, 4th ed. 2016.
- [6] M. Slater, "Enhancing Our Lives with Immersive Virtual Reality," vol. 3, no. December, pp. 1–47, 2016, doi: 10.3389/frobt.2016.00074.
- [7] É. Nagyné Hajnal, M. Seebauer, D. Marton, K. Széll, B. Tőke, and M. Rick, "Virtual Reality Laboratory in the Help of Research and Education," in *15th International Symposium on Applied Informatics and Related Areas organized in the frame of Hungarian Science Festival 2020: AIS 2020, 2020*, pp. 29–32. [Online]. Available: <https://m2.tmt.hu/api/publication/31662634>
- [8] M. Gonzalez-franco and J. Lanier, "Model of Illusions and Virtual Reality," *Front. Psychol.*, vol. 8, no. June, pp. 1–8, 2017, doi: 10.3389/fpsyg.2017.01125.
- [9] C. Games, "Vour - Virtual Tour Creation Tool." <https://assetstore.unity.com/packages/tools/utilities/vour-virtual-tour-creation-tool-188053>
- [10] V. Valls, "How to make a 360° image viewer with Unity3D." <https://medium.com/game-development-stuff/how-to-make-a-360-image-viewer-with-unity3d-b1aa9f99cabb>
- [11] D. Salmon, "Complete 360° Tour." https://assetstore.unity.com/packages/templates/systems/complete-360-tour-85014#asset_quality
- [12] "How to Use Equirectangular Image in Unity." https://www.google.com/search?rlz=1C1CHBD_huHU1015HU1015&sca_esv=568406902&cs=0&sxsrf=AM9HkKlk8ImxD-iL-BQBYkMogcjuCwff8A:1695704740126&q=Unity+360+image+Viewer&sa=X&ved=2ahUKewjpbpO1wMeBAxVA2AIHHWfAAw4QpboHKAB6BAGBEAI&biw=1707&bih=830&dpr=1.13#fpstate=ive (accessed Sep. 20, 2023).
- [13] H. McLellan, "15. virtual realities," no. 1992, 1994.
- [14] Matterport, "Tools for everything you want to do." <https://matterport.com/3d-capture-applications>

Surface restoration based on scanning data

Alexander Krasavin
*School of Digital Technologies and
 Artificial Intelligence*
*D Serikbayev East Kazakhstan
 Technical University*
 Ust-Kamenogorsk, Kazakhstan
akrassavin@ektu.kz

Maral Tolykbayeva
*School of Digital Technologies and
 Artificial Intelligence*
*D Serikbayev East Kazakhstan
 Technical University*
 Ust-Kamenogorsk, Kazakhstan
maralsamekenova@mail.ru

Assel Kussaiyn-Murat
*School of Digital Technologies and
 Artificial Intelligence*
*D Serikbayev East Kazakhstan
 Technical University*
 Ust-Kamenogorsk, Kazakhstan
akussaynmurat@edu.ektu.kz

Albina Kadyroldina
*School of Digital Technologies and
 Artificial Intelligence*
*D Serikbayev East Kazakhstan
 Technical University*
 Ust-Kamenogorsk, Kazakhstan
akadyroldina@gmail.com

Darya Alontseva
*School of Digital Technologies and
 Artificial Intelligence*
*D Serikbayev East Kazakhstan
 Technical University*
 Ust-Kamenogorsk, Kazakhstan
dalontseva@ektu.kz

Abstract— The main purpose of 3D scanning is to create a three-dimensional model of the scanned object. There are several different standard formats for describing 3D models, for example, those where the geometric shape of an object is specified by a set of slices, where the surface of the object is approximated by a triangular mesh. However, in a number of tasks, such as automatic generation of the trajectory of a robot processing a surface, an analytical description of the surface is most convenient. Often the scanned surface cannot be approximated by a smooth function with acceptable accuracy. However, the use of the surface segmentation procedure makes it possible to construct an analytical representation of the reconstructed surface by a piecewise continuous function. Segmentation is the division of a complex surface into geometrically homogeneous sections. Often, within a segment, the restored surface allows a simple analytical description. The paper describes a surface segmentation method based on calculating Gaussian and mean curvature for local surface approximations by second-order polynomials.

Keywords—surface restoration, point clouds, segmentation.

I. INTRODUCTION

The use of surface restoration methods is widespread in many fields of science and industry, including computer-aided design, medical imaging, safety monitoring, urban architectural renovation, reverse engineering, etc.

Surface reconstruction algorithms differ in terms of input point data and output reconstructed surfaces, where the input data can range from a single depth image to a point cloud or a point cloud with normals or scales, and the structure of the result can be divided into a surface representation, which is a parametric surface implicit surface or triangulated surface mesh, and dependence on the input data, in which the degree of dependence on the input data can vary from interpolation of all input data to interpolation of a subset of input data or approximation of input data [1].

The initial and important step in surface restoration is data acquisition or data collection. The data used to reconstruct the surface of objects is usually collected by scanning existing objects using 3D technology and is

obtained in the form of structured or unstructured point clouds. A point cloud is considered unstructured when it lacks connectivity information and structural information such as edge and face information. Typically, unstructured point clouds contain only spatial location information, accompanied by noise, incompleteness, and sampling irregularity [2].

To solve the difficulties that arise when working with unstructured point clouds, a number of surface restoration methods have been proposed in the literature, for example, also in [2] these methods include interpolation methods, approximation methods, learning-based methods, and soft computing surface restoration methods. The predominant surface restoration methods are the triangular mesh method, the 3D surface fitting method, and the surface restoration algorithm based on regional expansion [3].

Many surface reconstruction problems from point clouds can be more or less solved using various regularizations of surface geometry, but the problems of mismatches, missing points, and outliers remain unresolved, although data-driven approaches using deep learning show significant promise for surface modeling and reconstruction, including their ability to overcome various data deficiencies, systematic experiments suggest that these methods are difficult to generalize to complex shape reconstruction [4].

The process of constructing a 3D model of an object, in turn, occurs in 3 stages. At the first stage, the scanning plane is divided into many circles of the same radius, forming a coverage of the scanning area. The surface inside the circle is approximated by a second-order surface. At the second stage, surface segmentation is carried out, and small areas with completed local approximation are combined into geometrically homogeneous macroregions. At the third stage, the optimal parameters of the model as a second-order surface are calculated for each region.

II. METHODS

An important factor for the successful use of a point cloud when creating a 3D model in surface restoration is the segmentation stage. Segmentation is the division of a complex surface into geometrically homogeneous sections and reference points within the area in which point scanning with a simple analytical description will be performed. The greatest difficulty in building an adequate analytical 3D model is a surface with sharp kinks, since existing segmentation methods are mainly optimized for approximating smoother surfaces. Therefore, solving the

problem of surface segmentation remains relevant in the field of 3D scanning to enable scanning and analysis of all types of surfaces. The new segmentation algorithm used in this work has been proven and presented in detail in publications [5-9].

The immediate result of the scanning procedure is the so-called point cloud - an unstructured set of sets of spatial coordinates of points belonging to the scanned surface. The method of surface reconstruction from 3D scanning data described in the article was developed for processing data from a 3D scanner based on a laser triangulation distance sensor. Data from triangulation distance sensors are characterized by a high degree of noise, which does not allow the use of direct surface restoration methods. The proposed method is designed to reconstruct a surface from noisy data. Another important feature of the method is the output format of the recovery procedure. The proposed method constructs an approximation of the scanned surface by a piecewise smooth analytical function of two variables. Below we present a number of assumptions made when developing the method. It is assumed that the scanned surface can be described by the function $z(x,y)$, where z can be interpreted as the distance from a point on the surface with coordinates (x,y,z) in three-dimensional space to the XY plane (interpret z as the height of the point above the XY plane). The cloud of points is an unordered set of sets of coordinates of points $P_i = (x_i, y_i, z_i)$ (index i varies in the range from 1 to N , where N is the number of points equal to the number of distance measurements taken during the scanning procedure from the sensor to the scanned surface) in a three-dimensional Cartesian coordinate system. It is assumed that the projections of points onto the XY plane define a certain closed region D on the plane ("minimal" region covering all projections of cloud points onto the XY plane). (Note: the boundary of this area will, of course, be a polygon, the vertices of which will be the projections of some points of the cloud onto the plane.). The process of constructing a 3D model of an object, in turn, occurs in 3 stages. At the first stage, the area D is divided into many overlapping circles of the same radius, forming a covering of the scanning area D . The surfaces inside the circle are approximated by a second-order surface. At the second stage, surface segmentation is carried out, and adjacent small areas with a similar geometric structure are combined into geometrically homogeneous macroregions. At the third stage, the optimal parameters of the model as a second-order surface are calculated for each homogeneity region. The originality of the proposed method lies mainly in the segmentation procedure.

The main idea of the proposed segmentation method is to use, as criteria for the similarity of the geometric structure of surface areas, two numerical characteristics of a smooth surface area - average and Gaussian curvature at point P belonging to the surface area (it is assumed that this point represents one way or another a certain geometric center of this surface area). As is known, a paraboloid touching a smooth surface at point P has the same values of these quantities (Gaussian and mean curvature) at the point of contact as the surface. Moreover, based on the direction of the normal to the surface at point P and the values of the average and Gaussian curvature of the surface at this point, one can unambiguously reconstruct the paraboloid tangent to the surface at point P . Thus, if a group of adjacent sections of the surface has close (ideally coinciding) values

two of these parameters, then these areas can be combined into one "large" fragment of the surface, which can be approximated by a second-order surface. Below we will concretize what was said above, indicating the exact geometric meaning of the concepts of mean and Gaussian curvature and present a method for calculating the mean and Gaussian curvature from the coefficients of local approximation of the reconstructed surface by a second-order polynomial.

The concept of surface curvature is closely related to the concepts of principal directions at a point on the surface. In turn, the concept of principal directions naturally arises from consideration of the question of the curvature of curves on a surface passing through a given point on the surface. Let γ be a curve on an elementary surface Φ defined by the parametric equation $r = r(u, v)$. Let us define it by an equation with a natural parameter: $r = c(s)$, $c(s) = r(u(s), v(s))$. Let $P \in \gamma$, ν is the unit vector of the principal normal to γ at point P , and n is the unit normal vector to the surface. Let $\theta = \angle(\nu, n)$, and k is the curvature of the curve γ at point P . Let us denote $k_0 = k|\cos\theta|$, where $\ddot{c} \cdot n = L(\dot{u})^2 + 2M\dot{u}\dot{v} + N(\dot{v})^2 = II(\dot{c}, \dot{c})$.

As γ we consider the curve that is obtained in the section of the surface by the plane α passing through P parallel to the vector n (Fig. 1). Then the vector of the main normal ν to the curve γ at point P will lie in this plane and will be perpendicular to the tangent. This means $\nu \parallel n$ and $|\cos\theta| = 1 \Rightarrow k_0 = \pm k$. Therefore, the value k_0 is called the curvature of the normal section of the surface at point P in the direction of the curve γ or normal curvature. Let us give this quantity a sign so that the formula is correct

$$k_0 = \frac{II(c', c')}{I(c', c')} \tag{1}$$

It is in this formula that Meusnier's theorem lies.

We see that the value k_0 does not depend on the choice of a specific parameterization of the curve γ , but depends only on the direction of the tangent vector c' at point P . Therefore, we can determine the normal curvature of the surface in the direction of the vector ξ lying in the tangent plane:

$$k_0 = \frac{II(\xi, \xi)}{I(\xi, \xi)} \tag{2}$$

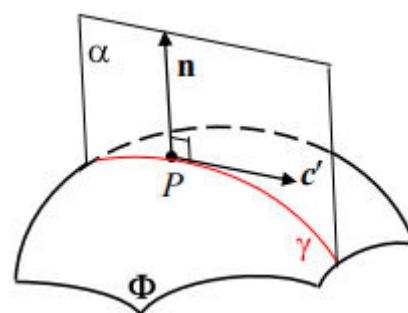


Fig. 1. γ curve in a section of a surface by a plane α passing through P parallel to the vector n

By choosing an orthonormal basis, any quadratic form in Euclidean space can be reduced to diagonal form. This means that by choosing an orthonormal basis (e_1, e_2) in the tangent plane π to the surface Φ at a given point P , we can reduce the II quadratic form to a diagonal form:

$$II(\xi, \xi) = 1 \cdot \xi_1^2 + 2 \cdot \xi_2^2 \quad (3)$$

Since the basis is orthonormal, then $I(\xi, \xi) = \xi \cdot \xi = \xi_1^2 + \xi_2^2$.

Let us denote $S^1 = \{\xi \mid |\xi| = 1\}$ - the set of all unit vectors from the tangent plane. Their ends form a circle. Then for $\xi \in S^1$ we have $I(\xi, \xi) = \xi \cdot \xi = 1$.

Let α will be the angle between vectors e_1 and ξ , and $k(\alpha)$ the normal curvature of the surface in the direction of vector ξ . Then $\xi_1 = |\xi| \cos \alpha$, $\xi_2 = |\xi| \sin \alpha$.

Substituting this into (3), we get

$$k(\alpha) = 1 \cdot \cos^2 \alpha + 2 \cdot \sin^2 \alpha \quad (4)$$

This formula is called Euler's formula. It follows from it that the maximum and minimum of the function $k(\alpha)$ are 1 and 2, and they are achieved at $\alpha = 0$ and $\alpha = \pi/2$, i.e. in the direction of vectors e_1 and e_2 .

Numbers 1 and 2 are called the principal curvatures of the surface at point P, and the directions of the vectors e_1 and e_2 are called the principal directions of the surface at point P. The value $K = 1 \cdot 2$ is called the Gaussian curvature of the surface, and $H = \frac{1}{2}(1 + 2)$ is the mean curvature. According to Vieta's theorem, 1 and 2 are the roots of the quadratic equation

$$2 - 2 \cdot H \cdot \lambda + K = 0 \quad (5)$$

Thus, knowing K and H, we can find 1 and 2.

For each point, the four local curvature values K, H, values 1 and 2 can be automatically obtained as functions of the coefficients of the approximating polynomial. In addition, such curvatures are invariant to the adopted reference system, which is a very important property when analyzing the shape of a surface, that is, depending on the average and Gaussian curvature and their combination, the type of surface being approximated is determined.

III. RESULTS AND DISCUSSION

After carrying out the local approximation procedure in all microregions, based on the data obtained, the second stage of constructing an analytical surface model is carried out - segmentation. To identify geometrically homogeneous areas of the scanned surface, we used one of the variants of the so-called region growing algorithm. Algorithms of this family are widely used in image processing technology to select areas in digital images that satisfy a certain specified criterion (for example, to select areas of the same color in color images). The region growth algorithm is very similar to the well-known wave algorithm in computer science (also known as Lee's algorithm [10]) for finding the shortest path between the vertices of a graph. The input of the algorithm is a graph. The vertices of the graph are the centers of circles (areas in which the surface is locally approximated by second-order polynomials), forming a rectangular grid. The mesh spacing is chosen so that the circles form a covering of the plane.

The algorithm operates with two sets of vertices (grid nodes) - a boundary, which can be considered as the front of a propagating wave, and a set of marked nodes, which includes internal points of the area limited by the boundary polygon (relatively speaking, these are points along which the wave has already "passed").

At the initialization stage, the set of boundary points consists of one element - the starting point, and the set of marked points is empty. Wave propagation is simulated by a procedure that constructs a new front based on the current position of the front. In this case, for each point included in the boundary (front) set, all points adjacent to it are viewed. If any of the adjacent points is not included in either the set of boundary or the set of marked points, does not belong to the new boundary being constructed and satisfies the similarity criterion, then it is included in the new boundary. In fact, at the stage of wave propagation, a simulation of the construction of a wave front occurs using the Huygens principle, i.e. each point of the wave front is considered as a point source of spherical waves. The iterations of constructing a new front (a set of boundary points) are resumed until it turns out that the procedure for constructing a new front returns an empty set (further expansion of the region is impossible).

The surface segmentation algorithm is based on the procedure for constructing a region of homogeneity at a selected starting point, as a sequence of iterations, schematically depicted in the block diagram shown in Figure 2.

The algorithm is a variation of the exhaustion method. The set of points that do not belong to any of the constructed homogeneity regions (indicated in the block diagram as the FreePoints set) is initially initialized by the entire set of vertices (centers of circles that define the local approximation regions). Using the GetSeedPoint procedure, a starting point is selected from the current set of free points (points that do not belong to any of the already constructed regions) for constructing a new region. The homogeneity region constructed from the selected starting point is added to the set of homogeneity regions NewRegions, and the points included in this region are removed from the FreePoints set.

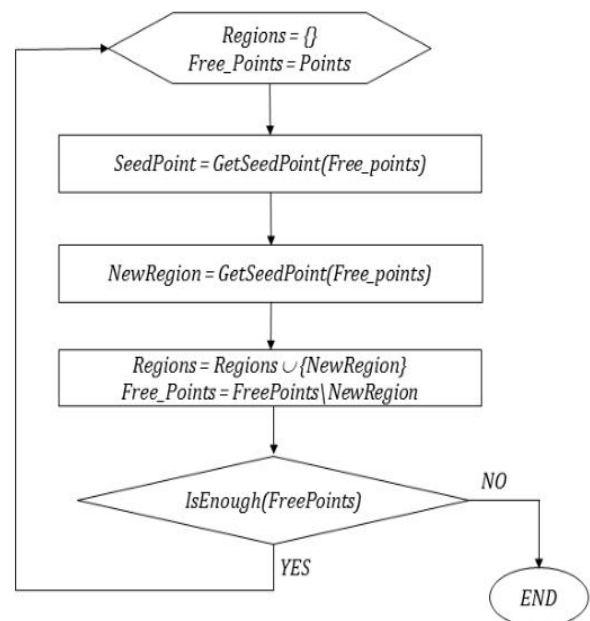


Fig. 2. Flowchart of surface segmentation algorithm [5]

The procedure is repeated until the number of points that do not belong to homogeneity regions is less than a given number (strictly speaking, the IsEnough procedure does not simply check the number of free points, but finds connected regions in the set of remaining “free” points and estimates the sizes of connected regions). During the experiments, we tested several different algorithms for selecting a starting point. According to our observations, a preferable selection algorithm is based on an analysis of the distribution of the parameter K , in which the point at which the value of the parameter K is closest to the “most probable value” found from the distribution is selected as the starting point. The last stage of the algorithm for constructing an analytical surface model - constructing an approximation in regions of homogeneity is quite standard and does not need description.

To restore the surface from 3D point scanning data, a computer program was developed in the C# programming language using the freely distributed IDE Microsoft Visual Studio Express 2017. The program takes as input a set of three-dimensional coordinates of surface points, the so-called point cloud, measured during the 3D scanning procedure. It is assumed that coordinate measurement data can be significantly noisy, so direct methods for surface reconstruction are not adequate for the task. The program builds a piecewise linear function of two variables (polygonal representation of a 3D surface), approximating the scanned surface, allows you to save a description of the reconstructed surface (strictly speaking, a polygonal approximation of a function of two variables describing the surface) in a text file for further use, and also visualize the resulting surface model. The interface of the developed program and images of the models obtained on it can be seen in Figures 3-5.

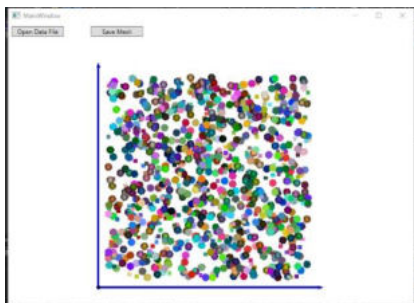


Fig.3. Screenshot of the main program window before loading data (immediately after starting the program)

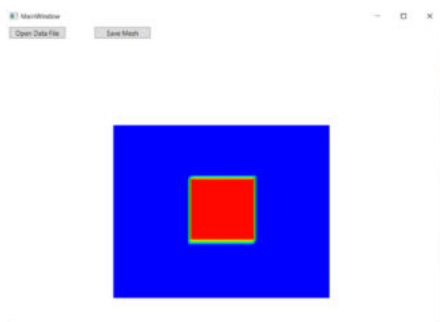


Fig. 4. Screenshot of the resulting model in three-dimensional space (top view)

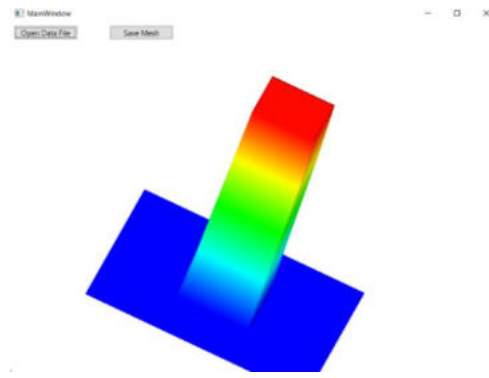


Fig. 5. Screenshot of the resulting model in three-dimensional space, obtained by simulating rotations

IV. CONCLUSION

In this study, an original algorithm for the surface segmentation procedure was developed with the construction of an analytical surface model, which creates convenience for solving the problem of automatically generating a robot trajectory. This method is based on calculating Gaussian and mean curvature for local approximations of the surface by second-order polynomials. The algorithm is based on the use of a local parametric model and the subsequent combination of local surface sections with a homogeneous geometric structure, which allows, without a priori assumptions about the geometric structure of the surface, to build an analytical 3D model of a surface with a complex structure.

Using a new algorithm developed, a program for surface restoration based on 3D point scanning data is proposed, which takes as input a set of three-dimensional coordinates of surface points, the so-called point cloud, measured during the 3D scanning procedure. The program allows you to save a description of the reconstructed surface in a text file in the form of a polygonal approximation of a function of two variables describing the surface for further use, as well as visualize the resulting surface model.

Since the software prototype was created, it was tested on the basis of synthetic data that was generated independently. Comparisons with existing methods were not carried out. Although we are satisfied with the results of the experiment, but this is not enough, additional work needs to be done to create software for comparative research. Software metrics were not obtained, since the software was created solely to indicate the operability and suitability of the algorithm.

ACKNOWLEDGMENT

This research was funded by the Science Committee of the Ministry of Education and Science of the Republic of Kazakhstan (Grant No. AP13068317).

REFERENCES

- [1] Matthew B., Joshua A. L., Luis G. N., Gabriel T., Claudio T. S. A benchmark for surface reconstruction // ACM Transactions on Graphics. – 2013. -Vol. 32, Issue 2. – P. 1-17.
- [2] You C.C., Lim S.P., Lim S. C., Tan J.S., Lee C.K., Khaw Y.M.J. A survey on surface reconstruction techniques for structured and unstructured data // IEEE Conference on Open Systems (ICOS). – 2020. P. 37–42.

- [3] Yuan-Zhi L., Min G., Ou Sh., Hong-Yu Zh. 3D Point Cloud Surface Reconstruction Based on Divide-and-Conquer Method in Laser Scanner // Journal of Physics: Conference Series. – 2020. – Vol. 1544, Issue 1. – P. 012118.
- [4] Zhangjin H., Yuxin W., Zihao W., Jinjuan R., Kui J. Surface Reconstruction from Point Clouds: A Survey and a Benchmark // Computer Vision and Pattern Recognition. -2022. - arXiv preprint arXiv:2205.02413
- [5] Kadyroldina A. *Intellektual'naya robotizirovannaya sistema dlya plazmennoj obrabotki izdelij slozhnoj formy*: Dissertaciya na soiskanie stepeni doktora filosofii (PhD) [Intelligent robotic system for plasma processing of complex-shaped products: Thesis for the degree of Doctor of Philosophy (PhD)]// Ust Kamenogorsk. –2021. - p. 44-55.
- [6] Alontseva D. L., Krasavin A., Shadrin G., Kadyroldina A., Kussaiyn-Murat A.T. Razrabotka sistemy upravleniya promyshlennym robotom-manipulyatorom dlya trekhmernogo skanirovaniya poverhnostej (Development of a control system for an industrial robotic manipulator for three-dimensional scanning of surfaces) // Vestnik VKGTU im. D.Serikbaeva. – 2019. - No 1. - p. 81-87.
- [7] Alontseva D. L., Krasavin A. L., Kadyroldina A. T., Kussaiyn-Murat A.T. Razrabotka sistemy 3D skanirovaniya dlya intellektual'noj robotizirovannoj sistemy plazmennoj obrabotki i rezki krupnogabaritnyh izdelij slozhnoj formy (Development of a 3D scanning system for an intelligent robotic system for plasma processing and cutting of large-sized products with complex shapes)// Vestnik VKGTU im. D.Serikbaeva – 2018. - No 1. – p. 7-19
- [8] Alontseva D., Krasavin A., Kadyroldina A., Kussaiyn-Murat A. Segmentation Algorithm for Surface Reconstruction According to Data Provided by Laser-Based Scan Point// Communications in Computer and Information Science. – 2019. -Vol 998. - p. 1-10.
- [9] Kadyroldina A., Kussaiyn-Murat A., Beszedes B., Alontseva D., A. Krasavin. Image Acquisition and Processing on Raspberry Pi in Matlab for 3D Scanning // 14th International Symposium on Applied Informatics and Related Areas (AIS 2019). – 2019. November 14, 2019. – p. 39-42.
- [10] Rubin F. The Lee Path Connection Algorithm // IEEE Transactions on Computers. – 1974. - Vol. C-23, Issue 9. – p. 907 – 914.

A novel method for the identification of flat curves

Alexander Krasavin

*School of Digital Technologies and
Artificial Intelligence*
D Serikbayev East Kazakhstan
Technical University
Ust-Kamenogorsk, Kazakhstan
akrassavin@ektu.kz

Darya Alontseva

*School of Digital Technologies and
Artificial Intelligence*
D Serikbayev East Kazakhstan
Technical University
Ust-Kamenogorsk, Kazakhstan
dalontseva@ektu.kz

Assel Kussaiyn-Murat

*School of Digital Technologies and
Artificial Intelligence*
D Serikbayev East Kazakhstan
Technical University
Ust-Kamenogorsk, Kazakhstan
akussaynmurat@edu.ektu.kz

Albina Kadyroldina

*School of Digital Technologies and
Artificial Intelligence*
D Serikbayev East Kazakhstan
Technical University
Ust-Kamenogorsk, Kazakhstan
akadyroldina@gmail.com

Arailym Orazova

*School of Digital Technologies and
Artificial Intelligence*
D Serikbayev East Kazakhstan
Technical University
Ust-Kamenogorsk, Kazakhstan
arailym-vko@mail.ru

Abstract—The article presents a new method for the identification of flat curves invariable to subgroup of 2D transforms (rotation and zooming). The key idea of the proposed method is that a flat curve is associated with a function of one variable specified on a fixed interval. This function, which we will call the characteristic curve function, is used directly in the feature extraction process. Namely, the coefficients of the Fourier series of the characteristic function of the curve are used as a set of features in the proposed method. The method was developed for handwritten character recognition tasks. In these applications, the input to the procedure was polylines obtained by applying a line extraction algorithm to a digital image. But the proposed method is also suitable for smooth plane curves identification. The article also discusses the possibility of applying the main ideas of the method to some robotics problems.

Keywords—flat curve identification, image recognition, symbol recognition.

I. INTRODUCTION

Image recognition has consistently remained a prominent research topic within the realm of computer vision. Its primary objective is to instruct models in the automatic identification of object categories present within a provided image. Image recognition technology emulates the cognitive process of human visual perception using computer technology, modern information processing techniques, and other technical tools. It involves extracting image features through various image processing methods and utilizes these extracted features as the foundation for the ultimate classification and recognition of objects within images. Over the past few years, as machine learning and computer vision have experienced rapid advancements, image classification and recognition have gained widespread application across diverse domains [1, 2]. For instance, it is employed in security for facial recognition technology, in transportation for vehicle recognition, and in aerospace for aviation remote sensing, among other areas.

In the initial stages of image recognition, the predominant approach was based on manual features. This approach encompassed several fundamental steps, including image preprocessing, extracting image characteristics, and designing classifiers. A critical aspect of traditional image recognition methods was the careful selection and design of

these manual features. These manual features typically encompassed attributes like color, texture, shape, and gradient, and specific examples included techniques such as Histogram Of Oriented Gradient (HOG), Local Binary Patterns (LBP), Scale Invariant Feature Transform (SIFT), Speeded-Up Robust Features (SURF), and Scale invariant local ternary pattern (SILTP). While this traditional approach demonstrated effectiveness for straightforward images, it fell short in terms of accuracy when confronted with more intricate or subtly distinct images, failing to meet the actual requirements of such applications.

The process of identifying graphical patterns stands out from other methods of pattern recognition due to its distinct approach. It involves several preliminary stages of preprocessing the input information. In the initial phases, the image undergoes transformations to make it suitable for subsequent analysis. Following this, a critical step involves selecting the type and quantity of informational attributes that can facilitate pattern recognition, whether with or without a reference sample [3].

Among these methods, the most crucial stage is the selection of informative attributes. These attributes play a pivotal role in distinguishing a pattern from a group of surrounding objects. Gostev, and Sevastianov in paper [4] presented the results of a methodology developed to establish a set of properties that remain invariant under such two-dimensional affine transformations. They explored two metrics that can be used to identify curves using a set of properties generated in a preprocessing step.

The proposed method for identifying plane curves was developed for use in handwritten character recognition tasks. Although applications of the method are not limited to the field of optical recognition of handwritten characters, in this article we will use examples from this area in which we have accumulated some experience. We focused our attention on character recognition methods based on transforming character images into a planar graph. According to the definition of a planar graph, there is a one-to-one mapping of the set of vertices of the graph to the set of points on the plane. Accordingly, each graph edge corresponds to a line segment in the plane, and the segments corresponding to different edges can intersect only at the end points. Each path in the graph corresponds to a simple polyline on the image plane. Suppose we have a digital

photo of handwritten symbols drawn with thin lines (for example, written in pen on paper). After applying the conversion procedure to this image, each isolated symbol will correspond to a connected component of the resulting planar graph. The curves forming the images of the symbol will be approximated by polylines (simple or closed) corresponding to the paths and cycles in the graph (see Fig.1). We have developed two algorithms for converting a raster image to a planar graph.

We developed software that implements these algorithms and used it for experiments with character recognition of decimal digits on real photos. Immediately, we note that the input data for character recognition procedures, including the feature extraction procedure, are the connected components of the planar graph. Thus, the planar graph obtained as a result of applying the conversion procedure contains all the necessary information for recognition, and after converting the image into a planar graph, the original image is not used in the recognition procedures.

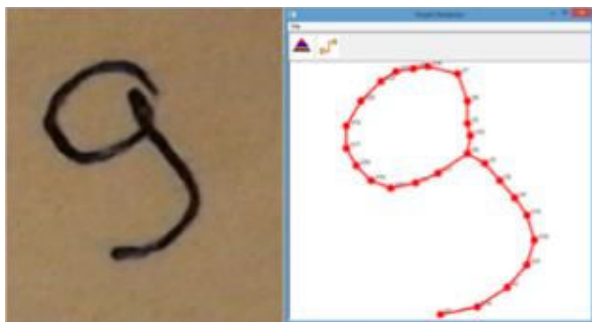


Fig. 1. A fragment of a digital photo (left image) and a screenshot of the "GraphRedactor" window (right image) with the image of the planar graph of the digit symbol "9" obtained when converting an image into a graph.

The key idea of the proposed flat curve identification method is the use of a special function to identify the shape of a simple smooth curve without self-intersections. We called this function the "curve angular characteristic function." This characteristic is invariant with respect to such transformations of the plane as rotation and zooming, which makes it very convenient for use in curve identification tasks. The mathematical construction of the function of the angular characteristics of the curve is easily transferred to simple broken lines. We use the vector coefficients of the window Fourier transform as a feature vector for identifying the polylines corresponding to the paths in the planar graph. The concept of the function of the angular characteristic of a curve is discussed in detail in the section "Function of the angular characteristic of a curve".

II. METHODS

Graph analysis and angular characteristic function

There are two types of geometric primitives that we can directly classify using the methods proposed in this paper, namely, curves without self-intersections with two ends and closed curves without self-intersections. In the planar graph of the symbol, the objects of the first type correspond to the paths between the vertices of the graph, and the objects of the second type correspond to the cycles of the graph. Some

symbols of decimal digits (for a specific spelling) are objects of the first group (for example, numbers 1 2 3 5), and their planar graphs are trees with two leaves. Obviously, if the planar graph is a tree whose vertices v_1 and v_2 are leaves and the graph has no other leaves, then a broken line corresponding to the path in the graph connecting the vertices v_1 and v_2 will be the most suitable object for classifying. But even if the connected component of a planar graph is a tree, then in more complex cases, the choice of paths between the vertices to classify this component becomes a task that allows for many solutions. For example, planar graphs of decimal digits 4 and 7 (in some cases of spelling) are a 'cross', i.e., a tree with 4 leaves, only one vertex of which A has a degree greater than 2 (more precisely $deg(A) = 4$) (see Fig. 2). In any case, it is necessary to apply some combinatorial procedures to select a classification scheme for such objects. For example, we can choose two unordered pairs from the set of the leaves of this tree, and use paths between pairs of vertices (B, D) and (E, C) for recognition. But it is clear that even if these paths are recognized as elements of the digit "4", this does not at all mean that we can classify this planar graph as the symbol of the digit "4". It is necessary to carry out additional procedures, based on the results of the first stage of classification, namely, to classify paths between the vertices (B, E) and (D, C).

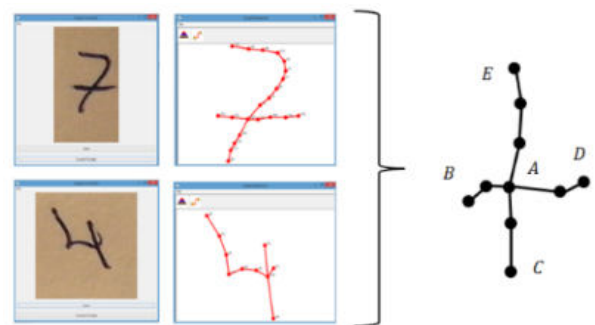


Fig. 2. Symbols of decimal digits '7' and '4' has same planar graph topology.

Thus, the results of the graph analysis stage determine the rules by which the classification procedure will be conducted. Graph analysis can be called a topological analysis of a planar graph. In some cases, the information obtained as a result of this analysis in combination with the results of the classification of geometric primitives may not be sufficient to classify a symbol as a whole. In such cases, the application of 'metric' algorithms of computational geometry, such as calculating areas of polygons, calculating the angles between lines, etc., are required. But in most cases (when recognizing digit characters), the role of such methods of computational geometry is insignificant, compared to the value of graph analysis methods and the recognition of geometric primitives. Thus, the fundamental role of the graph analysis procedure is to choose the recognition scheme for the connected component of the planar graph. But during the analysis of the graph, the procedures for eliminating artifacts that arise when converting an image into a planar graph are also performed. As mentioned above, we assume that each symbol corresponds to a connected component of a planar graph. Of

course, the first stage of image graph analysis is to find the connected components of this graph, and further graph analysis procedures are applied to each component. Below we describe the procedures for constructing the spanning tree of the connected component of the graph and generating cycles. In the course of these procedures, the elimination of artifacts is carried out and it is determined whether the component is a tree, or a graph having cycles. Below we describe the procedures for constructing the spanning tree of the connected component of the graph and generating cycles. These procedures are the first stage of analyzing a connected component of a planar graph. During these procedures, the elimination of artifacts is carried out and it is determined whether the component is a tree, or a graph that has cycles. Further graph analysis procedures related to the choice of a scheme for recognizing the corresponding connected component are rather complicated and require a lot of space for their detailed description. At the same time, the development of these procedures can be considered a technical task, since quite elementary and well-known methods are used to solve it. In this regard, we do not consider it appropriate to describe these procedures in this article.

Spanning tree of the connected component, cycle space and cycle’s generation procedure.

The spanning tree T of a connected graph $G(V, E)$ is the maximal acyclic connected subgraph (tree) of a given graph. All vertices of a graph are also vertices of its spanning tree (See Fig.3). Let E_T be the set of edges of the spanning tree T , and $E_C = E - E_T$. If $E_C = \emptyset$, then G is a tree. Otherwise, the cycle generation procedure described below is applied to the connected cyclic graph. Let $(a, b) \in E_C$ be the arbitrary edge of G , that is not an edge of spanning tree T . Then there is only one path γ in T , connecting the vertices a and b . If we add an edge (a, b) to the set of edges $E(\gamma)$, then we get a cycle of the graph G corresponding to the edge (a, b) . So, mapping $f: E_C \rightarrow C(G)$, where $C(G)$ is a set of cycles of the graph G , is defined. It is easy to show that a mapping f is a one-to-one mapping. (Suppose the opposite: Let $e_1, e_2 \in E_C$ and $f(e_1) = f(e_2)$. From this it follows that there is a path in the spanning tree T containing one of the edges e_1, e_2 , which is impossible). Let denote by $B \supset C(G)$ image of set E_C under mapping f . In the sequel, we will denote by $B(T)$ the set of cycles B defined in this way for an arbitrary spanning tree T of a connected graph G . In graph theory, it is proved that the set of cycles B is a basis of the linear space V of the cycles over the field \mathbb{Z}_2 .

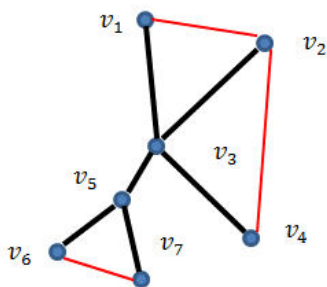


Fig. 3. Spanning tree of the connected graph. The edges of the spanning tree are highlighted in black. Edges belonging to the set E_C are highlighted in red.

In view of the importance of the concept of a linear space of the cycles for understanding graph analysis procedures, we give a brief description of this mathematical construction below. The elements (vectors) of the linear space V are some sets of edges of G . Each element of V can be represented as linear combinations of cycles of basis B , considered as sets of edges. For arbitrary $c \in V$ scalar multiplication is defined over $\{0,1\}$ as follows:

1. $0 * c = \{\}$, which shows that the zero-vector (the null set) is in Cycle Space
2. $1 * c = c$, which is identity

Let $a, b \in V$ then the addition operation $c = a + b$ be defined as a symmetric difference of the sets of edges: $a, b \in 2^{E(G)}$, $c = a \Delta b$. It is easy to show that $2^{E(G)}$ is an Abel group, relative to the addition operation defined in this way. It can be proved that for an arbitrary spanning tree T of a connected graph G , the corresponding set of cycles $B(G)$, defined above, will be the basis of the linear space of cycles V over the field \mathbb{Z}_2 , with scalar product $*: \mathbb{Z}_2 \times V \rightarrow V$ and addition operations $+: V \times V \rightarrow V$ defined above. The procedure of cycles generation for a given base B consists in generating the set of cycles $Q = \{c_1 + c_2 | c_1, c_2 \in B, E(c_1) \cap E(c_2) \neq \emptyset\}$ and building the union $C = B \cup Q$. The constructed set of cycles C does not contain all the cycles of the graph, but it is enough for solving the problems of removing the artifacts of the planar graph and generating the chains and cycles for proper symbol recognition.

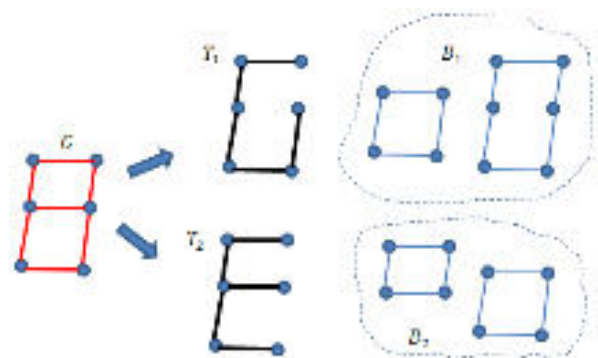


Fig. 4. Two spanning trees T_1 and T_2 of the graph G and the corresponding bases of the cycle space B_1 and B_2 .

The need to carry out the cycle generation operation can be explained with the example shown in Fig.4. The fact is that it is impossible to predict in advance which of the spanning trees will be generated by the program. In this example, if the program generates the T_1 spanning tree, then the corresponding cycle base B_1 will not contain a “small” cycle (the top loop of the “8” symbol).

III. RESULTS AND DISCUSSION

Angular characteristic function.

1. Introduction

The function of the angular characteristics of the curve completely determines the geometric shape of this curve.

More precisely, this function can be viewed as a mapping of the set of regular curves to the functional space $D \subset L^2$ of functions defined on the interval $I = [0,1]$. As shown in the “Properties of angular characteristics function” section, this mapping is invariant with to plane similarity transformations. The concept of the function of the angular characteristics is easily transferred to broken lines. The functions of the angular characteristics of a broken line can be put in accordance with the feature vector (the procedure for extracting features is described in detail in the “feature extraction” section), which allows to classify it. As mentioned above, the paths in the planar graph correspond to broken lines on the plane, which explains the key role of the concept of the function of the angular characteristics in the proposed method of recognizing handwritten characters.

2. Definitions

We will denote the set of vectors of unit length by E , so $E = \{\vec{e} \in \mathbb{R}^2 \mid |\vec{e}| = 1\}$. The oriented area of the parallelogram spanned by vectors $\vec{a}, \vec{b} \in \mathbb{R}^2$, we will denote by $S(\vec{a}, \vec{b})$. For an arbitrary Cartesian system on the plane, mapping $S: \mathbb{R}^2 \times \mathbb{R}^2 \rightarrow \mathbb{R}$ can be determined analytically by the formula (1)

$$S(\vec{a}, \vec{b}) = a_x \cdot b_y - a_y \cdot b_x \quad (1),$$

where $\vec{a} = (a_x, a_y)$, $\vec{b} = (b_x, b_y)$. If $\vec{e}_1, \vec{e}_2 \in E$, then

$$S(\vec{e}_1, \vec{e}_2) = \sin(\varphi) \quad (2),$$

where φ is the angle to turn the vector \vec{e}_1 counterclockwise so that it coincides with the vector \vec{e}_2 . We will denote mapping $E \rightarrow \left[-\frac{\pi}{2}, \frac{\pi}{2}\right]$, defined by (3) as $\angle(\vec{e}_1, \vec{e}_2)$.

$$\angle(\vec{e}_1, \vec{e}_2) = \arcsin(S(\vec{e}_1, \vec{e}_2)) \quad (3)$$

In view of the equality $\sin(\alpha) = \sin(\pi - \alpha)$, it would be incorrect in the general case to consider $\angle(\vec{e}_1, \vec{e}_2)$ as the angle between the vectors \vec{e}_1 and \vec{e}_2 . Below we provide the exact definition of the concept of ‘angle between vectors’ used in this article. For two nonzero vectors $\vec{a}, \vec{b} \in \mathbb{R}^2$ we determine the value δ by formula (4)

$$\delta = \arccos(\vec{e}_a * \vec{e}_b) \quad (4),$$

where \vec{e}_a is normalized vector \vec{a} (i.e. $\vec{e}_a = \frac{\vec{a}}{|\vec{a}|}$) and \vec{e}_b is normalized vector \vec{b} (i.e. $\vec{e}_b = \frac{\vec{b}}{|\vec{b}|}$). Then we define the function Ang as (5)

$$Ang(\vec{a}, \vec{b}) = \begin{cases} \delta, & \text{if } S(\vec{a}, \vec{b}) \geq 0 \\ -\delta, & \text{if } S(\vec{a}, \vec{b}) < 0 \end{cases} \quad (5)$$

3. Function of the angular characteristic of a smooth regular curve.

Let γ be a regular curve with end points A and B . If we choose one of the end points (for example, A), then we can parameterize γ as follows: For an arbitrary point $M \in \gamma$, we

define the corresponding value of the parameter s as the length of the curve segment AM . Thus, we define the mapping $[0, L] \rightarrow \gamma$, where L is the total length of the curve γ . For a given Cartesian coordinate system, this mapping defines two functions $x(s)$ and $y(s)$. In the case of a smooth regular curve under consideration, both functions $x(s)$ and $y(s)$ are differentiable. Let the mapping $[0, L] \rightarrow \mathbb{R}^2$ be given by formula (6)

$$\vec{v}(s_0) = \left(\left(\frac{dx}{ds} \right)_{s=s_0}, \left(\frac{dy}{ds} \right)_{s=s_0} \right) \quad (6)$$

As is known, for arbitrary $s \in [0, L]$ vector $\vec{v}(s) \in E$ is a tangent vector of the curve γ . It should be noted that the vector $\vec{v}(s)$ can be represented as (7)

$$\vec{v}(s) = (\cos(\alpha), \sin(\alpha)) \quad (7),$$

where α is the angle between the tangent line and the X axis (see Fig. 5).

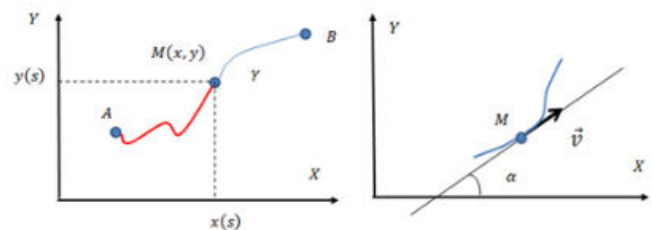


Fig. 5. Natural parameterization of regular curve. Parameter s is a length of the segment AM (left image), and tangent line (right image).

For an arbitrary point $M(s_0) \in \gamma$, we define $k(s_0)$ as (8):

$$k(s_0) = \lim_{\Delta s \rightarrow 0} \frac{\angle(\vec{e}(s_0 + \Delta s), \vec{e}(s_0))}{\Delta s} \quad (8)$$

It should be noted that $|k(s_0)| = \frac{1}{R}$, where R is the radius of the tangent circle, is the curvature of the curve γ at point $M(s_0)$. We define the function $\alpha(s)$ by the formula (9):

$$\alpha(s) = \int_0^s k(\tau) d\tau \quad (9)$$

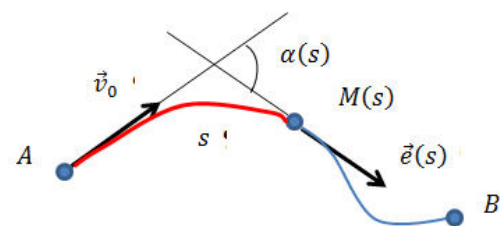


Fig. 6. Geometrical interpretation of function $\alpha(s)$.

Assuming some uncertainty, we can give the following clear geometric definition of the function $\alpha(s)$: Let $\vec{v}_0 = \vec{v}(0)$ be a tangent vector to γ at endpoint A . Then $\alpha(s)$ is the angle between the vectors \vec{v}_0 and $\vec{v}(s)$ (see Fig.6). The function $\alpha(s)$ is defined on the interval $[0, L]$, where L is the length of the curve γ . We define on the interval $I = [0,1]$ the function $\theta(x)$:

$$\theta(x) = \alpha(x \cdot L) \quad (10)$$

We will call $\theta(x)$ the function of the angular characteristic of the curve γ (or simply the angular characteristic of γ). As will be shown below, this function has properties that allow it to be effectively used in symbol recognition tasks.

4. Properties of an angular characteristic function.

- 1) Invariance to similarity transformations of the plane.

The most important property of the function of angular characteristics is its invariance to similarity transformations of the plane. Below we provide the necessary explanations: A similarity is a transformation of Euclidean plane which maps lines to lines and preserves the sizes of angles. The set of all similarities is the similarity group $S(2)$. Each similarity transformation can be viewed as a composition of translation, rotation, and uniform scaling. Let γ be a regular curve with endpoints A and B . Applying an arbitrary transformation $f \in S(2)$ to the plane transforms γ into a regular curve γ' with endpoints $f(A)$ and $f(B)$. Thus, if θ_1 is the function of the angular characteristic of γ , then it corresponds to the function of the angular characteristic θ_2 of the curve γ' . The statement about the invariance of the function of the angular characteristic to similarity transformations means that equality (11) holds.

$$\forall x \in [0,1] \theta_1(x) = \theta_2(x) \quad (11)$$

- 2) If the curve γ is a line segment, then its function of the angular characteristic θ of the γ is defined by (12)

$$\forall x \in [0,1] \theta(x) = 0 \quad (12)$$

- 3) If the curve is an arc of a circle cut off by an angle φ , then regardless of the radius of the circle, the function of the angular characteristics of this curve will be a linear function (13):

$$\theta(x) = \varphi \cdot x \quad (13)$$

It should be noted that the curves forming the symbol in the image can be approximated by curves made up of segments and arcs of a circle. The last two properties of the angular characteristics function make it easy to imagine the angular characteristics of these curves. In addition, the idea of approximating curves by joints of segments and arcs suggests an idea of using segmentation methods to recognize curves.

4) Function of angular characteristic of broken line.

We denote a broken line by a sequence of vertices $\{A_0, A_1, \dots, A_n\}$. Let (x_i, y_i) denote Cartesian coordinates of the i -th vertex. Then the broken line corresponds to a sequence of n vectors $\{\vec{v}_1, \vec{v}_2, \dots, \vec{v}_n\}$ given by equalities (14).

$$\vec{v}_i = (x_i - x_{i-1}, y_i - y_{i-1}) \quad (14)$$

We define the sequences $\{l_1, l_2, \dots, l_n\}$ and $\{\varphi_1, \varphi_2, \dots, \varphi_n\}$. by equalities (15) - (16).

$$l_i = |\vec{v}_i| \quad (15)$$

$$\varphi_i = \begin{cases} 0, & \text{if } i = 1 \\ \text{Ang}(\vec{v}_i, \vec{v}_{i-1}), & \text{if } i \neq 0 \end{cases} \quad (16)$$

Let x_0, x_1, \dots, x_n be a sequence of points on the X axis given by the equations (17)

$$x_i = \begin{cases} 0, & \text{if } i = 0 \\ \sum_{k=1}^i l_k, & \text{if } i \neq 0 \end{cases} \quad (17)$$

So, the interval $[0, L]$, where $L = \sum_{i=1}^n l_i$ is the length of broken line $\{A_0, A_1, \dots, A_n\}$, contains all points x_0, x_1, \dots, x_n . Now we define on the interval $[0, L]$ the step function α by (18)

$$\alpha(x) = \sum_{i=1}^n \varphi_i \cdot \chi_{D_i}(x) \quad (18),$$

where $\chi_{D_i}(x)$ is the indicator function of interval D_i (19), and sequence of intervals $\{D_1, D_2, \dots, D_n\}$ is defined by equations (20).

$$\chi_{D_i}(x) = \begin{cases} 1 & \text{if } x \in D_i \\ 0 & \text{if } x \notin D_i \end{cases} \quad (19)$$

$$D_i = \begin{cases} [x_{i-1}, x_i] & \text{if } 1 \leq i < n \\ (x_{i-1}, x_i] & \text{if } i = n \end{cases} \quad (20)$$

The function of the angular characteristic θ of a broken line will be determined (as for a regular smooth curve, see (10)) by equation $\theta(x) = \alpha(x \cdot L)$. An example of a broken line (strictly speaking, a planar graph representing a tree with two leaves) and the corresponding function of the angular characteristic is shown below (see Fig. 7)

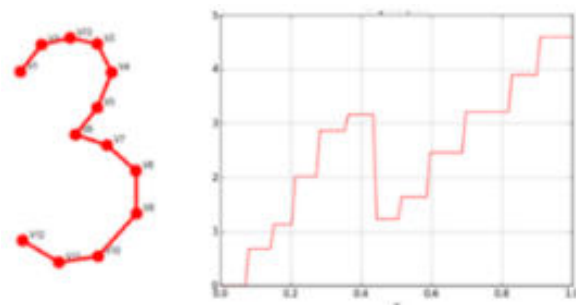


Fig. 7. Broken line (planar graph of real image) and plot of its angular characteristic function.

5) Feature extraction.

An arbitrary function f defined on an interval $[a, b]$ can be considered as a periodic function $\forall x \in \mathbb{R} f(x + T) = f(x)$ with a period $T = b - a$ (See Fig. 8) By definition, the function of the angular characteristics θ of arbitrary broken line is defined on the unit interval $I = [0, 1]$ and $\theta(0) = 0$, but in the general case $\theta(1) \neq \theta(0)$. Consequently, a periodic function θ in the general case will have jump

discontinuities. Due to Gibbs phenomenon, the partial sum of the Fourier series will be poorly approximated to the original function θ . To solve this problem, we use the following method: for a given function of angular characteristic θ , we define an even function Ψ defined on the interval $[-1,1]$ by equation (21)

$$\Psi(x) = \theta(1 - |x|) \quad (21)$$

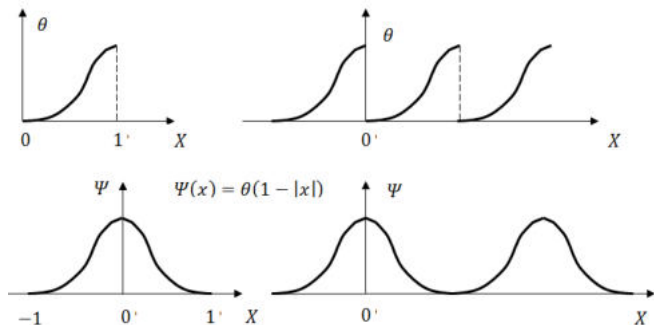


Fig. 8. Angular characteristic function θ and corresponding function Ψ .

As Ψ is a piecewise continuous bounded function it is possible to define its absolute value $\|\Psi\|$ by (22)

$$\|\Psi\| = \sqrt{\int_{-1}^1 \Psi^2(x) dx} \quad (22)$$

Let $\Omega = L^2([-1,1])$ be a L^2 space of functions, defined on interval $[-1,1]$. Then, $\Psi \in \Omega$, due to the fact that the norm $\|\Psi\| < \infty$ is defined by (2). As Ω is a L^2 space, Ω is a Hilbert space, where inner product of $f_1, f_2 \in \Omega$ is defined by (23):

$$\langle f_1, f_2 \rangle = \int_{-1}^1 f_1(x) \cdot f_2(x) dx \quad (23)$$

Each even function $g \in \Omega$ can be represented as a Fourier series in form (24)

$$g(x) = \sum_{i=1}^{\infty} c_i \cdot \varphi_i(x) \quad (24),$$

where functions φ_i is defined by equations (25)

$$\varphi_i(x) = \begin{cases} \frac{1}{\sqrt{2}} & \text{if } i = 1 \\ \cos(\pi \cdot i \cdot x) & \text{if } 1 < i \end{cases} \quad (25)$$

The system of functions (25) is orthonormal, which means that (26) holds true.

$$\forall i, j \langle \varphi_i, \varphi_j \rangle = \delta_{ij} \quad (26)$$

The coefficients $c_1, c_2 \dots$ of Fourier series expansion (24) are defined as the projections (27) of the vector $g \in \Omega$ onto the vectors of the orthonormal basis $\varphi_1, \varphi_2 \dots$:

$$c_i = \langle g, \varphi_i \rangle = \int_{-1}^1 g(x) \cdot \varphi_i(x) dx \quad (27)$$

For a given N , the N -th partial sum of the Fourier series (28) will approximate the original function.

$$g(x) \approx \sum_{i=1}^N c_i \cdot \varphi_i(x) \quad (28)$$

We will consider the real numbers $c_1, c_2 \dots c_N$, as components of the vector $\vec{g} \in \mathbb{R}^N$, so in some orthonormal basis of \mathbb{R}^N $\vec{g} = (c_1, c_2 \dots c_N)$. Let designate by $g \rightarrow \vec{g}$ correspondence between even function $g \in \Omega$ and vector $\vec{g} \in \mathbb{R}^N$ of Fourier series even coefficients. Then, for arbitrary even functions $f_1, f_2 \in \Omega$ approximations (29)-(30) holds true.

$$\langle f_1, f_2 \rangle \approx \vec{f}_1 * \vec{f}_2 \quad (29)$$

$$\|f - g\| \approx |\vec{f} - \vec{g}| \quad (30)$$

Both Hilbert space and Euclidean space are metric spaces. A metric in space (a set of points D) may be defined by the distance function d , defined for all pairs of points $A, B \in D$, which satisfies four conditions:

1. $\forall A, B \in D \ d(A, B) = d(B, A)$
2. $\forall A, B \in D \ d(A, B) \geq 0$
3. $\forall A \in D \ d(A, A) = 0$
4. $\forall A, B, C \in D \ \rho(AB) \leq \rho(AC) + \rho(CB)$

As is known, in the Euclidean space \mathbb{R}^N , distance d between $\vec{A}, \vec{B} \in \mathbb{R}^N$ is defined as $d(\vec{A}, \vec{B}) = |\vec{A} - \vec{B}|$. Similarly, for a Hilbert space L^2 metric d^* is defined by equation (31), where $f_1, f_2 \in L^2$

$$d^*(f_1, f_2) = \|f_1 - f_2\| \quad (31)$$

It is proved that conditions 1)–4) are satisfied for the metric d^* . Suppose that for a given function of the angular characteristic θ , the function Ψ is determined by the ratio (21) and $\Psi \rightarrow \vec{\Psi}$. If we consider the vector $\vec{\Psi}$ as a feature vector of the Euclidean feature space, then based on the above considerations, it can be argued that such a method of feature extraction will be good suitable for curve classification tasks. But in practice we need to classify the step characteristic functions of broken lines, containing discontinuous jumps. It is highly desirable to smooth out such functions. To do this, we apply the operation described below to the vector $\vec{\Psi}$ of the Fourier expansion coefficients of the function Ψ . Let denote by $g(x)$ Gaussian function, defined as (32)

$$g(x) = \frac{1}{\sqrt{2\pi}\sigma} \cdot e^{-\frac{x^2}{2\sigma^2}} \quad (32)$$

where $\int_{-\infty}^{\infty} g(x) dx = 1$, i.e., $g(x)$ is normalized. As g is an even function, equations (33)-(34), for arbitrary $\omega \in \mathbb{R}$ holds true.

$$\int_{-\infty}^{\infty} g(x) \cdot \cos(\omega \cdot x) dx = \int_{-\infty}^{\infty} g(x) \cdot e^{-i\omega x} dx \quad (33)$$

$$\int_{-\infty}^{\infty} g(x) \cdot \cos(\omega \cdot x) dx = e^{-\frac{\sigma^2 \cdot \omega^2}{2}} \quad (34)$$

For the values of the parameter σ , satisfying the non-equality $\sigma < \frac{2}{3}$, we can assume that $g(x) \approx x$ if $x \notin [-1, 1]$. Then the values g_k^* defined by (35)

$$g_k^* = \begin{cases} 1 & \text{if } k = 0 \\ e^{-\frac{\sigma^2 \cdot (k-1)^2}{2}} & \text{if } k > 1 \end{cases} \quad (35)$$

can be considered as the Fourier expansion coefficients of the function g^* , approximating the Gaussian function $g(x)$. Let $\vec{\varphi} = (\varphi_1, \varphi_2, \dots, \varphi_N)$ be the vector of the Fourier coefficients of the function Ψ , and $\vec{g}^* = (g_1^*, g_2^*, \dots, g_N^*)$ the vector of the Fourier coefficients of the function g^* . We define the vector $\vec{\varphi}_s = (\varphi_{s1}, \varphi_{s2}, \dots, \varphi_{sN})$ by equalities (36).

$$\varphi_{sk} = \varphi_k \cdot g_k^* \quad (36)$$

According to the convolution theorem for Fourier series, we can consider the components of the vector $\vec{\varphi}_s$ as the Fourier expansion coefficients of the function $\Psi_s(x)$, which is a result of application of a filter with Gaussian kernel g^* to the function Ψ (37)

$$\Psi_s(x) = \int_{x-1}^{x+1} \Psi(t) \cdot g^*(t) dt \quad (37)$$

Of course, the choice of the number n and the values of the parameter t strongly affect the quality of recognition.

The method for identifying plane curves described in the article was practically tested. We developed software that implements this method and used it for experiments with character recognition of decimal digits on real photos. At the first stages of the recognition procedure, the raster image was transformed into a planar graph. As mentioned above the planar graph obtained as a result of applying the conversion procedure contains all the necessary information for recognition, and after converting the image into a planar graph, the original image is not used in the recognition procedures. We have developed a simple text format for storing information about a planar graph in the form of s -expressions. To visualize the resulting planar graphs, a special stand-alone application was developed (we called it "Graph Redactor"), which also allows user to create artificial planar graphs using GUI tools (we used such artificially created planar graphs in experiments with character recognition software). All software was written in Python 2 language (Anaconda package). Since we used a small database to classify planar graphs corresponding to handwritten characters, the experimental results can only be considered as a proof of concept. But still, we consider it necessary to note that during the experiments we observed high reliability of the implemented recognition method.

IV. CONCLUSION

The suggested approach for recognizing plane curves was created with the intention of being utilized in tasks involving the recognition of handwritten characters. The core concept behind this method for identifying flat curves involves employing a unique function to discern the shape of a simple, continuous curve devoid of any self-intersections. Our primary focus was on character recognition techniques that involve the transformation of character images into a planar graph. This planar graph, generated through the conversion process, contains all the essential information required for recognition. As an outcome of our efforts, we designed software to put these algorithms into practice and applied it to conduct experiments involving the recognition of decimal digits in actual photographs.

Due to the radical difference between the proposed method and the existing ones, the software was created as proof of concept, solely to confirm the operability of the method. For the experiments, images of the symbols of the digits 1, 2, 3, 5 were used (numbers for which the planar graphs corresponding to their symbols do not contain cycles were used) generated in a relatively small number of instances (from 10 to 20 for each symbol) by the participant of the experiment. Based on this sample, a small database was created that allowed character recognition. Then an experiment was conducted to recognize characters generated by the same participant in the experiment. In the course of several similar experiments, 100% recognition accuracy was observed (no recognition errors). We emphasize that such experiments on small samples cannot be used for comparison with other methods and are only suitable as proof of concept.

ACKNOWLEDGMENT

This research was funded by the Ministry of Science and Higher Education of the Republic of Kazakhstan (Grant No. AP19679327).

REFERENCES

- [1] Yixian Zh. Researches advanced in image recognition, Proceedings of the 3rd International Conference on Signal Processing and Machine Learning ACE (2023) Vol. 4: pp. 205-214. <https://doi.org/10.54254/2755-2721/4/20230451>
- [2] Zheng Y., Meng F., Liu J., Guo B., Song Y., Zhang X., Wang L., Fourier Transform to Group Feature on Generated Coarser Contours for Fast 2D Shape Matching, in IEEE Access, vol. 8, pp. 90141-90152, 2020, <https://doi.org/10.1109/ACCESS.2020.2994234>
- [3] Gostev I. M. Recognition of Graphic Patterns. Part 1. Izv. Ross. Akad. Nauk. Teor. Sist. Upr. 2004. No. 1; Comp. Syst. Sci. 2004. V. 43, No. 1. pp 129.
- [4] Gostev, I.M., Sevastianov, L.A. About the identification of flat unclosed curves. Phys. Part. Nuclei Lett. 5, pp. 297-300 (2008). <https://doi.org/10.1134/S1547477108030345>

Identification of position by means of shape recognition in mixed reality systems

Zoltán Szilágyi
Óbuda University
Applied Informatics and Applied
Mathematics Doctoral School

Székesfehérvár, Hungary
szilagyi.zoltan@amk.uni-obuda.hu

Csaba Hajdu
Széchenyi István University
Department of Informatics

Győr, Hungary
hajdu.csaba@ga.sze.hu

Patrik Bajári
Óbuda University
Alba Regia Technical Faculty

Székesfehérvár, Hungary
bajari.patrik@stud.uni-obuda.hu

Abstract— One of the pillars of mixed reality systems, image processing techniques for position identification of real objects in space. These procedures can be implemented using different methodologies and technical backgrounds. These include identification using various visual codes (e.g., QR, ArUco), or model fitting and pattern matching. In this article, a possible implementation of the latter method is introduced, which aims to advance the use of mixed reality tools and solutions in the field of industrial robotics.

The object to be recognized is identified by means of a 3D model. After the recognition, the model is fitted on the real object to obtain the real position of the object. The model used in the method presented in this paper is a robot component, which allows the real spatial position of the industrial robot to be synchronized with the represented objects in the virtual space. The position identification method is part of a complex system that aims to increase the efficiency of industrial robots using mixed reality methods.

Keywords— mixed reality, augmented reality, industrial robotics, robotics, machine vision

I. INTRODUCTION

The implementation of emerging technologies is also essential in the field of industrial robotics. Such new technologies include augmented or mixed reality systems. This article aims to present an element of the work in this area. The aim of this research is to investigate methods for synchronizing real space and virtual reality to identify solutions suitable for application in industrial environments. Among these solutions, the 2D code marker identification (ArUco) was investigated, and traditional machine vision technology based on simple pattern matching. Object identification without fixed code offered a more flexible solution and the aim was to test the capabilities of the method and the system with a sample application. The sample application focuses on object recognition and position identification.

II. RELATED WORK

During the development, it was of utmost importance that the chosen software and software technologies are robot vendor independent, and that an operating system and platform independent solution can be created. The vendor independence aspect was important because the aim is to develop a general tool that can be used on all robots. Platform independence is of particular importance to ensure that the

system can be used on different hardware devices in the future. Consequently, numerous visual engines have been chosen, that are described in further detail in this section.

A. Vuforia Engine

The Vuforia Engine¹ is a popular and widely used software development kit (SDK) for creating augmented reality applications that allows us to recognize different images, objects and spaces. Using the kit, the application is able to recognize and track images, spatial models, markers, floor and table surfaces, or even a whole sofa from a database that have been created and populated. It has the advantage of being very stable and supports development in Unity, and can be used for Android, iOS and Universal Windows Platform (UWP) apps so it supports most phones, tablets and augmented reality glasses.

B. Unity

Unity² is a game development engine with a huge user base. Many games and applications are released every day that are built in Unity, but it is also increasingly used in industrial applications, as a small team can create any 2D, 3D, virtual reality (VR) and augmented reality (AR) application relatively quickly. Its popularity is greatly helped by the fact that it supports almost all platforms, and that there are many written and video tutorials available to help you learn.

For this project, Unity version 2021.3.10 was used with both the Android Build Support and Windows Build Support modules. This version was chosen for several reasons. First of all, it has a Long-Term Support (LTS) rating, which means that the version is constantly being improved and updated, so these are the most stable versions available in the development environment. Furthermore, the Netcode for GameObjects, Relay and Vuforia Engine packages that have been thoroughly used in the project, all are supported by this version. Since the start of development, newer versions of Unity have been released that have made major advances in the development of augmented reality games and applications, but the industry attitude is that the project is always built in the same version as it started in and you shouldn't change versions in the middle of development as this can cause a lot of problems later on, which is why version migration while the project was being developed is unfavorable.

¹ <https://developer.vuforia.com/#>

² <https://unity.com/>

C. Blender

To create a Model Target, a 3D virtual model of the real object is required. The virtual model was created using Blender, a free open-source modelling program. Blender can be used to create 3D models, render, create visual effects, and create 2D and 3D animations³.

D. Model Target Generator

The Model Target Generator builds a Vuforia Engine database from a 3D model, which you can then use to detect and track the Model Target. The program allows you to predict whether the model's characteristics are appropriate for later use. You can set up the Guide View and export the final database. The program can be downloaded for free from the official website.

III. CONCEPTUAL DESIGN

The conceptual design of the software operation is depicted in Fig. 1. It can be assumed that the necessary data is available to us in a suitable database. The project does not aim to develop the database and ensure the availability of the data. This is intended to be done in an independent work. The software will access the database and be able to process the required data. After processing, the appropriate information is sent to the AR tool. In the present project, this device is a tablet which acts as the AR device. A real AR display application will be part of further development. The main point of the software is to identify and position the right object using image processing and machine vision methods. The development will focus on this point. If the searched object is successfully identified in the camera image, the virtual object and the real object will be synchronously displayed on the AR device.

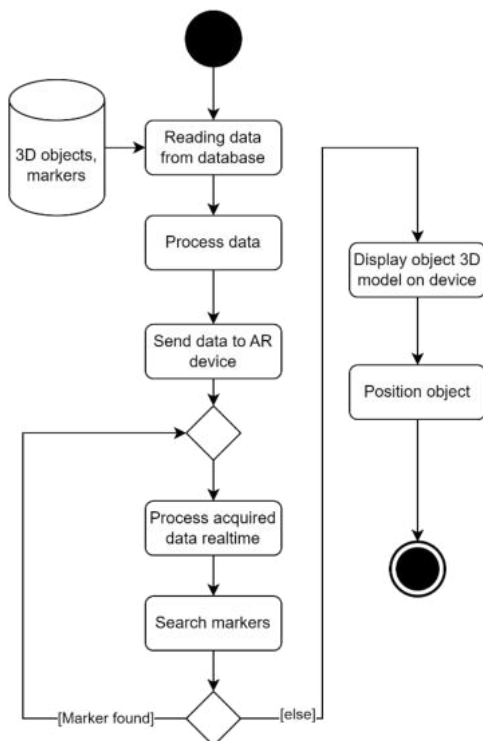


Fig. 1. Flowchart describing the application

The markers (e.g., Aruco [1], QR) associated with outlying objects can be detected with conventional computer vision methods, which are implemented in the free, open source Computer Vision Library (OpenCV) [2]. Besides marker detection OpenCV provides further image processing for realtime processing, preprocessing, and feature extraction [3]. The library mainly relies on Python and C++ languages, that enables rapid implementation and testing. In the current scope of this research, numerous feature extraction methods were tested with variable success. The methods required for the current implementation were performant enough to provide accurate results with relatively small latency.

IV. DETAILED DESIGN

The following section describes implementation details and software composition.

A. Model Target generation

To locate the robot in real space in augmented reality applications, you can create both model-based and image-based markers. The model target was chosen because it allowed the use a part of the robot as a marker and its position enables easier calculation of a specific point in the frame where the object is presumed to be placed. Conversely, if an image was as a marker, it would have been placed to a point on the robot and the position of the point calculate in space from there, but if the image was moved, the calculations will accumulate error, and the results shall be not as accurate. Consequently, the application will not work properly unless the object is placed back exactly into its predefined position. Once you have imported the 3D model you have used, you will be presented with the settings needed to generate it. Once the appropriate settings have been made, the database is then imported into your Unity project. The model target generation is shown in Fig. 2.

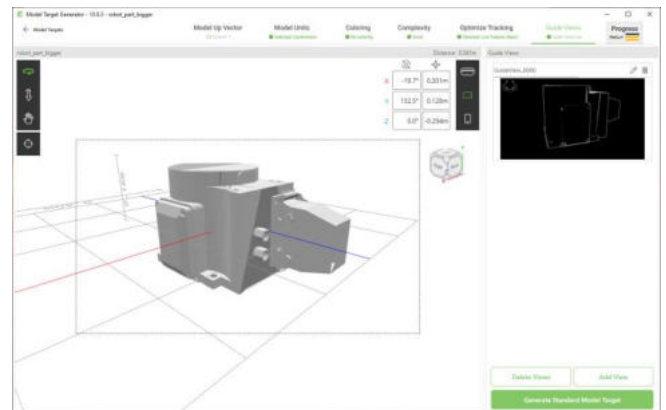


Fig. 2. Model Target generation

B. Set up Network Manager

To manage the data running on the network – and consequently communicate with the AR device –, a Network Manager component is required in runtime. Network Manager contains all the network-related settings for the project. To use the component, an empty object in the object hierarchy is needed and then it must be attached the *NetworkManager* component to this object so that it will run when the application starts. Once the file is attached, the variables and

³ <https://www.blender.org/>

settings for the program are displayed, and the network transport configuration is selected for Unity specific settings (*Unity Transport*). The network transport metrics are displayed real-time on the user interface. The *Relay* service is configured to Relay Unity Protocol. The next important change is *NetworkPrefabs*, which list all objects used on the network. If a network object is not in the list, it is essentially unavailable on the current network. It is important to note that if an object is on the network and is in the list, it must have an associated *NetworkObject* component. The *NetworkManager* object is continuously running in the background to maintain and manage network connections. In Unity such background processes are inserted into the *DontDestroyOnLoad* utility scene after the application startup. This scene serves as a utility scene and runtime context, thus the associated objects with this scene are not deleted until the application is stopped. The *NetworkManager*, *Unity Transport* (Script) and *NetworkObject* components are all C# code from the *Netcode for GameObjects* package.

C. Class composition

The software is composed of classes for specific tasks. In the following subsections each class and their primary function is described in more detail. The high-level class architecture is depicted in Fig. 3.

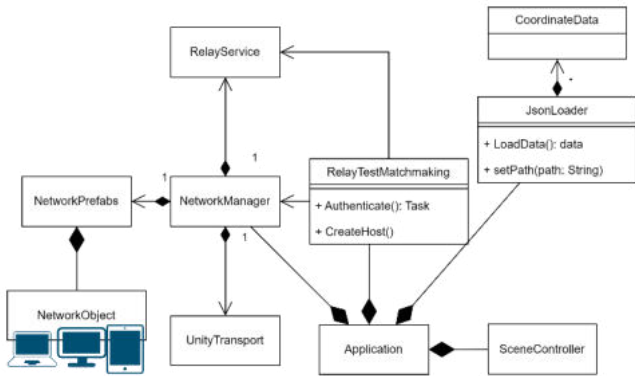


Fig. 3. Class composition architecture of the software

1) RelayTestMatchmaking class

The *RelayTestMatchmaking* class provides the connection to and setup of the *Relay* service. The program will authenticate the user through the sol-change after the application is started and the objects are loaded. After the host is created, the program generates a 6-digit code that clients can enter and then connect to the corresponding session. The process is depicted as a sequence flow in Fig. 4. Notice, that Unity classes are available as static singleton objects to call required methods, and the method returns a schedulable task that executes authentication on every external call.

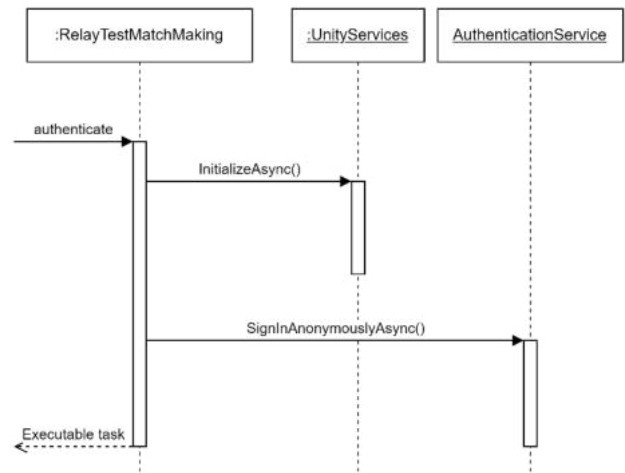


Fig. 4. Authenticate method

The *CreateHost()* function (depicted in Fig. 5) creates a host user by first allocating the session, with a maximum number of users specified. To create the host, a Relay service must be allocated, which primarily allocates space for the host and clients on the server. This allocation process also generate a six-digit code (*AllocationId*) for the clients to join. This is the code that is displayed for other devices as the value of the *joinCodeText* object to other actors on device side. The allocation information is then transported, with information containing the relay server IP address, port number, allocation ID number, allocation key and connection meta-information. Finally, the *StartHost()* method in *NetworkManager*, the host is created and running in the background.

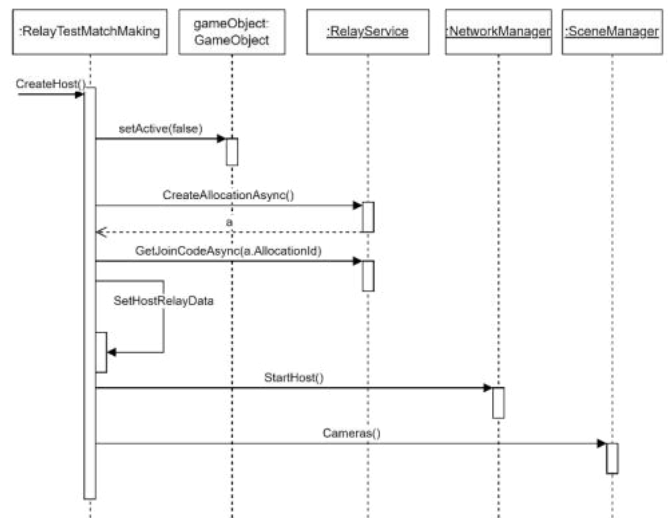


Fig. 5. Model CreateHost() method

The *JoinToHost()* function works with similar procedures as the *CreateHost()* function. The only difference is that instead of creating a new allocation, you join an existing one using the allocation ID and then connect as a client via the relay proxy after calling the *StartClient()* function in the *NetworkManager*. To stop the application, the *ExitTheApp()* method must be called. The method will first disconnect the client from the host using the *Shutdown()* method in *NetworkManager*, or in the case of a host, shut down the entire session. The user then exits the application.

2) SceneController class

Since currently network communication for users connected to a session is only possible within a given scene, the application has one such scene and varies depending on whether it is used in host or client mode. In Unity, the scene is an important program unit, it contains the "world" represented in the program with the models, virtual cameras, lights and all the components that are part of it [5].

The SceneController.cs program deletes the previously created ARCamera object from the hierarchy and creates a new virtual camera from a prefab of a pre-made camera. This is necessary because the PC (host) tries to use the device's camera when the application is started, but it is not necessary for the current scenario since data is required to be transmitted to the clients from this node.

The Cameras() function deletes the arCamera object and then creates the mainCamera object in the hierarchy by calling the Instantiate() function. This function is called by the CreateHost() function of the RelayTestMatchMaking program shown above.

3) JSONReader class

The JSONReader class is used to read and store the values of the database in a CoordinateData object. The SetPath() method saves the persistent path of the database in the pre-created persistentPath global variable. The persistentDataPath of Application.persistentDataPath is the path to a directory where the data is intended to be stored during runtime. The LoadData() method (Figure 6) reads the values of the data library stored in a JSON file (based on the value of persistentPath) and saves them to the CoordinateData object named data.

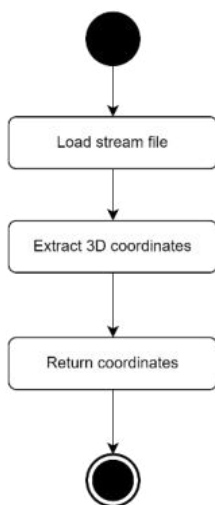


Fig. 6. LoadData() metod

4) TargetBehavior class

The TargetBehaviour.cs class sets the position of the origo object based on the coordinate values extracted from the database. The Vuforia Engine Target child object and the origo object used are stored as two variables, so their positions can be referred in space. Three more so-called network variables are created to store the values of the coordinate axes in the network. With network variables the properties between server or host and clients can be synchronized continuously without the need to use RPCs (Remote Procedure Call) or custom messages. To define variables, several criteria must be

met. First, the variable is only available in a class derived from the NetworkBehaviour class, and the object to which it is attached as a component must also have a NetworkObject component. In addition, the network variable type must be restricted to an unmanaged type. The variables must be initialized at the first creation, where the default value was initialized to zero and allowed the clients to read the value of the variables.

The goToTarget() method sets the position of the origin object to the position of the selected target object. This is necessary because the object assigned to the target will disappear when the target is detected and tracked and the position of its coordinate value will not be visible, but since the localization has already been done, the position of the robot in space is known, so even if the target is lost, its position is saved in the variable of a 3-dimensional vector to recognize the desired position of the origin object, until the robot is moved from its predefined original position.

The SetCoordinates() method calls the LoadData() function of the JSONReader class, which reads the values from the database as described earlier and saves them to the data object and convert entries to cartesian coordinates. The database is presumed to store coordinates in millimeters, so proper conversion is required in the preprocessing steps. Then the values of the network variables are changed to the values stored in the data object, but since the coordinate values in the robot are in millimeters and in unity a coordinate unit is counted in meters, it is required to divide by thousands to get the correct scale. NetworkVariable requires synchronization on external events and explicit data update.

Finally, the TestMoving() method sets the location of the origin object of choice in the target position and configures required network variable values.

D. Results of the robot armless testing

The robot is intended to carry out a typical pick-and-place problem prominent in industrial robot control scenarios [4]. The program read the values stored in the database without errors and after the conversion from millimeters to meters the values were the same as the position values were recalculated. After reading these values and converting them into the correct form, the coordinate value obtained by the application accurately positioned the origo object at this point on both the computer and the device side. The peer-to-peer communication between the two sides worked properly. The data served on the computer was received by all three devices connected simultaneously, as described earlier, and none of the clients had any problems with the accurate placement of the origo object.

In addition to the optimal operation of the application's functions, the performance of the program running on different Android devices have been examined. In general, all three devices ran at an average of over 30 frames per second (fps). On the network connection to a server, required a lot of computational power, the display real-time transmission stopped momentarily, but restored as the connection to the remote server is completed. During testing, remote server connection required a time amount of 1-2 seconds.

E. The result of testing with the robotic arm

During testing, the robot's pedestal was recognized by the application even when a small part of it was hidden from the camera. The previously tested mechanics also worked

properly and the origin object was moved to the correct position. During testing it was observed, that the application was very fast at detecting and accurately tracking robot pedestals even in mediocre lighting conditions in the robot laboratory. In further research, the accuracy is needed to be measured, but in the scope of the current research this was not carried out for technical reasons.

V. FUTURE WORK

Currently the zero point indicator of the origin object is displayed at the lower center point of the robot's pedestal, so the displayed object is estimated to be accurate when the user also defines it at this point on the robot arm. This could be eliminated by enabling the user to move the indicator object that defines the origin point using the mouse within the application. Since Unity is a multi-platform visual engine, in the future it would be possible to run the client-side application on phones tablets, and apparently on augmented reality glasses, (e.g., Magic Leap 2, Microsoft HoloLens 2) with Universal Windows Platform (UWP) support.

VI. CONCLUSION

The final application consists of two main viewpoints. One side is the device (client side), and the application runs on Android phones and tablets, where it can locate a Fanuc LR Mate 200iD/4S robot arm in real space and display an object around the robot based on the coordinate values. The other side is a general-purpose computer (host side) and its task is to read the values of the robot's user frame 3D coordinates from a database and then transmit these coordinates to the client side via a peer to peer connection. Furthermore, using a separate program, it can retrieve the user frame data to be displayed from the Fanuc robot and save it to the appropriate database.

Since Unity cross-platform game engine was used to create the application, it is possible to easily run it on both Android and Windows operating systems. It is also possible to deploy it on other operating systems (e.g., iOS, macOS and Linux).

Considering that the solution using pattern matching based on object identification is considered promising for the realization of the task, the aim is to apply the system on an AR device. The requirements to deploy the application in an industrial-grade context are high, thus further development is required to achieve this goal.

REFERENCES

- [1] Garrido-Jurado, S., Muñoz-Salinas, R., Madrid-Cuevas, F.J., & Marín-Jiménez, M.J. (2014). Automatic generation and detection of highly reliable fiducial markers under occlusion. *Pattern Recognit.*, 47, 2280-2292.
- [2] I. Culjak, D. Abram, T. Pribanic, H. Dzapo and M. Cifrek, "A brief introduction to OpenCV," 2012 Proceedings of the 35th International Convention MIPRO, Opatija, Croatia, 2012, pp. 1725-1730.
- [3] R. Szeliski, *Computer Vision: Algorithms and Applications*, 2010
- [4] Siegwart, R.Y., Nourbakhsh, I.R., & Scaramuzza, D. (2004). *Introduction to Autonomous Mobile Robots*.

POSTER SESSION II.
Geodesy and Geoinformatics

The Role of Building Information Modeling in Facility Management

János Király
Óbuda University Alba Regia
Technical Faculty
Székesfehérvár, Hungary
kiraly21.98@gmail.com

Kinga Teszárs
Óbuda University Alba Regia
Technical Faculty
Székesfehérvár, Hungary
kinga.teszars@gmail.com

János Katona
Óbuda University Alba Regia
Technical Faculty
Székesfehérvár, Hungary
katona.janos@amk.uni-obuda.hu

Abstract— The paper summarises how BIM is created and the benefits of using it. In addition to a general description, the paper describes the survey and BIM creation of a concrete building. The second half of the paper examines the role of BIM in facility management. The practical relevance of BIM in facilities management is illustrated through a concrete building (a dormitory).

Keywords— *Building Information Modelling, Facility Management, Laser scanning.*

I. INTRODUCTION

Building Information Modeling (BIM) is the simulation and optimisation of building design and construction processes using comprehensive digital models. From the point of view of the operation of buildings throughout their life cycle, BIM offers significant advantages over traditional design methods, as it provides detailed information on any building component at any time.

Building information modelling as a concept was first used in 1992, but has only gained ground thanks to the digitalisation that has been gaining momentum over the last two decades. Digital tools are now widely used in building design, but valuable information is often lost between the different steps. The solution to this is BIM, which ensures a consistent and continuously updated state during design, construction and operation. [1] [2].

BIM includes the three-dimensional geometry of buildings, but can also include spaces, zones, schedules and building structures in addition to physical objects. Within a building, the different objects are usually well distinguishable and are identified by specific information such as type of component, material, technical parameters, price or cost [3] [4].

Facilities management, as an organisational function, is responsible for ensuring that the needs of the whole organisation for facilities management services are met at an optimal level, i.e. the smooth running of the core business of the organisation. In the course of its activities, it has a fundamental impact on the organisation, the well-being of its employees and the effectiveness of the organisation's operations by managing change. The scope of services includes services related to buildings as well as work-related services, such as:

- building maintenance and other technical services, cleaning, energy management, security services, etc.,

- catering services, occupational health services, information and communication services, local disaster prevention and response, fire safety services for facilities, furniture, removals, asset protection, occupational safety and health, site management, etc.

II. DATA AND METHODS

The dormitory "A" building of the University of Óbuda, located at Hosszúsétatér 8, Székesfehérvár, was chosen for the presentation of the topic. The three floors of the dormitory can accommodate 94 students.

A. Building Surveying

The primary instrument for data collection was a Leica P40 laser scanner. This instrument is capable of surveying both interior and exterior spaces, measuring vertically from -55° to $+90^\circ$ and horizontally at 360° . The measuring range is 270 metres.



Fig. 1. One of the survey's instrument stations

The detail measurement is based on control points and can be integrated into the EOVS system. The control points were defined using a CHCNAV i73 GNSS receiver and the associated CHCNAV HCE320 controller. Around the building, 10 control points were stationary, which were determined by 30 epoch measurements.

The laser scanner was set up at locations where most of the building's detail points were visible. From each position, at least two control points were visible. Measurements were taken outside the building over a given angular range, and inside the building over the full angular range. During the measurement, the "Scan+Image" function was set up so that, in addition to the laser scan, the instrument also took photographs.

The point cloud is generated by processing the raw measurements. The processing steps in the Leica Cyclone software were as follows:

1. Creating a database
2. Import measurement data
3. Contrast adjustment
4. registration
5. transforming the data into a point cloud
6. Point cloud cleaning
7. Export point cloud

Based on the verification measurements, the average geometric accuracy of the model is 0.134 m [5]

B. Creating BIM

The BIM was produced in Revit 2023 software, but first had to be converted to the appropriate file format using Autodesk Recap Pro software. To create the BIM, first a project had to be defined and then the point cloud was imported. To define the building levels, a vertical cross-

section of the point cloud had to be created first. The next major step was to design the walls and then the foundation of the building. This was followed by placing the doors, windows, furniture and utilities in the model. On the ground floor alone, 66 doors and 23 windows of different types, materials and sizes were installed. After the floor was constructed, the staircase connecting the ground floor and the first floor was modelled. The type of staircase could be selected and its slope could be specified, as well as the levels between which the staircase would run. To create the ceiling, a ceiling level for the ground floor had to be created. The first floor essentially had to repeat the tasks performed at ground level. The modelling of the second floor started with the modelling of the roof, as this floor is now located in the attic. The difficulty in modelling the roof was caused by the fact that the roof is of mansard design, consisting of a 28 degree hipped roof and an 80 degree pitched gable roof. To realistically model the roof, skylights had to be cut into the roof planes.

The structural modelling was followed by the placement of utility and operational objects (e.g. furniture, electronic devices). For the latter, information provided by the manufacturer (e.g. dimensions, average consumption, price of the product, electronic link to the full product specification) can be included.

The equipment of bathrooms and kitchens can also be modelled, since they are included in the predefined elements. As with electronic equipment, useful information can be provided in the data table for these items. Lastly, devices relating to lighting and fire protection are included. The data plate for lamps provides information on consumption, the type and life expectancy of light bulbs and neon tubes, and for fire protection equipment, maintenance data is useful [5].

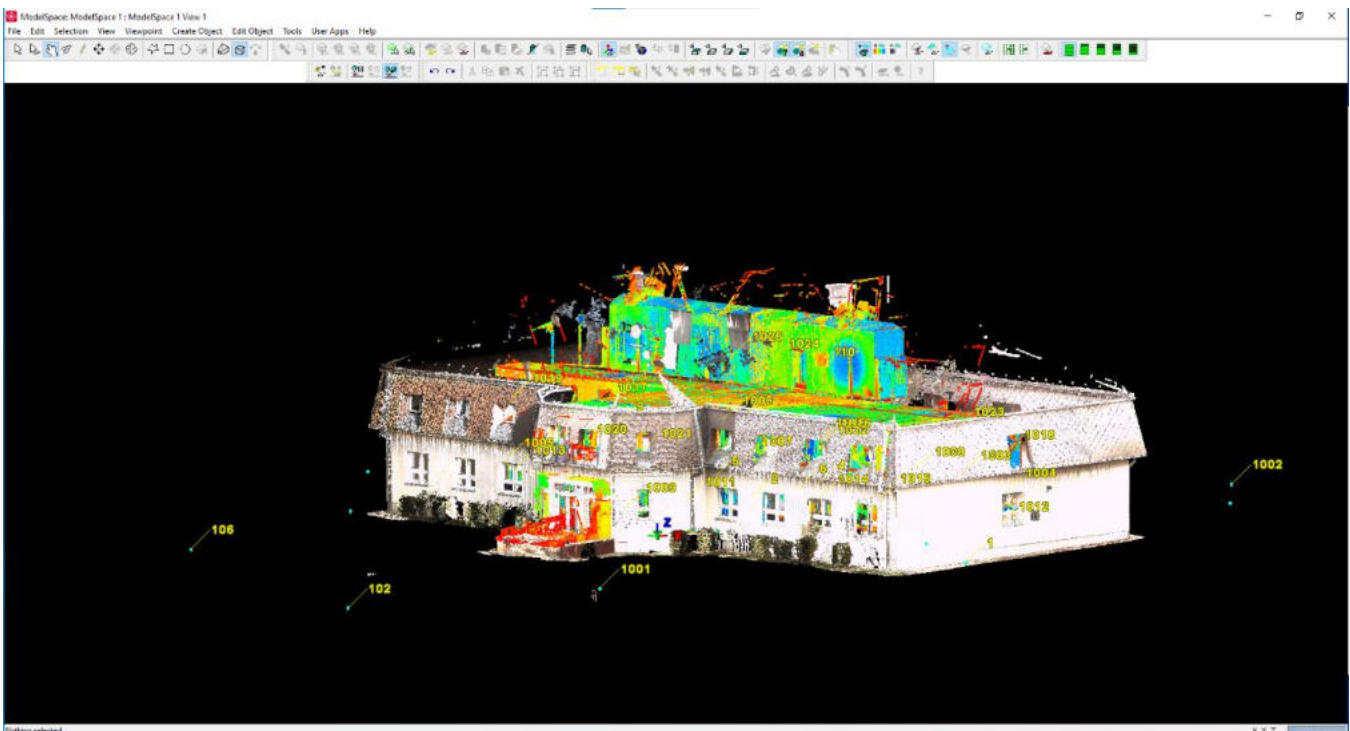


Fig. 2. Representation of the cleaned point cloud

C. The benefits of BIM for facilities management

Asset management is an important field of facilities management. In practice, asset management is a visual information system that provides a transparent system for both the operator and the user. Asset management is a process that is based on a BIM model and a facility model. With CAFM (Computer Aided Facility Management), furniture and objects in a room can be assigned to specific people and rooms, and an inventory can be created. It can even be useful in the event of a move, by moving furniture from one location/room to another.

Identification can be greatly simplified by placing unique barcodes and other unique identifiers. It can also facilitate the inventory process for larger facilities and institutions. Asset and equipment types, maintenance records, and possibly purchase and warranty information can be digitally assigned to them in one place in the model and stored. In addition to acquisition and warranty data, you can also have specific information about the condition and obsolescence of assets using the asset management BIM model.

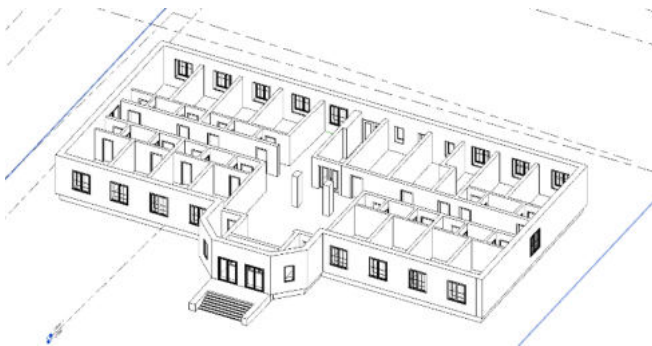


Fig. 3. BIM model of the ground floor of the dormitory

III. RESULTS

The model created can be used for maintenance, inventory and technical refurbishment.

The building of dormitory was last completely renovated between 2011 and 2012. A new boiler was installed, the walls, plinth, high roof and facade were fully insulated and the roof was replaced. In addition, the windows and doors were replaced. All this was done with the aim of saving energy throughout the entire operation, minimising the environmental impact and the temperature difference between the rooms.

Inventory management in the dormitory is simplified by the installation of unique identifiers and barcodes. This way it could be perfectly managed and organised within the BIM model. All the furniture and equipment in the rooms are uniquely identified. In building A of the dormitory, the number of beds in each room is 94, exactly the number of places provided. Keeping track of the number of chairs and tables is not so easy, as more of them are placed in the common and common areas. The beds were replaced in the summer of 2018. In BIM, once the bed objects have been collected, it is possible to assign all the same information at the same time, i.e. the type and the exact time of replacement. In addition, if a bed is destroyed or a new mattress is installed, it is possible to individually assign additional data to the bed concerned.

On the ground floor and the first floor there is a bathroom with a washbasin with mirror and a shower for every 2 bedrooms. On the second floor, sinks and mirrors are located inside the rooms. These are guaranteed accessories in the rooms. In addition, the dormitory provides additional facilities for students. These include an extension cord, table lamp and internet cable. Each person can request one of these accessories. As they keep a detailed record of which person "lives" in which room, this can be documented in the BIM model. In addition, not only can a person be linked to a room, but the devices they wear can also be assigned to their name by their unique identifier [6].

Family:	F2405 - Bed, Non-medical, Single	Load...
Type:	F2405 - Bed, Non-medical, Single	Duplicate...
		Rename...
Type Parameters		
Parameter	Value	
Constraints		
Default Elevation	0.0	
Materials and Finishes		
Material secondary	habszivacs	
Material main	fa	
Identity Data		
Youtube clip		
Technical description		
Product data url	http://bimobject.com/seps2bim/	
Product certification		
Product Guid	37b41116-7304-427e-9999-8228e89	
Installation instructions		
EAN code		
Description	Single bed, approximately 18" high	
Type Image		
Keynote		
Model		
Manufacturer		
Type Comments	Első használat 2018	
URL		
Assembly Code		
Cost	90000.00	
Assembly Description		
Type Mark	Egyszemélyes	
OmniClass Number		
OmniClass Title		
Code Name		
IFC Parameters		
IFC Class Description		

Fig. 4. Data table of the object

With this solution, it is possible to track possible replacements, but also to track both theft and damage. The descriptive data can be extended with any number of additional data depending on what is needed, what the premises are, what the routines are and what the failure possibilities are. A list of this type can be created for any premises and tailored to your needs.

Preparing and carrying out the renovation in such a large institution is no easy task, especially considering the fact that students are inside the dormitory building twenty-four hours a day, 365 days a year. In the case of the dormitory,

particular attention must be paid to the maintenance of the facilities and the regular painting of the cleanliness of the building. During 2022, light bulbs in all rooms and common areas were replaced with energy-saving bulbs. Beds should be replaced every 7-10 years for reasons of hygiene, so new beds will be needed again between 2025-28. The last cleanliness painting took place in the summer of 2021, so this should be done next in 2024.

The BIM model can help the dormitory management to carry out all these works in a cost-effective way.

IV. SUMMARY

This paper highlights the wide range of applications of the BIM model in the field of facilities management through an example. The BIM model has been created using state-of-the-art technology that can stand its ground in the market. The model presented can replace the college's previous databases for maintenance and inventory, as well as making operations more predictable.

REFERENCES

- [1] Zagorác M.-Szabó B., BIM KÉZIKÖNYV-BEVEZETÉS AZ ÉPÜLETINFORMÁCIÓS MODELLEZÉSBE, 1. kötet-1. kiadás, Lechner Tudásközpont, 2018, 128 p.
- [2] Ladai, A. ; Toth, C. ; Toth, Z. Indoor Mapping with an Omnidirectional Camera System, PERFORMANCE ANALYSIS INTERNATIONAL ARCHIVES OF PHOTOGRAMMETRY AND REMOTE SENSING (2002-) XLIII-B1-2022 pp. 347-352. , 6 p.
- [3] Érces, G. -Vass, Gy., Okos épületek és városok tűzvédelmének BIM alapú fejlesztési lehetőségei, In: Gyapjas, János; Varjassy, László (szerk.) KONFERENCIA KIADVÁNY : X. Lakiteleki Tűzvédelmi Szakmai Napok, Kecskemét, Magyarország : Bács-Kiskun Megyei Katasztrófavédelmi Igazgatóság (2023) 444 p. pp. 291-301. , 11 p.
- [4] Manish K. D. et al., Integration of facility management and building information modeling (BIM): A review of key issues and challenges, Department of Construction Science, Texas A&M University, College Station, Texas, USA, 2018, 29 p.
- [5] Király, J., Épületfelmérés épületinformációs modell (BIM) létrehozásának céljából, Alba Regia Technical Faculty of Óbuda University, 2022, 45 p.
- [6] Teszárs, K., Épületinformációs modell (BIM) létrehozása az üzemeltetés optimalizálása céljából, Alba Regia Technical Faculty of Óbuda University, 2022, 44 p.

Water Resources in Efficient Networks (WREN) project overview and presentation of the research results carried out during the first year

Malgorzata Verőné Wojtaszek
Alba Regia Technical Faculty
Óbuda University
Székesfehérvár, Hungary
wojtaszek.malgorzata@amk.uni-obuda.hu

Gábor Molnár
Alba Regia Technical Faculty
Óbuda University
Székesfehérvár, Hungary
molnar.gabor@amk.uni-obuda.hu

Valéria Balázsik
Alba Regia Technical Faculty
Óbuda University
Székesfehérvár, Hungary
balazsik.valeria@amk.uni-obuda.hu

Andrea Pődör
Alba Regia Technical Faculty
Óbuda University
Székesfehérvár, Hungary
podor.andrea@amk.uni-obuda.hu

Gábor Nagy
Alba Regia Technical Faculty
Óbuda University
Székesfehérvár, Hungary
nagy.gabor@amk.uni-obuda.hu

János Katona
Alba Regia Technical Faculty
Óbuda University
Székesfehérvár, Hungary
dr.katona.janos@amk.uni-obuda.hu

Erick Noboa
John von Neumann Faculty of Informatics
Óbuda University
Budapest, Hungary
erick.noboa@irob.uni-obuda.hu

Bence Ádám
Alba Regia Technical Faculty
Óbuda University
Székesfehérvár, Hungary
adambence1989@gmail.com

György Eigner
John von Neumann Faculty of Informatics
Óbuda University
Budapest, Hungary
eigner.gyorgy@nik.uni-obuda.hu

György Györök
Alba Regia Technical Faculty
Óbuda University
Székesfehérvár, Hungary
gyorok.gyorgy@amk.uni-obuda.hu

Abstract—The aim of the WREN project is to create a real-time complex decision support system that facilitates climate change adaptation by monitoring and forecasting drought damage. The goal is to enhance the spatial and temporal resolution of the current drought monitoring system, by combining remotely sensed and local data.

The article presents the results of the research tasks, mainly related to field tests experiments since the launch of the project in April, 2022.

For field soil moisture measurements a study area was selected. For understanding the spatio-temporal variations of the soil moisture a spatial database was created for topographic, meteorological, and pedological, data of the study area. Field soil moisture measurements during the growing season were compared with vegetation indices and a modelling procedures and field measurements.

Index Terms—Remote Sensing, Drought monitoring, Soil moisture, OPTRAM model

I. INTRODUCTION

A. Drought phenomena and drought monitoring

Currently we are witnessing an intensive change of climate on a global scale, which, along with anomalies in weather patterns, poses a major risk of shrinking water resources,

potentially leading to critical situations in agriculture. Drought is not a new issue; however, in recent decades, it has been occurring more frequently and causing increasingly significant damage worldwide. In Hungary, this is becoming an increasingly significant and recurring problem as well.

According to several climate simulations, we should prepare for an expansion of drought-prone areas in the future. In general, drought damage can be estimated at 40 billion HUF annually, but in 2015, it caused a damage of about 400 billion HUF in agriculture. According to some sources, the precipitation deficit in the year 2022 resulted in agricultural losses exceeding 500 billion HUF.

As a general-purpose definition, the World Meteorological Organization (WMO) defines drought as follows: 'Drought is a prolonged dry period in the natural climate cycle that can occur anywhere in the world. It is a slow onset phenomenon caused by a lack of rainfall.' [1].

Depending on the area of application, meteorological drought, hydrological drought, and agricultural drought can be distinguished.

Meteorological drought began to be addressed in the 1960s. In this article titled 'Meteorological Drought' in 1965, Palmer

defined drought as a prolonged and abnormal moisture deficit [2]. Several researchers started working on meteorological drought around the mid-1980s [3],[4], and the common element in the definitions they formulated is a precipitation deficit below the long-term average.

Hydrological drought can be interpreted as a water scarcity in water systems, appearing as abnormally low streamflow in rivers, abnormally low water levels in lakes and reservoirs, and abnormally low groundwater levels [5].

The definition of agricultural drought generally approaches the issue from an unfavorable physiological perspective of plants or a decrease in soil moisture content. According to the European Drought Observatory (EDO), agricultural drought occurs when the low soil moisture content due to meteorological drought limits water availability for vegetation [6].

Quantification is essential for monitoring, analyzing, and forecasting the phenomenon of drought over time. Several calculation methods are available, resulting in the characterization of drought as a so-called *drought index*. However, there is no single unified drought index that can be universally applied across all climates and for all purposes.

For example, the National Water Directorate of Hungary uses a station network established across the entire territory of Hungary for drought monitoring. To track drought, they use a drought index developed in 2015, called the Hungarian Drought Index (HDI), developed by Fiala and colleagues, in 2018 [7]. Based on the scope of data provided by the stations, the index has three variations:

- **HDI0:** The baseline HDI, calculated using daily precipitation and daily mean temperature.
- **HDI1:** This variation of the index takes into account the heat stress experienced by plants. In addition to precipitation and temperature, it simplistically considers potential evapotranspiration.
- **HDI2:** The combined index that not only considers meteorological elements but also incorporates soil moisture and soil water management properties.

These variations of the HDI provide different levels of insight into drought conditions, allowing for a more comprehensive assessment of the phenomenon.

The National Meteorological Service of Hungary (OMSZ) uses the Standardized Precipitation Index (SPI) recommended by the World Meteorological Organization (WMO) for drought monitoring.

In recent decades, satellite remote sensing has provided Earth observation capabilities with relatively high spatial and temporal resolution. Remote sensing imagery offers extensive, spatially continuous spectral measurements over large areas, reflecting both atmospheric and surface characteristics. As a result, remote sensing data are increasingly used for drought monitoring. For example, numerous vegetation indices derived from satellite data have been developed for local and global-scale drought observations. Currently, several systems operation is based on the evaluation of indices derived from satellite imagery.

The European Drought Observatory (EDO) is a drought monitoring system operated by the Joint Research Centre of the European Commission, based on the evaluation of data from the Copernicus program. The majority of the data related to drought generated by the European and global drought monitoring centers can be downloaded from the following links: <https://edo.jrc.ec.europa.eu/gdo/php/index.php?id=2112> and <https://edo.jrc.ec.europa.eu/gdo/php/index.php?id=2000>.

The European Drought Observatory continuously monitors drought in Europe by calculating various drought indices. Typically, these indices highlight the statistical anomaly of the current situation compared to a longer reference period. Different indices can be used to examine various elements of the hydrological cycle (precipitation, soil moisture, water levels, streamflow, groundwater levels) or their impacts (water stress). In addition to the Standardized Precipitation Index (SPI), EDO tracks and forecasts drought by continuously calculating other indices.

The Comprehensive Agricultural Drought Monitoring System, is a system developed at the Remote Sensing Centre of the Institute of Geodesy and Cartography of Poland for monitoring agricultural conditions [8]. This system utilizes a 1 km² spatial resolution index based on Terra MODIS satellite imagery to assess the state of agricultural crops. The DISS (Drought Identification Satellite System) index is a combination of the Temperature Condition Index (TCI) and the Hydrothermal Coefficient (HTC), which characterizes the climatic conditions prevailing in Poland. The DISS drought index is generated in successive eight-day periods within the vegetation season, starting from the end of March. The index values are divided into five categories, representing different levels of moisture: extreme drought, drought, average moisture, good moisture, and high moisture. (<http://www.igik.edu.pl/en/drought-detection>).

B. The Application of Artificial Intelligence in the agriculture sector

The use of artificial intelligence (AI) in agriculture has rapidly increased in recent years, with the potential to revolutionize the way crops are grown and the way they can be managed. Between the facilities that AI can provide in the agriculture sector it worth to mention that it can be used to optimize planting and harvesting times, monitor crop growth, detect diseases and pests in early stage in order to suggest actions to the farmers, and provide recommendations for irrigation and fertilizer management [9],[10]. Additionally, AI-powered drones and robots can help farmers automate tasks such as soil analysis, planting, and harvesting, improving efficiency and reducing costs [10].

With the help of AI, farmers can make data-driven decisions, resulting in higher yields and healthier crops [11]. However, there are also concerns about the ethical and social implications of AI in agriculture, such as loss of jobs and data privacy. Overall, the implementation of AI-based systems in agriculture has the potential to transform the industry and address many of the challenges facing global food production [12].

The history of AI in agriculture can be traced back to the 1980's when the first attempts were made to develop AI-based systems to assist farmers in crop management [13]. In the early years, AI was primarily used to develop Decision Support Systems (DSS) to help farmers make better-informed decisions about irrigation, fertilizer, and pesticide management [10].

One of the first AI-based DSS was the Agro-ecological Information System (AEIS), developed by Davis at University of California, in 1984. AEIS was a knowledge-based system that provided recommendations for soil and water management to improve crop yield [14]. The system used a combination of expert knowledge and data from soil and weather sensors to generate recommendations for farmers.

In the 1990s, the development of precision agriculture technologies led to the integration of AI with precision farming practices [9]. This included technologies such as GPS, remote sensing, and robotics to monitor and manage crops on a more granular level, where AI was applied to analyze data obtained from these technologies to provide suggestions for crop management, such as adjusting irrigation, fertilizer, and pesticide application based on the specific needs of the crop.

Another important milestone in the history of AI in agriculture was the development of machine learning algorithms for crop classification and yield prediction. In 2004, researchers at the University of Illinois developed an AI-based system that used machine learning algorithms to predict corn yield based on weather and soil data [13].

In recent years, the development of AI-powered drones and robots has revolutionized the way farmers manage crops. Drones equipped with sensors and cameras can collect data on crop health, plant count, and soil moisture, while AI-powered robots can automate tasks such as planting and harvesting [10].

The agricultural sector has always been one of the most important pillars of the economy, and with the advent of Industry 4.0, it has undergone a major transformation. Industry 4.0, also known as the fourth industrial revolution, is characterized by the integration of digital technologies into the manufacturing and production process, which has led to a significant increase in productivity, efficiency, and sustainability. One of the most important components of Industry 4.0 is the Internet of Things (IoT), which has played a vital role in revolutionizing this economical sector.

In agriculture, IoT is used to monitor various aspects of the farming process, including soil moisture, temperature, and nutrient levels. This data can be used to make informed decisions about irrigation, fertilization, and other farming practices, resulting in higher crop yields and reduced costs. In this regard, precision farming involves the use of IoT sensors and data analytics to make more precise decisions about planting, harvesting, and other farming practices [10]. This allows farmers to optimize their operations and reduce waste, resulting in higher profits and greater sustainability [11].

The integration of agriculture and Industry 4.0 has not only resulted in increased productivity and sustainability but has also created new opportunities for innovation and en-

trepreneurship. Startups and established companies alike are developing new technologies and solutions to meet the needs of the modern farmer, leading to a growing agricultural technology (AgTech) industry [15].

One of the most powerful AI-based tool available for agriculture is the Object-Based Image Analysis (OBIA), which uses machine learning algorithms to analyze satellite or drone images of crops. The OBIA process involves identifying individual objects within an image and classifying them based on their properties, such as size, shape, and texture [16]. In agriculture, OBIA can be used to identify different crop types, detect crop diseases, and assess crop health. By analyzing crop images, farmers can make data-driven decisions about irrigation, fertilizer, and pesticide management, resulting in higher yields and healthier crops.

One of the key advantages of OBIA is its ability to handle large amounts of data. With the increasing availability of high-resolution satellite and drone images, there is a need for automated methods to analyze these images quickly and efficiently. This tool can process large datasets in a relatively short amount of time, allowing farmers to make timely decisions about the management of their crops. Another advantage of OBIA is its ability to capture spatial variability within an image. Crop health and yield can vary significantly within a field, and this kind of analysis can identify and classify these variations, providing farmers with a detailed understanding of the crop's health and growth.

Due to this reasons, OBIA has been used in several agricultural applications, including crop mapping, crop yield prediction, and disease detection [17]. For example, an Object-Based Image Classifier (OBIC) has been used to identify different types of crops in a field, such as corn, soybeans, and wheat, by analyzing the size, shape, and color of the crops.

OBIC has also been used to detect crop diseases such as fusarium head blight (*Fusarium sp.*) analyzing the texture and color of the wheat heads, OBIC can identify the presence of the disease and provide farmers with recommendations for treatment.

C. WREN

The main aim of the project is to create a real-time complex decision support system (named WREN - Water Resources in Efficient Networks) that facilitates climate change adaptation, drought damage prevention and drought forecasting, and is able to enhance the spatial and temporal resolution of the current drought monitoring system through a fusion of remotely sensed and local data, using mathematical models based on geographic information and artificial intelligence. Within this, our further goal is to create a specially equipped satellite platform, capable of on-board preprocessing of signals to support the aims. The components of the system are: (1) the custom satellite (2) the numerical models that convert satellite data to soil water content distribution (3) the computing infrastructure designed for this purpose and (4) the web application and the associated public API that deliver results to users (Fig. 1).



Fig. 1. The components of the WREN system

The main goal of the project is to create an artificial intelligence-based information system that utilizes machine learning algorithms to estimate and predict soil moisture, enabling drought monitoring and prediction. The system leverages expert knowledge, remote sensing data, and complementary data to generate information for site-specific management support, aiming to improve optimal irrigation and crop yield. Machine learning encompasses algorithms and methods that create models from available data. The key feature of machine learning is automatic knowledge discovery and intelligence-based decision-making. Machine learning is an essential component of artificial intelligence, with the objective of developing behavioral algorithms for systems based on empirical data.

II. DATA

A. Study area

1) *Selection of the study area:* For selecting the study area, the spatial variability of the arable land was considered, both from pedological and from topographical point of view. Another selection criteria was the application of precision agricultural technology (or most elements of it) on the study area. During project preparatory talks with the land owners, the property of the Gyermelyi Zrt. Company's has been selected. The company owns 8300 hectares in the vicinity of its headquarter in Somodorpuszta, Hungary. The area of the fields varies from 20 to 200 hectares, where, because of the hilly landscape, the soil degradation is a common problem. The company contributes to the project with *in situ* data gathered during fieldwork (e.g. crop yield data).

Two fields were selected for regular *in situ* soil moisture measurements and sampling: *Csolnok-73* and *Szomor-11* fields (Fig. 2 and 3).

2) *Topography of the study area:* Topography, besides the landcover and meteorological and soil properties of the area is the key factor in drought development. All these factors affect the utilisation of insufficient amounts of precipitation. The infiltration of a given amount of precipitation into the soil, even at the same precipitation intensity, can vary significantly due to topography characteristics such as slope steepness, length of slopes in the area, and the retention of moisture already in

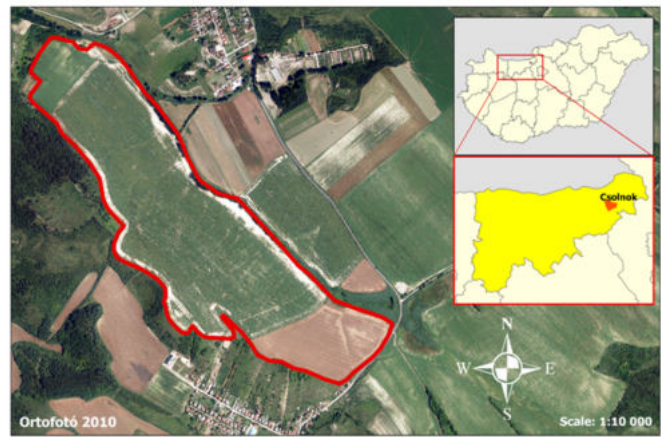


Fig. 2. The location of the study are, field: "Csolnok-73"

the soil depends on evapotranspiration, which are influenced by slope exposure and vegetation cover.

A Digital Elevation Model (DEM) of the 400 ha sample area of the project was generated based on grid points derived from a 1:25 000 scale topographic map with a horizontal resolution of 10m. This resolution, together with the vertical accuracy of +/-0.8 m and +/- 2.5m for flat and hilly areas, makes it suitable for drainage network analyses, however for calculating precipitation infiltration and surface erosion a more detailed DEM, representing the micro-morphology is required.

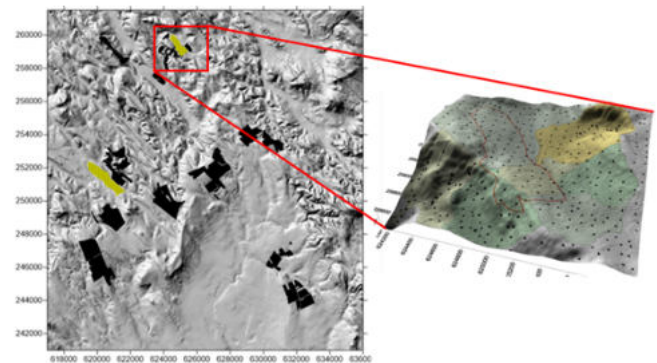


Fig. 3. Digital elevation model of the sample area and Csolnok-73 field is marked in red on 3D figure

3) *UAV measurements:* In order to build a mathematical model describing as accurately as possible the relationship between the remotely sensed data from the proposed WREN satellite and the reference data measured in the field, we also produced a 4cm resolution orthophoto-mosaic and a 1m horizontal resolution digital elevation model of one of the agricultural field of the study area: "Csolnok-73". Using UAV technology, we took around 1800 aerial photographs of the neighbouring 100 ha area and determined the coordinates of nearly one and a half billion points of the surface using LIDAR technology.

These high-resolution topographic data will allow a more

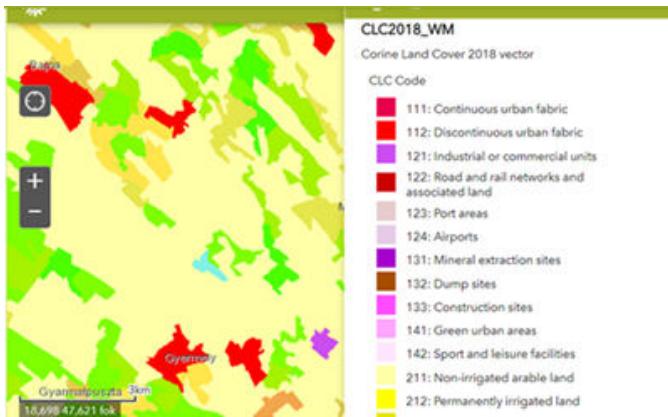


Fig. 4. Landcover map of a part of the sample area



Fig. 5. Field data collection, UAV aerial photography and LIDAR laser scanning of the agricultural field "Csolnok-73"

accurate mathematical modelling, increasing the effectiveness of the drought mapping.

4) *Landcover of the study area:* Due to the European Union's Copernicus Earth Observation program, a 1:50 000 scale Corine Land Cover (CLC50) database is available for the whole country, with a minimum mapped area of 4 ha and a linear minimum of 50 m.

One of the main categories is agricultural fields, which includes irrigated and non-irrigated land separately (Fig. 4).

5) *Soil data for the sample area:* The drought sensitivity of soils is related to their water balance. Water balance is influenced by several factors and different properties at different saturation states help to classify them. In the near saturation state, the water holding capacity of soils is correlated with the bulk density and the total porosity. At low moisture contents, the micro-structure and mechanical composition of the soils are closely related to the amount of water retained. In dry conditions, the quantity and quality of organic matter and inorganic colloids are the determining factors for water holding capacity.

The spatial data from the following databases were used for the analysis:

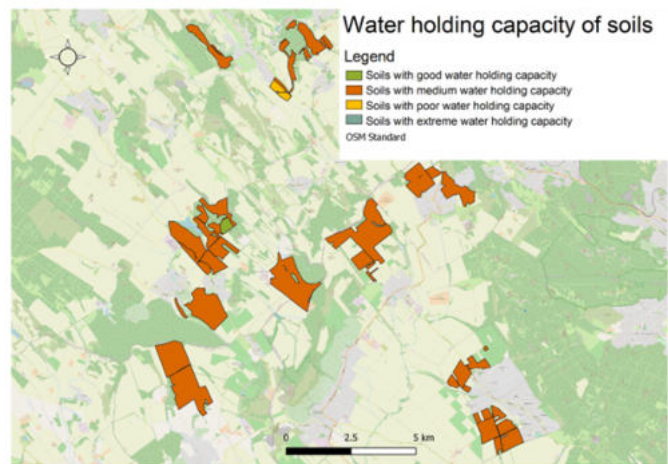


Fig. 6. Water holding capacity of soils in the vicinity of sample area

- TAKI AGROTOPO database (genetic soil type, physical and chemical characteristics, topsoil thickness, organic matter stock, soil water management properties)
- Digital, Optimized, Soil Related Maps and Information in Hungary (Clay Content, Sand Content, Silt Content, Lime Content, Organic matter Content)

According to these databases, 97 % of the sample area is covered by Ramann brown forest soil. This soil type is characterised by strong clay loam and weak acidification.

The analysis shows that more than 97 % of the sample area is of medium water absorption and water conductivity, with high water storage capacity and good water holding capacity. In addition, 1 % to 1 % of the area contains soils with 'High water absorption and conductivity, medium water storage capacity, poor water holding capacity' and 'Good water absorption and conductivity'.

6) *Meteorological Data:* In accordance with the European Union directives, Hungary implemented an open meteorological data policy from 1. January, 2021. According to this policy, the National Meteorological Service of Hungary, (OMSZ) will be able to provide data through the odp.met.hu open data server (Meteorological Data Repository). The data is free of charge and for free use.

The time series are measured by the National Meteorological Service's network of stations. These measurements can be used to study a shorter period of time, data include the extremes measured at the stations. However, these data are not recommended for the study of long-term climate change. The data available for each meteorological station:

- monthly rainfall in mm,
- monthly mean temperature in °C,
- monthly minimum temperature °C
- monthly maximum temperature °C
- monthly average horizontal visibility in m,
- monthly average instrument air pressure in hPa,
- monthly average relative humidity %,
- monthly average gamma dose nSv/h,

- monthly global radiation amount in J/cm²,
- monthly UV radiation amount MED,
- monthly average wind speed m/s,
- monthly mean sea level pressure in hPa,
- monthly average wind speed in m/s,

Another important data source is General Directorate of Water Management in Hungary (OVF), providing *Operational Water Shortage Assessment and Forecasting System* data. The network has more than 150 stations. Data from this network, which was specifically created for drought monitoring, can be downloaded via Internet: <https://aszalymonitoring.vizugy.hu/index.php?view=custommap> By selecting the station name, the user can select the data to be downloaded:

- Soil temperature (20-75 cm depth) (°C)
- Soil moisture (10 cm to 75 cm depth) (V/V)
- Relative humidity (%)
- Precipitation (mm)
- Drought index
- Water deficit(35 cm) (mm)
- Water deficit(80 cm) (mm)
- EOV (Unified National Map Projection of Hungary) coordinates of the station
- Station name
- Air temperature (°C)

B. Field data acquisition

In the present study, the precipitation data measured at meteorological stations and *in situ* measurement of soil moisture were applied. The soil moisture content measurement was carried out four times on two agricultural fields (Csolnok-73 and Szomor-11). Measurement dates:

- 15 July, 2022 (during a dry period), only Csolnok-73 field
- 27 July, 2022 (during a dry period), only Szomor-11 field
- 22 August, 2022 (after rainfall)
- 10 October, 2022 (period without extreme meteorological events)

Soil moisture measurements were taken at depths of 10 cm and 20 cm from the surface. To return to the same sampling points measured during previous measurements, we used a mobile GPS application with an accuracy of 1-2 meters. The selection of measurement points took into account the heterogeneity of the field based on satellite images (Sentinel-2).

The sensor used for the measurements was the WaterScout SM100 Soil Moisture Sensor with a FieldScout Soil Sensor Reader. The sensor was calibrated for mineral soil and the Volumetric Water Content (VWC%) of soil was measured. FieldScout Soil Sensor Reader (Item number: 6466) was used to read the values of the sensor. The relationship between the results obtained was investigated by correlation and regression analysis.

The results of field measurements (July) at "Csolnok-73" field: soil moisture at a depth of 10 cm was ranged from 1.9% to 13.7%. In case of "Szomor-11" field: soil moisture at a depth of 10 cm was ranged from 1.1% to 4.7%, and at a depth of

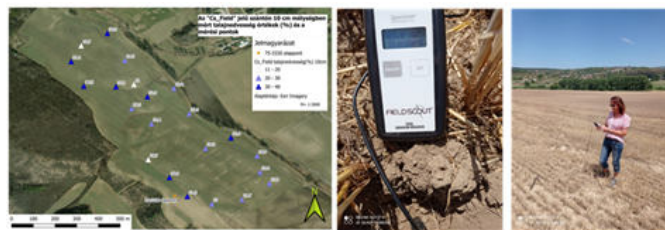


Fig. 7. Soil moisture sampling sites on "Csolnok-73" field. Soil moisture measuring instrument, and field measurement

Dataset	Data type	Fields	
		Csolnok-11	Szomor-73
Sentinel-2	Spectral resolution VIS NIR, SWIR (bands: 3, 4, 8, 12)	12, 20 Aug 2022 09 Oct	1,21,28 July 2022 12, 20 Aug 09 Oct
Meteo station	Precipitation accumulated total	15, 27 July (0 mm) 20 Aug (35 mm) 20 Aug (5 mm)	23 July (0 mm) 20 Aug (40 mm)

TABLE I
REMOTE SENSING AND METEOROLOGICAL DATA

20 cm, was ranged from 2% to 7.8%.

The results of field measurements (August) at "Csolnok-73": Soil moisture at a depth of 10 cm was ranged from 11.0% to 37.1%, and at a depth of 20 cm, was ranged from 7.1% to 40.1%. "Szomor-11": Soil moisture at a depth of 10 cm ranged from 8.3% to 35.2%, and at a depth of 20 cm, was ranged from 11% to 38.2%.

The results of field measurements (October) in "Csolnok-73": Soil moisture at a depth of 10 cm was ranged from 6.7% to 27.5%, and at a depth of 20 cm, was ranged from 19.7% to 34.6%. "Szomor-11": Soil moisture at a depth of 10 cm was ranged from 13.8% to 34.5%, and at a depth of 20 cm, was ranged from 18.7% to 36.8%.

III. METHODS

A. Remote sensing data analysis

Multispectral Sentinel-2 satellite images acquired from the European Space Agency's Sentinel Scientific Data Hub were used in this study. The investigated period was between July and October, 2022. A total of 15 cloud-free images were available, but after preliminary interpretation, 6 of them were selected for further processing. Meteorological (the amount and the intensity of precipitation) data were taken into account in the selection. The characteristics of the data used in the research are included in Table I.

Technically, this research was performed in *eCognition Developer* software. The images and the model were processed using object-based image analysis. Workflow illustrating the main steps of data analyses for mapping surface soil moisture with OPTRAM algorithm (see later) is depicted in Fig. 8.

The data extraction includes the following steps: data pre-processing, multi-level image segmentation, delimitation of indices and the application of the optical trapezoid model.



Fig. 8. Satellite data analysis steps for mapping surface soil moisture with OPTRAM algorithm. [18]

It is important to note that the Sentinel-2 Level-1C processing includes geometric and radiometric corrections including ortho-rectification and calculation of the TOA (the top-of-atmosphere) reflectances. Hierarchical framework was used to identify the boundary of study area at super-object level and determine the unit of investigation (20 m) at the second level for mapping surface moisture.

After pre-processing, indices like Normalized Difference Vegetation Index (NDVI) and Shortwave Infrared Transformed Reflectance (STR) were calculated.

The most common vegetation index used in the water stress models is the NDVI. Reflectance at the red band (B4: 665 nm) and the near infrared (B8: 842 nm) were used to calculate the NDVI.

Reflectance at the SWIR band (B12: 2190 nm) was used for calculation of the STR following [18]:

$$STR = \frac{(1 - S_{SWIR})^2}{2S_{SWIR}} \quad (1)$$

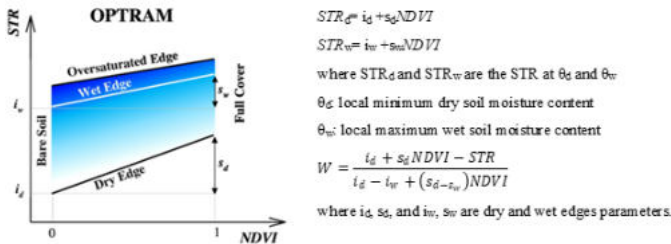


Fig. 9. NDVI-STR diagram illustrating the parameters of OPTRAM model [19]

B. OPTRAM model

The Optical TRapezoid Model (OPTRAM), developed for Soil Water Content (SWC) estimation using optical satellite data is based on the linear physical relationship between soil moisture and STR [19]. OPTRAM requires a parametrization at a given location based on the pixel distribution within STR-NDVI space (Fig. 10, Table II). The model parameters can be obtained for a specific location from the dry and wet edges of the optical trapezoid. During the work, dry (id and sd) and wet (iw and sw) edges were determined by visual inspection of the STR-NDVI diagram, so that the trapezoids surrounded the majority of the pixels. From id and sd (dry edge parameters) and iw and sw (wet edge parameters), the normalized moisture content (W) was estimated for each pixel. The formulas required for the calculation are shown in Fig. 9.

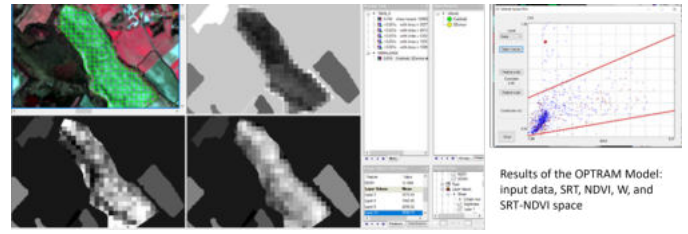


Fig. 10. Development of the OPTRAM model within eCognition environment

Data	Dry edge (id)	Dry edge (sd)	Wet edge (iw)	Wet edge (sw)
27 Aug 2022	0,3	2	0,7	2,25
09 Oct 2022	0,4	2,8	0,7	6,5

TABLE II
OPTRAM PARAMETERS OBTAINED FOR THE STUDY AREA (CSOLNOK-73) BASED ON SENTINEL-2 (2022)

IV. RESULTS

Pearson's correlation coefficient is a statistical measure that quantifies the strength and direction of a linear relationship between two continuous variables. It is widely used in statistics and data analysis to assess the degree of association or correlation between two sets of data. Pearson correlation values can vary from -1 to +1. A correlation value of +1 indicates a perfect positive linear relationship, meaning that as one variable increases, the other also increases proportionally. A correlation of -1 indicates a perfect negative linear relationship, meaning that as one variable increases, the other decreases proportionally. A correlation of 0 indicates no linear relationship or a very weak linear relationship between the two variables. The formula for calculating Pearson correlation is as follows:

$$r = \frac{\sum(X_i - \bar{X})(Y_i - \bar{Y})}{\sqrt{\sum(X_i - \bar{X})^2} \sqrt{\sum(Y_i - \bar{Y})^2}} \quad (2)$$

where:

- r is the Pearson correlation coefficient
- X_i and Y_i are individual data points in the two datasets
- \bar{X} and \bar{Y} are the means (averages) of the respective datasets

The results of Table III show a strong positive linear relationship between the soil moisture data measured during field surveys and the soil moisture values estimated by using OPTRAM model.

V. CONCLUSIONS

During statistical analysis the OPTRAM-based moisture estimates were compared with soil moisture ground truth data. Taking into account the results of the model calculation, the moisture value (W) of the points was determined at which a local measurement (WC) was also performed. Based on the value of the Pearson correlation coefficient, that a strong positive relationship was found between the two variables (r

augusztus			október		
10cm	20cm	W	10cm	20cm	W
11	7,1	-0,242799568	6,7	16,5	-0,492539003
19,7	16,9	-0,23133975	9,3	19,7	-0,215083704
19,7	18,7	-0,211558851	11,2	22,7	-0,180587166
20,2	24,2	-0,207494664	11,2	24,3	-0,094233741
21,7	25,5	-0,203976777	12,2	25,2	0,12008608
24,2	26	-0,20162519	12,6	28	0,12597996
26,4	26	-0,08461995	18,3	28,5	0,299855586
26,5	26,9	-0,009468904	27,5	34,6	0,481198679
26,8	28	0,014628648			
27	30,1	0,046135048	Pearson: 10 cm - W		0,900170641
27,3	31,3	0,080244107	Pearson: 20 cm - W		0,971120131
27,8	31,8	0,104775354			
28,2	32,2	0,105100347			
29,8	32,8	0,134867114			
30,6	33,4	0,144796686			
31,2	33,8	0,148337604			
31,2	34,4	0,249605868			
32,2	35,4	0,269062895			
32,4	35,4	0,315511376			
33,9	37,1	0,386820702			
36,5	37,6	0,486709269			
37,1	40,1	0,53935856			
Pearson: 10cm - W		0,926576953			
Pearson: 20cm - W		0,877088646			

TABLE III
THE CORRELATION BETWEEN ESTIMATED DATA (W) AND FIELD MEASUREMENTS (WC)

= 0.8-0.9). Statistical analyses show that the values calculated by the model (W) were strongly correlated with the values measured *in situ*. Therefore, the results could confirm the applicability of the model.

In the further research we plan spread soil moisture measurements for more agricultural fields and use them in validation.

According to earlier [18] and current research results the method proved to be useful for developing satellite image based drought monitoring system.

ACKNOWLEDGMENT

The authors gratefully acknowledge the support provided for this research by the GINOP_PLUSZ-2.1.1.-21-2022-00040 Project. The project is supported by Széchenyi Plan Plus, co-funded by the Government of Hungary and the European Union. Authors are very grateful to Zsolt Keresztes director of the Plant Production (Gyermelyi Zrt. Company, Hungary) for providing data and ensuring the possibility for field soil moisture measurements.

REFERENCES

- [1] P. Board, Ed., *State of the Climate in Europe 2022*. World Meteorological Organization, 2022, vol. WMO-No. 1320.
- [2] W. Palmer, *Meteorological Drought* (Meteorological Drought 30). U.S. Department of Commerce, Weather Bureau, 1965. [Online]. Available: <https://books.google.hu/books?id=kyYZgnEk-L8C>.
- [3] M. J. Sadowski, "Climatological premises of soil drought forecasting," *Journal of Climatology*, vol. 4, no. 6, pp. 637–643, 1984. DOI: <https://doi.org/10.1002/joc.3370040607>.

- [4] M. H. Glantz, *Drought & Hunger in Africa*. Cambridge University Press, 1988, p. 480, ISBN: 9780521368391.
- [5] A. F. V. Loon, "Hydrological drought explained," *WIRES Water*, vol. 2, no. 4, pp. 359–392, Apr. 2015. DOI: 10.1002/wat2.1085.
- [6] *European drought observatory*. [Online]. Available: <https://edo.jrc.ec.europa.eu/edov2/php/index.php?id=1000>.
- [7] K. B. Károly Fiala, B. Benyhe, I. Fehérváry, J. Lábdy, G. Sipos, and L. Györfly, "Operational drought and water scarcity monitoring system," *Hungarian Journal of Hydrology*, vol. 98, no. 3, pp. 14–24, 2018.
- [8] K. Dabrowska-Zielinska, A. Malinska, Z. Bochenek, *et al.*, "Drought model DISS based on the fusion of satellite and meteorological data under variable climatic conditions," *Remote Sensing*, vol. 12, no. 18, p. 2944, Sep. 2020. DOI: 10.3390/rs12182944.
- [9] K. Jha, A. Doshi, P. Patel, and M. Shah, "A comprehensive review on automation in agriculture using artificial intelligence," *Artificial Intelligence in Agriculture*, vol. 2, pp. 1–12, Jun. 2019. DOI: 10.1016/j.aiaa.2019.05.004.
- [10] S. Pitla, S. Bajwa, S. Bhusal, *et al.*, "Ground and Aerial Robots for Agricultural Production: Opportunities and Challenges," *Biological Systems Engineering: Papers and Publications.*, no. 727, 2020.
- [11] T. Talaviya, D. Shah, N. Patel, H. Yagnik, and M. Shah, "Implementation of artificial intelligence in agriculture for optimisation of irrigation and application of pesticides and herbicides," *Artificial Intelligence in Agriculture*, vol. 4, pp. 58–73, 2020. DOI: 10.1016/j.aiaa.2020.04.002.
- [12] P. Zhang, Z. Guo, S. Ullah, G. Melagraki, A. Afantitis, and I. Lynch, "Nanotechnology and artificial intelligence to enable sustainable and precision agriculture," *Nature Plants*, vol. 7, no. 7, pp. 864–876, Jun. 2021. DOI: 10.1038/s41477-021-00946-6.
- [13] A. Cavazza, F. D. Mas, P. Paoloni, and M. Manzo, "Artificial intelligence and new business models in agriculture: A structured literature review and future research agenda," *British Food Journal*, vol. 125, no. 13, pp. 436–461, Jul. 2023. DOI: 10.1108/bfj-02-2023-0132.
- [14] M. Carozzi, S. Bregaglio, B. Scaglia, E. Bernardoni, M. Acutis, and R. Confalonieri, "The development of a methodology using fuzzy logic to assess the performance of cropping systems based on a case study of maize in the po valley," *Soil Use and Management*, vol. 29, no. 4, pp. 576–585, Jul. 2013. DOI: 10.1111/sum.12066.
- [15] A. Cavallo, A. Ghezzi, and B. V. R. Guzmán, "Driving internationalization through business model innovation," *Multinational Business Review*, vol. 28, no. 2, pp. 201–220, Jul. 2019. DOI: 10.1108/mbr-11-2018-0087.

- [16] L. Ma, M. Li, X. Ma, L. Cheng, P. Du, and Y. Liu, “A review of supervised object-based land-cover image classification,” *ISPRS Journal of Photogrammetry and Remote Sensing*, vol. 130, pp. 277–293, Aug. 2017. DOI: 10.1016/j.isprsjprs.2017.06.001.
- [17] M. Vogels, S. de Jong, G. Sterk, and E. Addink, “Agricultural cropland mapping using black-and-white aerial photography, object-based image analysis and random forests,” *International Journal of Applied Earth Observation and Geoinformation*, vol. 54, pp. 114–123, Feb. 2017. DOI: 10.1016/j.jag.2016.09.003.
- [18] M. Veróné Wojtaszek, V. Szabó, J. Kauser, A. Kocsis, and L. Lippmann, “55. mapping of soil moisture variability within a field by the OPTRAM model,” in *Precision agriculture '21*, Wageningen Academic Publishers, Jun. 2021. DOI: 10.3920/978-90-8686-916-9_55.
- [19] M. Sadeghi, S. B. Jones, and W. D. Philpot, “A linear physically-based model for remote sensing of soil moisture using short wave infrared bands,” *Remote Sensing of Environment*, vol. 164, pp. 66–76, Jul. 2015. DOI: 10.1016/j.rse.2015.04.007.

Common aspects of 3D modeling and vision solutions in robotics and geoinformatics

Tamás Jancsó
Alba Regia Technical Faculty
Óbuda University
Szekesfehervar, Hungary
jancso.tamas@amk.uni-obuda.hu

Károly Széll
Alba Regia Technical Faculty
Óbuda University
Szekesfehervar, Hungary
szell.karoly@amk.uni-obuda.hu

Gergely Vakulya
Alba Regia Technical Faculty
Óbuda University
Szekesfehervar, Hungary
vakulya.gergely@amk.uni-obuda.hu

József Borbély
Alba Regia Technical Faculty
Óbuda University
Szekesfehervar, Hungary
borbely.jozsef@amk.uni-obuda.hu

János Katona
Alba Regia Technical Faculty
Óbuda University
Szekesfehervar, Hungary
katona.janos@amk.uni-obuda.hu

Gábor Nagy
Alba Regia Technical Faculty
Óbuda University
Szekesfehervar, Hungary
nagy.gabor@amk.uni-obuda.hu

Abstract— The solutions of image-based 3D modeling in photogrammetry and the possibilities of 3D vision in robotics show common problems and solutions. Such common areas are, for example, the mapping of the virtual world, the automated creation and classification of point clouds, the detection and tracking of 3D objects. The common features of the applied methods are the stereo vision, the image matching, the motion detection and, finally, the intelligent object recognition. This article provides a brief overview of the methods used in these two areas and the challenges we face.

Keywords— 3D modelling, 3D vision, robotics, geoinformatics, photogrammetry, image matching

I. INTRODUCTION

3D modeling plays a significant role in robotics and is applied in various areas, from design and simulation to control. Here are some important areas where 3D modeling can be useful in the field of robotics:

- Robot design and pre-design analysis: 3D modeling allows visualization of the concept and appearance of robots even before physical prototypes are created. This enables identifying and correcting design errors before actual hardware production.
- Robot prototyping and testing: Through 3D modeling, physical prototypes of robots can be created and tested in a virtual environment even before the actual hardware is manufactured. This allows for trying out different design variations and functionalities, optimizing, and making improvements.
- Simulation and control development: 3D modeling enables the creation of realistic simulations of robot behavior and operation. This allows for the development of control algorithms, optimization of navigation, and planning tasks for the robots.
- Collaborative robots (Cobots) and human-robot collaboration: Using 3D modeling, the conditions for human-robot interactions can be designed and simulated, making cobots safer and more efficient in collaboration with humans. Designing and simulating the robot's physical appearance and movements through 3D models can enhance human-robot interaction by making the robot more relatable and user-friendly.

- Object Recognition and Manipulation: 3D models of objects in the environment can be used for training and testing object recognition algorithms. The robot can use these models to recognize and manipulate objects, enhancing its interaction capabilities.
- Localization and Mapping (SLAM): 3D models assist in simultaneous localization and mapping (SLAM) algorithms, where the robot constructs a map of its environment while estimating its own position within it (Fig. 1, [4]). These 3D maps provide richer spatial information compared to 2D maps. 3D models are also aiding tools in collision detection algorithms. The robot's movement and path can be simulated within the 3D environment, allowing for the identification of potential collisions and the optimization of motion paths to avoid obstacles.

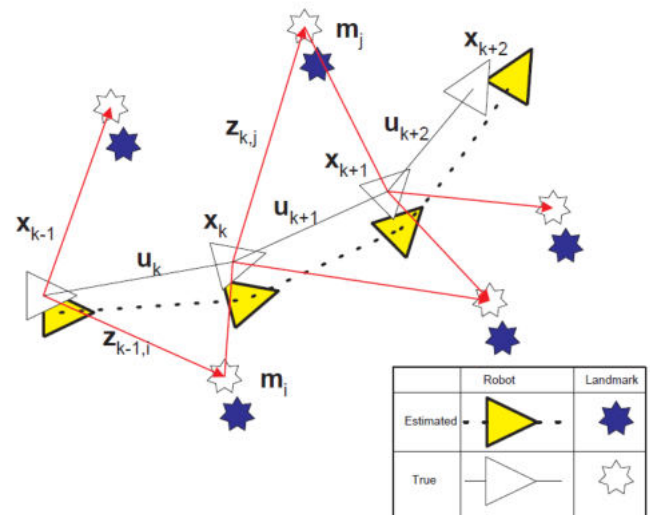


Fig. 1. A typical SLAM task of a mobile robot with built-in sensors

- Augmented Reality (AR) and Visualization: Overlaying 3D models onto the real-world environment using AR techniques enhances the robot's perception and visualization, aiding in tasks like navigation and object interaction.
- Training Machine Learning Models: 3D models can be used to generate training data for machine learning models. Simulated environments allow for generating diverse datasets to train algorithms for various robot-

related tasks, such as object recognition, grasp planning, and locomotion.

- Teleoperation and Remote Control: 3D models can be used to create user interfaces for teleoperation and remote control of robots, providing an intuitive way for operators to visualize and control the robot's actions.
- Education and Training: 3D models are valuable tools for educating and training individuals in robotics. They facilitate a better understanding of robot anatomy, kinematics, and dynamics.

Overall, 3D modeling provides the capability to pre-plan, test, and optimize robots, facilitating their more efficient and safer application in various domains of robotics.

On the other hand, 3D modeling is a versatile tool in geoinformatics, enabling the representation, visualization, and analysis of geographical data in three-dimensional space. Here are several important applications of 3D modeling in the field of geoinformatics:

- Terrain modeling and topographic mapping: 3D modeling allows for the precise representation of topographic features and landforms. It is crucial in creating accurate 3D models based on elevation data, which are essential for various applications such as urban and landscape planning, as well as disaster management.
- Urban and city planning: 3D modeling plays a vital role in urban and city planning, enabling the creation of detailed plans for buildings, infrastructure, and public spaces. It allows planners to assess the spatial layout and impacts of buildings and infrastructure within an urban environment.
- Environmental modeling and conservation: Through 3D modeling, environmental elements such as forests, rivers, and other natural objects can be modeled and visualized. This helps in analyzing environmental changes and their impacts, aiding in environmental protection efforts (Fig. 2).

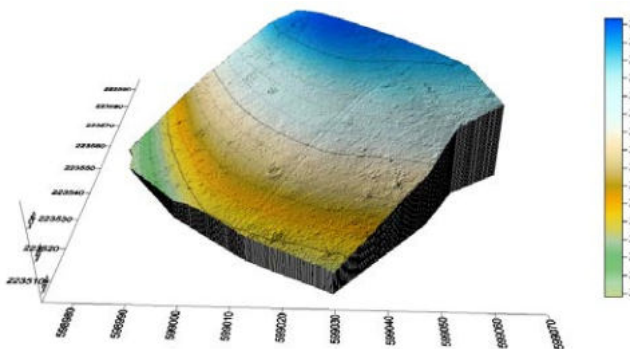


Fig. 2. Digital terrain model based on drone images

- Infrastructure and utility modeling: 3D modeling is used to accurately model infrastructure elements such as roads, bridges, airports, and utility networks like electrical and communication grids. This assists in better planning, maintenance, and development of these essential public facilities.
- Telecommunications and satellite communication: In geoinformatics, 3D modeling is used to model

telecommunication towers and satellite communication systems. It helps optimize the network layout and analyze the coverage for better communication infrastructure planning.

- Simulation and crisis management: 3D modeling is an aiding tool in simulations and predictions related to various crises such as floods, earthquakes, or wildfires. Preemptive modeling and visualization assist in developing crisis management plans and understanding potential impacts.
- Archaeology and cultural heritage preservation: 3D modeling is employed to create digital representations of archaeological sites and cultural heritage assets. This aids in documentation, analysis, and preservation of historical sites.
- GIS (Geographic Information Systems): 3D models can enhance for example the navigation systems providing three-dimensional representations of landscapes and structures.
- Natural resource management: 3D modeling is utilized in managing natural resources such as mines, forests, and water bodies. It aids in efficient planning and utilization of these resources.

By utilizing 3D modeling in these various applications, geoinformatics professionals can better visualize, analyze, and plan activities related to geography, urban planning, environmental management, and more, ultimately leading to more informed decision-making and sustainable development.

Next section puts forward the methods for 3D modelling regarding solutions in robotics and image matching in photogrammetry.

II. 3D MODELLING METHODS

Image matching for 3D modeling is a critical process for tasks such as structure from motion (SfM), simultaneous localization and mapping (SLAM), and 3D reconstruction. Innovations in this field are driven by advancements in computer vision, machine learning, and the integration of sensor technologies. Here are some of the most innovative methods in image matching for 3D modeling:

- Structure from Motion (SfM) with Bundle Adjustment: SfM is a fundamental technique for 3D reconstruction. Modern SfM approaches incorporate bundle adjustment to jointly optimize camera poses and 3D structure, resulting in highly accurate reconstructions.
- Feature matching and correspondence estimation: Utilizing advanced local feature descriptors (e.g., SIFT, SURF, ORB) and robust matching algorithms for establishing correspondences between features in images, aiding in accurate 3D reconstruction.
- Direct methods for depth estimation: Direct methods bypass feature extraction and matching by directly estimating depth from image intensities. These methods leverage photometric and geometric constraints to estimate depth maps.
- Depth from stereo and depth from motion: Techniques that leverage multiple images or video frames to

estimate depth information, crucial for generating accurate 3D models.

- Multi-View Stereo (MVS): MVS algorithms aim to estimate 3D geometry by combining information from multiple images to generate dense, detailed 3D reconstructions.
- PatchMatch and PatchMatch Stereo: PatchMatch is an efficient algorithm used in stereo matching and image correspondence tasks, providing high-quality results in terms of depth estimation and 3D reconstruction.
- Convolutional Neural Networks (CNNs) for depth estimation: CNN-based approaches are increasingly being used for depth estimation from monocular images, stereo pairs, or video sequences, leveraging large datasets for training.
- Graph Neural Networks (GNNs) for 3D Structure Estimation: GNNs can be employed to model relationships and dependencies between 3D points or patches, aiding in reconstructing accurate 3D structures from 2D images.
- Learning-based depth fusion: Techniques that combine depth information from various sources, including stereo matching, monocular depth estimation, and depth sensors, to obtain a more reliable and accurate depth map.
- Semantic 3D reconstruction: Integrating semantic information into the 3D reconstruction process to obtain semantically meaningful 3D models, useful in various applications like robotics and AR/VR.
- Real-time and incremental 3D reconstruction: algorithms that enable continuous 3D reconstruction in real-time, important for applications like augmented reality and robotic navigation.
- Global optimization techniques: Leveraging global optimization methods, such as loop closure detection and optimization, to refine the 3D reconstruction by correcting drift and improving overall accuracy.

Incorporating these innovative methods into the image matching pipeline for 3D modeling has significantly advanced the field, enabling accurate, detailed, and real-time 3D reconstructions for a wide range of applications, including virtual reality [4], robotics, geospatial analysis, and more.

A. Possible solutions in robotics

Detecting and tracking 3D objects in robotics is a crucial task for various applications, including autonomous navigation, object manipulation, and scene understanding. This process involves using sensor data, often from cameras or depth sensors, to identify and continuously monitor the position, orientation, and shape of objects in a 3D environment.

Here's a high-level overview of the steps involved in detecting and tracking 3D objects in robotics:

- Sensor data acquisition: Robotics systems typically use sensors such as RGB cameras, depth cameras, LiDAR (Light Detection and Ranging), or a combination of these to gather data about the environment. RGB cameras provide color information, while depth

sensors or LiDAR offer depth information, aiding in the creation of 3D representations.

- Preprocessing: Raw sensor data often requires preprocessing to enhance its quality and relevance. This may involve noise reduction, calibration, synchronization of multiple sensors, and rectification to align the data accurately.
- Object detection: Object detection is the process of identifying and locating objects within the sensor data. In the context of 3D object detection, algorithms analyze the 3D data (point clouds or depth maps) to identify objects and estimate their 3D bounding boxes and/or poses.
- Feature extraction: Extracting relevant features from the detected objects is important for accurate tracking. These features might include color information, surface normal vectors, shape descriptors, or unique patterns.
- Object tracking: Object tracking involves associating the detected objects over time, maintaining their identities and positions across successive sensor readings. Tracking algorithms utilize object features and motion models to predict and update the object's position, orientation, and other relevant parameters.
- Data Fusion: In many robotics applications, data from multiple sensors are fused to improve object detection and tracking accuracy. Fusion algorithms combine information from different sensor modalities to create a more comprehensive and robust representation of the environment.
- Kalman filtering or extended Kalman filtering: These filtering techniques are commonly used for object tracking. They incorporate prediction models and sensor measurements to estimate the object's state (position, velocity, etc.) and update the estimates iteratively as new measurements are received.
- Mapping and localization: Concurrently with object detection and tracking, robotics systems often build maps of the environment and localize the robot within these maps [9]. This helps in understanding the spatial context in which the objects are detected and tracked.
- Integration with robot control: The detected and tracked objects' information is integrated into the robot's control and decision-making processes. This could involve path planning, obstacle avoidance, or manipulation planning based on the detected objects' positions and characteristics.
- Feedback and adaptation: Robotics systems often incorporate feedback loops to adapt the object detection and tracking algorithms based on the performance and real-world interactions. Machine learning techniques may be used to continuously improve the system's accuracy and reliability.

Efficient and accurate 3D object detection and tracking are critical for enabling various robotic applications, from autonomous driving to robotic manipulation tasks, and are an active area of research and development within the field of robotics.

Motion detection and intelligent object recognition are fundamental components of computer vision and play an important role in various applications, including surveillance, robotics, human-computer interaction, automotive safety, and more. Here, we'll discuss the methods and application areas for both motion detection and intelligent object recognition.

a) *Motion Detection Methods*

- **Frame differencing:** Frame differencing involves subtracting consecutive frames in a video sequence to detect regions with significant pixel intensity changes, indicating motion.
- **Optical flow:** Optical flow methods estimate the motion of pixels between consecutive frames, providing information about the direction and speed of motion [1].
- **Background subtraction:** Background subtraction algorithms model the stationary background in a video and identify regions where there are significant differences between the current frame and the background.
- **Blob analysis:** After detecting motion regions, blob analysis groups adjacent pixels into objects or "blobs" based on certain criteria, such as size, shape, and connectivity.
- **Machine learning and deep learning:** Advanced techniques, including supervised learning and deep learning, can be employed to train models for motion detection. Convolutional neural networks (CNNs) and recurrent neural networks (RNNs) can learn motion patterns and detect complex motion events.

b) *Motion detection application areas*

- **Surveillance and security:** Motion detection is widely used in surveillance systems to monitor and detect suspicious activities, intruders, or unusual behavior in restricted areas.
- **Automotive safety:** Motion detection is critical for advanced driver assistance systems (ADAS) to detect moving vehicles, pedestrians, and other objects to enhance road safety and enable features like collision avoidance and adaptive cruise control.
- **Gaming and human-computer interaction:** Motion detection is used in gaming systems and gesture-based interfaces to track movements of players and interpret gestures for controlling gameplay or interacting with devices.
- **Healthcare:** Motion detection is utilized in healthcare for monitoring patient movements, fall detection for the elderly, and assessing rehabilitation exercises.
- **Retail and marketing:** Retailers use motion detection to analyze customer movements and behavior in stores, helping optimize store layouts and marketing strategies.

c) *Intelligent object recognition Methods*

- **Haar cascades:** Haar cascades are used for rapid object detection using a cascade of increasingly complex classifiers, often applied in faces and object detection.

- **Histogram of oriented gradients (HOG):** HOG computes the distribution of gradient orientations in an image, which is used for object detection, particularly in pedestrian detection.
- **Convolutional Neural Networks (CNNs):** CNNs have revolutionized object recognition by learning hierarchical features directly from images, making them highly effective for complex object recognition tasks.
- **Region-based CNNs (R-CNN, faster R-CNN, mask R-CNN):** These models combine CNNs with region proposal networks to efficiently detect and segment objects in images.
- **You Only Look Once (YOLO):** YOLO is an efficient and fast real-time object detection algorithm that divides the image into a grid and predicts bounding boxes and class probabilities directly.

d) *Intelligent object recognition application areas*

- **Autonomous vehicles:** Object recognition is critical for autonomous driving systems to identify and track vehicles, pedestrians, cyclists, and road signs to make driving decisions.
- **Augmented Reality (AR) and Virtual Reality (VR):** Object recognition is used to overlay virtual objects seamlessly into the real world in AR applications and for enhancing immersive experiences in VR.
- **Robotics:** Object recognition is employed in robotic systems for tasks like object manipulation, pick-and-place operations, and scene understanding.
- **Medical imaging:** Object recognition assists in medical image analysis, such as detecting and segmenting tumors, organs, or anomalies in medical imaging data.
- **Retail and e-commerce:** Object recognition is used in product recognition, inventory management, and recommendation systems in retail and e-commerce platforms.

In both motion detection and intelligent object recognition, ongoing advancements in machine learning, deep learning, and computer vision techniques are continually improving accuracy, speed, and applicability across a wide range of real-world scenarios and domains.

B. *Image matching in photogrammetry*

Image matching in photogrammetry refers to the process of identifying corresponding points or features in multiple images of a scene or object, with the goal of creating accurate three-dimensional (3D) models and measurements. Photogrammetry uses the principles of geometry and mathematics to extract 3D information from two-dimensional (2D) images [2], [3], [6]. Image matching is a fundamental step in photogrammetry as it establishes correspondences between images, enabling the creation of accurate and detailed 3D models used in applications like mapping, surveying, remote sensing, archaeology, and urban planning.

The area-based image matching (ABM) with normalized cross-correlation is a widely used technique to find correspondences or similarities between image regions or patches by measuring the cross-correlation between the intensity values within these areas. Cross-correlation is a

mathematical operation that describes the similarity or resemblance between two signals (in this case, image patches) as they are shifted relative to each other.

ABM with cross-correlation is widely used in various computer vision applications, including stereo matching, optical flow estimation, object tracking, template matching, and registration in medical imaging. ABM is a technique used in computer vision, photogrammetry, and remote sensing to establish correspondences and match regions or areas in multiple images based on their pixel intensities or other properties. Unlike feature-based matching that focuses on distinct key points, ABM operates on larger image regions or patches, considering a more extensive area for matching.

ABM is useful in various areas including the following typical tasks:

- Stereo matching and depth estimation: By comparing patches in stereo images, it helps estimate the disparity or depth information for each patch, which is crucial for 3D reconstruction.
- Change detection: Comparing patches in images acquired at different times helps identify changes in the scene, useful for monitoring and detecting alterations in landscapes, urban areas, and environmental conditions.
- Orthoimage generation: In aerial or satellite imagery, matching patches is essential to create seamless orthoimages by aligning and mosaicking overlapping images.
- Remote sensing and GIS: ABM is used for feature extraction, land cover classification, and image registration, aiding in various remote sensing and geographic information system (GIS) applications [7].

Overall, area-based image matching provides a broader perspective on matching image regions and is vital in many image processing and computer vision tasks.

As an alternative, the semi-global image matching (SGM) is a powerful stereo vision technique used for dense disparity map estimation from stereo image pairs. It aims to find correspondences or disparities for each pixel in the left and right images, providing valuable depth information for 3D reconstruction. SGM is particularly effective in cases where traditional local matching approaches struggle, such as for symmetrically textured and textureless regions.

Semi-global image matching has several advantages, including robustness in handling occlusions, slanted surfaces, and textureless regions. It produces dense disparity maps, providing detailed depth information across the entire image.

Applications of SGM include 3D reconstruction, autonomous vehicles (e.g., for obstacle detection), robotics (e.g., for navigation and mapping), augmented reality, and various computer vision tasks that require accurate depth estimation from stereo imagery.

III. CONCLUSION

In summary, 3D modeling and vision solutions are fundamental components in both robotics and geoinformatics, serving to understand and navigate complex environments. There is an overlap in technology and tools, since both domains may utilize similar software and tools for data

processing, analysis, and visualization, including GIS (Geographic Information Systems) software, computer-aided design (CAD) tools, and 3D modeling software. Here's a summary highlighting their common aspects, and differences in methods, in the representation and analysis of three-dimensional data and environments.

A. Common aspects

All the common aspects and differences are summarized in Fig. 3. followed by a detailed explanation.

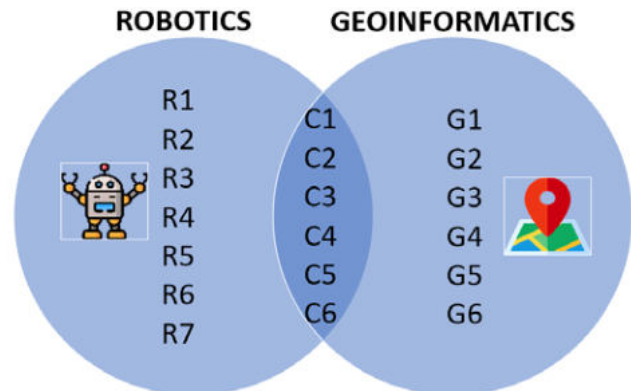


Fig. 3. Specific and common aspects

- Representation of 3D environment (C1): In general, 3D modeling focuses on creating digital models of objects, landscapes, or structures, while geoinformatics emphasizes representing geographical or spatial data in three-dimensional space. Both domains involve creating and representing 3D models of the environment to aid perception, analysis, and decision-making. These models may include terrain, objects, structures, and other spatial entities.
- Sensor integration (C2): Both domains involve data acquisition and subsequent processing, and they rely on sensors like LiDAR, RGB-D cameras, stereo cameras, and other depth-sensing technologies to capture 3D data and imagery. Integration and fusion of data from various sensors enhance accuracy and completeness of 3D representations. Geoinformatics mainly involves the acquisition of spatial data through technologies like GPS, LiDAR, or aerial/satellite imagery, followed by data processing and analysis. In robotics, various sensors such as cameras, LiDAR, IMUs (Inertial Measurement Units), and others are combined to obtain comprehensive spatial information, as well [11].
- Feature extraction (C3): Extracting salient features, key points, or landmarks from sensor data is crucial for understanding and reconstructing the environment. Common methods like SIFT, SURF, or CNN-based features are applied for feature extraction.
- Image processing and Computer Vision (C4): Both domains heavily utilize computer vision and image processing techniques including edge detection, filtering, and object recognition to enhance and manipulate images and data for further analysis. Computer vision methods aid in object detection, tracking, and image-based 3D reconstruction. It means, similar computer vision algorithms are used in robotics and geoinformatics to analyze images or sensor data,

detect features, track objects, and extract meaningful information.

- Spatial analysis and visualization (C5): Both domains involve spatial analysis and visualization. Geoinformatics utilizes spatial analysis techniques to derive insights and patterns from geographical data. 3D modeling in robotics and geoinformatics enables the creation of visualizations and simulations for better understanding and analysis of spatial information.
- Depth estimation (C6): Estimating depth information is vital for both domains. Depth estimation methods, such as stereo vision, structure from motion (SfM), or depth from monocular cues, contribute to 3D perception.

B. Differences in methods

- Mapping and localization (R1): Creating maps of the environment and localizing the robot or objects within these maps are specific tasks for mobile robots. Simultaneous Localization and Mapping (SLAM) and related techniques are extensively used for this purpose [5], [8].
- Focus and purpose: In robotics, the emphasis is on real-time control, navigation, and interaction with the environment. Methods often prioritize efficiency, low latency, and adaptability to dynamic and unknown environments (R2). In geoinformatics, the focus is on precise mapping, analysis, and understanding of geographic spaces, often emphasizing accuracy and high-resolution models (G1).
- Sensor suites: Robotics often utilize a broader range of sensors, including proximity sensors, IMUs, and haptic sensors, to enable close interaction and safe navigation (R3). Geoinformatics primarily centers around remote sensing technologies such as satellites, aerial imagery, and LiDAR (G2).
- Complexity of environments: Robotic applications deal with varying, unstructured, and dynamic environments, necessitating robustness and adaptability (R4). Geoinformatics typically deals with more structured and predictable natural or man-made environments (G3), [10].
- Real-time requirements: Robotics often require real-time processing and decision-making to ensure safe and efficient robot operations (R5). Geoinformatics applications may prioritize accuracy over real-time constraints, allowing for more elaborate post-processing and analysis (G4).
- Integration of Artificial Intelligence (AI) and Machine Learning (ML): While both domains leverage AI and machine learning, robotics often integrate AI for real-time decision-making, obstacle avoidance, and path planning (R6)). In geoinformatics, AI and ML are commonly used for data analysis, classification, change detection, and pattern recognition (G5).

- Scale of analysis: Geoinformatics frequently deals with large-scale geographic areas, requiring methods for handling massive datasets and distributed processing (G6). Robotics, on the other hand, may focus on local or regional scales, necessitating different approaches for data handling and processing (R7).

Understanding these similarities and differences is crucial for tailoring methods and techniques to suit the specific requirements of robotics and geoinformatics applications, enabling efficient and effective use of 3D modeling and vision solutions in each domain.

ACKNOWLEDGMENT

The paper was supported by the Bilateral Chinese-Hungarian Project No. 2019-2.1.11-TÉT-2020-00171 with the project title of “Investigation of the characteristics of surface shapes in rural environment based on point clouds and remote sensing data”.

REFERENCES

- [1] Károly A. I., Nagyné Elek R., Haidegger T., Széll K., Galambos P., “Optical flow-based segmentation of moving objects for mobile robot navigation using pre-trained deep learning models”, In: IEEE (szerk.) 2019 IEEE International Conference on Systems, Man and Cybernetics (SMC), Piscataway (NJ), USA : IEEE, pp. 3080-3086. , 7 p., 2019.
- [2] Kertész G., Szénási S., Vámosy Z., “Multi-Directional Image Projections with Fixed Resolution for Object Matching”, Acta Polytechnica Hungarica 15 : 2 pp. 211-229. , 19 p., 2018.
- [3] Molnár A., Lovas I., Domozi Zs., “Practical Application Possibilities for 3D Models Using Low-resolution Thermal Images”, Acta Polytechnica Hungarica 18 : 4 pp. 199-212. , 14 p., 2021.
- [4] Nagyné Elek R., Haidegger T., “Robot-Assisted Minimally Invasive Surgical Skill Assessment – Manual and Automated Platforms”, Acta Polytechnica Hungarica 16 : 8 pp. 141-169. , 29 p., 2019.
- [5] Nátrán A., Széll K., “Mobile Robot Environment for SLAM”, In: Csuka, Ildikó; Simon, Gyula (szerk.) AIS 2021-16th International Symposium on Applied Informatics and Related Areas – Proceedings, Székesfehérvár, Hungary: Óbuda University, pp. 80-83. , 4 p., 2021.
- [6] Reskó B., Herbay D., Krasznai P., Korondi P., “3D Image Sensor based on Parallax Motion”, Acta Polytechnica Hungarica 4 : 4 pp. 37-53. , 17 p., 2007.
- [7] Shi W., Meng Q., Zhang L., Zhao M., Su C., Jancsó T., “DSANet: A Deep Supervision-Based Simple Attention Network for Efficient Semantic Segmentation in Remote Sensing Imagery”, Remote Sensing, 2022; 14(21):5399. <https://doi.org/10.3390/rs14215399>, 2022.
- [8] Széll K., “SLAM in Simulation and Test Environment”, In: Orosz, Gábor Tamás (szerk.) AIS 2019 : 14th International Symposium on Applied Informatics and Related Areas organized in the frame of Hungarian Science Festival 2019 by Óbuda University, Székesfehérvár, Hungary : Óbuda University, pp. 5-8. , 4 p., 2019.
- [9] Vámosy Z., “Map building and localization of a robot using omnidirectional image sequences”, Acta Polytechnica Hungarica 4 : 3 pp. 103-112. , 10 p., 2007.
- [10] Wang X., Meng Q., Liu X., Zhang L., Hu X., Bi Y., Jancsó T., “Evaluation of Fairness of Urban Park Green Space Based on an Improved Supply Model of Green Space: a Case Study of Beijing Central City”, Remote Sensing, 2023.
- [11] Wolf, Á., Troll P., Romeder-Finger S., Archenti A., Széll K., Galambos P., “A Benchmark of Popular Indoor 3D Reconstruction Technologies: Comparison of ARCore and RTAB-Map”, Electronics (Switz) 9 : 12 p. 2091 , 15 p., 2020.

Processing 3D panoramic photos into point cloud modell

Regina Hanna BALATON

Institute of Geoinformatics
Óbuda University, Alba Regia
Technical Faculty
Székesfehérvár, HUNGARY
reginahannabalaton@gmail.com

Gergely LÁSZLÓ

Institute of Geoinformatics
Óbuda University, Alba Regia
Technical Faculty
Székesfehérvár, HUNGARY
laszlo.gergely@amk.uni-obuda

Zoltán TÓTH

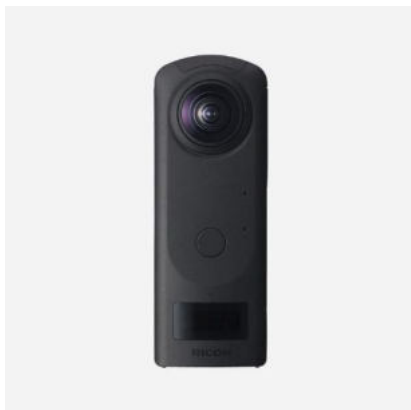
Institute of Geoinformatics
Óbuda University, Alba Regia
Technical Faculty
Székesfehérvár, HUNGARY
toth.zoltan@amk.uni-obuda

Abstract — 3D modeling based on traditional photographs is a fairly long-used and widespread method in photogrammetry. In this article, we present the process of model production based on 360° panoramic images, describing the problems, advantages, and disadvantages of the procedure. We use a Ricoh Theta Z1 camera for photos, and Agisoft Metashape software for processing.

Keywords — photogrammetry, panoramic images, 3D modeling

I. INTRODUCTION

Agisoft Metashape is a stand-alone software product that performs photogrammetric processing of digital images and generates 3D spatial data to be used in GIS applications, cultural heritage documentation, and visual effects production as well as for indirect measurements of objects of various scales. [1]



1. Figure - Ricoh Theta Z1 camera

The RICOH THETA Z1 supports approximately 23-megapixels resolution (6720 x 3360 pixels) 360-degree still image photo shooting as a high-end model of the RICOH THETA camera series, which can shoot spherical images in a single shot, giving consumers the opportunity to adventure, discover and capture life in 360. [2]

A three-dimensional survey of building interiors may be necessary more and more often, as designers and operators of registers have realized on the one hand that in many situations

it is not possible to represent objects in a complex way in 2D, and on the other hand, BIM (building information modeling), which is a procedure that includes the creation and management of digital spatial models of physical and functional properties of places.

To satisfy the spatial information needs of these systems, there are several survey methods, starting from traditional total station surveys, 3D laser scanning and terrestrial photogrammetry. In a different way than these, but in each case, we get a final result in which there are points with x, y, z coordinates and some quality information. There are several differences between the procedures given in the above example, one of which is the absolutely not negligible asset investment aspect. Of the three, the tool for the photogrammetry process examined in the article is the cheapest, so this was one of the aspects of our choice.

II. TERRESTRIAL PHOTOGRAMMETRY

The branch of science dealing with the preparation and processing of measurement images and photographs designed for measurement and evaluation purposes from the ground position is called terrestrial photogrammetry. It can be used where an unobstructed view of the area, object, or surface to be measured is ensured. Nowadays, its application in cartography is beginning to come to the fore again with the spread of 3D databases, previously it was only used in those specialist areas where not only the processing of metric data is important, but also the additional information provided by the photograph.

III. CHARACTERISTICS OF TERRESTRIAL PHOTOGRAMMETRY

- it is not necessary to approach the examined object or facility during the measurement (this is why terrestrial photogrammetry is also a type of remote sensing),
- the time required for the field measurement is short,
- due to the short exposure (exposure) time, it is also suitable for measuring fast processes,

- the measurement images contain a lot of information (quantitative and qualitative),
- the evaluation is fast and can be easily automated.

IV. RECORDING ARRANGEMENTS OF TERRESTRIAL PHOTOGRAMMETRY

In terrestrial photogrammetry, we also speak of single-image or planar photogrammetry and two-image, or spatial photogrammetry. Recording layouts can also be grouped accordingly:

- one-shot procedure,
- spatial photogrammetry procedure.

From the point of view of this article, the spatial solution is important.

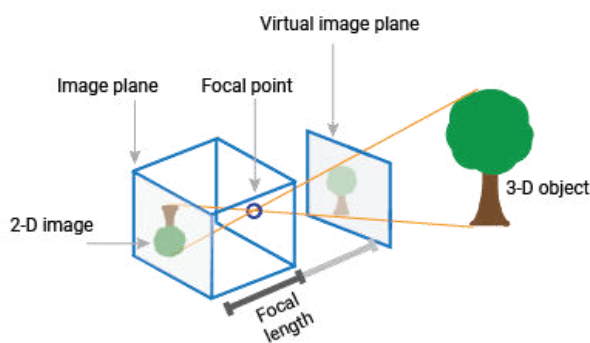
In spatial photogrammetry, we aim for the spatial (three-dimensional) determination of the points to be measured, for which we need to take at least two pictures of the object to be measured. In both pictures, the object to be measured must be on it. In previous, traditional procedures, the photographs taken for measurement purposes were taken from positions with known horizontal and height data, where the direction of the camera axes was also known.

Nowadays, the evaluation and model creation is done with a multi-image 3D reconstruction process. The essence of photographing is to depict spatial objects in a plane, this means that depth is lost, the process we use is the opposite of this.

In doing so, we need several images, since we cannot determine from a single image where a spatial point is located on the projection line, and which point on this line actually corresponds to the pixel. If we already have two images that depict the point in question from different locations, the position of a 3D point can already be determined as the intersection of the two projection rays. This process is known in the literature as triangulation. The key to the process is knowing the relationship between the recording locations, on the basis of which the appropriate transformation equations can be written.

Reconstruction is a multi-step process.

In the first step, we need to calibrate the camera, during which the internal and external orientation parameters are determined. Photogrammetric processing cannot be performed without this step.



2. Figure - Imaging Process

By internal parameters we mean the location of the optical center on the image plane, the focal length and the optical distortion parameters of the lens. Described in matrix form, they are:

$$K = \begin{bmatrix} a_x & \gamma & u_0 & 0 \\ 0 & a_y & v_0 & 0 \\ 0 & 0 & 1 & 0 \end{bmatrix}$$

The K contains 5 intrinsic parameters of the specific camera model. These parameters encompass focal length, image sensor format, and camera principal point. The parameters $a_x = f * m_x$ and $a_y = f * m_y$ represent focal length in terms of pixels, where m_x and m_y are the inverses of the width and height of a pixel on the projection plane and f is the focal length in terms of distance. γ represents the skew coefficient between the x and the y axis, and is often 0. u_0 and v_0 represent the principal point, which would be ideally in the center of the image.

Nonlinear intrinsic parameters such as lens distortion are also important although they cannot be included in the linear camera model described by the intrinsic parameter matrix. Many modern camera calibration algorithms estimate these intrinsic parameters as well in the form of non-linear optimization techniques. This is done in the form of optimizing the camera and distortion parameters in the form of what is generally known as bundle adjustment.

External orientation parameters

$$\begin{bmatrix} R_{3x3} & T_{3x1} \\ 0_{1x3} & 1 \end{bmatrix}_{4x4}$$

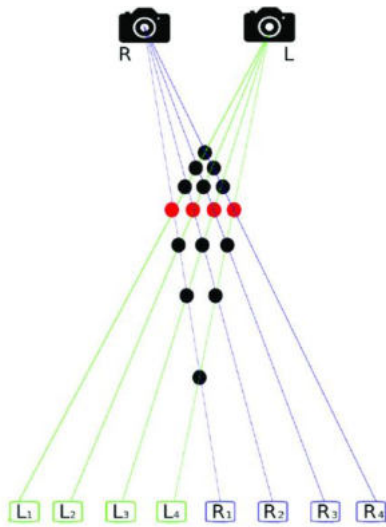
R and T are the external orientation parameters that denote the transformations of the coordinate system from the coordinates of the 3D world to the coordinates of the 3D camera. Accordingly, the external parameters determine the position of the center of the camera and its orientation in world coordinates.

T is the position of the origin of the world coordinate system given in the camera-centered coordinate system. The position of the camera C can be expressed in world coordinates based on the following formula: [3]

$$C = -R^{-1}T = -R^T T \text{ (since } R \text{ is a rotation matrix)}$$

Determining the depth of field

Determining depth of field is the most challenging part of the process, as this is where the important spatial information missing from images is determined - depth. The correspondence problem, finding the match between the two examined images, thus the position of the matched elements in 3D space, is the question to be answered.



3. Figure – Restore depth of field

Mesh creation

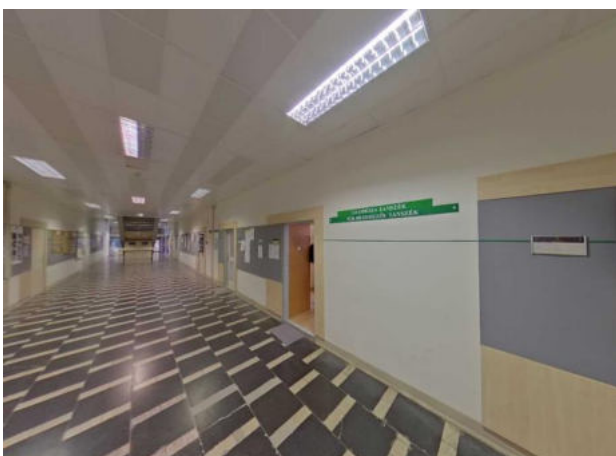
Once we have the multiple depth maps, we need to combine them to create the final mesh by calculating the depth and projecting it from the camera. Camera calibration will be used to identify where the many meshes created by depth maps can be combined to create a larger mesh that already provides viewing from multiple viewpoints.

Coloring the mesh model

In this step we have a full 3D mesh, which may be the ultimate goal, but usually we want to apply the color of the original photos to the mesh. This can range from randomly projecting images onto the mesh for super-resolution, to combining textures, to segmenting the mesh by material, including things like reflections and diffuse properties.

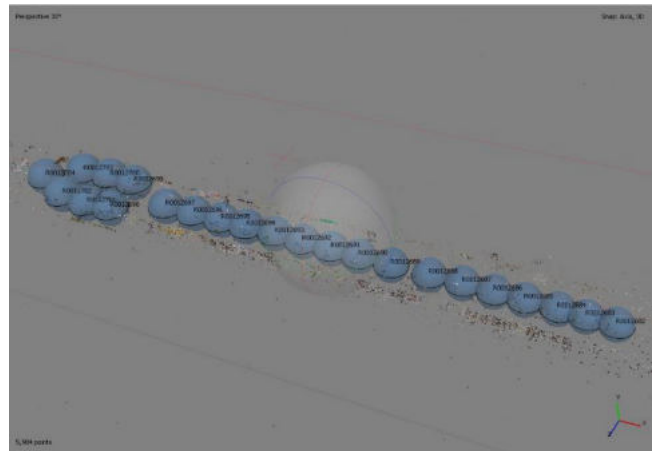
V. PRESENTATION OF THE SURVEY

The survey was carried out with a Ricoh Theta Z1 360° camera, which we borrowed from the Slovak University of Technology in Bratislava. The surveyed area was the ground-floor corridor of the Pirosalma street building of the Alba Regia Technical Faculty of Óbuda University.



4. Figure - The test area

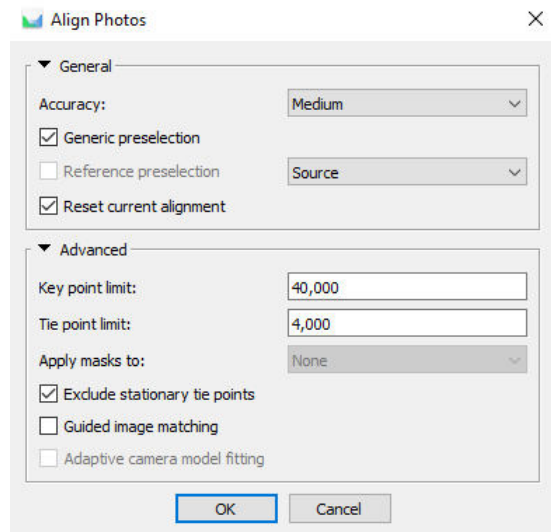
On this occasion, we did not use the point signals provided by Matterport for the survey, as we did not want to do the processing with its own program, so that we could export a point cloud. A total of 23 images were taken with appropriate overlap in the arrangement shown in the image below:



5. Figure – The places of the pictures

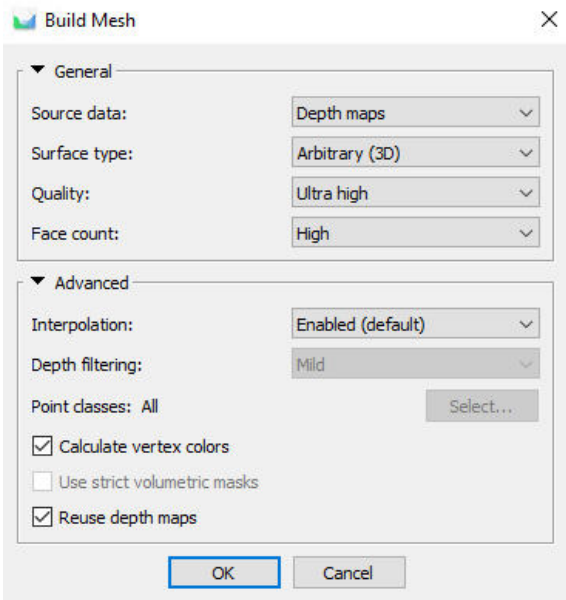
Processing

The processing was done with the Agisoft program. First, we imported the saved JPEG format images into a new project, then set the camera properties to use a spherical camera model for processing. The first step of the processing was the relative alignment of the photographs performed at the same time as the calibration. This is done in such a way that the program searches for identical points on each pair of images, thereby creating a sparse point cloud.



6. Figure - Align Photos properties

The second step, as previously described, was to define the depth-of-field map, thereby restoring the 3D nature of the surveyed data. With this, the creation of the mesh model is also done in one function, as the first 3D visualized final product.

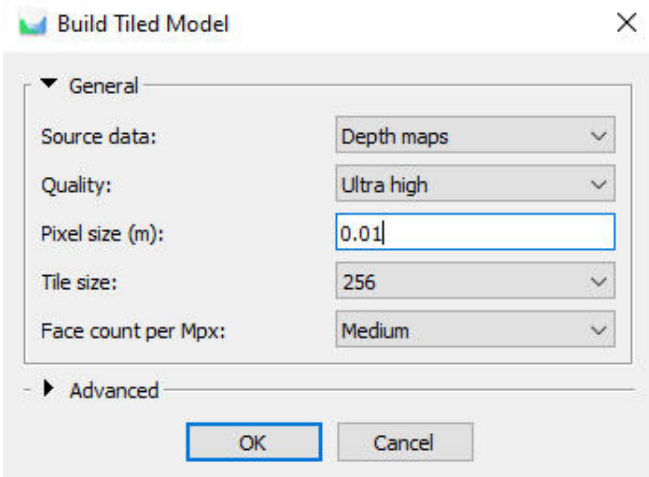


7. Figure - Mesh properties

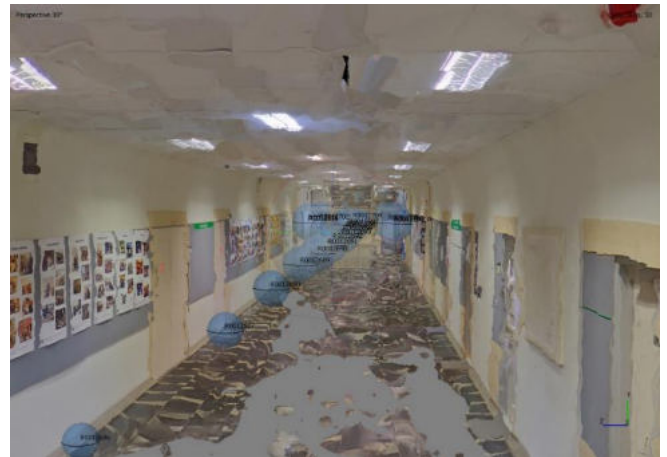


8. Figure - Mesh Model

During the third, optional step, a tiled model can be made from the mesh model, which can be exported to formats supporting 3D models for further processing with external software.

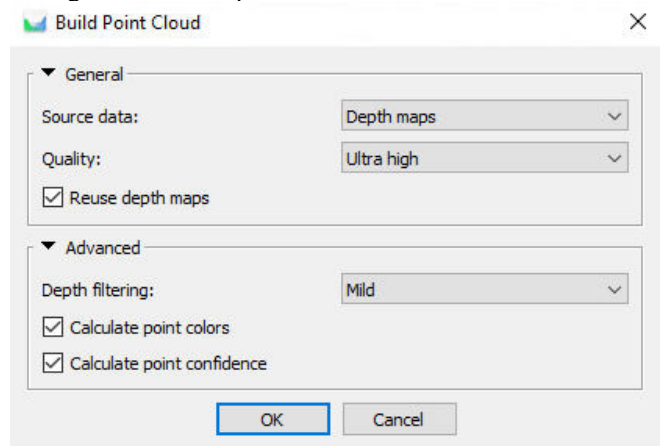


9. Figure - Tiled Model properties

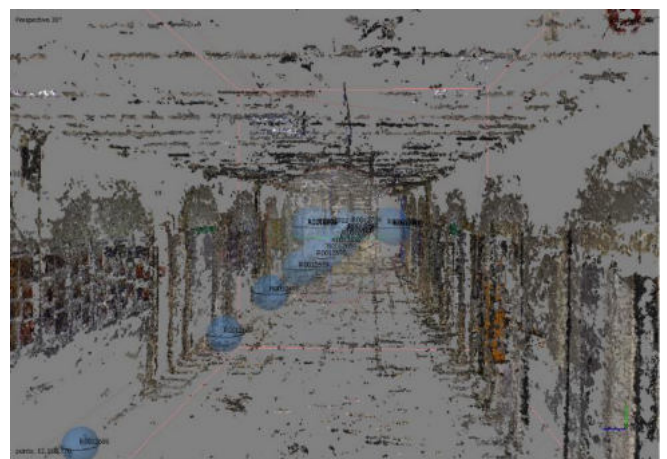


10. Figure - Tiled Model

In the last step, the 3D point cloud is created, using the results created in the first two phases. The pictures below show the settings and the final product:



11. Figure - Point Cloud properties



12. Figure - Point Cloud

VI. DISCUSSION

The images of the results show that the method has weaknesses. First of all, there will be no spatial information about visually homogeneous surfaces, such as the floor, wall and ceiling, because the software and the procedure it uses cannot calculate spatial intersection points, so there could only

be a point formed on those parts if we interpolated a plane to those places, which would negatively affect accuracy. Another obvious problem is that dots are formed in places where they obviously shouldn't be. These can be caused by reflections or camera distortion. Their repair could be solved by manual cleaning or calibration.



13. Figure - Generated noise below floor level

VII. CONCLUSION

In the case of images taken on inhomogeneous surfaces, a point cloud of adequate density can be created for the entire area, but under average conditions, you have to account for parts with missing data. By solving the problem of camera calibration, the points formed on the edges of the camera would improve in terms of accuracy. In any case, geometrical validation would be necessary in comparison with other measurement methods.

ACKNOWLEDGMENT

The research was supported by the New National Excellence Program 2023 (ÚNKP 2023). In addition, we are grateful to the Slovak University of Technology in Bratislava for the loan

of the RICOH THETA Z1 360° camera, which is essential for the realization, without which the survey of the research could not have been realized.

We would like to express our special thanks to Ján Erdélyi and Richard Honti, who gave us a quick and professional guide regarding the use of the camera and the processing.



REFERENCES

- [1] <https://www.agisoft.com/>
- [2] <https://ricohtheta.eu/products/ricoh-theta-z1>
- [3] B. Triggs; P. McLauchlan; R. Hartley; A. Fitzgibbon (1999). "Bundle Adjustment — A Modern Synthesis" (PDF). ICCV '99: Proceedings of the International Workshop on Vision Algorithms. Springer-Verlag. pp. 298–372. doi:10.1007/3-540-44480-7_21. ISBN 3-540-67973-1.
- [4] Image and depth from a conventional camera with a coded aperture Anat Levin, Rob Fergus, Fredo Durand, William T. Freeman, MIT
- [5] Martinello, Manuel; Favaro, Paolo (2012). "Depth estimation from a video sequence with moving and deformable objects". IET Conference on Image Processing (IPR 2012) (PDF). p. 131. doi:10.1049/cp.2012.0425. ISBN 978-1-84919-632-1.
- [6] https://www.nive.hu/Downloads/Szakkepzesi_dokumentumok/Bemeneti_kompetenciak_meresi_ertekelesi_eszkozrendszerenek_kialakitasa/20_2241_004_100915.pdf

Safety Aspects of the Urban Green Cadaster

Levente Dimén

Faculty of Informatics and engineering
1 Decembrie 1918 University of Alba Iulia
Alba Iulia, Romania
ldimen@uab.ro

Clement Negruț

Faculty of Informatics and engineering 1
Decembrie 1918 University of Alba Iulia
Alba Iulia, Romania
clement.negrut@uab.ro

Alina Cristina Nuță

School of Economic Sciences and Business
Administration Danubius University
Galați, Romania
alinanuta@univ-daniubius.ro

Abstract— This paper aims to present a GIS-aided safety map related to the non-invasive assessment of trees in urban green areas. The goal is to create an urban GIS-based evidence of the green areas focused on hidden tree pathology, in order to increase the safety of urban parks and provide an instrument for decision-making to eliminate trees that pose a danger to citizens due to hidden pathology. This is especially important in light of the tremendous physical destruction, injury, loss of life, and economic damage caused by wind disasters, as well as concurrent heavy rains and flooding, which have become increasingly common in recent decades. Improved observational capabilities and recordings of such events have led to greater public awareness of severe weather events.

Keywords—green cadaster, urban green, GIS, climate change

I. INTRODUCTION

Climate alter is an verifiable reality that's changing the world as we know it. Among its wide-ranging consequences, one of the foremost concerning is the escalated and expanded recurrence of wind calamities. Wind designs are unpredictably connected to climate frameworks. The change of climate designs due to worldwide warming has come about in shifts in wind concentrated, course, and dispersion. Hotter seas, for occurrence, give the fuel for tropical storms to create into more effective storms and tropical storms. Also, changes in temperature angles and air conditions can impact the arrangement and conduct of tornadoes. These changes in wind designs have driven to an expanded event of extraordinary wind occasions over the globe. Climate alter has contributed to a rise in extreme climate occasions having genuine impacts within the urban green zones.

This paper investigates the application of Geographic Data Framework (GIS) in setting up a comprehensive database for overseeing green spaces in urban ranges. It talks about the duty of neighborhood governments to conduct inventories of open green spaces and make an prove registry for effective administration. The center is on examining the green ranges inside authoritative boundaries, considering components such as zone scope, vegetation quality, availability, and security. By receiving an individualized approach for each green space entity, a more exact understanding of the whole green infrastructure within regional regulatory units can be accomplished, empowering viable measures for support and administration.

A. THE URBAN GREEN AREAS

In 2015, the entire region of urban green spaces in Romania was 25,778 hectares. This speaks to an increment of 4,145 hectares compared to 1991. This data is given by the National Established of Measurements (2017) and alludes to the range of green spaces created within the frame of parks, open gardens, squares, plots with trees and blooms, forests, cemeteries, grounds of sports grounds and offices that are found within the buildable edges of the territories, i.e. open green spaces.

These figures reflect an increment within the zone of urban green spaces in Romania over a few 24 a long time. It is critical to note that these information allude as it were to green spaces formally created and perceived as open green spaces. Other shapes of green spaces, such as undeveloped natural areas or rural arrive in or close regions, may not be included in these insights. This increment within the sum of urban green space may reflect the endeavors of specialists and communities to advance and create green regions to move forward the quality of life within the urban environment and preserve biodiversity. Be that as it may, it is imperative to proceed endeavors to preserve and reasonably create green spaces inside cities to guarantee a solid and adjusted urban environment for inhabitants.

Looking at the province scale, concurring to Figure 1, 27 provinces in Romania appear an increment within the sum of urban green space. This shows that endeavors have been made in these districts to develop and extend green spaces in urban zones. These increments may be the result of nearby activities and arrangements advancing natural assurance, progressed quality of life and feasible advancement of cities. Province and neighborhood specialists can actualize programs and projects aimed at creating parks, open gardens and other green spaces inside communities. It is gratifying to see that there's intrigued and commitment to expanding the sum of urban green space in most districts in Romania. This will contribute to more advantageous, more wonderful and economical urban situations, giving recreational and relaxation opportunities for communities and advancing biodiversity. Be that as it may, it is imperative to proceed to screen and back the advancement of urban green spaces in all districts to

ensure a fitting adjust between the wants of urban advancement and natural preservation.

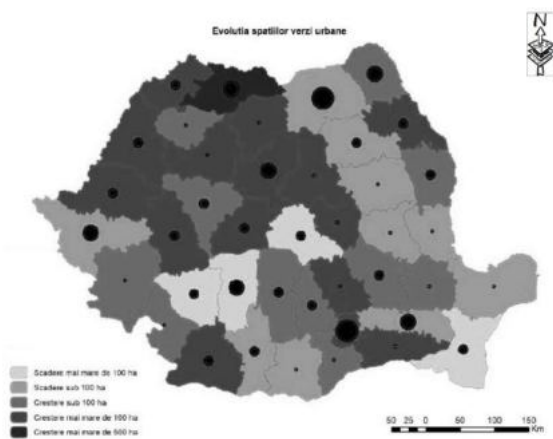


Figure 1. Evolution of the area of urban green infrastructure between 1991 and 2015 (data source Institutul Național de Statistică – 2017) cited by Udvardy, Borșan 20230

B. Creation the databases related to the green cadastre

Nowadays, GIS is one of the most instruments utilized to analyze green spaces and vegetation in urban ranges. These frameworks are utilized for green cadastre databases, coordinates administration plans and the foundation of mediation stages for urban vegetation.

One of the major preferences of GIS frameworks is their capacity to create complex, geo-referenced databases that can be powerfully reexamined and overhauled. These databases offer the plausibility to oversee nitty gritty data almost green spaces and urban vegetation, encouraging educated decision-making and fitting arranging of intercessions. Another vital advantage of GIS frameworks is their flexibility, permitting coordinate communication with particular innovations for top-down approaches to green cadastre as well as bottom-up mapping strategies. This implies that information from a assortment of sources can be coordinates, from adherent pictures and orthophotos to locally collected client information. The framework can therefore be utilized to urge a complete and point by point picture of green spaces and vegetation within the urban environment.

In expansion, advanced innovation permits the utilize of UAVs to gather GIS information. These UAVs can be prepared with different rebellious such as high-performance cameras, temperature and mugginess sensors, infrared sensors and others. This permits much more complex and comprehensive databases to be gotten than with conventional strategies.

To enroll trees in a GIS database, an approach is utilized to incorporate diverse traits pertinent to each group/entity

- Uniq ID - each tree can have a special identifier to permit person recognizable proof and administration of each tree within the database.

- Species - trait showing the species of the tree (e.g. oak, spruce, acacia, etc.).

- Trunk breadth - the trait that records the breadth of the tree trunk, either at the base or at the tallness of 1.3 meters

from the ground. Valuable for evaluating tree development and for arranging suitable care.

- Trunk size - the property that records the size of the trunk of the tree measured at a given tallness over the ground (e.g. 1.3 meters over the ground). This quantification is significant for surveying tree estimate and development.

- Trunk height - the property that records the stature of the tree trunk, measured from the base of the tree to the primary quarter or primary department. This could be valuable for deciding the structure of the tree and its vertical measurement.

- Crown breadth - the property that records the breadth of the crown of the tree, as a rule measured at the most extensive portion of the crown. This will be valuable for evaluating the flat estimate of the tree and the zone the crown involves.

- Shaft deviation - the attribute that records the deviation of the shaft pivot from the vertical. It can be communicated in degrees and demonstrates whether the tree is vertical or slanted to the vertical. This data is critical for surveying shaft steadiness and deciding potential auxiliary issues.

- Wellbeing status - an trait that shows the by and large wellbeing of the tree, counting evaluation of conceivable infection, harm or other issues.

- Geographic area - the trait that contains the tree's geographic/geographic/ rectangular facilitates (scope and longitude) to permit precise situating of the tree on the outline within the GIS database.

- Year planted - quality that records the year the tree was planted or set up to permit the age and history of the tree to be followed.

When designing the database, particular codes will be allotted to each quality, depending on the sort of data it'll contain.

- Content - this information sort is utilized to store printed data, such as tree species name, street title or any other printed portrayal. In common, a maximum length is indicated for the content field as required.

- Numbers - is utilized to store entirety numbers, such as trunk circumference or trunk tallness. A least and maximum value is indicated to constrain the run of values acknowledged.

- Genuine number - is utilized to store genuine numbers such as crown breadth or crown stature. A exactness (number of digits after the decimal point) is additionally indicated to control the detail of the genuine values.

- Date - is utilized to store calendar dates, such as the date of planting or the date of the final record. It permits chronological operations and comparisons to be made.

- Boolean - this information sort is used to store coherent values, such as tree wellbeing status (yes/no, true/false). It allows the representation of twofold data.

MATERIALS AND METHODS

Hidden tree pathologies

Spoiling of trees alludes to the common rot handle that happens when a tree's natural matter breaks down over time. It could be a characteristic portion of the life cycle of trees and is fundamentally caused by organisms and microscopic organisms. When a tree passes on or is harmed, the method of deterioration starts, driving to the breakdown of the tree's

basic components.

The spoiling handle ordinarily begins from the interior of the tree and advances outward- Figure 2. Organisms, particularly wood-rotting parasites, play a vital part in breaking down the tree's wood fibers. These organisms emit proteins that break down the complex particles within the wood into less difficult compounds, such as carbon dioxide and water. This handle makes a difference reuse supplements back into the environment.

The decaying process can moreover posture dangers and challenges. Trees that are broadly rotted may gotten to be basically powerless and more inclined to falling, posturing a security risk. Usually especially concerning in urban zones where falling trees can harm property or imperil individuals. Hence, standard tree assessments and support are vital to recognize and address potential dangers related with decaying. It's worth noticing that not all decaying is unmistakable from the exterior. Trees may show up solid and vigorous on the surface whereas encountering noteworthy inside rot. Hence, the utilize of specialized instruments and strategies, such as sonic tomography or resistograph, can offer assistance arborists and tree specialists evaluate the inner condition of trees and make educated choices with respect to their administration and security.



Figure 2. Internal rotting

Risks and difficulties can also arise from the rotting process. Trees with widespread rot may weaken structurally and become more likely to fall, creating a safety threat. This is especially worrying in cities where falling trees can cause property damage or put people in danger. Therefore, it's crucial to identify and manage any potential concerns related to rotting by performing regular tree inspections and care.

It's important to remember that not all rot is apparent from the outside. Trees may appear strong and healthy from the outside while suffering from serious internal deterioration. Thus, arborists and tree professionals can examine the internal condition of trees and come to wise management and safety judgments by using specific equipment and techniques, such as acoustic tomography or resistograph.

NON INVASIVE ASSESSMENT

Various anomalies that impact the course of sound waves can be found using a diagnostic equipment that measures the sound speed perpendicular to the fiber. Internal cavities, decay, and extensive fissures within the material are a few examples of such anomalies. The average sound speed perpendicular to the fiber in healthy, unbroken wood is between 1800 and 2000 m/s.

However, the speed of sound is dramatically decreased in the presence of a fiber run break, increasing the measured propagation time. This shift in propagation time may be a sign of internal wood problems. The depth of a crack can also be determined by using this measurement method. While the penetration depth of a thin plate can be used to estimate the depth of a surface fracture, the crack route is not necessarily straight. As a result, the measurement may not precisely reflect the crack's depth.

The propagation time over the crack and the propagation time over the same distance in an unaffected area without a fracture are compared to determine the crack depth (C). Divós et al. describe a formula for calculating crack depth that can be used for this purpose.

$$C = \frac{D}{2} \sqrt{\left(\frac{T_{crack}}{T_{solid}}\right)^2 - 1}$$

Where:

C - crack depth

D is the length of the propagation path

T crack is the Propagation time in the cracked surface

T solid is the propagation time in the crack free surface

It operates by comparing the sound velocities of many sensors placed around the trunk.

The fundamental premise of measurement is that if a hole or density difference occurs between sensors, sound velocity will decrease.



Figure 3. Sound velocity measurement

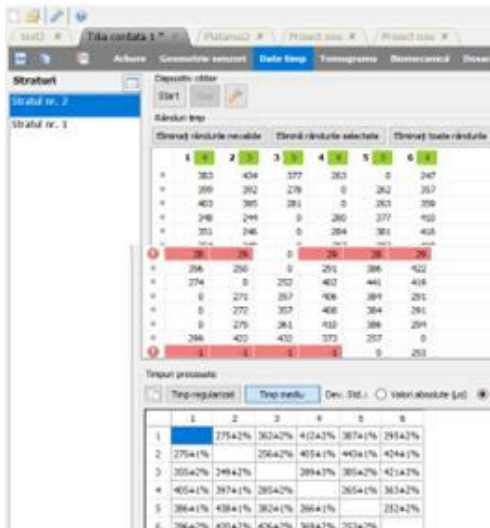


Figure 4. The time passing data through the trunk between the sensors/corrections

RESULTS AND DISCUSSIONS

Defect identification using measurements taken perpendicular to the fiber has proven to be successful. This approach is especially beneficial when the sound waves pass through a different path between the sensors. However, in order to detect faults that are not visible from the outside, more than two sensors may be required. This approach, known as acoustic tomography, has been used successfully in the evaluation of urban trees and is useful for investigating big cross-section timber and living trees.

Acoustic tomography uses several sensors placed around the trunk or structure to measure the speed of sound. Sound velocity data can be compared to provide important insights. The sound velocity will decrease if there is a void or hole between two sensors. This theory underpins the measurement technique and provides an effective method for discovering hidden faults. This technology, which employs many sensors and measures sound velocities, is useful for investigating big cross-section timber and living trees, as well as examining urban tree health and integrity.

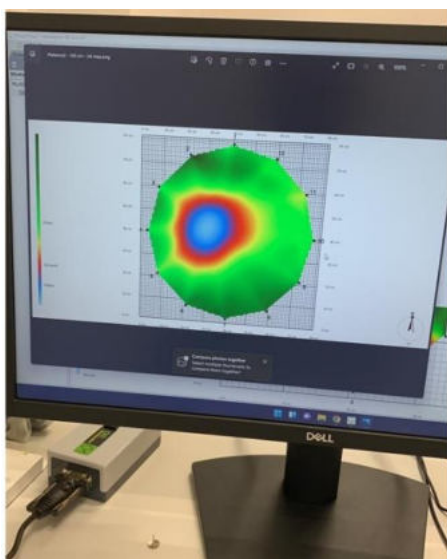


Figure 5. Example of internal assessment



Figure 6. Tilia cordata

We can estimate the propagation speed on all available routes by tapping the sensors, for $N = 12$ sensors on $N(N-1) / 2 = 66$ routes. The 3D device reconstructs the speed map of the inspected cross-section based on the 66 sound speed measurements. Figure 4 depicts the time flowing data along the trunk between the sensors, while Figure 5 depicts the imaging expression of the processing of physical data collected from the sensor.

The colors represent the tree's condition. Red areas indicate destruction, whereas blue regions imply a hollow.

CONCLUSIONS

The acoustic tomography approach was tested in urban green spaces for its capacity to identify interior degradation in high-value trees. Based on preliminary study of acoustic tomograms, we conclude: - Acoustic tomography proven to be an efficient method for detecting internal structure change in urban trees; - The tomogram can show the position, relative size, and form of internal rotten areas; and -

- Green cadaster should record special data relating to the hidden disease of the trees in green cadaster.

- The idea of Urban Green Safety must be taken into account in any assessment and data collection connected to urban green areas.

ACKNOWLEDGEMENTS

This research work was carried out with the support of project: Improvement of the educational infrastructure in the D and H buildings of the University 1 December 1918 in Alba Iulia" SMIS code 120779, financed by P.O.R. 2014-2020 Reference number and date of the Financing Contract: Financing Contract no. 4159/06.05.2019 SMIS 120779

References

- [1] Coppock, J.T., Rhind, D.W. (1991). The history of GIS, Grossmont College paper, pp.25-40.
- [2] Divós, F. (1999). Fahibák, bélkorhadás feltárása a hangsebesség mérésével, In: DIVÓS, F. (szerk.): Roncsolásmentes faanyagvizsgálat, Mérési útmutató, Soproni Egyetem, 1-5. old
- [3] Divós, F., Németh L., Major B., (2015) Új technológiák bemutatása a faszerkezetek felülvizsgálata területén, Magyar Mérnöki Kamara
- [4] Divos, E and L. Szalai. (2002). Tree evaluation by acoustic tomography. In: Proc. of the 13th International Symp. on Nondestructive Testing of Wood, Aug. 19-21, Berkeley, CA. pp. 251-256.
- [5] Gavrilidis, A., Alexandru, et al. (2015). "Land use and land cover dynamics in the periurban area of an industrialized East-European city. An overview of the last 100 years." Carpathian Journal of Earth and Environmental Sciences.
- [6] Grecea, C., Ienciu, I., Dimen, L., Bala, A.C., Oprea, L. (2012). Impact of Surveying Engineering on the Environmental Protection Problems. J Environ Prot Ecol, 13 (1), 352.
- [7] Foote, K.E., Lynch, M. (1995). The Geographer's Craft Project, Department of Geography, The University of Colorado at Boulder.
- [8] Marulli, J., et al. (2005). "A GIS methodology for assessing ecological connectivity: application to the Barcelona Metropolitan Area." Landscape and Urban Planning.
- [9] Munteanu, L. et al, (2016). Strategic environmental assessment (a case study: transylvania motorway project, romania), International Multidisciplinary Scientific GeoConference : SGEM; Sofia, Vol. 3,
- [10] Oprea, L., (2018). Green Cadastre Of Romania – Between Necessity and Realisation, Journal of Environmental Protection and Ecology 19, No 1, 208–215.
- [11] Wade, T., Sommer, S. (2006). A to Z GIS, ESRI Press, Redlands, California.
- [12] Fakopp homepage <https://www.fakopp.com/en/product/arbersonic/> accessed 2023/05/21.
- [13] Institutul National de Statistica (2017). Baza de date TEMPO - Date teritorial-administrative si date asupra dinamicii spatiilor verzi;
- [14] Norme Tehnice pentru aplicarea Legii nr.24/2007 privind reglementarea și administrarea spațiilor verzi din zonele urbane (Elaborarea Registrului Local al Stațiilor Verzi).

Estimation of the location of bee pastures in Hungary based on SENTINEL satellite images

Balázs Böröcz
Alba Regia Technical Faculty -
Óbuda University
Institute of Geoinformatics
Székesfehérvár, Hungary
boroczbalazs@stud.uni-obuda.hu

Abstract

*In my research, I want to estimate the honeybee pastures in Hungary, using satellite earth observation. The data source will be the SENTINEL-2 satellite images of the European Space Agency (ESA) COPERNICUS programme. The processing will be carried out using remote sensing tools and the analysis will be followed by setting up of a geospatial database. The database will be a raster data structure, which will contain the spatial distribution of the isolated plant species and the estimated time of expected flowering, with special emphasis on the periodic isolation of white acacia (*Robinia Pseudoacacia*) in the south ('lower acacia') and north ('upper acacia'). The resulting database is the bases for an open database in the form of a Web Map Service (WMS).*

Keywords:

- *Bee pastures*
- *Satellite earth observation*
- *Geospatial database*

I. Introduction

Hungary has one of the most important beekeeping industries in the EU. Currently there are 1.2 million bee colonies in Hungary and 20,000 beekeepers, of which 20% are full-time beekeepers, 70% are part-time beekeepers and 10% are hobby beekeepers. 60 % of beekeepers are migratory beekeepers travelling across the country from flowering to flowering, the remaining 40 % keep a stationary apiary. The number of colonies per square kilometre varies widely across the European Union, with an average of 4.04 colonies per square kilometre, but in Hungary there are up to 13 colonies per square kilometre, currently the highest in the EU [1]. Unfortunately, high bee density not only has a negative impact on overgrazing, but also contributes to spread infections more rapidly.

Major bee pastures in Hungary [2]:

There are three major type of plants, that are important for beekeeping, because of their economic relevance:

1. Rapeseed (*Brassica napus*): herbaceous plant of the Brassica family, one of our most important honey plants. The weather does not particularly affect the quality of the rapeseed flowering, which starts to bloom at about the same time throughout the country, around 15th of April. The flowering period for bee pastures lasts on average two weeks. The bright yellow colour of the flowers makes them easy to identify from satellite imagery [3]. Interestingly, the optimal pH of the honey makes it suitable for people with stomach problems, as it can also be used to relieve acid overload.

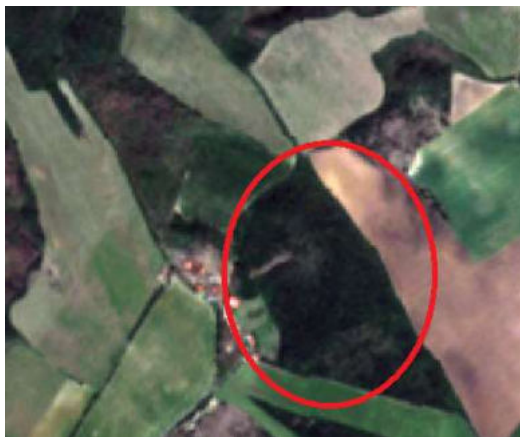


1. Figure: rape flowering, beekeeping container on the right



2. Figure Rapeseed fields from satellite imagery. The yellow fields are clearly identifiable during flowering period.

2. White acacia (*Robinia pseudoacacia*), is the most important honey plant in Hungary. The time, quality and length of its flowering is greatly influenced by the weather, which is usually 10 days (\pm 1-2 days). The flowering propagates from south to north, and in beekeeping terminology it is distinguished from the lower (southern) acacia, and the upper (northern) acacia. When the upper acacia starts flowering, the lower acacia finishes flowering. If the lower acacia is poor quality, the beekeepers will often migrate to the central acacia (central part of the country). Identification of the flowering by satellite imagery is not as straightforward as for rape. For the ease of identification, it is worth identifying the woods themselves first, on a pre-flowering image, and then comparing with the presumed flowering date. It will then be easier to identify the acacia stands to be surveyed.



3. Figure: Acacia forest before flowering in tru color optical satellite image.



4. Figure: The same acacia forest during the flowering. Clearly visible whiteish patches appeared on the forest.

3. Sunflower (*Helianthus annuus*), a plant with significant industrial and apicultural benefits, the main use for the oil that can be extracted from the seeds. The quality of its flowering is partly influenced by the weather, with the main influence being on the length of flowering, which lasts 2 weeks in average, but in rare cases may last up to one month. Varietal honey is difficult to collect from the flower, as several field plants (such as the stitchwort (*Stachys annua*), which is typically found in pastures and wheat fields) flower at the same time as the sunflower, and is therefore usually sold as mixed flower honey. It is the last of the three major bee pastures in Hungary to flower, so it plays an important role in preparing bees for winter.



5. Figure: Sunflower flowering in satellite image. During flowering, a yellowish-green colour appears on the otherwise green-coloured board.



6. Figure: Sunflowers blooming. Because the flowers are not fully upward facing, they do not look as spectacular in satellite images as in rape flowering.

II. DATA

The focus of my research is the mapping of honeybee pastures in Hungary, using the SENTINEL-2 satellites of the SENTINEL satellite family, developed by the European Space Agency's (ESA) Copernicus Programme. SENTINEL-2 is a pair (2A and 2B) of high-resolution earth observation satellites equipped with multispectral sensors, which are phased at 180° to each other and orbit in a sun-synchronous orbit [3]. The satellites have a return period of 10 days, so they take images of the same area in every 10 days, but because they are in pairs, images of the same area are available every 5 days. One of their missions is to monitor the Earth to gather information for agriculture, forestry and to track changes in the Earth's surface cover. By using multispectral sensors, it captures images in 12 bands of visible light, near infrared and mid-infrared part of the spectra, The images are freely available via Interned [3]. For my project I will mainly use the visible light range (400 nm - 700 nm). The aim of my research is to create a map that will cover the whole of Hungary, provide beekeepers with statistical information and be openly accessible to them.

The source of the data is the Earth Observation Information System ("FIR") [4], from which I downloaded the satellite images. The FIR is operated by Lechner Tudásközpont Nonprofit Ltd (LTK), the Government Agency for Information Technology Development (KIFÜ), the National Infocommunication Service Company (NISZ) and the Digital Government Agency (DKÜ). The website is open to the public and free of charge. The aim of the website is to pre-select the Sentinel images that cover the territory of

Hungary and to make them available in the national projection system of Hungary (EOV). Before downloading, the user has to select the satellite images he/she wants to download (in our case Sentinel 2), select the period and select the interested area. The selection can be made on the current viewpoint, on a specific point, draw a polygon or a simple rectangle, or even upload a shape file of its own that selects the area to be searched. The result can then be filtered. For each type of satellite you can apply different filters. For Sentinel 2, you can filter by satellite ID (Sentinel 2A, or Sentinel 2B), product type, relative orbit number, and maximum tolerance for cloud cover in percent.

The screenshot shows a web-based search interface for satellite images. The title is "Műholdkép keresés". There are tabs for "Keresés", "Találatok", "Megjelenítés", and "Kosár". Below the tabs, there are sections for "Rendezés:" (sorted by "Érzékelés kezdete") and "Írány:" (sorted by "Csökkenő"). The "Időszak" section shows dates from "2023-05-15" to "2023-05-31". The "Terület szűrő" section has icons for map, location, rectangle, and polygon. The "Műhold" section has "Sentinel-1" unchecked and "Sentinel-2" checked. There are input fields for "Műhold azonosító:", "Termék típus:", "Relatív orbit szám (1-143):", and "Felhőborítottság %:" with a value of "20". A "Keresés" button is at the bottom right.

7. Figure: Detail of the FIR query graphical user interface

Images can be previewed before downloading, either in real colour or in false color. When downloading, the user also has the option to pre-select which bands he/she wants to download.

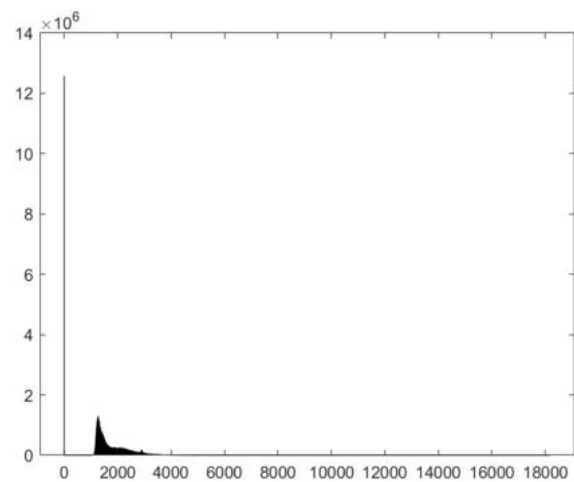
III. METHODOLOGY

I started processing the data in Matlab, with using the "Mapping Toolbox" add-on. With the Mapping Toolbox, I was able to call up GeoTIFF files previously downloaded from FIR's system and retrieve descriptive data from them. The scanned GeoTIFF files were stored in Matlab in 3-dimensional matrixes. I first selected the bands that were of interest to me and then viewed the histograms of those bands. Based on the histograms I plotted, I decided which range of values for the bands was the most relevant, and I rescaled the distribution of values between the minimum and maximum values of the range using the "rescale" command [6]. The rescaling was necessary to make the images interpretable, without the process, the images are very dark and practically uninterpretable (this process is called histogram equalization).

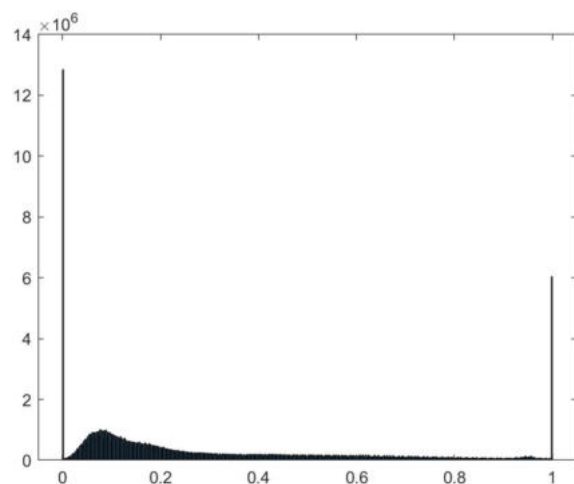
After the rescaling was done, I can start analysing the images. I started by detecting the bee pastures.

For this I had the help of several beekeepers, (including István Böröcz, personal communication), who provided me with coordinates of the bee pastures they grazed during the beekeeping season. I analyzed each flowering periodically, at times before, during, and after bloom.

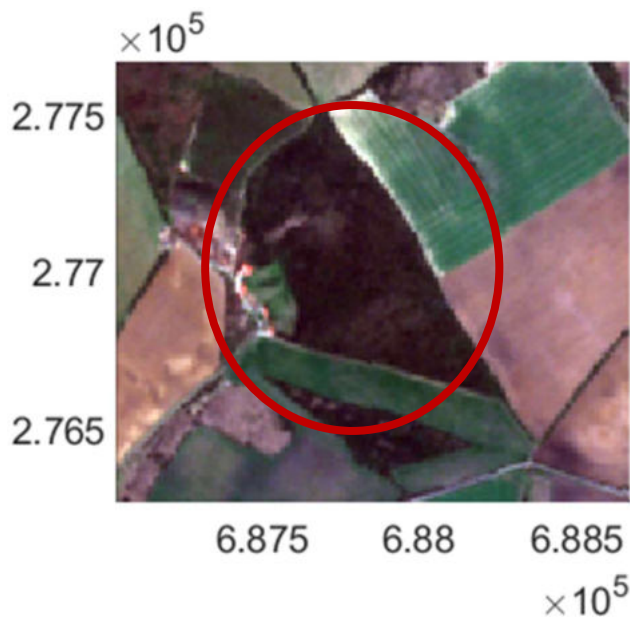
Using the Mapping Toolbox I was able to display the scanned images in EOV coordinate system. First I located the area in the image where the bloom was visible. Then, using the "ginput" command, I subtracted two EOV Y and X coordinates, which formed two opposite corners of a square. I then used the "mapcrop" command to crop the square, and then used the same EOV coordinates to crop the same area from the other satellite images.



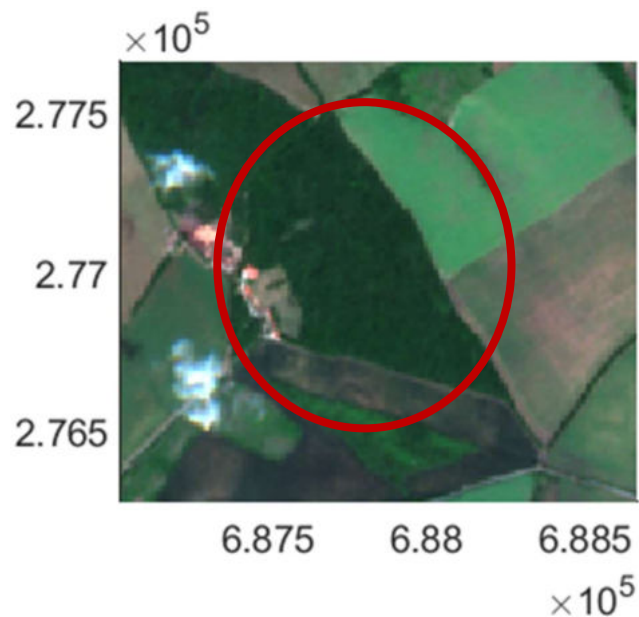
8. Figure: Histogram of the red band (B4) of one of the satellite images in Matlab, before the rescaling. It can be clearly seen that there is a huge value area within the band, but the significant values are between 1100 and 3000. In Sentinel-2 images, the grayscale values are stored in 12 bits, so their values range from 0 to 4095. However, as observed in the diagram, the images downloaded from the FIR system can exhibit grayscale values over a much larger range. Nevertheless, I have not found an explanation for this wider range within the FIR system.



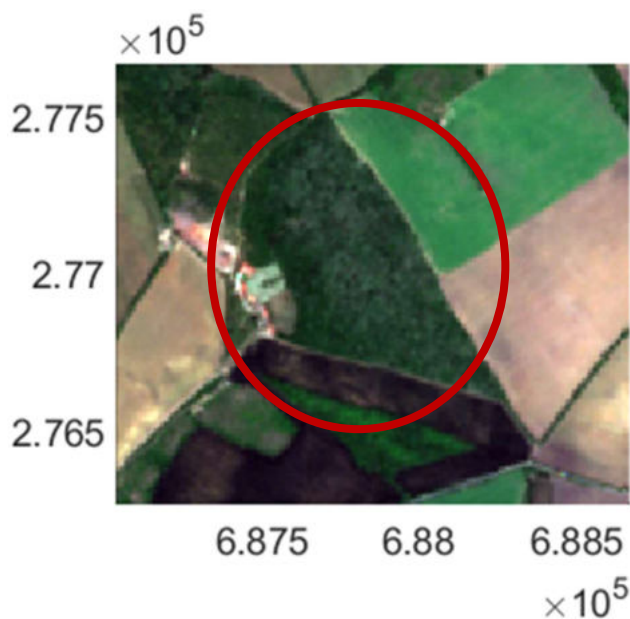
9. Figure: The same satellite image histogram, after the rescaling. The values are clearly distributed between 0 and 1.



10. Figure: Acacia forest surveyed as seen on SENTINEL-2 true color satellite image, in spring (04.02.2020) before flowering, near Szirák (north Hungary). Map coordinates are in EOVC coordinate system



12. Figure: The same acacia forest as on Fig. 11 and 12. after flowering (06.06.2020.). In the forest, observable white patches have disappeared.



11. Figure: The same acacia forest as on Fig. 11. during the flowering period of the examined acacia forest (05.22.2020). The whitish spots are the trees, while darker spots represent tree shadows.

V. References

- [1] P. De La Rúa, R. Jaffe, R. Dall'Olio, I. Munoz and J. Serrano, „Biodiversity, conservation and current threats to European honeybees.,” *Apidologie*, p. 263, May 2009.
- [2] J. Sebestyén, Virágporos Méhlegelő, Budapest: Országos Magyar Méhészeti Egyesület (OMME), 2014. (in Hungarian)
- [3] J. Han, Z. Zhang and J. Cao, „Developing A New Method to Identify Flowering Dynamics of Rapeseed Using Landsat 8 and Sentinel-1/2,” *Remote Sensing*, %1. kötet13, p. 105, 12 2020.
- [4] V. Fernandez, P. Martimort, F. Spoto, O. Sy and P. Laberinti, “Overview Of Sentinel-2,” *Proceedings of SPIE*, October 2013.
- [5] „Földmegfigyelési Információs Rendszer,” [Online]. Available: <https://efold.gov.hu/>.
- [6] T. Bjørk, *Gray Scale Image Analysis: Image analysis program for use with MATLAB*, Oslo: University of Oslo, 2006.
- [7] B. Böröcz, „Developing a GIS Based Application for Bee-Keeper,” Székesfehérvár, 2023. (in Hungarian)

IV. Discussions

In Hungary the primary bee pastures are rape, white acacia and sunflower. They can be identified from satellite imagery, but, with the exception of rape, this task requires the analysis of several images. Because satellite images are not always taken of the same area, it is not possible to select the areas to be analysed using image coordinates, and it is necessary to use Georeferenced images. Matlab makes it easier to process satellite imagery, but because of its many functions, it is essential to use the Mapping Toolbox, which allows Matlab to handle projection systems and perform various mapping operations, such as map cropping. Thanks to the Matlab Mapping Toolbox, I could display the original image in a projection system and then to select the boundaries of the area to be cropped on the map, which can be used to perform the cropping on other images without the need to locate the area again. I have saved the resulting crops in GeoTIFF format so that I do not have to create new crops for later parts of the work.

In the future, I intend to use the clippings for a machine learning system to automate the extraction of the searched areas, and to link the resulting data to the Hungarian Beekeeping Geospatial Support System [7] I developed earlier in the form of a WMS service.

The Present and Future of Satellite Gravimetry: Advancements, Applications, and Prospects

Xinling Wang
School of Geodesy and Geomatics
Wuhan University
Wuhan, China
wangxinling892@gmail.com

Xiaojing Li
School of Geodesy and Geomatics
Wuhan University
Wuhan, China
180877263@qq.com

Zhe Chang
School of Geodesy and Geomatics
Wuhan University
Wuhan, China
396742082@qq.com

Abstract—Satellite gravimetry has emerged as a powerful tool for monitoring Earth's gravitational field variations, revolutionizing our understanding of geophysical processes and their impacts on our planet. This scientific paper provides an overview of the current state of satellite gravimetry, highlighting recent advancements, applications, and future prospects in this field. We discuss the technological developments that have enabled more accurate and comprehensive measurements, explore the diverse applications across geophysics, climate science, and hydrology, and outline the potential directions for satellite gravimetry in the coming years.

Keywords—gravimetry, gravity field, satellite geodesy

I. INTRODUCTION

Satellite gravimetry, also known as satellite-based gravity mapping, has become an indispensable technique for monitoring and understanding Earth's dynamic processes. This method involves the precise measurement of variations in the gravitational field by tracking the motion of orbiting satellites. The data obtained from satellite gravimetry have applications ranging from studying the Earth's interior to monitoring changes in the polar ice caps and detecting subsurface water resources. In this paper, we provide an overview of the current state of satellite gravimetry, discussing its evolution, technological advancements, applications, and future prospects.

II. BACKGROUND

A. Mathematical Background

A square integrable function, such as the gravity field of the Earth in the outer space, can be represented by spherical harmonic functions, defined on the surface of infinite number of concentric spheres [1].

$$V(r, \theta, \lambda) = \frac{GM}{r} \sum_{l=0}^{\infty} \left(\frac{a}{r}\right)^l \sum_{m=0}^l P_{lm}(\cos \theta) (C_{lm} \cos m\lambda + S_{lm} \sin m\lambda) \quad (1)$$

where GM is the gravitational constant times mass of Earth; r, λ, θ are the spherical geocentric coordinates of computation point (radius, longitude, latitude); a is a reference length (mean semi-major axis of Earth) = 6371 km; $P_{lm}(\cos \theta)$ are the associated Legendre functions; l, m are the degree, order of spherical harmonics; C_{lm}, S_{lm} are spherical harmonic (or Stokes') coefficients of the potential.

Similar equations can be derived for $T=V-U$ disturbing potential, where U is the normal potential [1]:

$$T(r, \theta, \lambda) = \frac{GM}{a} \sum_{l=0}^{\infty} \left(\frac{a}{r}\right)^{l+1} \sum_{m=0}^l \bar{P}_{lm}(\cos \theta) (\Delta \bar{C}_{lm} \cos m\lambda + \Delta \bar{S}_{lm} \sin m\lambda) \quad (2)$$

and for the deflection of the vertical [1]:

$$\xi(r, \theta, \lambda) = \frac{GM}{r^2 \gamma} \sum_{l=0}^{\infty} \left(\frac{a}{r}\right)^l \sum_{m=0}^l \frac{\partial \bar{P}_{lm}(\cos \theta)}{\partial \theta} (\Delta \bar{C}_{lm} \cos m\lambda + \Delta \bar{S}_{lm} \sin m\lambda) \quad (3)$$

$$\eta(r, \theta, \lambda) = -\frac{GM}{r^2 \gamma \cos \phi} \sum_{l=0}^{\infty} \left(\frac{a}{r}\right)^l \sum_{m=0}^l \bar{P}_{lm}(\cos \theta) (-m \Delta \bar{C}_{lm} \sin m\lambda + m \Delta \bar{S}_{lm} \cos m\lambda) \quad (4)$$

where ζ is the meridional direction value and η is the vertical direction value. Also, two forms of spherical harmonics representation of the variations of the gravity, the first derivative of the potential are used, the gravity anomaly [1]

$$\Delta g(r, \theta, \lambda) = \frac{GM}{a^2} \sum_{l=0}^{\infty} (l-1) \left(\frac{a}{r}\right)^{l+2} \sum_{m=0}^l \bar{P}_{lm}(\cos \theta) (\Delta \bar{C}_{lm} \cos m\lambda + \Delta \bar{S}_{lm} \sin m\lambda) \quad (5)$$

and the gravity disturbance [1]

$$\delta g = -T_r = \frac{GM}{a^2} \sum_{l=0}^{\infty} (l+1) \left(\frac{a}{r}\right)^{l+2} \sum_{m=0}^l \bar{P}_{lm}(\cos \theta) (\Delta \bar{C}_{lm} \cos m\lambda + \Delta \bar{S}_{lm} \sin m\lambda) \quad (6)$$

The second derivatives of the potential are referred to as gravity gradients. The gravity gradients are 9 different second derivatives of the potential, each are different combinations of derivatives with respect to r, ϕ and λ . These are forming the Marussi tensor [1].

$$M = \nabla T = \begin{bmatrix} \frac{\partial^2 T}{\partial r^2} & \frac{\partial^2 T}{\partial \phi \partial r} & \frac{\partial^2 T}{\partial \lambda \partial r} \\ \frac{\partial^2 T}{\partial r \partial \phi} & \frac{\partial^2 T}{\partial \phi^2} & \frac{\partial^2 T}{\partial \lambda \partial \phi} \\ \frac{\partial^2 T}{\partial r \partial \lambda} & \frac{\partial^2 T}{\partial \phi \partial \lambda} & \frac{\partial^2 T}{\partial \lambda^2} \end{bmatrix} \quad (7)$$

Among them, the largest is the vertical gravity gradient, which is [1]

$$T_{rr} = \frac{GM}{a^3} \sum_{l=0}^{\infty} (l+1)(l+2) \left(\frac{a}{r}\right)^{l+3} \sum_{m=0}^l \bar{P}_{lm}(\cos \theta) (\Delta \bar{C}_{lm} \cos m\lambda + \Delta \bar{S}_{lm} \sin m\lambda) \quad (8)$$

Gravity gradients are more suitable to be described in local coordinate systems, with considering the gradient along the North (N), East (E) and Up (Z) directions. The Marussi tensor is symmetric and is defined by six quantities which, in the north-oriented system centred on the observation point, are

T_{NN} , T_{EE} , T_{ZZ} , T_{NZ} , T_{EZ} , T_{EN} ; five of these are independent as the trace ($T_{NN} + T_{EE} + T_{ZZ}$) is equal to zero. The formulas for the north-oriented gradients are [2]

$$T_{NN} = \frac{1}{r^2} \left(\frac{\partial^2 T}{\partial \varphi^2} + r \frac{\partial T}{\partial r} \right) \quad (9)$$

$$T_{NE} = \frac{1}{\cos \varphi r^2} \left(\frac{\partial^2 T}{\partial \varphi \partial \lambda} + \frac{\tan \varphi \partial T}{\partial \lambda} \right) = T_{EN} \quad (10)$$

$$T_{NZ} = \frac{1}{r} \left(\frac{\partial^2 T}{\partial \varphi \partial r} - \frac{1}{r} \frac{\partial T}{\partial \varphi} \right) = T_{ZN} \quad (11)$$

$$T_{EE} = \frac{1}{\cos^2 \varphi r^2} \left(\frac{\partial^2 T}{\partial \lambda^2} + r \cos^2 \varphi \frac{\partial T}{\partial r} - \cos \varphi \sin \varphi \frac{\partial T}{\partial \varphi} \right) \quad (12)$$

$$T_{EZ} = \frac{1}{r \cos \varphi} \left(\frac{\partial^2 T}{\partial \lambda \partial r} - \frac{1}{r} \frac{\partial T}{\partial \lambda} \right) = T_{ZE} \quad (13)$$

$$T_{ZZ} = \frac{\partial^2 T}{\partial r^2} \quad (14)$$

The potential directly cannot be measured, but the deflection of the vertical, the gravity anomaly / gravity disturbance and gravity gradients can be observed. For large scale observations, satellite-borne methods are used, named satellite gravimetry.

B. Demand on Application of Satellite Gravity Data

Satellite gravimetry is a scientific technique that involves using satellites to measure the Earth's gravitational field [3][4]. The primary task of satellite gravimetry is to provide precise and detailed information about the distribution of mass within the Earth, which can be used for a variety of purposes, including:

- **Monitoring changes in the Earth's Gravity Field:** this can be used to track movements of mass within the Earth, such as the melting of ice sheets [5][6], changes in groundwater storage [7][8], and shifts in the distribution of ocean water [9][10].
- **Geodesy and Reference Frames:** satellite gravimetry helps in improving the accuracy of geodetic reference frames, which are essential for activities like navigation [11][12], land surveying [13][14], deformation monitoring [15][16], and the study of Earth's shape and size [17][18].
- **Sea-Level Rise and Ocean Circulation:** by measuring changes in ocean mass and circulation, satellite gravimetry provides valuable data for studying sea-level rise, ocean currents, and their impact on climate and coastal regions [19][20].
- **Earthquake and Volcano Monitoring:** it can be used to monitor subtle changes in the Earth's crust that may indicate tectonic plate movements, potential earthquake hazards, and volcanic activity [21][22].
- **Hydrology and Water Resources Management:** satellite gravimetry helps in assessing changes in terrestrial water storage, which is crucial for managing

water resources, predicting droughts or floods, and understanding the Earth's water cycle [23][24].

- **Glacial Mass Balance:** by measuring changes in the mass of glaciers and ice sheets, satellite gravimetry contributes to our understanding of global climate change and its impact on polar regions [25][26].
- **Atmospheric Studies:** it can also be used to study variations in atmospheric mass, such as changes in air pressure and moisture content, which are important for weather forecasting and climate research [27][28].
- **Environmental Disaster Monitoring:** relevant natural disasters are tied to mass redistributions, many of them can efficiently benefit from the temporal varying gravity data. Direct impacts such as the melting of the permafrost melting [29][30], and indirect impacts such as related medical problems [31][32] are all witnessed.

III. EVOLUTION AND TECHNOLOGICAL ADVANCEMENTS

The concept of satellite gravimetry was first proposed in the 1960s. The methods have been further improved in the 1980s and 1990s. Theoretical developments were implemented in the 2000s by the launch of the CHAMP, GRACE and GOCE satellites missions [33].

CHAMP (Challenging Mini-satellite Payload): CHAMP was a German satellite mission launched in July 2000 with the primary objective of studying Earth's magnetic field and gravity field [33]. In order to complete the geomagnetic measurements, it had been equipped with a long boom at its face (Fig. 1).

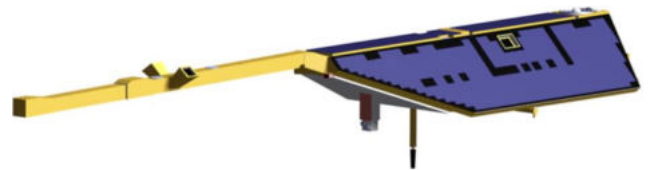


Fig. 1. CHAMP [34]

GRACE (Gravity Recovery and Climate Experiment): The GRACE mission, launched in 2002 and succeeded by GRACE-FO in 2018, is a collaborative effort between NASA and the German Aerospace Center (DLR) [33]. GRACE is known for its unique approach to measuring Earth's gravity field by observing range rate variations between the identical satellites (Fig 2.), GRACE A and GRACE B with high-precision laser interferometry [34].

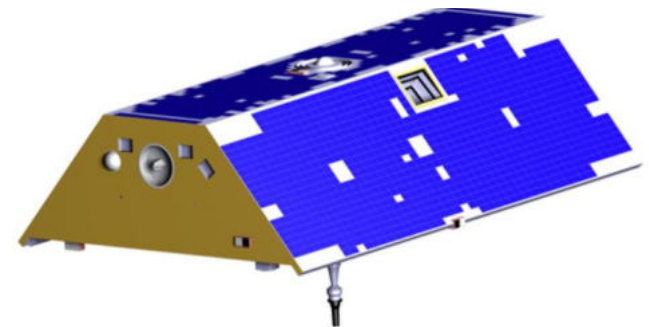


Fig. 2. GRACE [34]

GOCE (Gravity field and steady-state Ocean Circulation Explorer): GOCE was an Earth observation satellite mission launched by the European Space Agency (ESA) in 2009 [33]. It was dedicated to measuring Earth's gravity field with very fine spatial resolution by implementing the gravity gradiometry technique in space (Fig. 3).

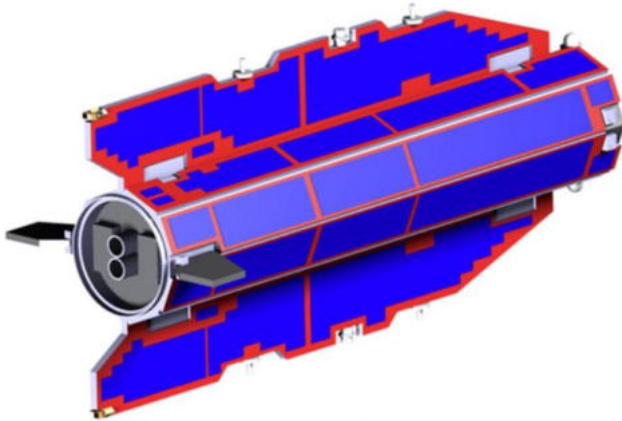


Fig. 3. GOCE [34]

These satellite missions, CHAMP, GRACE, and GOCE, have played vital roles in advancing our understanding of Earth's gravity field, geophysical processes, and their impacts on our planet, making significant contributions to various scientific disciplines. All these three missions could have been realized primarily due to the development of high-precision blackjack GPS receivers and ultra-stable accelerometers. Additionally, technological advancements in satellite design (GOCE), range-rate laser interferometry (GRACE), and precise tracking systems have improved measurement accuracy. Upcoming mission GRACE-FO (Follow-On) continued to push the boundaries of precision [35].

IV. PRESENT STATUS OF SATELLITE GRAVIMETRY

By the mid-2010s, CHAMP, GRACE and GOCE has ceased operation. As GRACE has provided useful time series of mass variation, its follow-on mission has been settled.

The Gravity Recovery and Climate Experiment-Follow-On (GRACE-FO) Mission was launched on 22 May 2018, which is jointly operated by NASA and GFZ, and provides a continuity for the GRACE temporal gravity field models [35].

The primary objective of the GRACE-FO is to obtain precise global and high-resolution models for static and temporal components of the gravity field. As in the original GRACE mission, this goal is achieved by making precise measurements of the inter-satellite range between the two identical satellites. The satellites are revolving on a co-planar, polar, low altitude orbit tracked by a K/Ka-Band microwave system. The innovative observation of the mission is the Laser Ranging Interferometer (LRI) for ranging the distance between the satellites. For positioning, both satellites carry high-precision Global Navigation Satellite System (GNSS) receivers, and for ranging from the ground a Laser Retro-Reflector (LRR), and for observing non-gravitational accelerations influencing the satellites, high-accuracy accelerometers are carried in their center of mass [36].

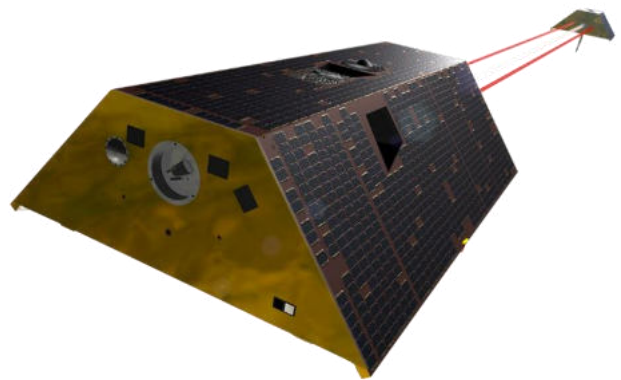


Fig. 4. GRACE-FO [37]

V. FUTURE PROSPECTS

The GRACE-FO performs well, but its planned mission lifetime is already over as it was planned to stay in orbit and delivering observations until May 2023 [38]. Therefore, future perspectives are under considerations.

After GOCE, GRACE and GRACE-FO, there is still a need for improvement of spatial resolution [39]. The demand can be defined as

- a 40 km to 100 km spatial scale static gravity field, and
- time-varying gravity fields on scales smaller than 500 km.

Figure 5 shows the spectral signal power of the gravitational field components. The time varying gravity signal is less than the static, and it decrease essentially increasing resolution [40]. Both accuracy and resolution can be improved by future satellite gravity missions, for static and time varying gravity field as well.

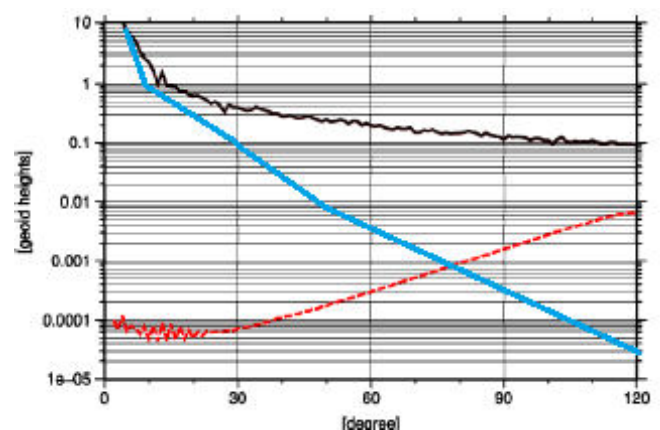


Fig. 5. Spherical harmonic spectrum of gravity field signal (black curve), and the time variable gravity signal (blue curve). The accuracy spectrum of the present best available gravity field model, EGM08 (red curve).

For geodetic applications, the spectral omission error due to the improper spatial resolution of satellite-borne observations is a limiting factor [41]. The recommended method for extending the spatial resolution of future missions as much as possible, while improving the modelling of the small-scale gravity components involved by inclusion of ground-based gravity information and topographic models.

Geodetic needs for improved gravity models are defined in several applications, such as developing

- precise vertical reference systems,
- applicability of GNSS/levelling techniques,
- proper use of inertial navigation,
- precise orbit determination, and
- for precise positioning.

Nowadays, global height systems with an accuracy of 1 cm are needed to study sea level and ocean circulation. This can be achieved by a future satellite mission with higher spatial resolution, combined with improved modelling of local and regional gravity fields. Similarly, determination of physical heights by GNSS levelling from the decimeter to the centimeter level may be improved by the increase of the accuracy of the global height systems. Any improvement in global gravity field models for inertial vehicle navigation, in particular for the guidance of submarines, aircraft and missiles, would contribute to improving reliability and the radius of the operation [42].

Now the technical and methodological developments is summarized, which can lead to achieve the demanded improvements in accuracy and resolution of the global gravity field models. Here are some issues to be taken into account for future developments.

A. Enhanced Accuracy

Continued advancements in satellite technology will lead to even more precise gravity measurements. Integration of laser interferometry and quantum sensors may further enhance measurement capabilities. Relevant expectations are established based on the applicability of the achievements of quantum technology under space environment.

B. Expanded Coverage

Smaller, more cost-effective satellite missions may enable increased spatial and temporal coverage. Collaborative efforts among space agencies worldwide will enhance global monitoring.

C. Multidisciplinary Collaboration

Increased collaboration between satellite gravimetry, remote sensing, and climate science will yield a more holistic understanding of Earth's systems. Interdisciplinary research will address complex challenges, such as climate change and natural hazards.

D. AI and Machine Learning

The application of artificial intelligence and machine learning algorithms will facilitate data analysis and interpretation. These techniques will enable real-time monitoring and more robust predictions.

VI. FUTURE PROSPECTS

Satellite gravimetry has rapidly evolved, offering invaluable insights into Earth's dynamic processes. Advancements in technology and increasing international collaboration are poised to propel this field further into the future. With its multifaceted applications and potential for addressing pressing global challenges, satellite gravimetry remains a crucial tool for Earth scientists and policymakers alike.

ACKNOWLEDGMENT

The research is supported by the National Science and Technology Planning Project in China (H.-B.L.) and NSF grant EAR3420671/2022 (E.E.B.). The authors also thank to the anonymous reviewers for their substantive review and valuable comments.

REFERENCES

- [1] ZH Li, "Space Geodesy (Chinese Edition)", Wuhan University Press, 2010. ISBN-10: 7307075741, ISBN-13: 978-7307075740
- [2] C Braitenberg et al, "The enigmatic Chad lineament revisited with global gravity and gravity-gradient fields", Geological Society, London, Special Publications, 357, 1, 329-341, 2011. DOI 10.1144/SP357.18J.
- [3] L Foldvary et al. "Gravity inversion techniques for high-low SST applied to a simulated GOCE orbit" Acta Geodaetica et Geophysica Hungarica 1217-8977 1587-1037 2213-5820 40 1 1-13, 2005. DOI 10.1556/ageod.40.2005.1.1
- [4] M Wermuth et al. "Mission Simulation and Semi-Analytical Gravity Field Analysis for GOCE SGG and SST", Observation of the Earth System from Space pp. 193-208, 2006. DOI 10.1007/3-540-29522-4_14
- [5] A Blazquez et al "Exploring the uncertainty in GRACE estimates of the mass redistributions at the Earth surface: implications for the global water and sea level budgets" Geophys. J. Int., 215, 415–430, 2018. DOI 10.1093/gji/ggy293
- [6] L Foldvary "Mass-Change Acceleration in Antarctica from GRACE Monthly Gravity Field Solutions" Geodesy for Planet Earth. Proceedings of the 2009 IAG Symposium pp. 591-596, 2012.
- [7] A Kiss "Comparison of seasonal hydrologic variations in the La Plata basin from GRACE monthly solutions with in situ tide gauge water level data" Acta Geodaetica et Geophysica 1214-9705 14 2 145-152, 2017. DOI 10.13168/AGG.2016.0035
- [8] K Abdelmohsen et al. "Water Density Variations of the Aral Sea from GRACE and GRACE-FO Monthly Solutions" Water 2073-4441 p. 1725, 2023 DOI 10.3390/w15091725
- [9] Q Wang et al "Improving the Resolution of GRACE/InSAR Groundwater Storage Estimations Using a New Subsidence Feature Weighted Combination Scheme" Water 15, 1017, 2023. DOI 10.3390/w15061071
- [10] D Zhong et al. "Spatiotemporal Downscaling of GRACE Total Water Storage Using Land Surface Model Outputs" Remote Sensing 13, 900, 2021. DOI 10.3390/rs13050090
- [11] M Rogobete et al "Using Gravity Potential Field and Inertial Navigation System in Real Time Submarine Positioning" 2018 IOP Conf. Ser.: Earth Environ. Sci. 172 012005. DOI 10.1088/1755-1315/172/1/012005
- [12] G Toth et al. "Upward / downward continuation of gravity gradients for precise geoid determinations", Proceedings of The 2nd International GOCE User Workshop pp. 249-254, 2004
- [13] MB Aminjanova et al "Vertical Deformation Analysis Based on Repeated Measurements of a Shopping Building" The herald of Kyrgyz state university of construction, transport and architecture named after N.Isanov, 74(4): 534-544, 2021. DOI 10.35803/1694-5298.2021.4.534-544
- [14] A Ruziev et al "Comparison of the Reliability of the Most Frequently Used Surveying Techniques" Journal of Geographical Society of Uzbekistan, 62: 181-189, 2022.
- [15] C Egeto et al. "Variations of the gravity field due to excavations of the Budapest Metro4 subway line" Periodica Polytechnica-Civil Engineering 0553-6626 1587-3773 58 2 131-136, 2014 DOI 10.3311/PPci.7489
- [16] T Huszak et al. "The effect of tunnelling on repeated precise levelling measurements for vertical deformation control of the Metro4 project" Journal of Geodetic Science 2081-9943 3 2 95-102, 2013 DOI 10.2478/jogs-2013-0015

- [17] M Wermuth et al. "Comparison of Different Gravity Field Solution Methods Applied to CHAMP Gravity Field Modelling" Österreichische Beiträge Zu Meteorologie Und Geophysik 1016-6254 31 45-50, 2004.
- [18] M Wermuth M et al. 'A gravity field model from two years of CHAMP kinematic orbits using the energy balance approach' Geophysical Research Abstracts 1029-7006 1607-7962 6, 2004.
- [19] N Sneeuw N et al. "One year of time-variable CHAMP-only gravity field models using kinematic orbits" A Window on the Future of Geodesy pp. 288-293, 2005. DOI 10.1007/3-540-27432-4_49
- [20] ZH Duan et al "Monitoring and Mapping of Soil Salinity on the Exposed Seabed of the Aral Sea, Central Asia" Water 2022, 14, 1438 DOI 10.3390/w1409143
- [21] G Laszlo et al "Application of Sentinel-1 data for determination of surface deformation due to volcanic and seismic events" Modern Technologies for the 3rd Millennium, p. 55-60, ISBN 978-88-87729-49-8, 2018
- [22] G Laszlo et al "Determination of 3D surface deformation for the 2018 Oaxaca earthquake using InSAR" Selected papers of the 5th International Conference on Research, Technology and Education of Space (H-SPACE 2019), pp. 17-22. Paper: HSPACE2019-FP-18, 2019
- [23] L Foldvary "Applicability of GRACE and GRACE-FO for monitoring water mass changes of the Aral Sea and the Caspian Sea" Proceedings of the International Conference Intercarto/InterGIS 2414-9179 2414-9209 26 2 443-453, 2020 DOI 10.35595/2414-9179-2020-2-26-443-453
- [24] T Bauer et al. "The Making of a Joint E-Learning Platform for Remote Sensing Education: Experiences and Lessons Learned" Remote Sensing 2072-4292 13 9, 2021. DOI 10.3390/rs13091718
- [25] A Kiss et al. "Uncertainty of GRACE-borne long periodic and secular ice mass variations in Antarctica" Acta Geodaetica et Geophysica 2213-5812 2213-5820 52 4 497-510, 2017. DOI 10.1007/S40328-016-0185-1
- [26] L Foldvary et al. "Accuracy investigations of GRACE-borne ice mass variations in Antarctica". Dixue Qianyuan / Earth Science Frontiers 1005-2321 22 4 239-246, 2015
- [27] L Foldvary et al. "IB and NIB hypotheses and their possible discrimination by Grace" Geophysical Research Letters 0094-8276 1944-8007 28 4 663-666, 2001. DOI 10.1029/2000GL011775
- [28] L Zenner et al "Using atmospheric uncertainties for GRACE de-aliasing: first results" Proceedings of IAG Symposium in Buenos Aires, IAG Symposia Series, Vol. 131., 147-152, 2016.
- [29] Y Fukuda et al. "Environmental corrections for the precise gravity observations by mean of satellite gravity data" Journal of the Geodetic Society Of Japan 0038-0830 47 2 679-685, 2001.
- [30] N Gido et al. "Studying permafrost by integrating satellite and in situ data in the northern high-latitude regions" Acta Geophys. 67, 721–734, 2019. DOI 10.1007/s11600-019-00276-4
- [31] I Turdimambetov et al. "Influence of Adverse Ecological Factors on the Incidence of Malignant Neoplasms" E3S Web of Conferences 2555-0403 2267-1242 227, 2021
- [32] E Varga et al. "Optimalization of Density and Distribution of Stereograph Measurement Points for a Face" Proceedings of the Third Hungarian Conference on Biomechanics pp. 387-394, 2008
- [33] GF Balmino et al "CHAMP, GRACE and GOCE: Mission Concepts and Simulations", Bollettino di Geofisica Teorica e Applicata, 40(3-4): 309-320, 2001.
- [34] G March et al. "High-fidelity geometry models for improving the consistency of CHAMP, GRACE, GOCE and Swarm thermospheric density data sets" Advances in Space Research 63(1), 213-238, 2019. DOI 10.1016/j.asr.2018.07.009
- [35] RP Kornfeld et al. "GRACE-FO: The Gravity Recovery and Climate Experiment Follow-On Mission" Journal of Spacecraft and Rockets, 56(3) 931-951, 2019. DOI 10.2514/1.A34326
- [36] F. Flechtner et al "What Can be Expected from the GRACE-FO Laser Ranging Interferometer for Earth Science Applications?" Surveys in Geophysics 37, 453–470, 2016. DOI <http://doi.org/10.1007/s10712-015-9338-y>
- [37] Official GRACE-FO website:
<https://www.jpl.nasa.gov/missions/gravity-recovery-and-climate-experiment-follow-on-grace-fo>
- [38] GRACE-FO project EO portal: <https://www.eoportal.org/satellite-missions/grace-fo#eop-quick-facts-section>
- [39] Z Polgar et al. "Filter design for GOCE gravity gradients" Geocarto International 1010-6049 1752-0762 28 1 28-36, 2013. DOI 10.1080/10106049.2012.687401
- [40] G Toth et al. "Practical aspects of upward / downward continuation of gravity gradients" Proceedings of The 3rd International GOCE User Workshop pp. 115-120, 2007.
- [41] L Foldvary "Desmoothing of averaged periodical signals for geodetic applications" Geophysical Journal International 0956-540X 1365-246X 201 3 1235-1250, 2015. DOI 10.1093/gji/ggv092
- [42] J Flury et al "Future Satellite Gravimetry For Geodesy" Future Satellite Gravimetry and Earth Dynamics, Springer New York, 13-29, 2005. DOI 10.1007/0-387-33185-9_2

POSTER SESSION III.
Enterprise and Economics

Process and quality development of an automotive production cell

Anita Lengyel
Alba Regia Technical Faculty
Óbuda University
Szekesfehervar, Hungary
lengyelanita.14@gmail.com

József Németh
Hydro Extrusion Hungary
Szekesfehervar, Hungary
jozsef.a.nemeth@hydro.com

Monika Pogatsnik
Alba Regia Technical Faculty
Óbuda University
Szekesfehervar, Hungary
pogatsnik.monika@amk.uni-obuda.hu

Abstract— In recent decades, the automotive industry has been about cutting costs and increasing profits. Companies have improved their processes and reduced the amount of scrap to maximize their performance. This idea is driven through practical perspective in this study. Optimize the process we were using lean process improvement tools such as workday recording and the standard work chart. Besides the standard work chart, we use some other classic lean techniques such as 5S or kaizen. 5S is the basis for orderly, quality work. Kaizen is a process consisting of small improvement actions, which is mostly cost-free, making it an excellent tool for companies that want to improve their processes and reduce costs, how to make a production system in an automotive environment more efficient. The article describes the status of the production cell, describes the kaizen proposals. After the corrective measures have been carried out, the cell is presented so that the increase in capacity can be detected. It illustrates quality and process engineering tasks and solutions.

Keywords— Automotive industry, Production cell, 5S, Kaizen, Quality engineering

I. INTRODUCTION

In today's automotive industry, companies need to produce a product of sufficient quality to satisfy their customers, in addition to maximizing profits and environmental targets. Minimizing the amount of scrap is also important from an environmental point of view, and it also plays a big role in reducing costs. Companies also aim to improve their work processes. It is also important to ensure the safety of workers and create an orderly working environment.

The main objective is to increase the efficiency of production equipment and processes, thereby increasing customer satisfaction. To increase the efficiency of the production process, sources of loss must be eliminated. Companies should use methods that maximize capacity with the highest efficiency at the lowest cost. So, we are not talking primarily about automation, but about small changes that may be insignificant individually, but over a longer time horizon are very effective in increasing production capacity. The moves and methods in people's work processes must be found that have no added value and are therefore redundant. By eliminating these movements, rearranging the working environment, and making some small changes, work can be simplified, and process efficiency increased.

Perhaps the best method is to adopt a lean approach, because lean refers to all activities that do not create value as waste and aims to eliminate them.

II. ABOUT LEAN IN GENERAL

The lean management in short, it is about reducing costs, losses and inventories, thereby in short, to increase quality and added value [1].

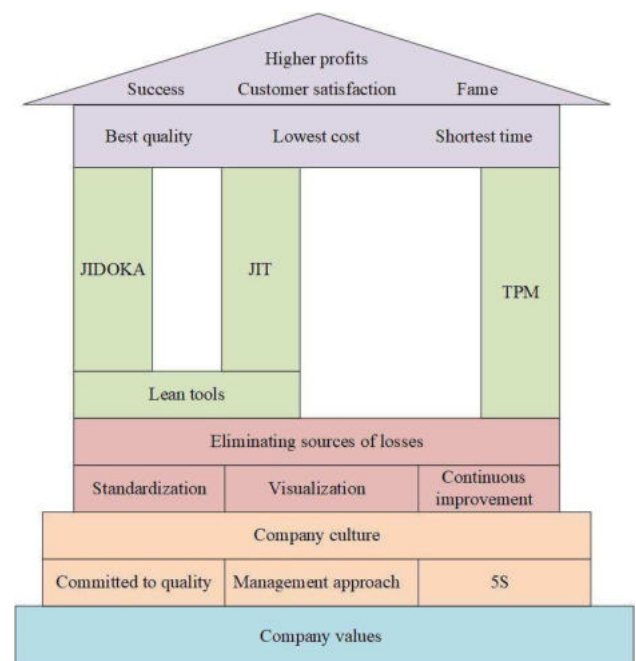


Fig. 1.: "Lean House" (Source: own editing)

Figure 1 shows the "lean house", also known as the "lean church". This figure illustrates the Toyota production system (TPS) [2], which shows that the companies have to produce the best quality, in the shortest time, at the lowest cost, thereby minimizing their losses and maximizing their profits. At the lowest level are the company values, followed by the corporate culture. At the next level are standardization, visualization and Kaizen, which are tools to minimize or eliminate sources of loss. Jidoka [3] is one of the pillars of TPS and is basically nothing more than automation. The two basic principles of Jidoka are: machines can stop automatically when an anomaly is detected; and human and machine work must be separated. On the same "pillar" is the term Poka-Yoke [4], which is a set of devices and solutions that indicate faults electronically or mechanically, designed to avoid them. JIT (Just in Time) [5] is the other pillar of TPS and its essence is very simple: the necessary product, in the required quantity, at the required time. Heijunka, or balanced production, is a prerequisite for JIT. By applying it, inventories are

significantly reduced, so that production becomes more flexible, making it easier for companies to respond to and meet customer demand [6].

Companies that follow a lean approach, use tools that enable production processes such as 5S, SWC and Kaizen. Standard work chart (SWC) is a tool that provides a visual representation of the way of work in the workplace. It includes a layout drawing, as well as the length of the workflow, so it maps the workflow in its entirety, showing the material flow. 5S [7] comes from the initial letters of 5 Japanese words. These are the following words:

- Sort
- Set in order
- Shine
- Standardize
- Sustain

The 5S guarantees orderly, accident-free and efficient work and a transparent working environment. The Japanese word Kaizen [8] is usually defined as continuous improvement. Mostly a process of costless or low-cost improvement measures, that minimize or eliminate losses in production processes. A Kaizen idea can be effectively implemented and implemented without major financial investment a competitive advantage for the company [9].

The most important task for companies adopting a lean approach is to constantly look for, analyze and eliminate losses. Losses are defined as any activity that does not directly generate value for the customer.

Let's see how lean identifies the basic sources of loss. Basically, we can identify 7 main losses, which we call the 7 MUDAs. The following figure illustrates these.



Fig. 2.: 7 wastes (Source: own editing)

We talk about overproduction when we produce

more than our customers' needs, which means that our stocks are also higher. The biggest loss in production processes is overproduction because, if it occurs, then all the other losses will be present. Because in this case our stocks increase, and consequently the waiting time, so that unnecessary activities which do not add value to production appear. In addition, a series of movements carried out by the workers which do not increase the value of the product value added, are a significant source of losses. If the working conditions of workers are ergonomically inadequate, their performance and ability to concentrate at the end of the working day will be significantly reduced. Consequently, there is an increase in the production of scraps, as well as other errors and operations that are not justified to produce the product. And the plus 1 or 8th loss is untapped human knowledge.

Eliminating these losses is therefore the goal of any organization that wants to run its processes economically and efficiently. Loss reduction options are basically divided into two groups, the extensive and the intensive methods.

Extensive methods include overtime, i.e., increasing working time, putting unused shifts into production. Intensive methods include the increased involvement of intellectual work. This step is crucial for the efficient and quality-conscious operation of a company. Other methods include the rationalization of productive work and the general application of best working practices.

III. STANDARD WORKING, STANDARD WORK CHART

The Standard Work Chart (SWC) is a tool that provides a visual representation of the way of work in the workplace. A summary operations sheet describing the standard work, structured as a schematic layout plan, a spaghetti diagram, production organization basic values. It follows the standard work steps of a standard operation and accounts for their time units. In the standard work chart, 3 main parts can be highlighted. In the standardized operation chart, a layout description which visualizes the layout of the work area and the flow of material. It indicates the locations (finished goods and raw material locations) and the work the quantity of materials in work in progress. It shows the way in which the worker follows the standard work route and the locations where the material passes through the product realization process.

The other important part of the standard work chart is the norm calculation and the data required for takt time and cycle time planning. It can also be referred to as a Kaizen tool, because it can be used to reveal problems in the work processes. It maps the process, including sub-processes, activities, operations, and operational elements. It examines the differences between TT (Takt Time), HTT (Hungarian Takt Time), CT (Cycle Time).

Time analysis is a basic technique for understanding and improving current processes. To identify standard workflows, we need to know the time required for all operations. Through time analysis, we can find the hidden problems in processes, and it helps us to find

ways to improve them.

The Standard Work Chart contains a layout plan which shows the material flow and human movement. It also includes the following statistics: number of working days in a month, monthly piece count, length of a shift, number of operators, and the utilization rate. From these data, the number of pieces per day and per shift, the takt time also can be calculated. In addition, it also shows the differences in the load of each operator. The monthly number of units divided by the number of working days in a month, then we get the daily number of pieces. The number of pieces per shift can be calculated from the number of shifts and the number of products produced per month [6].

IV. THE WORK OF IMPROVEMENT

The first and most important step in a development project is to map the current situation, presentation of the current situation. If we know each step of the current process in detail, we will be able to really improve the manufacturing cell in the future. It is important to check the processes in several shifts and take several measurements to get a complete picture of the current state of the production cell.

In the present study, the assessment of the baseline condition of the automotive production cell started with the observation and measurement of the processes and elementary operations. The above mentioned is illustrated in the layout drawing.

When developing a process, it is important to know that the operators do exactly and how long each part of their activity lasts. After measuring the length of each elementary operation and movement, we know the operator's manual time, walking time and waiting time, so we can see exactly where there are time intervals that can be exploited to increase the number of pieces produced.

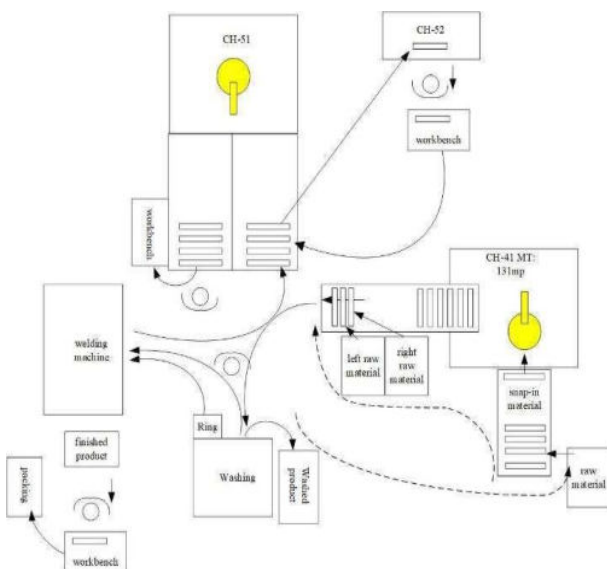


Fig. 3: Production cell layout drawing (Source: own editing)

These data are stored in the Standard Work Chart. The SWC contains the layout drawing, the manual and

machine times and all the data we needed for the calculations [10].

The layout shows that there are basically four operators working in the above cell. It can be clearly seen the individual elements of the operation and the paths of travel within the cell. One operator works at the Chiron 51 milling machine (CH-51), two at the welding machine and the washing machine, and one at the SLP station, where the parameters of each finished product are checked individually. The operator working on the Chiron 51 milling machine goes to the conveyor belt to pick up the part, prepares it and replaces it with the part in the milling machine, then starts the program. Operator deburring the removed part and placed on the conveyor. A check measurement is made on the part every hour to check the size of the holes, the depth of the threads and the overall length of the profile.

Meanwhile, another operator walks to the Chiron 41 (CH-41) infeed conveyor and loads the material. He walks back to the Chiron 42 (CH-42) unloading conveyor, pairs the parts, picks up the already paired part, puts it in the washing machine and starts the program. Meanwhile, he puts two rings in the welder, then takes the paired part out of the washer and puts it in the welder and starts the program. At the end of the program, he places the welded part on the Chiron 51 infeed conveyor. The washed finished product from the washing machine is placed in the OK pallet.

In parallel with these processes, operator 3 picks up the raw material from the conveyor belt and deburr it. He then places the part in the washing machine, takes it out and puts it in the OK pallet and walks back to the conveyor. He takes a measurement every hour on the given profile. The operator also performs bore and thread inspection and full-length measurement.

The last step is to weigh and package all the parts that have been made so far. In this step, the operator checks the holes, alignment, threading and bending of each part. He visually checks the measured profile, then inserts it into the machine, locks it in place, followed by the welded joint check. The final operation is the packing.

The baseline assessment of the manufacturing cell was followed by its development. Suggestions for improvements were introduced that affected the working environment, the measurement tools and the measurement process. The most important kaizen proposal was the moving of the operational element.

In Figure 4, the diagram shows that operator 3 (OP3) is the bottleneck in the process since he has the longest hand time (orange) and he therefore he is the most overloaded. In the case of the longest elementary operations, which are the preparation of the raw material and the and skimming, are moved to operator 2 (OP2), then the manual time of operator 3 (OP3) is 50,1 seconds. With the transfer of the activity, the production of a cell with a capacity of 81 units per shift was increased to 94 units per shift. This will result in an additional production of 13 pieces per shift. This

increases to 39 pieces in one day, based on a 3-shift working schedule, resulting in 195 pieces in 5 working days. This is more than 2 shift capacity. The cell currently employs 4 operators, so the above calculation allows us to save 8 operator shifts when they can be involved in other value-adding processes, and the cell can be maintained and improved.

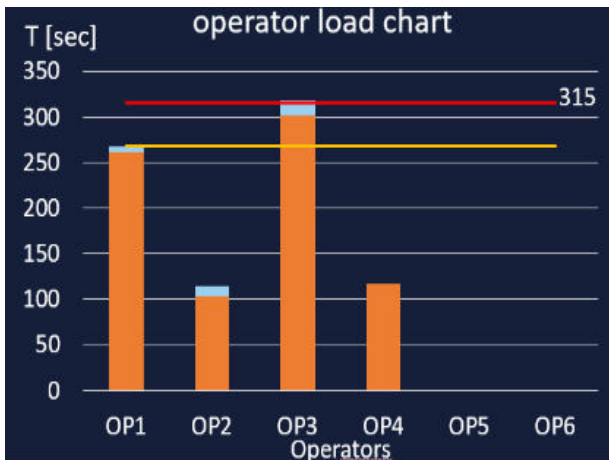


Fig. 4.: Operator load charts before the development (Source: own editing)

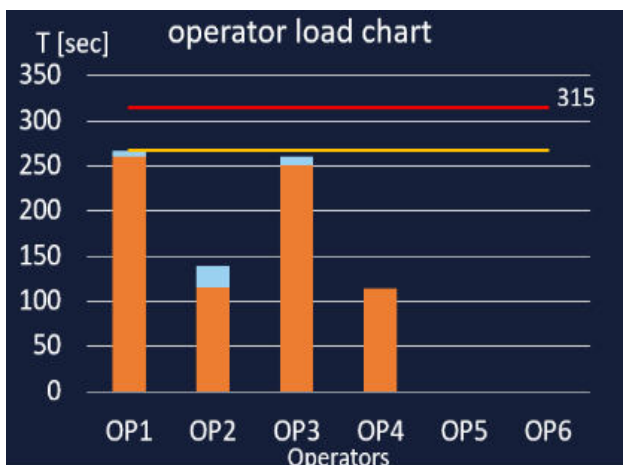


Fig. 5.: Operator load charts after the development (Source: own editing)

The takt time of the process has been reduced from 311.1 seconds to 268.1 seconds, which gives a surplus of 13 pieces in 1 shift, 39 pieces in 1 day, 195 pieces in a week and 780 pieces in a month.

Overall, the result of the above kaizen proposals is that the production cell can produce 7 shifts faster.

V. DISCUSSION

Our article introduces the lean approach, including its main tools and their use. It follows in detail the method and steps of process improvement of an automotive production cell. It goes through the individual development proposals and their demonstrable effects in a case study approach. It presents and analyses the operation of a production cell, breaking down the different operational elements through a Standard Work Chart. This has led to the identification of losses that can be eliminated to make the cell work more efficiently, thus enabling the customer's order to be fulfilled in a shorter

time. By eliminating losses, leaner production could be achieved. Most of the proposals are cost-free or can be implemented at very low cost. By reorganizing the layout, a more ergonomic, orderly, and accident-free working environment for workers has been created. Thanks to the recommendations on measurement, the operator's previous walking time was eliminated and, together with the digital gauge attachment, the measurement process was shortened by 13 seconds. In the SLP area, the layout has been rearranged to create a more ergonomic working environment. The transfer of work tasks has resulted in a more even workload, so that the operators in the cell have almost the same workload. Transferring operations, we were able to increase the production of the cell from 81 units per shift to 94 units per shift, an increase of 13 units per shift, which is 39 units per day.

So, overall, the more efficient operation of the cell is guaranteed by the introduction of the kaizen proposals. In this case, the manufacturing cell can produce the customer's order faster than before. Operators can work in a safe and orderly working environment. However, we cannot sit back and relax, because the essence of kaizen is continuous improvement, so we need to reassess its status from time to time and look for possible improvement points.

We have further summarized the improvement proposals mentioned in my article in an Ishikawa diagram in Fig.6.

Ishikawa diagrams are sometimes referred to as fish bone diagrams or cause-and-effect diagrams created by Isikava Kaoru in 1968. Isikava made major breakthroughs in quality management, making him one of the founding fathers of modern management, and his basic concept of the fishbone diagram, first published in 1920, has since been regarded as a fundamental tool of quality control. We often use the Ishikawa diagram in development work because it helps us to outline the stages and steps of the production process.

This diagram can help us identify where quality control problems may arise, so we could determine what resources are needed to solve them [11].

In this case, it shows that the development proposals are basically divided into 5 groups with further sub-categories:

- Method
- Measurement
- Layout
- Ergonomics
- Work organization

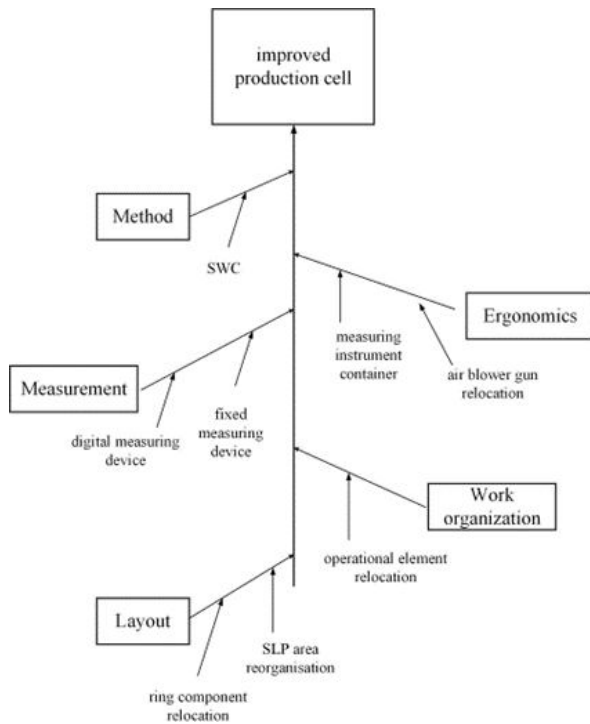


Fig.6: Ishikawa diagram (Source: own editing)

In this article, the herringbone diagram is not used in the usual way, as it does not follow a cause-and-effect structure but contains the proposals for improvement. The implementation of these kaizen suggestions led to a more efficient operation of the production cell. The Ishikawa diagram shows how, within each category, the implementation of these suggestions has helped to increase capacity while maintaining a safe and orderly working environment.

VI. REFERENCES

- [1] A. Koncz, "A lean szemlélet eszköztára", 2017.
- [2] T. Ohno, "Toyota production system: beyond large-scale production", Productivity press, 2019.
- [3] M. H. A. Soliman, "Jidoka: The Toyota Principle of Building Quality into the Process", 2020.
- [4] S. Shingo, "Zero quality control: Source inspection and the poka-yoke system". 2021, Routledge.
- [5] R. R. Fullerton, and C. S. McWatters, "The production performance benefits from JIT implementation", Journal of operations management, 2001, 19(1), 81-96.
- [6] J. Kosztolányi and G. Schwahofer, "Lean szótár", Budapest: Kaizen Pro Kft., 2015.
- [7] F. C. Filip, and V. Marascu-Klein, "The 5S lean method as a tool of industrial management performances", In IOP conference series: materials science and engineering (Vol. 95, No. 1, p. 012127).2015, IOP Publishing, 2020.
- [8] M. Helmold. "Lean management and kaizen", Springer international publishing.
- [9] J. P. Womack and D. T. Jones, "Lean thinking", New York, 1996.
- [10] L. Berényi, "A Toyota-módszer hatása a minőségmenedzsmentre", Miskolc, 2015.
- [11] O. Fehér, "Ishikawa diagram távoktatási jegyzet" , Budapest, SIRIUS Bt. 2014.

What is a Startup Ecosystem About?

Richard Veres
 Alba Regia Technical Faculty
 Óbuda University
 Szekesfehervar, Hungary
 veres.richard@amk.uni-obuda.hu

Abstract — In this short paper, I want to explore what the startup ecosystem is all about, what its key elements are and what it can mean for a city in its development. My aim is to find out what conditions are conducive to the creation of such an innovation network, what role science and innovation parks can play in this, what social missionary activities (education, research) of higher education institutions are conducive to the diffusion of an entrepreneurial, startup culture. I use a literature analysis to clarify the necessary knowledge and conceptual framework. I will use the assumption that science and innovation parks have a role for the dissemination of startup culture and in the building of the ecosystem. I assume that a startup ecosystem can have a strong impact on retaining talented young people in large cities and increasing the competitiveness of the region.

Keywords — *key elements of startup ecosystem, science and technology parks, keeping young talents at hometown, regional competitiveness*

INTRODUCTION

The city of Székesfehérvár is facing the same urbanisation and global challenges as most other cities in Hungary and Western Europe. To maintain their competitiveness in the international economic space, they need to keep developing, otherwise they will be left behind and, from the investors' point of view, will only appear as a shrinking area on the map until they are completely out of sight. There is a growing demand from city dwellers for urban life to be more liveable, more likeable, healthier, greener, and more sustainable. The problem of keeping young people in their place is also a problem in all cities, and it is important that their fresh vision and new ideas are somehow retained and that their ideas are incorporated into the development opportunities of the city.

One possible response to the challenges identified could be to build a local start-up ecosystem, which could be an alternative to keep talented young people in the city, while at the same time responding to global or local problems, implementing their innovative ideas, and starting new businesses, contributing to the development of the city and its region, and improving the lives of its residents.

In 2023, the municipality has arrived at the gateway to a development opportunity with the planned Science and Innovation Park programme in Székesfehérvár, where the coordinated work of potential actors can help to increase the innovative capacity of the municipality and local society by supporting the matching of potential actors. This in turn can have an impact on the growth of the local economy, improve efficiency, create jobs, increase visibility in the international arena and, through complementary activities to shape attitudes, improve the well-being of the local population. The development of a start-up ecosystem that can be linked

to and integrated into the Science and Innovation Park will create a vibrant, inspiring, and entrepreneurial atmosphere in which young people interested in the subject can find their place locally and in the international network. The city could thus become a winner in the fight to retain young talent, who can contribute to local R&D processes with their fresh ideas and innovative ideas, and in the medium term contribute to increasing the number of knowledge-intensive activities. One of the seven areas identified in McKinsey's study "*Fueling the Hungarian start-up ecosystem*" is to ensure support (e.g. attracting) talent, and to retain or attract young talent from other cities, including from the international market [1].

The aim of the literature review is to define the concept of the startup ecosystem, to identify the key elements and to understand the role of science and innovation parks in the diffusion of startup culture. During the research, I have selected from the literature those that each bring us closer to understanding the field under study through a different perspective, to defining the startup ecosystem and to identifying the elements of the system, so that it can be framed and interpreted in a scientific perspective in further research in relation to the situation of a specific city.

In addition to the peer-reviewed literature, during my research to find the relevant literature, I came across several blog posts, case studies and reports on cities, which I do not wish to present at this time, but the number of hits proves the popularity and importance of the topic.

DEFINITION OF THE STARTUP ECOSYSTEM

To define the startup ecosystem and to identify its key elements, I refer to the study Insights into startup ecosystems through exploration of multi-vocal literature by Nirnaya Tripathi, Pertti Seppänen, Ganesh Boominathan, Markku Oivo, Kari Liukkonen, published in Information and Software Technology in 2019. In it, the authors provide an overview of the definitions of startup ecosystems, the important elements that make up the system, and how they influence startups in their product development phases. The authors used a "multivocal" literature analysis approach to the startup ecosystem, as they found little relevant literature on the novelty of the field. 18310 articles were filtered using various search engines, with results also examining "grey literature" (blog posts, web articles, white papers, etc.) that would not have been found through electronic databases. Finally, 63 articles were selected for their analysis, describing startup ecosystems around the world in some form. Three definitions of startup ecosystem were highlighted in their study, as defined by other authors, before they defined their own concept.

Cukier et al. define it as "*a region defined within a 30-mile (or one-hour travel) radius, made up of people,*

startups and various support organisations, working together as a complex system to create new startups and develop existing ones" (Cukier et al., 2016) [2]. In this approach, a network system to support innovative enterprises is presented in terms of activities within a specific geographical area.

As Cervantes and Nardi (2012) state, "The startup community uses the term 'ecosystem' to describe the network of people, institutions and resources needed to build startups. This ecosystem includes entrepreneurs with diverse backgrounds, skills and experience, as well as private investors, public and private funding institutions, large companies that create infrastructure, and universities" [3]. In this interpretation, the focus is on the supportive environment, which contributes to the start-ups' launch through its resources.

As defined by Krajcik and Formanek (2015), "A regional startup ecosystem is an effective way to support regional innovation, improve the business environment, ensure domestic product growth and employment in the country" [4]. The authors link the definition of the ecosystem to the level of the regions, which can have an impact on regional competitiveness through innovation outcomes and employment creation.

Tripathi et al (2019) defined the elements of the startup ecosystem in eight themes and additional sub-elements: entrepreneurs, supporting factors, finance, demographics, market, education, human capital, technology [5]. They conclude their study by concluding that start-ups play a role in job creation and can become an important factor for economic development. And ecosystem elements are crucial to the creation of startups. Several common characteristics of startup ecosystems were highlighted:

- multidimensional phenomenon.
- It can be local or regional.
- support actors are thought of as a network of collaborators with a vested interest in the system, acting as stakeholders.
- Supporting infrastructure, which on a smaller scale focuses on the creation of new start-ups/enterprises; on a larger scale, it can have an impact on the growth of domestic production and the creation of new jobs.
- an effective way to support innovation and improve the business environment.

KEY ELEMENTS OF THE STARTUP ECOSYSTEM

The elements of the startup ecosystem are defined by Tripathi et al (2019) in eight themes and additional sub-elements: entrepreneurs, supporting factors, finance, demography, market, education, human capital, technology. These are expanded in detail as follows:

The entrepreneur is identified as a key element, whose goal may be self-employment or the development of opportunities. In the context of the entrepreneurial approach, both over-optimistic and realistic attitudes come to the fore, which can determine the development trajectory of an organisation.

The **supporting factors** include a number of specific sub-elements: *incubators* and *accelerators* (important for early-stage startups, founders and startups); *co-working spaces* (where actors can collaborate to develop startups, network); *events* (provide a framework for meeting each other, contribute to the spread of startup culture); *government* (government subsidies, programmes to help create the "environment"); *legal framework* (taxes, intellectual property rights, facilitating business entry, immigration); *media* (social media opportunities, role of blogs and news agencies); *mentoring* (developing entrepreneurial mindset, boosting entrepreneurs' confidence).

Finance is also a central element in the ecosystem, as startups need financing adapted to their life stages. In principle, two types of funding can come into the system, one from *the state* and one from *the private sector*. These in turn can be diverse: large corporate funding, seed investments (bootstrapping, angel investors, incubators, accelerators, FFF), venture capital funds (business expansion, further growth), bank loans, community funding.

Demography is an important factor, and its components have an impact on the system as a whole: Within this, the importance of *culture* and *language* (may determine the creativity of the local population, presence or absence of startup culture); *the impact of GDP* (for the development of the economy; favourable GDP = may lead to easier financing); *geography* (location of the municipality and the determination of the economic structure); *history* (positive impact of startup success stories); *immigrants* (due to language and cultural differences, they see entrepreneurship and learning new technologies as a way of making a living).

The **market** can be local, if start-ups can find a market for their products, or global, if the local market is small and there is no uptake. Startups need to focus on the needs of their customers. In this respect, the population of large cities is more favourable to start-ups than smaller municipalities.

Education is a key area for startup ecosystems. Within this, the role of *higher education institutions* is crucial (entrepreneurship, dissemination of knowledge; development of an innovation-driven economy; role of talent management). *Experience* is also valued (involvement of someone with a strong entrepreneurial background and experience; familiarity with global markets). The role of the *media* is also emerging as a channel for information sharing and awareness raising. The *family* is not only involved as part of the FFF (friends, family, fools) in the seed stage as a financier, but also as a provider of education and moral support, by passing on the experience and knowledge accumulated in the business created in the family ties.

Human capital is an important part of the system because of the talent it brings. Factors that play a role in developing human capital include *educational institutions* (by creating education and training programmes; spreading entrepreneurship; providing information about open startup jobs); *government* (by creating programmes to help identify talent; encouraging international cooperation to attract talent); and reaching out to *young talent*.

Technology impacts on ecosystems and their actors. Also, within this category, the relationship between

geography, technology and *industry* is very closely linked (what technology is diffused within the geographical unit and what industry is built on it). What *large companies* are present in the region, what technology they use, can influence early-stage startups. The technology background of the *founders* of the startups. Another important element is the *product* developed, which is closely linked to the technology used and its innovative features.

Tripathi et al (2019) conclude that startups can become an important tool for job creation and a driver of economic development. Together, these ecosystem elements are crucial for the creation of startups.

THE IMPACT OF UNIVERSITY TEACHING AND RESEARCH ACTIVITIES ON THE ENTREPRENEURIAL DISPOSITION

Chiara Marzocchi, Fumi Kitagawa & Mabel Sánchez-Barrioluengo authors The Journal of Technology Transfer journal 44. Evolving missions and university entrepreneurship: academic spin-offs and graduate start-ups in the entrepreneurial society, published in the 2019 issue of the Journal of the Journal of Higher Education (JRC), they provide an overview of the impact of university teaching and research activities on the entrepreneurial disposition, ethos and actions of the higher education institution, which have a direct impact on the emergence of spin-off companies and student start-ups in the entrepreneurial society [6].

Their study focuses on England within the United Kingdom. The analysis is based on a longitudinal database of Higher Education Business Community Interaction (HE-BCI) surveys and data from the Higher Education Statistics Agency (HESA), covering 163 higher education institutions. Their work also refers to related European Commission reports from 2012 and 2015, which underline the link between student entrepreneurship and regional/national economic performance, as there is a rise in the ranks of HEIs that encourage the development of student start-ups and the spread of entrepreneurship.

Marzocchi and co-authors (2019) have the following findings for the English higher education sector:

- The creation of spin-off companies has been stable over the period, and the generation of start-ups created by graduates has increased significantly.
- Both research and education play a role in determining the chances of creating or growing entrepreneurial organisations.
- In universities where there is a tradition of research activities and the aim is to develop and strengthen them, this favours the creation of academic spin-offs in the short term.
- For institutions traditionally focused on education, the focus is on student start-ups rather than academic spin-offs.
- The entrepreneurial skills needed to stimulate business are underpinned by both education and research.
- Universities are diverse, with different types generating different types of academic entrepreneurial organisations, depending on the

internal characteristics of the institution (strengths, external environment, historical traditions).

"Within higher education institutions, there is competition between student startups and spin-off companies, which can be reflected in their values and drivers. Spin-off companies are market-driven, their growth strategy and entrepreneurial characteristics may change over time. As their relationships and links with the university change. In the case of student start-ups, some may be driven by socially motivated goals, while others may be driven by commercial goals. Universities may support student startups in the teaching and learning environment, while the nature of the student enterprise may change over time." (Marzocchi et al., 2019).

At the end of their findings, the authors of the study asked further questions: should higher education institutions choose between supporting student start-ups and academic spin-off companies? How can support measures be used to develop both forms of entrepreneurship while balancing education and research? These are the games that are at play in the sphere and together influence the way in which a given higher education institution defines its own mission and influences the forms and dynamics of its entrepreneurial activities.

THE ROLE OF SCIENCE AND INNOVATION PARKS IN SPREADING STARTUP CULTURE

The authors *Bálint Vasvári, Gábor Mayer, László Vasa* in their study entitled The role of science and innovation parks in the development of the knowledge economy and the innovation ecosystem, published in the journal *Tér-Gazdaság-Ember* in the 2nd issue of the VIII. volume 2020, review the concepts and tasks of science and innovation parks, present the Bolzano Science Park and the Singapore Science Park in the form of case studies, and formulate useful experiences for the Hungarian development policy [7].

To summarise the concepts and tasks of science and innovation parks (TIPs), the authors draw on the definitions of the IASP (International Association of Science Parks and Areas of Innovation), the UKSPA (The United Kingdom Science Park Association) and the success factors identified by the European Commission. For me, the definitions are important specifically because of the references to the place of start-ups in the system in the parks supporting the creation of innovation ecosystems, which can be identified in all three cases. In the UKSPA SIP's term we find startups named: *„traditionally, it describes a business support environment that encourages and supports startups, the launch, incubation and development of high-growth, knowledge-based businesses..."* [8]. The IASP understands the role of parks to include *"facilitating the creation and growth of innovation-based companies through incubation and spin-off processes"* [9]. The European Commission has identified incubation and acceleration activities as one of the key elements of a science and innovation park (SIP), which could be one of the elements to be considered in the design and development process when setting up a new SIP. Rowe points out that he is *"enthusiastic to animate and inspire the STARTUP and Co-working scene for academics and young entrepreneurs"* [10].

In this case study on the *Bolzano Science Park* (Nature of Innovation), the authors look at the science park in Bolzano, in the South Tyrol province of northern Italy. They find that the park's strategy focuses on supporting young people to become entrepreneurs and on bringing the research results of academic actors to the market through start-up and technology transfer services. They identify as a strong activity the entrepreneurship education activities and the infrastructure and service framework provided for the start-up culture: start-up incubation programmes adapted to the different life cycles; technology transfer actions; innovation management (student camps, grants, product innovation programmes).

The case study on the *Singapore Science Park* is also important because the authors present the SIP development vision of the city-state, voted the world's most competitive economy in 2019 by the World Economic Forum [11]. It was highlighted that the move of the National University of Singapore's Centre for Entrepreneurship Development to the park in 2000 marked a spectacular turnaround in innovation promotion. Technology transfer, the launch of start-up and spin-off programmes, and the „Overseas Colleges” initiative, through which a significant number of students have gained entrepreneurial internships with international start-ups. International agreements have been signed with 10 world-class universities to ensure quality services for their students.

Vasvári and co-authors highlight among the lessons that can be drawn from this experience for domestic development policy:

- from the NOI Science Park model to strengthen the start-up culture, focused investment incentives and the involvement of research institutions.
- In the context of the Singapore Science Park model, the city-state is a hotbed for world-class companies that create the critical mass for the knowledge economy, as well as measures to encourage youth entrepreneurship.

The development of levels of the education system and the development of entrepreneurial attitudes through the development of young people's assertiveness, independent thinking and risk-taking capacity are seen as a model for promoting innovation in the country.

SUMMARY AND FURTHER RESEARCH PROPOSALS

With the selected literature review, following Tripathi et al (2019), an interpretative framework was found in which the supporting elements of the startup ecosystem can be identified at the local level. Marzocchi and co-authors (2019), examining UK higher education institutions, have explored the entrepreneurial spirit of universities and the relationship between the scale of teaching and research activities to identify cases that favour the emergence of startups or spinoffs. In addition to its strong teaching activities, the Alba Regia Technical Faculty, Óbuda University is also working to broaden its research activities with its teaching and research community, which provides scope for the development of student start-ups and the emergence of research spin-offs. The two types of business development activities can be fully complementary, not in

competition, and both can help to promote a more innovative approach, thus also promoting entrepreneurship.

Vasvári and colleagues (2020), who analysed international case studies to define the concept and tasks of science and innovation parks, suggest that the proposals for domestic development policy could serve as a model for innovation promotion at the educational system level, for the development of entrepreneurial attitudes among young people and for the strengthening of start-up culture. The UKSPA, the IASP's definition of a SIP, as well as the European Commission's success factors, identify start-ups as innovative forms of entrepreneurship to be supported with incubation and acceleration services. It is therefore appropriate to design the science and innovation park in Székesfehérvár in such a way that activities supporting start-ups and culture can be included, together with student orientation.

Székesfehérvár is not only the "city of kings", but also the home of businesses and economic organisations. As a result of the conscious industrial development of the city, it has become one of the country's leading economic power centres over many years. It is in an advantageous position, since in the years following the change of regime the local economic structure was not based on one dominant enterprise, but on a great number of large companies and small and medium-sized enterprises, with a presence in several sectors, grouped in 5 industrial parks.

Two higher education institutions offer a wide range of courses in the municipality, the Kodolányi János University, the Alba Regia Technical Faculty of Óbuda University and the Keleti Károly Faculty of Business and Management, which means that there is a diverse student community. The municipality is open, proactive, supportive of new ideas and plays a catalytic role in the life of the municipality.

Thanks to the cooperation of local higher education, economic actors and the municipality, the dual higher education system was established and consolidated from 2015 onwards and has become one of the strengths of the city. I would like to examine the functioning of this local triple helix model as a possible starting point for a future study on how and under what conditions a start-up ecosystem based on cooperation can be created in the municipality. The spiral model, extended to a new segment, civil society, can bring new perspectives to innovation collaborations by reflecting the views and interests of the local population and by enforcing cultural and environmental aspects.

This short paper has been prepared with the aim to provide a literature review to understand the conceptual framework of the startup ecosystem at the local level, to understand its conditions and its feasibility to be designed in a local science and innovation park.

Further research on this topic is important to retain young talent and, through them and their potential entrepreneurial activities, to increase the competitiveness of the city and its region, to set it on a sustainable development path and to ensure the well-being of its inhabitants.

REFERENCES

- [1] G. Bacsó, A. Havas, L. Jánoskúti, M. Matécsa, M. Mazza, T. Vecsernyés, “Fueling the Hungarian start-up ecosystem,” McKinsey & Company, 2023.
<https://www.mckinsey.com/featured-insights/europe/fueling-the-hungarian-start-up-ecosystem#/> (Last viewed: 2023.10.04.)
- [2] D. Cukier, F. Kon, T.S. Lyons, “Software Startup Ecosystems Evolution - The New York City Case Study,” 2nd International Workshop on Software Startups (2016).
- [3] R. Cervantes, B. Nardi, “Building a Mexican startup culture over the weekends,” ICIC '12: Proceedings of the 4th international conference on Intercultural Collaboration, March 2012, pp. 11-20.
- [4] V. Krajcik, I. Formanek, “Regional startup ecosystem,” European Business & Management, 1(2):14–18, 2015.
- [5] N. Tripathi, P. Seppänen, G. Boominathan, M. Oivo, K. Liukkunen, “Insights into startup ecosystems through exploration of multi-vocal literature.” Information and Software Technology, Vol. 105, pp. 56-77., 2019.
<https://www.sciencedirect.com/science/article/pii/S095058491830168X>
 (Last viewed: 2023.09.15.)
- [6] C. Marzocchi, F. Kitagawa, M. Sánchez-Barrioluengo, “Evolving missions and university entrepreneurship: academic spin-offs and graduate start-ups in the entrepreneurial society,” The Journal of Technology Transfer, Vol. 44, pp. 167–188., 2019.
<https://link.springer.com/article/10.1007/s10961-017-9619-3> (Last viewed: 2023.09.15.)
- [7] B. Vasvári, G. Mayer, L. Vasa, “A tudományos és innovációs parkok szerepe a tudásgazdaság és az innovációs ökoszisztéma fejlesztésében,” Tér Gazdaság Ember, 2020/2. 8., pp. 95-107., 2020.
https://www.researchgate.net/publication/347440181_A_tudomanyos_es_innovacios_parkok_szerepe_a_tudasgazdasag_es_az_innovacios_okoszisztema_fejleszteseben_The_role_of_science_and_innovation_parks_in_the_development_of_innovation_ecosystems (Last viewed: 2023.09.15.)
- [8] About the UKSPA, <https://www.ukspa.org.uk/how-to-join> (Last viewed: 2023.09.15.)
- [9] About the IASP, <https://www.iasp.ws/our-industry/Definitions> (Last viewed: 2023.09.15.)
- [10] D. Rowe, “Setting up, managing and evaluating eu science and technology parks,” Publications Office of the European Union, Luxembourg, p. 162., 2014.
<https://s3platform.jrc.ec.europa.eu/en/w/setting-up-managing-and-evaluating-eu-science-and-technology-parks-an-advice-and-guidance-report-on-good-practice-may-2014-> (Last viewed: 2023.09.17.)
- [11] <https://www.weforum.org/agenda/2019/10/competitiveness-economy-best-top-first-singapore-secret-consistency> (Last viewed: 2023.09.17.)

Entrepreneurial spirit among young people

Ildikó Csuka Petőné
Alba Regia Technical Faculty
Obuda University
Székesfehérvár, Hungary
csuka.ildiko@amk.uni-obuda.hu

Csilla Czeglédi
Faculty of International Management
and Business
Budapest Business University
Budapest, Hungary
czegledi.csilla@uni-bge.hu

Abstract— This paper aims first to describe the definition of entrepreneurship and the business demography in Hungary. By examining the intention to start a Hungarian business the authors outlines the basic models of intention. The study analyses the factors affecting entrepreneurs. Due to space constraints, this article does not address the external factors (i.e. the impact of the entrepreneurial ecosystem), although previous research (including the GEM report) has shown that this is a significant factor influencing business start-ups and entrepreneurial activity. The impact of this factor has been analyzed in a previous article [11]. We focused in particular on the factors influencing the start-up decisions of young people, especially students. The entrepreneurial propensity of young people were examined. The results of one of the largest entrepreneurship research projects, GUESSS, were used for the analysis. Universities are of paramount importance in increasing entrepreneurial willingness and ambition. Age and educational qualification have a significant influence on the propensity to engage in entrepreneurship. Finally, the authors pointed out that entrepreneurial spirit is highest among young adults with a degree.

Keywords—*entrepreneurship, young people, entrepreneurial intention, entrepreneurial spirit, business demography*

I. INTRODUCTION

The innovation ability of a country and thus its economic performance is crucially influenced by the level of entrepreneurship. To develop the economic development strategy, greater attention should be paid to entrepreneurs.

There is no single precise definition of entrepreneurship. The research of entrepreneurship owes much to Joseph Schumpeter. He argued that the innovation and technological change of a nation come from the entrepreneurs. He created the concept “entrepreneurial spirit” and asserted that “... the doing of new things or the doing of things that are already being done in a new way” stemmed directly from the efforts of entrepreneurs [12]. “Other scholars understand entrepreneurship as a process of opportunities discovery with the final purpose of creating new wealth.” [10]

World Economic Forum in its report defines the following short definition: “The pursuit of opportunities beyond the resources you currently control.” [14].

European Commission states [16]: “Entrepreneurship is a skill that can be learnt. You don't have to be born an entrepreneur to run a successful business. You can become one by developing an entrepreneurial mind set and skills. As Europe needs more entrepreneurs creating jobs, it's necessary to support this type of education in all EU countries. The main objective of the European Commission is to promote entrepreneurship education and stress its importance at all levels from primary school to university and beyond.”

II. TYPES OF ENTREPRENEURSHIPS AND THE PROPENSITY OF THEIR START

A. Types of entrepreneurs

The following types of entrepreneurs can currently be set up by individuals in Hungary: sole proprietorship, sole proprietorship company, one-person LLC, general partnership, limited partnership, limited liability company, joint-stock company. The most popular type of company is the sole proprietorship, which can be set up almost free of charge with a minimum initial investment and simple electronic administration. It is a one-person company with a small initial capital and easy to use electronic system. This one-person entrepreneurship, which has no legal personality, can be inherited and can be transformed into another company at any time. It can be suspended at any time and then resume within two years. The disadvantage is that the entrepreneur is solely responsible for the debts with his own assets.

A sole proprietorship company can be created by transforming a previously established sole proprietorship. It requires the person to have a deed of incorporation, a countersignature by a lawyer or registration with the Companies Court. It can be either limited and unlimited liability. The initial capital requirement is lower, as there is no need to pay the 3,000,000 HUF initial capital at the start-up. Double taxation is typical of it, optional KATA (small taxable enterprises) or KIVA (small business tax) taxation. Its advantage is that there is no obligation to have a partner.

A one-person Ltd. can be established under the Civil Code (Ptk.), which can be created by the establishment of an individual enterprise, an individual company, or a one-person Ltd., or by the transformation of business companies. A natural or legal person is required for the establishment. The minimum capital requirement is 3 million HUF, which is not a monetary asset, it can be an asset, or assets or cash. It is subject to corporate tax, the KATA is not may opt instead of corporate taxation, but may be taxed according to KIVA.

A Public Limited Company, also known as a limited company, usually refers to family businesses. Its establishment requires a minimum of two members, unlimited joint and several liability for debts. There is no minimum capital requirement for incorporation and it can usually be set up with a few hundred thousand forints in the presence of a lawyer. The KIVA or KATA taxation can be chosen for taxation purposes.

The next type of company is the limited partnership (Bt.), a company form that combines the characteristics of a sole proprietorship and a limited liability company. It requires at least two people to set up, where there must be an outside member with limited liability, while the inside member has unlimited liability. When setting up no minimum capital is

required, usually a few hundred thousand forints are needed to start a limited partnership. It is essential to consult a lawyer to set up this kind of company, and the double-entry bookkeeping is compulsory.

The limited liability company (Kft.) is a business usually planned for a longer period of time. It requires at least one person to set up. It has a higher start-up cost of 3,000,000 HUF. It has more favourable tax conditions, and also KIVA taxation is optional.

A joint-stock company is a business company that can be incorporated with a share capital consisting of a fixed number of shares of a fixed nominal value. In Hungary, its establishment is governed by the Civil Code (Ptk.) At least one person is required for its establishment. A distinction is made between public and private limited companies. A public limited company (Nyrt.) is generally the legal form of a large company, while the Zrt. is the legal form for medium-sized enterprises. The minimum value of the share capital at the time of incorporation is 20 million HUF for a public limited company and 5 million HUF for a private limited company. As in the past, this can also be a monetary asset, an asset or cash. The voting rights of the owners are divided in proportion to the capital, and a lawyer is always required to be supplied by establishing a company. It is subject to corporate tax for taxation purposes.

TABLE 1 BUSINESS DEMOGRAPHY IN HUNGARY (KSH, 2022) [7].

Types of business	2017	2018	2019	2020	2021	2022
1. Limited liability company	380 082	376 304	375 884	380 870	398 016	406 246
2. Joint-stock company	6 783	7 083	7 351	7 700	8 150	8 448
3. Public limited company	3 299	3 096	2 850	2 603	2 403	2 191
4. Limited partnership	126 825	122 126	117 459	111 893	107 580	99 868
A Business company	516 989	508 609	503 544	503 066	516 149	516 753
5. Cooperative	4 865	4 539	3 845	3 436	3 173	2 935
6. Other legal entities	6 027	6 109	6 202	6 313	6 448	6 653
B Company with legal personality (A+5+6)	527 881	519 257	513 591	512 815	525 770	526 341
7. Partnership without legal personality	1 727	1 746	1 683	1 666	1 681	1 671
Partnership enterprise (B+7)	529 608	521 003	515 274	514 481	527 451	528 012
9. Self-employed entrepreneur	1 189 993	1 236 486	1 279 135	1 295 875	1 329 408	1 310 708
9/a Sole proprietorship (from self-employed)	450 901	493 958	531 617	556 191	586 368	567 158
D Total enterprises (C+9)	1 719 601	1 757 489	1 794 409	1 810 356	1 856 859	1 838 720
E Budget and non-profit organisation	150 814	151 319	151 342	152 137	152 723	153 695
Total organisation (D+E)	1 870 415	1 908 808	1 945 751	1 962 493	2 009 582	1 992 415

As shown in the first table, according to the KSH by the end of 2019 there were nearly two million business organisations operating in Hungary. The number of these has been steadily increasing for years until the beginning of the COVID-19. Increase is due to the rise in the number of sole proprietorships, while the number of partnerships is steadily decreasing. The main reason for this change is the impact of the introduction of KATA and KIVA. The other reason is the introduction of more strict rules on company formation to curbe the abuses (e.g. the increase of the registration fee). Most organisations were registered as a sole proprietor in the category of other self-employed taxable individuals.

The number of active businesses exceeded 1 million in 2022, mainly due to an increase in the number of self-employed sole proprietors. The number of sole proprietors who ceased their activities (103,000) almost doubled compared to 2021 due to the change in the KATA rules. The contribution to the country's economic performance of large companies, with fewer than 1,000 employees but more than 250 employees, remained key important, but their share in the contribution has declined slightly compared to the same a year ago [7].

B. Intention of Hungarian entrepreneurship

The theoretical model of Ajzen's planned behaviour is that at its core is the individual's intention to perform some behaviour (Fig.1.). So-called motivational factors act as incentives for the intention. Such motivational factors are attitudes, subjective norms and perceived behavioural control. The stronger the intention, the higher the probability of occurrence. The model distinguishes between intention and action, which play a central role. Actual action can only be expected if the intention is strong [8].

Farkas and Gubik [17] further developed the behavioural model in the figure and added the actual behavioural control, which has two types of effects on action and intention: incentive and self-efficacy.

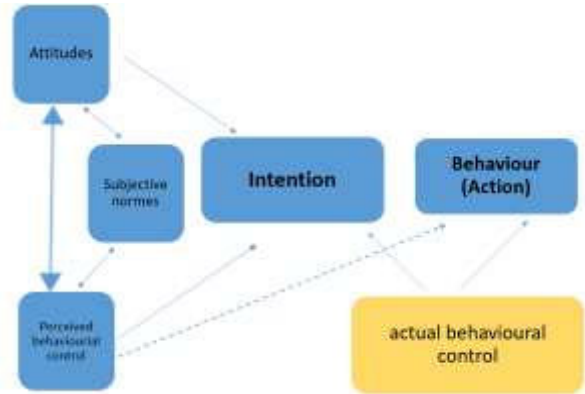


Fig. 1. Planned behaviour model (own edit according to [8])

Figure 2. shows that intention has three drivers: perceived desirability, willingness to act and perceived feasibility. These indicate that there are many motivational factors that can facilitate the start-up of a business [9]. The weakest motivator for starting a business is compulsion, when we only start because we feel there is no other option. Then the business is unlikely to deliver the expected profitability. It may also be motivated by the acquisition of material wealth and independence. The best motive for starting a business is, of course, to have an idea of your own, which you want to implement anyway.

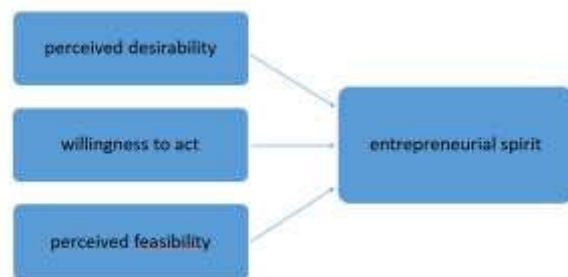


Fig. 2. Entrepreneurial intention model (own edit [9])

C. Factors affecting entrepreneurship start-up

The analysis of entrepreneurial activity is not only an indirect purpose having an important role in generating value-added and new workplaces but also conduces to the growth of economy and society. The extent of positive impacts depends on the entrepreneurial ecosystem. [11].

Several surveys show that in the United States is more typical among people to choose entrepreneurial status than in

EU member states. In Hungary the preference for employee status is particularly marked. The preferences are influenced by several economic, social, historical and cultural circumstances.

Both external and internal factors influence the propensity to become an entrepreneur. The 18-24 age group is known to be the most entrepreneurial, with university and college students being the most likely to start a business, although many of them have not yet developed a concrete idea of what they want to start or what they would like to do. 64% of them think they could realise their dreams by starting their own business. Of course, other factors play a role, including family, cultural background, education, skills learned and acquired, and others.

It is also important to talk about motivation as a factor. 83% of the respondents considered autonomy to be the most important factor. Here this can be understood as the desire to be as independent as possible, to manage their own finances or to come up with a unique idea to create something new. Flexible working hours came second with 30%. Almost a quarter of respondents (24%) thought that they could earn more as an entrepreneur, so it can be seen that this is also a key factor for many. Entrepreneurship is most common among graduates and men working as employees. 64% of survey respondents want to use their own resources to finance the start-up of their own business, while those under 25 would use their savings would use their savings. 35% would use one third of their own resources and the rest from tenders or state aid. One in two of those surveyed would rather start a business individually than in a group. [13].

The 2016 GUESSS survey of university students examined the factors that influence students' propensity to become entrepreneurs, in particular the propensity to start a business among students who have already started a business during their university studies. The data showed that gender (men's entrepreneurial propensity higher), increasing age, approaching the end of studies (the less time left until graduation, the more likely the university student to be an entrepreneur), and the higher intensity of entrepreneurship education in business studies and the entrepreneurial parental background all have a positive impact on becoming an entrepreneur. Researchers have found that students who are already entrepreneurs during their studies are more likely to become entrepreneurs in the long term [5].

III. ENTREPRENEURIAL SPIRIT

A. Entrepreneurial Spirit researches

Entrepreneurial propensity is to be distinguished from the willingness to become an entrepreneur. While the latter only refers to someone who is open to the idea of entrepreneurship and is ready for it, ready to seize the business opportunity that arises [15], the former refers to a firm intention, possibly having a concrete idea of starting a business and when to start it. Csehné and her co-author found in one of their studies entrepreneurial thinking is rather scarce in the examined population and they would desire to gain their first experience mainly in the environment of multinational companies as full time employees [18].

The country's innovation ability and thus to its economic performance is crucially influenced by the level of entrepreneurial spirit. The Global University Entrepreneurial Spirit Students' Survey (GUESSS), a series of biannual

surveys examines the entrepreneurial intentions and activities of university students. In 2018 more than 208,000 students from 3,000 universities in 54 countries, and more than 9,000 students from Hungary, completed the questionnaires. With these indicators GUESSS is one of the most largest entrepreneurship research project in the world. According to their latest research, conducted in autumn 2021 17.8% of all surveyed students directly after completing their studies and 32.3% of them plan to become an entrepreneur 5 years after completing their studies [6]. This latter study shows that universities play a key role in increasing entrepreneurial willingness and ambition. Age and educational qualification have a significant influence on the propensity to engage in entrepreneurship. In terms of age, it can be assumed that the youngest age group has the highest propensity to entrepreneurship. Those with the highest educational attainment (college and university) have the highest propensity to entrepreneurship.

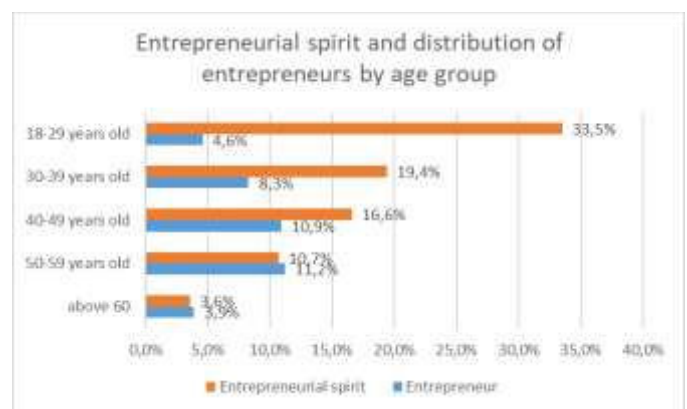


Fig. 3. Entrepreneurial spirit and distribution of entrepreneurs by age group [1]

Young people were also asked about their propensity to become entrepreneurs and their views on employment. Among the 18-29 age group, 62% do not want to be entrepreneurs, 34% would like to be entrepreneurs and 5% are already working as entrepreneurs. (Figure 3).

One reason for this difference may be the age difference, as the survey [1], which only included young people, also looked at the age group who are not yet of working age and cannot work as entrepreneurs. In terms of the proportion of potential young entrepreneurs, the two surveys produced broadly similar results: 33.5% (18-29 year olds) and 37.6% (15-24 year olds). It is interesting to compare young people's propensity to become entrepreneurs with their attitudes towards employment. 61.3% of them would be reluctant to become self-employed and a large proportion (77%) also have a poor opinion of employment, believing that workers are mostly or completely at the mercy of their employer, with only 5.2% of respondents disagreeing. This suggests that a high percentage of young people would prefer to be self-employed, but responses on entrepreneurship showed that young people are also mostly averse to entrepreneurship. This may be partly due to the fact that a large proportion of respondents (39%) to the survey believed that job security was more important than the income they could earn, and just over a tenth (11%) chose not to put money before job security. This is also explained by the fact that 69% of respondents think that starting a business

is a high risk and more than half (51%) think that it is possible to live in prosperity as an employee.

These results suggest that a higher proportion of young people, although they believe that they could really fulfil their potential in a business, would prefer to be employed, which may offer less income but more security. It would be interesting to examine what might determine this attitude, such as parental patterns (whether they are entrepreneurs or employees), or the influence of the media or peers' views on the subject.

The results show that entrepreneurship declines with age. Among other things, this is probably because the older people get, the less risk-taking they are and the more they seek security, so they are reluctant to start a business, preferring to be employed. Further research should explore the possible reasons for this.

However, the proportion of entrepreneurs in each age group varies inversely with the development of entrepreneurial propensity: the proportion of people who are actually self-employed increases with age. While in the youngest age group, where the propensity to be an entrepreneur was 33.5%, the proportion of entrepreneurs was only 4.6%, it was 8.3% in the 30-39 age group, 10.9% in the 40-49 age group and the highest, 11.2%, in the 50-59 age group. However, it can be assumed that the relatively high rates among 50-59 year olds and 40-49 year olds compared to other age groups may have historical reasons (Fig. 3.). This generation was made up of young adults during the change of regime, when full employment was lost within a few years and the 5 million people registered as employed at the time fell by more than 1 million. Many of those who were unable to retire early on pension schemes entered forced employment for existential reasons, but there was also a high proportion of those who took up business opportunities in the changed economic environment brought about by the change of regime. This could be a further avenue for research.

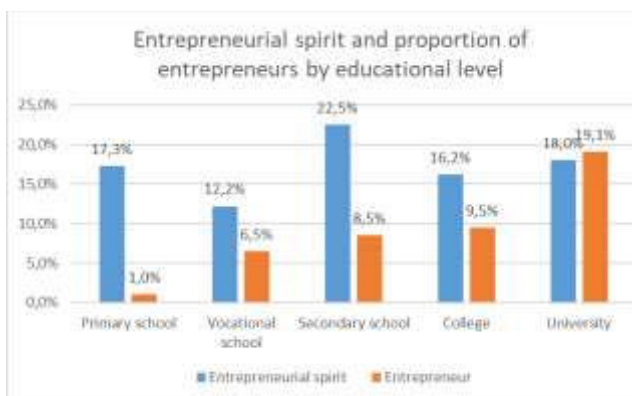


Fig. 4. Entrepreneurial spirit and distribution of entrepreneurs by educational level [1]

The highest proportion (22.5%) of those with a secondary education would like to be entrepreneurs. The second highest propensity to be an entrepreneur is among people with a university degree (18.0%). Among those with primary education, 17.3% would like to be entrepreneurs. Members of this group have the lowest labour market prospects and think that entrepreneurship could be a solution for them. 16.2% of college graduates would be entrepreneurs, while the lowest

propensity to be an entrepreneur is 12.2% among those with vocational school qualification. The results show that higher educational attainment is not associated with higher entrepreneurial spirit (Fig.4.).

As regards those who are actually self-employed, the proportion of those with higher education who run their own business, is higher. University graduates are the most likely to be self-employed (19.1%) in their business. This value is exceptionally high compared to the other groups, with the next highest value being 9.5%, which shows the entrepreneurial activity of college graduates. 8.5% of secondary school graduates, 6.5% of skilled workers and only 1.0% of primary school graduates are self-employed (Fig.4.).

Several conclusions can be drawn from this. The propensity to be an entrepreneur among primary school leavers does not seem realistic in relation to the proportion of people who are actually self-employed, which may mean that they do not really have a serious intention to be self-employed, but it is rather only a kind of wishful thinking. They may believe that their education would make it easier for them to start a business than to find a job in the labour market. Another explanation may be related to education: without the right knowledge, they may not be able to realistically assess what starting an own business might mean. A relatively high entrepreneurship rate among university graduates could be considered a good result. It would also be important to investigate the proportion of university and college graduates who are computer and high-tech literate, open to innovation and able to incorporate it into their business. Of course, further research is needed to confirm these results. However, the experience in Hungary is that such professionals prefer to work as employees in a large company for a high salary, because they can avoid the risks of entrepreneurship.

Several studies show that entrepreneurial ambitions are highest among young adults with a degree. That is the reason Tesseniyk and Kun conducted a survey [2] among university students. Students (323) from two rural universities in Hungary, in the faculties of economics, horticulture and engineering, were surveyed about their expectations and plans 5 years after graduation and asked their opinions on entrepreneurship and their own attitudes.

The GEM's 25-year study series includes the Adult Population Survey (APS), which analyses the entrepreneurial characteristics, motivations and ambitions of individuals who start a business, as well as their social attitudes towards them ('entrepreneurial spirit'), which we have processed for our article. According to the GEM studies, a typical person starting their own business is a middle-aged (35-45 years old) male, usually with a college or university degree [4]. Szerb-Imreh writes this finding in their study in 2007 according to Hungarian research. [3]. In fact, entrepreneurship education has a positive impact on becoming an entrepreneur, and on the person who wants to become an entrepreneur. Based on data collected by GUESS in 2016 [5], university students were classified into 4 basic types based on their entrepreneurial inclination: achievers, dreamers, procrastinators and stay-aways. Based on this, different suggestions were made to increase entrepreneurship. Universities should adapt their entrepreneurship programmes according to the 4 types of entrepreneur and the implementers and stimulate the growth of the entrepreneurial type.

Figure 5 illustrates the typical differences in future intentions. A significant proportion of students immediately after graduation wanted to work in a large or small and medium-sized enterprise or small and medium sized enterprises, preferring to work as an employee. They also found the public sector attractive. Overall, 74.4% of students intended to work as an employee after graduation. Five years later, the attractiveness of being an employee is declining, replaced by an increase in the proportion of people planning a career as an entrepreneur. This may mean that students want to gain some work experience rather than to be employees and they want to use the work experience in their entrepreneurial careers. In both surveys (before graduation and five years after graduation), the proportion of those who are relatively uncertain about their future career, is high (nearly 12%)[6].

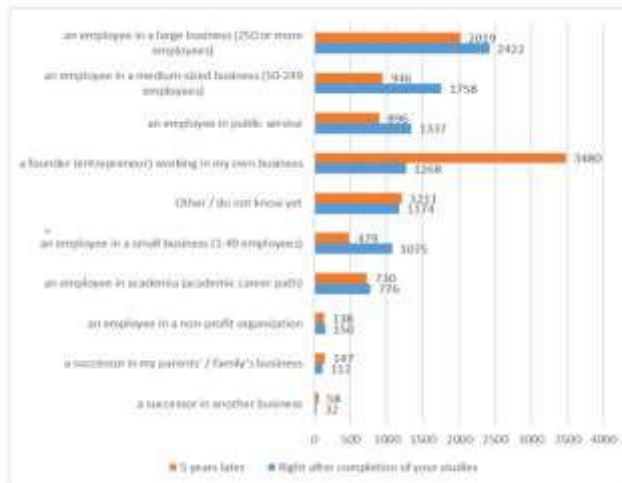


Fig. 5. : Career aspirations right after graduation and five years after studies N=10.104 [6]

Entrepreneurship education and training, creating an entrepreneurial environment, and supporting problem groups in society are central to helping entrepreneurs in Europe. Education is seen as a key priority for job creation, competitiveness and economic growth. It is important to start entrepreneurship education at an early age and this is being given even greater emphasis. The European Commission research programmes on entrepreneurship education have, among other things, identified and analysed how entrepreneurial spirit is reflected in national curricula.

IV. CONCLUSION

This study aimed to examine the entrepreneurial spirit of among young people in Hungary with analysing the business demography in Hungary and the propensity of their start. The most popular type of business is the sole proprietorship until the beginning of COVID-19. The number of this type of entrepreneurship significantly increases as a result of introduction of KATA and KIVA. The number of partnerships has been decreasing after the introduction of more strict rules.

The findings showed that age and educational qualification have a significant influence on the propensity to engage in entrepreneurship. In terms of age, it can be assumed that the youngest age group has the highest propensity to entrepreneurship. Those with the highest educational

attainment (college and university) have the highest propensity to entrepreneurship. The study confirms that higher intensity of entrepreneurship education in business studies and the entrepreneurial parental background have a positive impact on becoming an entrepreneur. Other finding is that students who are already entrepreneurs during their studies are more likely to become entrepreneurs in the long term

In developed market economies the small and medium-sized enterprise sector is given more attention because it has been recognised that it plays a significant role in domestic production and in the mitigation of the unemployment problem due to its ability to soak up the workforce, and so due to its economic power it can potentially play a stabilising role in the economy [19].

This study suggests that, first, the government institutions and universities need to be concerned about entrepreneurial programs to promote young entrepreneurs. Second, in starting a business, it is necessary to involve several stage holders in supporting their business activities, faced by young entrepreneurs. Third, young entrepreneurs still have the locus of control that needs to be increased. They need a more global mindset that makes them able to survive to run their business well. In this condition, the need for high motivation for these entrepreneurs to be able to work hard independently. Fourth, the formation of the attitude of young entrepreneurs who are very supportive of business activities is essential. In this case, entrepreneurs can make an appropriate and future-oriented analysis and have a high creative power. The need to participate in some business communities, both with beginners and those who have succeeded, will have an impact on the formation of young entrepreneurs' character. The results show that entrepreneurship declines with age. Among other things, this is probably because the older people get, the less risk-taking they are and the more they seek security, so they are reluctant to start a business, preferring to be employed. Further studies need to consider this assumption.

V. REFERENCES

- [1] Á. Tóth (2013): "The entrepreneurial spirit of the Hungarian population and openness to innovation - national survey results," TAMOP-4.2.2.A-11/1/KONV-2012-0058 research, University of Pécs, Pécs, 2013
- [2] J. Tessenyi- Zs. Kun (2022): Entrepreneurship among university students STATISZTIKAI SZEMLE, 100. ÉVF. Number 11. pp. 1010–1024., Budapest, 2022
- [3] L. Szerb. – Sz. Imreh (2007): Entrepreneurship Education and Entrepreneurial Attitudes of Hungarian Students: An International Comparison. 5th International Conference on Management, Enterprise and Benchmarking June 1–2, 2007, Budapest, Hungary. https://kgk.uni-obuda.hu/sites/default/files/6_Szerb.pdf (downloaded: 15/09/2023)
- [4] Global Report (2022): Global Entrepreneurship Monitor, 2021/2022. <https://www.gemconsortium.org/reports/latest-global-report> (downloaded: : 20/09/2023)
- [5] GUESSS 2016 Report, P. Sieger – T. Zellweger – U. Fueglistaller, Student Entrepreneurship 2016: Insights From 50 Countries November 2016 https://www.guesssurvey.org/resources/PDF_InterReports/GUESSS_2016_Global_Report.pdf (downloaded: : 12/09/2023)
- [6] P. Sieger – L. Raemy – T. Zellweger – U. Fueglistaller. – I. Hatak (2021): Global Student Entrepreneurship 2021: Insights From 58 Countries. St.Gallen/Bern: KMU–HSG/IMU–U.

- https://www.guesssurvey.org/resources/PDF_InterReports/GUESSS_2021_Global_Report.pdf
(downloaded: : 12/09/2023)
- [7] Ksh (2022): Number of registered business organisations.
(downloaded: : 08/09/2023)
<https://www.ksh.hu/docs/hun/xftp/idoszaki/gazd/2022/index.html>
- [8] I. Ajzen (2002): Perceived Behavioral Control, Self-Efficacy, Locus of Control, and the Theory of Planned Behavior, *Journal of Applied Social Psychology*, Volume 32, Issue 4
Pages: 665-683, April 2002
<https://doi.org/10.1111/j.1559-1816.2002.tb00236>
- [9] C. Schlaegel and M. Koenig (2014) Determinants of Entrepreneurial Intent: A Meta-Analytic Test and Integration of Competing Models. *Entrepreneurship Theory and Practice*, No. 38, pp. 291-332.
<https://doi.org/10.1111/etap.12087>
- [10] D. Egerová, I. Ubreziová, W. Nowinski, Cs. Czeglédi (2016): Entrepreneurship Education Opportunities and Challenges for Universities in Visegrad Countries, *Visegrad Fund, NAVA, Plzeň*, 2016
- [11] I. Petóné Csuka (2022): Entrepreneurial activity and ecosystem in Hungary. In: Petóné Csuka, Ildikó; Simon, Gyula (szerk.) *AIS 2022 - 17th International Symposium on Applied Informatics and Related Areas – Proceedings*, Székesfehérvár, Magyarország : Óbudai Egyetem pp. 152-156. , 5 p
- [12] J.A. Schumpeter (1947). *The Creative Response in Economic History*. *Journal of Economic History*, 7, pp. 149-159.
- [13] Budapest Bank: 2016, Hungarians want to start their own business
https://piacesprofit.hu/kkv_cegblog/
- sajat-vallalkozasra-vagyik-a-magyar-mar-az-otlete\ -is-megvan/, (downloaded: : 12/09/2023)
- [14] WEF (World Economic Forum): Enhancing Europe’s Competitiveness Fostering Innovation-driven Entrepreneurship in Europe
https://www3.weforum.org/docs/WEF_EuropeCompetitiveness_InnovationDrivenEntrepreneurship_Report_2014.pdf (downloaded: : 08/09/2023)
- [15] Gy. Lengyel. (2012): Potential Entrepreneurs. *Entrepreneurial Inclination in Hungary, 1988-2011*. Corvinus University of Budapest, pp. 1-162.
- [16] European Commission (2015). Entrepreneurship education. Available at: http://ec.europa.eu/growth/smes/promoting-entrepreneurship/support/education/index_en.htm. (downloaded: : 08/09/2023)
- [17] G. Farkas –A. S. Gubik (2013): Methodological specificities of research on entrepreneurial attitudes of university-college students. *Statisztikai Szemle*. 91. évf. 10. sz.
- [18] Cs. Molnár – I. Csehné Papp (2022): Challenges of Industry 4.0 on Skill Requirements towards new Entrants to the Labour Market In: Pásztor, Rita; Gál, Katalin; Székedi, Levente (szerk.) *A társadalomtudományok harminc éve a Partiumban Kolozsvár, Románia, Nagyvárad, Románia: Kolozsvári Egyetemi Kiadó, Partium Kiadó* 242 p. pp. 23-36. , 14 p
- [19] B. Parragh (2017) Competitiveness and Economic Stimulus. *New Dimensions and Instruments of Monetary Policy*. *Polgári Szemle: Gazdasági és Társadalmi Folyóirat*, 13 (Spec.). pp. 151-166.

Investigating the financing of secondary vocational education

Zoltán Trenka
University of Óbuda Alba Regia Faculty of
Technology,
Székesfehérvár 8000
E-mail: zoltan.trenka@gmail.com

Csaba Bráda
University of Óbuda Alba Regia Faculty of
Technology,
Székesfehérvár 8000
E-mail: brada.csaba@amk.uni-obuda.hu

Abstract. - Nowadays, the public media deals significantly with teacher salaries and the need for a salary increase. This question, although it has a significant social content, covers only a small part of the issue. The basic issue includes the maintenance and operation of the entire vocational training system. This includes the maintenance costs and material expenses of the vocational training institutions - as an especially important issue, the material and equipment costs, - development, and salary costs of the practical trainings belonging to the vocational training. The available information does not allow us to evaluate the issue of financing vocational training based on the above criteria. However, it is possible to determine, taking into account the budget data, how much room for maneuver the government has to expand the financing of vocational training. In our study, we took into account the data of the annual budget of Hungary, together with the statistical data of the KSH, from which the level of state support per capita was compared with the payments of employees by different types of tax. Based on a market approach, we try to prove the truth of the slogan "education, investment in the future". In the final chapter of the study, we also examined the realistic basis for transferring the financing of vocational training to market funds.

Keywords – education, financial, market approach

I. INTRODUCTION - GENERAL ECONOMIC FINDINGS

The economic processes of a country are basically influenced by the factors of two sectors. One is the productive sector, which basically operates on the basis of interest in profit and is the determinant of the country's GDP production. These include individual businesses that provide services, trade and produce products, small and medium-sized companies and multinational companies. The other is the unproductive sector, which basically includes organizations that ensure the functioning of the state. This includes public administration organizations, such as municipalities, document offices, etc. as well as armed organizations such as the police, military, and national defense, and this includes social, health organizations and education.

The difference between the two sectors can be seen basically in the availability of the funds necessary for operation.

The productive sector, as already stated in the introduction, basically covers its operating costs from the sales revenue of its activities, and carries out its developments from its profits - or from tender funds. The unproductive sector, as it does not produce and sell actual products, does not directly receive income. It must obtain the funds necessary for its operation indirectly, i.e. it takes it from the productive sector - typically in the form of taxes - and redistributes it to the sectors maintained within the sector - public administration, law enforcement, education, etc. - in the direction of.

In very simplified terms, in order to ensure operation, on the one hand, maintenance costs must be provided, which includes, among other things, the provision of material and immaterial assets, such as real estate and their maintenance costs, energy fees, infrastructural and technical equipment costs, etc. On the other hand, the coverage of wages and salary-type costs must be ensured. All of this is quantified in the country's annual budget.

From the above, it is clear that there is a significant difference in the resources of the two sectors. Based on the sources, the unproductive sector is at a significant disadvantage compared to the productive sector. It has significantly less room for maneuver in the individual financing areas, the most striking point of which is perhaps the wage. In the past year and a half, we can constantly see reports and movements about teacher salary adjustments in the media. Let us note in parentheses that the problem affects not only teachers, but all workers in the unproductive sector.

The purpose of this study is to examine the question of whether education, or certain parts of it, can be placed on a market basis, and if so, in what form and under what conditions. Operation on a market basis is the typical form of operation of the productive sector, which is determined by the relationship between supply and demand, and which determines the price of the product, ultimately the sales revenue.

II. STUDY OF THE CURRENT FINANCING SYSTEM OF EDUCATION.

In Hungary, education and training are currently carried out at three levels. There is basic, intermediate and advanced training. In the case of secondary and higher education, there is general and professional education. For our study, we chose the system of secondary professional training, as this form of training seems to be the most suitable for transfer to market foundations.

Currently, education is financed on the basis of state norms, the amount of which is determined as a percentage of GDP. (Fig. 1)

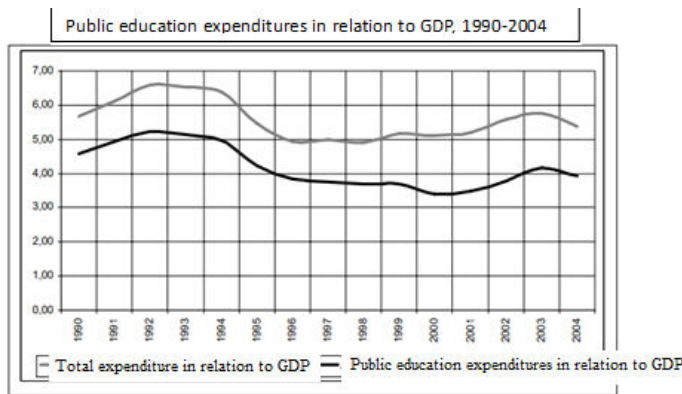


FIGURE 1 Public education expenditures in relation to GDP, 1994-2004: [1].

The amount of support per student can also be determined from this normative amount. (Figure 2) In its details, the annual state budget includes the framework figures for the given year.

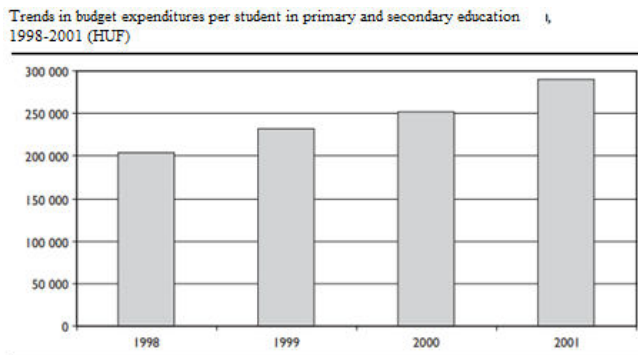


FIGURE 2. Trends in budget expenditures per student in primary and secondary education 1998-2003. [2].

Taking all of this into account, the annual budget of an educational institution can be easily calculated based on the number of students. However, it should also be emphasized that in the case of secondary education, the form of the education has a significant impact on the costs of the education. A distinction must therefore be made between the costs of a high school and a vocational training institution.

Even in the case of vocational training, significant cost differences can be found in the case of different professions. The differences are mainly due to the material and equipment requirements.

In summary, education is financed according to the scheme below. The state allocates part of its annual income to finance education, which amount is distributed among the schools - currently the institutions that control and regulate the operation of the schools (KLIK, Vocational Training Centers) - based on the number of students participating in the training. The maintaining institution ensures the material and personal conditions, as a result of which the student, upon completion of his studies, acquires professional knowledge, which enables him to find a job on the labor market.

As a final result, the community investment is realized in individual results and individual profits.

Apparently.

III. THE MARKET VIEW OF EDUCATION FINANCING

There is a well-known slogan that goes roughly like "education is an investment in the future". We tend to interpret this slogan only on a social level, even though it also has significant economic content. Before explaining this statement, let's look at the interpretation of the financing of education on a market basis.

A. Identification of market-oriented participants in the education process.

TABLE 1.

Participant designation	Market-based equivalent
Hungarian State	Investor
Training institution (school)	Production company
Graduate student	Product or "finished product"
Company that employs the graduate	Customer

The investor: He is willing to tie up his available funds in a specific activity, in the hope of long-term return and profit.

The production company: By using its existing resources, by transforming the raw material, it produces a new product and a new value. In education, the existing resources are the institution and its infrastructure, as well as the professional knowledge of the instructors. The "basic material" is the student enrolled in the education, whose professional knowledge increases during the education, and his way of thinking and attitude develop as a result of the educational work, i.e. the instructors change their quality with added value.

Finished product: The graduated student who, with his professional knowledge, is able to independently carry out quality work, make professional decisions, or manage the

work of others. Furthermore, with his professional knowledge, he is able to make corrective, modernizing and developmental suggestions.

Buyer: A workplace employing a student entering the labor market.

B. Fundamentals of market processes.

1. In the case of a market-based system, the investor is always willing to tie up his capital in the given activity and risk it for the sake of profit. In some cases, it is accepted that there is no profit, i.e. revenues and costs are the same - see non-profit organizations - however, operating at a loss is not allowed in this case either.

2. The production company can continue its primary activity as long as the investments and sales revenue from the sale of the product cover the costs of operation.

3. The market price of the product is determined by the supply-demand relationship.

C. Forms of profit.

Here we would like to refer back to II. to the closing thought of the chapter and to explain why only individual profit is apparent and why the slogan is completely correct from an economic point of view.

Upon completion of the training, the student sells his/her ability to perform work on the labor market, enhanced by the acquired knowledge and/or practical experience. The company that employs him incorporates this ability to perform work into its own system, with which it tries to increase its production capacity, sales revenue and profitability. In parentheses, I would like to note that we are usually talking about the sale of labor, but the wage can be seen more as a cover for the maintenance and reproduction costs of the labor force, if I look at the areas of use of the wage, such as buying food, clothing, covering housing costs, or expenses for raising children. Maintenance expenses are also expenses that can be assigned to rest and recreation.

Payment for labor - the purchase of labor - could be realized by paying the producer. The vocational training contribution paid by the company to the school could be considered a payment of this kind. This solution, even if numerically it does not meet the rules of market operation, but in terms of its principle, it meant financing entirely on the market principle, until January 1, 2021, when the vocational training contribution system was abolished.

The processes and the conclusions that can be drawn from them can be very narrowly defined, and it can be stated that workplaces today have access to "productive equipment" worth several million forints for free and without wages.

Returning to profitability, the profit of the investor, i.e. the Hungarian state, is realized in the form of various taxes. A higher education usually means a more profitable

job, so higher income is associated with higher taxes. The tax burdens examined in the later part of the study develop as follows in the examined period:

TABLE 2. Taxes on work

Examined period	2020	2021
Personal income tax	15%	15%
Social security contribution	18.5%	18.5%
Social contribution tax	17.5% from July 1 15.5%	15.5%
Vocational training contribution	1.5%	1.5%

A better-educated workforce is capable of cost-effective and economical production, optimization of production processes, product and process development, thus contributing to the company's profitability to a greater extent. The profit tax charged on the company's profit also appears as state revenue. Finally, higher income brings with it the need for a higher standard of living, which in turn is reflected in consumption and its growth, which means VAT revenue for the state.

From the point of view of financing, an important question is, in what proportion does the amount received from taxes cover the costs of the training? We are trying to answer all this based on the data of two years, 2020 and 2021. For the investigation, we used the data of the KSH and the budget guidelines for the years 2020 and 2021 as a basis.

IV. FINANCING EDUCATION IN THE VIEW OF THE NUMBERS

It can be considered an almost classic research aspect to express education expenses as a proportion of the gross domestic product produced in the country in a given period. If we plot the data, the following picture is drawn. (Figure3.)

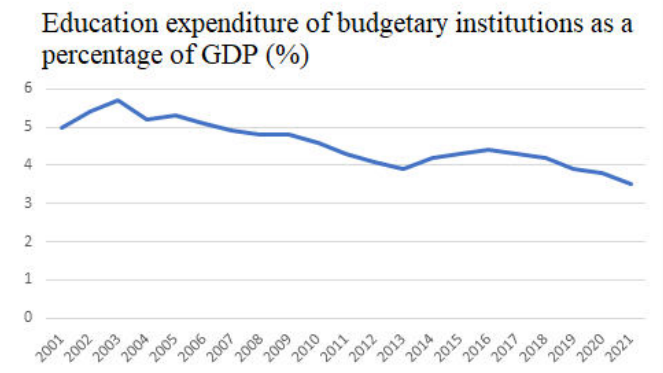


Figure 3. Education expenditure of budgetary institutions as a percentage of GDP % [3].

The number of students in primary and secondary education in the last few years and the amount spent per student are summarized below.

➤ TABLE 3. Funds per student

Year	Amount spent on primary and secondary education (HUF)	Number of students in primary and secondary education (person)	Amount spent per student
2010.	694 709 000 000 Ft	1335000	520 381 Ft
2011.	649 804 000 000 Ft	1315000	494 148 Ft
2012.	620 591 000 000 Ft	1283000	483 703 Ft
2013.	586 474 000 000 Ft	1250000	469 179 Ft
2014.	676 849 000 000 Ft	1219500	555 022 Ft
2015.	770 885 000 000 Ft	1196000	644 553 Ft
2016.	839 326 000 000 Ft	1176200	713 591 Ft
2017.	837 998 000 000 Ft	1160500	722 101 Ft
2018.	894 645 000 000 Ft	1142700	782 922 Ft
2019.	909 269 000 000 Ft	1131000	803 951 Ft
2020.	895 933 000 000 Ft	1126578	795 269 Ft
2021.	938 980 000 000 Ft	1154455	813 353 Ft

[4].

Among the indicators of education, the amount of educational expenditure determined as a proportion of GDP (gross domestic product) is very often mentioned, and we have already examined this with regard to public education institutions. We are currently subjecting it to a narrowed examination, focusing specifically on primary and secondary education.

In 2020 and 2021, which we mentioned, looking at the entire educational spectrum, this gives values of 3.8 [5]. and 3.5 [6]. percent. However, if we examine the resources spent on education, only on primary and secondary education, the values are smaller than this. This value was 2.77% [7]. in 2018, which was already relatively low in international comparison. If we examine 2020, we will find a value of 1,85%%, while in 2021 we will get values of 1,7%.

TABLE 4. Fund and resources spent on secondary education

Year	The value of the gross domestic product million HUF	Fund and resources spent on secondary education (million HUF)	GDP %
2020	48,425,421	895 933	1,85%
2021	55,255,130	938 980	1,7 %

It is clearly visible that the proportion of primary and secondary education to GDP shows a noticeable decrease in the years presented.

From the data briefly described above, it is clear that even if the amount spent on basic and secondary education shows a nominal increase, this was not enough to keep the expenditure proportional to the GDP at the same level.

As we mentioned above, a better-educated workforce and an employee with better experience are able to sell their labor (knowledge) at a higher value (secondary education is extremely important here, including professional education, which cannot achieve success without primary or elementary school education). In this way, the state, which can be considered an investor in the education system, would be able to realize higher revenues. A higher amount can be reinvested from higher revenues in order to further increase the standard of education.

In the following, we summarized the taxes and contributions paid to the budget in connection with the wages of the employees, in order to be able to examine how much income the state, as an investor, derived from incomes strongly linked to education. We performed this summation for both 2020 and 2021 data, with the following result:

TABLE 5. The evolution of examined taxes

	2020 million forint	2021 million forint
Personal income tax	2,527,742.30	2,888,586.10
Social security contribution Ny. Part of the fund and pension contribution	1,536,379.20	1,715,162.90
Social insurance contribution E. Part of the fund and health insurance contribution	1,042,910.80	1,169,149.30
Vocational training contribution	105,783.30	114,329.40
Social contribution tax Ny. Part of the fund	1,703,512.60	1,692,116.00
Social contribution tax E. Part of the fund	670,548.50	670,057.00
Tax revenues directly related to wages	7,586,876.70	8,249,400.70
General sales tax	4,669,039.80	5,397,233.40
Total	12,255,916.50	13,646,634.10

[8].

By plotting the obtained data, it becomes more visible that the nominal value of the examined tax revenues increased by more than HUF 1,390 million in the two years examined, which means an increase of 11%. The rate of growth itself exceeds the sum spent on primary and secondary education in 2021.



Figure 4 Own figure. [9].

If we examine the obtained data from the side of the state funds spent on primary and secondary education, we can conclude that in 2020, nearly 12% of the examined taxes related to employment were spent on education. If the general sales tax is also taken into account, this value is 7,3%.

In 2021, the amount spent on primary and secondary education accounted for 11,3% of work-related tax revenues, i.e. of the more than HUF 8 thousand billion in work-related income, the state will finance education with only HUF 938 980 million He paid HUF.

In the event that, as an easily connected form of tax, the general sales tax is also included in the projection base, then this ratio does not even reach 10%. Considering VAT as a form of tax is possible because a better-educated workforce contributes to the state's higher revenues by spending a higher proportion of its higher wages. (Figure 5)

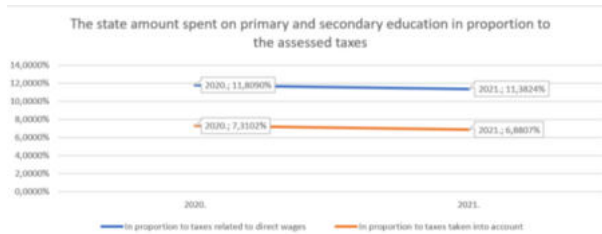


Figure 5. The state amount spent on primary and secondary education in proportion tot he assessed taxes [10].

From the data presented above, it can be seen that both in proportion to GDP and in terms of tax revenues closely related to employment, we received decreasing data in the two years under review.

Returning to the original thought process of the study, in the examined years the "producer" realized a decreasing income in terms of the examined indicators. Practically, based on the two years examined, although nominally a larger amount was allocated to primary and secondary education in Hungary, this did not result in a substantial increase in resources for the schools.

In the following, we examined the number of employees who paid the taxes we examined and their amount. In this way, the average amount of taxes paid by one employee can be determined.

TABLE 6. Tax payment per employed person [11].

Year	2020.	2021.
Paid amount of examined taxes (HUF)	12,255,916,500,000 HUF	13,646,634,100,000 HUF
Number of employees (Main)	4,603,200	4,634,600
Tax payment per employed person (HUF)	2,662,478 HUF	2,944,512 HUF

It is clear that compared to 2020, both the number of employees and the average amount of tax paid increased in the following year.

After that, we determined the amount of tax revenues related to paid work that the state would spend on primary and secondary education, if the level of expenditure were the same as the level of expenditure proportional to GDP.

TABLE 7. Work-related taxes amount spent on education at the level of expenditure proportional to GDP [12].

Year	2020.	2021.
Tax payment per employed person (HUF)	2,662,478 HUF	2,944,512 HUF
GDP ratio spent on primary and secondary education	1,85%	1,7%
Work-related taxes amount spent on education at the level of expenditure proportional to GDP	49 259.28 HUF	50, 037.66 HUF

It is clear that this value would be between HUF 49 and 52 thousand in both years.

At the same time, we also examined the ratio of those who are employed and those who participate in primary and secondary education. In other words, we determined how many main employees should cover the education costs of a student.

TABLE 8. Development of the number of students and employees [13].

Year	2020.	2021.
Number of employees (Main)	4,603,200	4,634,600
Number of students	1,523,980	1,555,863
Number of employees per main student	3.02051208	2.978796976

It can be clearly seen that while in 2020 more than 3 employees had to cover the costs of one student, in 2021 this value dropped to a minimum of 3 employees.

After that, it is easy to determine the amount with which employees contribute to a student's education.

This value is HUF 148,78826 in 2020, and HUF 149,052.04 in 2021. Of course, these amounts are far below the amount spent on primary and secondary education per person. In other words, in addition to the previously mentioned calculation methodology, the state must still provide more than HUF 640,000 in support every two years for primary and secondary education.

V. CLOSING THOUGHTS

At the beginning of the preparation of the study, we had an assumption that we wanted to prove with numerical data in the study. This assumption was that it would be covered by tax revenues, and in the worst case would show a slightly lower value than the amount intended to finance education. However, during our investigation, it was revealed that tax revenues make up roughly 1/16 of the financing amount, so the state has a significant financial role at the expense of other revenues.

From what was described in the previous chapters, it can be seen that education is faced with somewhat low funding both in proportion to GDP and in relation to work. Returning to the original thought process of the study, it must be stated that the biggest beneficiaries of the results of education are the employers appearing on the labor market.

It would be worth examining how the labor market using graduates, including the employers who employ them as employees, could contribute to better financing of education.

Taking customer, producer and investor behaviors as a basis, several options are available for better financing of primary and secondary education. In the event that the state imposes higher taxes, it would worsen the economic situation and also the opportunities of employers. If the internal structure of the budget were to be changed in favor of education, it would, by definition, worsen the prospects of other state-financed sectors.

But there is also the possibility of trying to finance education in a slightly more direct way from employers, as if they were actually paying for the "product", i.e. well-educated employees. For example, so that they could donate a certain proportion of their taxes directly to the benefit of vocational training centers. In the case of such a more direct financing, the customer, i.e. the employer, could gain a greater insight into the education and be able to target at least partially finance those areas that fall within the scope of his well-understood business interests.

Producers, i.e. schools, would be in more direct contact with the labor market, and this would enable them to earn more directly. With this step, it would perhaps be possible to better finance more financially demanding training courses, such as construction or mechanical engineering, and to purchase new technologies.

In the short term, perhaps only the investing state would be at a disadvantage, since such a system inevitably entails a loss of income in the short term. The short-term loss of income, on the other hand, may be compensated in the long term by the possibility that, due to the more direct impact, the customer receives a better "product", i.e. a better qualified workforce. The education system is able to achieve a higher level of education as a result of more direct funding. Because of the above, the product, i.e. the student

himself, is more likely to be able to find a job, for a higher wage, which would increase the state's income in the longer term.

- [1]. ISTVÁN POLÓNYI-JÁNOS TÍMÁR THE COSTS AND FINANCING OF EDUCATION (OTKA T 049593) , Competitio.2006
- [2]. MIKLÓS BALOGH - GÁBOR HÁLÁSZ REPORT ON HUNGARIAN PUBLIC EDUCATION 2003, Országos Közoktatási Intézet. 2003. Budapest.
- [3]. Central statistical office - Education expenses of budgetary institutions. https://www.ksh.hu/stadat_files/okt/hu/okt0002.html (Retrieved:2023.08.31)
- [4]. Own editing table based on the data sources below: Central statistical office https://www.ksh.hu/stadat_files/okt/hu/okt0002.html and <https://www.ksh.hu/docs/hun/xftp/idoszaki/oktat/oktatas1011.pdf>, <https://www.ksh.hu/docs/hun/xftp/idoszaki/oktat/oktatas1112.pdf>, <https://www.ksh.hu/docs/hun/xftp/idoszaki/oktat/oktatas1213.pdf>, <https://www.ksh.hu/docs/hun/xftp/idoszaki/oktat/oktatas1314.pdf>, <https://www.ksh.hu/docs/hun/xftp/idoszaki/oktat/oktatas1415.pdf>, <https://www.ksh.hu/docs/hun/xftp/idoszaki/oktat/oktatas1516.pdf>, <https://www.ksh.hu/docs/hun/xftp/idoszaki/oktat/oktatas1617.pdf>, <https://www.ksh.hu/docs/hun/xftp/idoszaki/oktat/oktatas1718.pdf>, <https://www.ksh.hu/docs/hun/xftp/idoszaki/oktat/oktatas1819.pdf>, <https://www.ksh.hu/docs/hun/xftp/idoszaki/oktat/oktatas1920/index.html>; <https://www.ksh.hu/docs/hun/xftp/idoszaki/oktat/oktatas2021e/index.html>, <https://www.ksh.hu/docs/hun/xftp/idoszaki/oktat/oktatas2122e/index.html>; Retrieved:2023.08.31)
- [5]. Central statistical office - Education expenses of budgetary institutions. https://www.ksh.hu/stadat_files/okt/hu/okt0002.html (Retrieved:2023.09.02)
- [6]. Central statistical office - Education expenses of budgetary institutions. https://www.ksh.hu/stadat_files/okt/hu/okt0002.html (2023.08.31)
- [7]. A közoktatás inikátorrendszer 202, Szerkesztette: Varga Júlia (KRTK KTI)
- [8]. Government of Hungary (Magyarország Kormánya). 2022. Preliminary balance of the central government

subsystem <https://cdn.kormany.hu/uploads/sheets/b/b3/b3c/b3c5a9df03b4f81b138f293ccbfl18c5.pdf> (2023.09.07)

[9]. Government of Hungary (Magyarország Kormánya). 2022. Preliminary balance of the central government subsystem <https://cdn.kormany.hu/uploads/sheets/b/b3/b3c/b3c5a9df03b4f81b138f293ccbfl8c5.pdf> (2023.09.07)

[10]. Government of Hungary (Magyarország Kormánya). 2022. Preliminary balance of the central government subsystem <https://cdn.kormany.hu/uploads/sheets/b/b3/b3c/b3c5a9df03b4f81b138f293ccbfl8c5.pdf> (2023.09.07)

[11]. own calculation

[12]. own calculation

[13]. own calculation

POSTER SESSION IV.
Information Systems in Education

Challenges in Higher Education in Light of Teaching the Digital Technology

Nikoletta Tolner
Alba Regia Technical Faculty
Óbuda University
Szekesfehervar, Hungary
tolner.nikoletta@amk.uni-obuda.hu

András Dávid
Alba Regia Technical Faculty
Óbuda University
Szekesfehervar, Hungary
david.andras@amk.uni-obuda.hu

Monika Pogatsnik
Alba Regia Technical Faculty
Óbuda University
Szekesfehervar, Hungary
pogatsnik.monika@amk.uni-obuda.hu

Abstract: *Over the past two decades, higher education has undergone significant changes that have created challenges for both teachers and students and set new directions for the universities of the future. The development of information technology and the rise of the Internet have fundamentally changed the way education is delivered. Online learning and the new opportunities offered by smart devices have radically transformed the educational process. Teachers are now required to use not only traditional curricular elements but also online content and tools. Educational institutions need to develop skills and knowledge in students that are relevant to the labour market. Education must be increasingly accessible and diverse. Learning processes should become more interactive and personalized to help students solve complex problems more effectively. In the face of these changes and challenges, higher education needs to evolve continuously to remain relevant and effectively serve the needs of society and students. In this article, we explore the changes in higher education through the teaching of Digital Technology.*

Keywords: *transformation of higher education, online learning, educational challenges, future universities*

I. INTRODUCTION

The subject of Digital Technology is part of the professional core material in the electrical engineering major at the Alba Regia Technical Faculty of the Óbuda University. Students study the course for 2 semesters. According to the sample curriculum (currently F), Digital Technology I. has 2 hours of lectures per week for 4 credits in the 2nd semester, Digital Technology II. has 1 hour of lectures per week for 4 credits and 2 hours of laboratory exercises in the 3rd semester. The main objective of the course is to provide the basic hardware knowledge necessary for the logical design and testing of digital circuits. Therefore, the students can deepen their theoretical knowledge through practical exercises. Lectures will focus on the design of elementary, complex combinational and sequential networks, while laboratory exercises will include simulation and measurement exercises of the designed logic networks.

First time, we look at the changes in higher education, and then, in the case of Digital Technology, how the way lectures and lab exercises are delivered has changed. The changes are presented in terms of teaching methodology, the role of the teacher, technology, and student needs.

II. CHANGES IN HIGHER EDUCATION

A. Methodological changes in education

Teachers' teaching methods have changed significantly in universities in recent years. This was and is necessary because of societal expectations, changes in the labour market and the ever-changing needs of the digital generation. The following is a comparison between the methods used in the past and the new teaching methods that have emerged in universities.

In the past, traditional lectures and notes dominated teaching. Lecturers would lecture to students, who would take notes and then learn independently from the lectures. Much of the teaching material came from books and printed sources. Examinations and written assessments (essays, papers) were the most common assessment methods used to measure students' knowledge. Teaching and learning were more passive, with students having less interaction with instructors and peers in class.

Today, instructors are increasingly using interactive teaching methods that allow students to participate and work in groups. This includes small group discussions, project-based learning, and practical applications. Online content and learning platforms, such as virtual classrooms and online courses, are becoming increasingly common in education. They allow students to learn on their own schedule and access digital resources. Assessment methods have also changed. Tutors are supplementing traditional exams with assessments such as portfolios, presentations, group work and practical projects. Instructors are increasingly using digital technologies and tools in their teaching, such as smartboards, video conferencing systems and smartphone apps. Instructors are increasingly seeking to personalise the learning process, i.e., to consider the individual needs and learning styles of students [1]. Table 1 compares the differences between traditional and modern forms of education.

These changes show that education is constantly evolving and adapting to new technologies and the needs of students. Educators need to find a balance between traditional and modern teaching methods to effectively serve students and facilitate the acquisition and application of knowledge in real life.

TABLE 1. COMPARISON OF TRADITIONAL AND MODERN EDUCATION (OWN EDITING)

Viewpoints	Traditional	Modern
educational methods	lecture, frontal	interactive
teachers' roles	lecturer	mentor
student activity	passive	active
course material	printed textbooks, notes	online content
tools	traditional whiteboards, notebooks, writing tools	smart devices, online platforms
learning methods	note-taking, tutoring	use of digital tools and learning materials, practice
assessment	exam	exam, project, group work
interaction	minimal	high level
location	classroom	online place
educational form	personal	e-learning, hybrid

B. The changing role of the teacher

Over the past 20 years, the role of teachers in higher education has undergone significant changes. The role of teachers has expanded and become more versatile. Whereas they used to focus mainly on teaching and learning, they now have a range of additional responsibilities. These include research, project management, student mentoring [2] [3]. This change shows that teachers are increasingly important actors in the university community and academic institutions. Technological developments have transformed the work of teachers. Online teaching platforms, virtual teaching tools and educational software enable more effective teaching and support for learning. However, the shift to digital education has also brought new challenges, for example in the areas of online assessment, student motivation and data protection. The paradigm of student-centred education has been reinforced in recent years. Teachers need to place increasing emphasis on understanding students' individual needs and learning styles and adapt their teaching methods accordingly. In higher education, we encounter an increasingly diverse student community and, accordingly, teachers have an important task to develop intercultural competencies and respect cultural diversity. The role of teachers also includes teaching sustainability and social responsibility. Teachers must be prepared to make students more sensitive to environmental, social, and ethical issues.

Teachers are also evaluated and held accountable for teaching effectiveness and results. These changes show that the teaching role in higher education is becoming increasingly complex and challenging. Teachers need to adapt to new demands and opportunities while continuing to focus on the quality of teaching and the development of students. Figure 1 summarises the roles of teachers today.

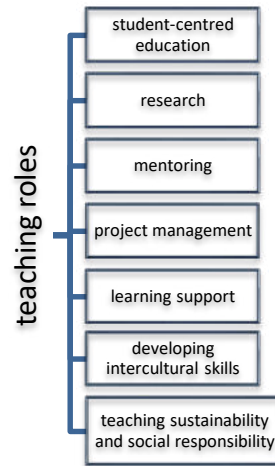


Figure 1. Teachers' roles today (own editing)

C. Technological changes

Over the past 20 years, technology has revolutionised education, from online courses and virtual classrooms to interactive teaching tools. The coronavirus epidemic has given an even greater impetus to online teaching and the use of digital tools, creating challenges, and accelerating the spread of distance learning. The emergence of new innovations and technological tools in education has increasingly made it possible to adapt to individual needs and to learn more effectively [4]. Web platforms such as Moodle, Blackboard or Canvas have emerged that allow teachers and students to create and participate in online courses. Virtual classrooms and 3D simulations allow interactive learning and simulation of hands-on experiences in online environments such as surgery simulators or chemistry labs. Instructors can present material on interactive whiteboards or projectors, allowing for dynamic lectures and student participation. Storing and sharing educational materials and documents on cloud-based platforms such as Google Drive or Dropbox facilitates collaboration and access to materials between students and instructors. Mobile apps allow students to access educational content and devices anywhere and anytime, making learning more flexible. For online learning, video conferencing systems such as Zoom or Microsoft Teams enable live communication and interaction between students and instructors. Data storage and analytics tools used in education help instructors to better understand student performance and needs, enabling more personalised instruction. AR (Augmented Reality) and VR (Virtual Reality) technologies allow for combining reality and virtual reality or creating fully virtual learning environments, for example for history lessons or spatial planning. Automated assessment tools, such as plagiarism-checking software or adaptive learning systems, help educators to assess more effectively and objectively.

These innovations and technological tools allow educational institutions and instructors to deliver material more effectively and interactively, and to personalise the learning experience according to the needs and style of students [5] [6].

D. The needs of Generation Z

Members of Generation Z (those born after 1997) have different expectations and needs from university lecturers, which create new challenges and opportunities for teaching and learning.

Generation Z has grown up with digital technologies and the Internet, and they are more inclined to interactive and experiential learning [7]. They expect educators to deliver information not only through monologue methods, but also to provide opportunities for group work, project work and hands-on experience. Generation Z members bring digital competencies with them to the university and expect instructors to use online tools and platforms in their teaching. In addition, they expect instructors to be equipped to manage online learning environments and communication. They value flexibility in teaching. Online learning opportunities, distance learning and different learning formats offer students the possibility to adapt to their individual needs. Tutors are expected to offer flexible learning opportunities. Generation Z values community and diversity. Educators are expected to promote inclusive and diverse learning environments and initiatives that foster community building among students. Members of this generation place a strong emphasis on applicable knowledge and practical skills that can help them succeed in the labour market. Educators are expected not only to provide theoretical knowledge but also to develop skills that are useful in real life. Generation Z is committed to social responsibility and sustainability, and they share this value system with their university lecturers. They expect educators to help them understand and address global challenges. Figure 2 shows Generation Z's expectations of academics.



Figure 2. Generation Z's demands on university teachers (own editing)

University teachers need to find a balance between using new technologies and teaching methods, considering the individual needs of students, and imparting valuable knowledge and skills. Flexibility, innovation and respect for the values and expectations of students are needed to ensure that education effectively and valuably serves Generation Z [8].

III. TRACKING CHANGES IN DIGITAL TECHNOLOGY

The course includes both a lecture and a lab exercise, so you will follow the changes in both cases. We will also cover methodological and technological changes, as well as changing social conditions. The epidemic situation has also brought huge changes and has moved education towards

the online space, which has been extremely challenging for both students and teachers.

A. Lecture

For two decades, lectures in Digital Technology were also frontal, with the instructor standing on the lectern and talking about the current course material. Learning was facilitated by printed notes and books written by the instructor. There was little interaction between the students and between the lecturer and the students. The students took handwritten notes and used them to prepare for the quizzes. In 2012, our university introduced Moodle (Modular Object-Oriented Dynamic Learning Environment). Moodle is an LMS (Learning Management System) application, an e-learning framework. As it is a web-based system, it requires Internet access to use it. After several months of work, we created a fully e-learning version of the Digital Technology course, which we have been running on the university's Moodle platform on the KMOOC (Carpathian-Mediterranean Online Education Centre) site. The material is also used in full-time education as a supplement to classroom lectures, mainly for practical exercises. The course contains a summary of theoretical and practical material, supplemented with videos of exercises and tests to assess comprehension. The existing e-learning course on Moodle was very useful during the pandemic, as it allowed a smooth transition to online learning. We also had face-to-face contact via the Teams application, but with the existing online materials, students were able to work through the course material at their own pace. Examinations were also conducted via the Moodle interface. In order to minimise misuse, everyone wrote their quizzes at the same time, and everyone was given a different set of tasks. The introduction of dual training also meant that we had to face the fact that most of our students spend most of their time at their chosen workplace, especially when they are involved in larger projects, so they are not always able to attend lectures. The e-learning course helps to overcome this, as it allows them to keep up with the course material and work to their own timetable. In the case of the correspondence course, a fully e-learning course has been introduced, so students have fewer days to come, which is also an advantage for them because of work and family commitments. We try to organise the lectures in such a way that students who are present in person, but also preparing at home, have the opportunity to learn the material and pass the exam.

B. Laboratory exercise

The aim of the laboratory exercises is to practice and apply what has been learned in the theory class, and to acquire the knowledge needed to measure digital networks. Below is a look at how the organisation of laboratory exercises has evolved over time for the subject [9].

The UNILAB (Figure 3) was a tool used in the 1980s for hands-on digital technology training. This device had individual digital integrated circuits mounted on panels, with outputs accessible via terminal boards. From these integrated circuits, the network to be measured had to be assembled by the students by wiring. The input signals and levels (high and low) could be set by switches, and the status and level of the outputs could be controlled by LEDs.

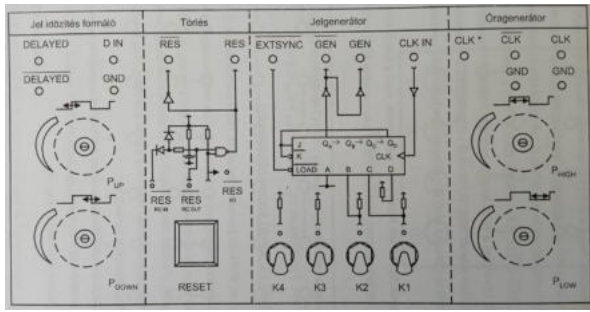


Figure 3. The front panel of the UNILAB clock generator (own editing)

The advantage of UNILAB was that the students practised building and wiring digital networks. The disadvantage was that some students had problems wiring the network together, often making mistakes and thus not getting the right measurement results. Another problem was that the connectors were not stable, there were many contact errors and the connectors often broke. The instrument had a high maintenance requirement [10].

Later, one of our teaching colleagues designed and produced a measuring card. The students took measurements on it. The measuring card was used to perform delay time and signal level measurement tasks (Figure 4).

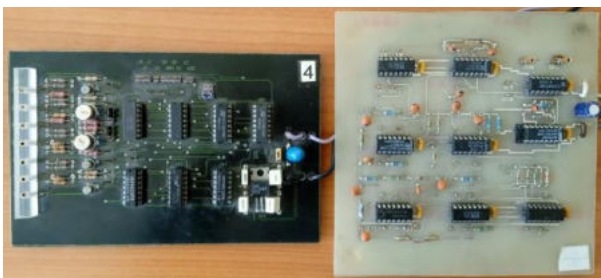


Figure 4. Single measuring cards (own editing)

The advantage of using these measurement cards was that the students no longer had to deal with wiring the digital networks together, so they could concentrate on the measurement task. The primary disadvantage of these cards was the failure of the connectors, and contact failure, but they also required a lot of maintenance. The advent of programmable logic integrated circuits and subsequent developments have moved in this direction [11].

During the 2000s, in parallel with the emergence and development of programmable logic ICs, digital engineering colleagues developed measurement panels where the digital network to be measured was implemented with a programmable logic IC. Software and hardware development tools have made it possible to implement the digital networks to be measured using circuit diagrams and hardware description languages. The obvious advantages of this solution are the flexibility resulting from programmability and the reduction of development time. Much time and cost could be saved by not having to physically build the digital networks to be measured. However, the disadvantage is that students only see the digital networks to be measured at the level of the schematic, they do not see the physical architecture of the

networks and therefore do not get practice in the physical implementation. Several types of programmable logic have been used and are presented below.

- Lattice

The Lattice measurement panels (Figure 5) are based on the Lattice ispLSI 1016 Programmable Logic Device (PLD).

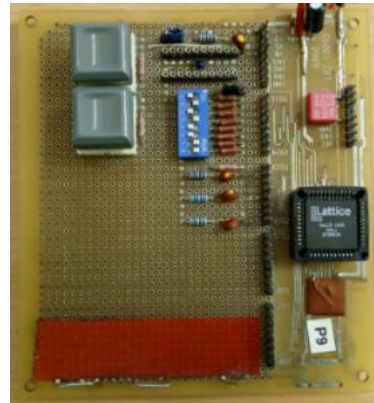


Figure 5. Measuring card with Lattice programmable IC (own editing)

For the development of the measurement programs, our colleague used the Xilinx ISE WebPack (Integrated Software Environment) software environment. This development system is a free software developed by Xilinx for FPGAs and CPLDs, which can be freely downloaded from the company's website. The development system contains all the elements needed for schematic-based and hardware description language-based development. The designer can enter his ideas and designs in the form of a schematic drawing, using the schematic creator and input program, or in hardware description language. This is supported by the HDL editor part. The supported languages are Verilog and VHDL. After input, you can simulate your circuit to make sure that it works as expected.

The Xilinx ISE WebPack simulator is the Xilinx ISE Simulator. To run the simulation, the model must be operated, "excited", so the model inputs must be fed with appropriately variable signals. This is done by specifying a series of so-called test vectors. The test vectors can be specified by the designer using an HDL specification (test bench). The simulator can be used to test the operation of the circuit over time (Figure 6).

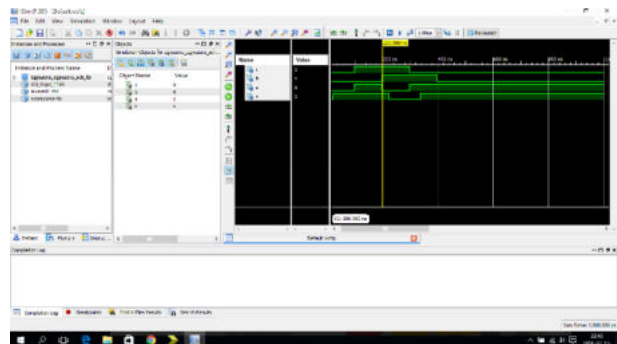


Figure 6. Simulation of a simple combinational network with Xilinx ISE WebPack simulator (own editing)

In addition to the flexibility of the device, the disadvantage was that a separate measurement program was created for each type of digital network (due to the limited capabilities and capacity of the programmable IC), so at the beginning of each hour a new measurement program had to be downloaded into the device, and the programmable logic IC had to be reprogrammed. Unfortunately, the Lattice IC used was severely limited in its reprogrammability, so the Lattice ICs often had to be replaced due to failure. After a while, the IC was no longer available, so another solution had to be found.

- XILINX

The next technological step was the writing of a measurement program implemented by our colleague using a measurement card from XILINX company containing a programmable CPLD circuit (XC9572XL). To create the measurement program, our colleague used the Xilinx ISE WebPack development system (Integrated Software Environment). One of our colleagues designed a measurement box (Figure 7) to perform the measurements. The signals to be measured were available on a spike line and could be tested with an oscilloscope [12].



Figure 7. XILINX CPLD Programmable Logic Integrated Circuit (PIC) based test box (own editing)

The advantage of the device was its reprogrammability. Here, our colleague had managed to use the same measuring program for a semester, so that we did not have to download a new measuring program for each lab exercise. This increased the lifetime of the programmable IC. The problems with this solution were: breakage of interconnecting wires; soldering problems; errors due to repeated reprogramming. Replacing the programmable ICs solved some of the problems for a short time, but it was not a permanent solution, as the programmable logic ICs used were also difficult to obtain.

- Basys3 board

The Basys 3 board was introduced in digital engineering lab classes in 2023. This board is a complete digital circuit generation platform based on the Artix-7 FPGA device from XILINX. With Basys 3, combinational and sequential networks can be easily implemented. The development of the measurement programs was done using the VIVADO

software system from XILINX company. VIVADO is a free software developed by Xilinx company for FPGAs, which contains all the elements needed for schematic-based and hardware description language-based development. To perform the measurements, one of our collaborators designed an additional panel where the signals to be measured can be accessed on a spike line and tested with an oscilloscope (Figures 8 and 9).

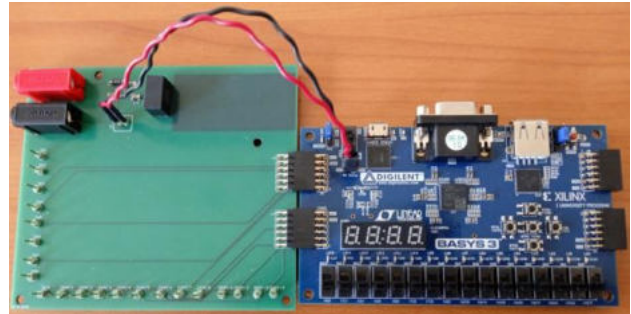


Figure 8. The Basys 3 board with the additional panel (own editing)

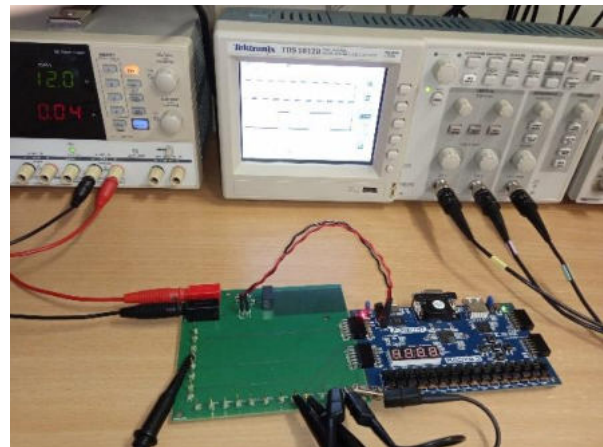


Figure 9. Testing the operation of a serial network using an oscilloscope (own editing)

The advantage of the tool is its flexibility, with the VIVADO program it is easy to implement digital networks. Each digital network is implemented in VHDL, and the networks are combined into a block at the level of a circuit diagram. The blocks are the measurement programs. At the moment there are 4 measurement programs available: combinational networks; three-bit stateful sequential networks; stateful sequential networks implemented with a step register and stateful sequential networks implemented with synchronous counters.

The VIVADO software system from XILINX is also suitable for simulation tasks. After entering the network to be tested, a test bench file must be created, which provides a set of test vectors. The simulator can be used to test the operation of the circuits over time (Figure 10).

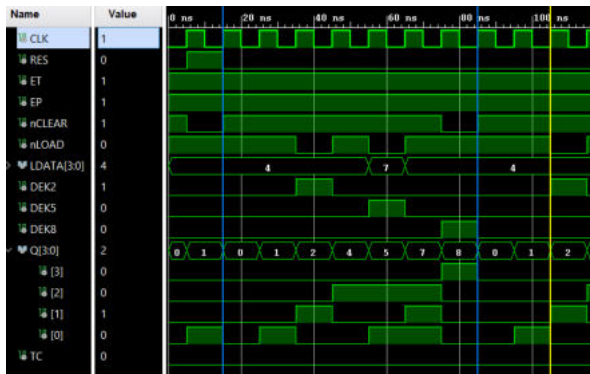


Figure 10. Simulation result of a sequential network with counter 162
(own editing)

IV. THE FUTURE

Considering the challenges of our time and the needs of Generation Z, we want to create a subject where both lectures and laboratory exercises can convey the necessary curriculum to students in an enjoyable, thorough, and professional way. It also meets the needs of industry and society. Taking these into account, the theoretical teaching of the subject would be tailored to the individual needs of the students, with a greater emphasis on mentoring. Students could work to their own timetable, but by the end of the semester, they would have to master the required material and give several assessments of their knowledge. For lectures, the emphasis would be on individual work, while for laboratory exercises, students would work mainly in groups. In the labs, students would work in teams on project tasks. Here, they would be asked to solve a predefined task, from designing a programmable IC, through implementation, to checking operation and recording the results. The Artix-7 based FPGA device Basys3 from XILINX is currently the right tool for this.

The technical higher education of the future will be a diverse and flexible system that meets multiple needs. Institutions will strive to provide students with a broad range of knowledge and skills. Through online education and virtual reality technologies, students can access education anywhere and at any time. Adaptive learning systems help to personalise the curriculum while also playing an important role in developing practical skills. In addition, technical higher education is at the heart of sustainability and social responsibility, preparing students for the challenges and opportunities of the future.

REFERENCES

- [1] András István, Rajcsányi-Molnár Mónika, Bacsa-Bán Anetta, Balázs László, Németh István Péter, Szabó Csilla Marianna és Szalay Györgyi (2016). Módszertani megújulás a felsőoktatásban : Az új oktatói szerepek megfelelő oktatásmódszertani megközelítés. DUNAKAVICS, 4 (6). pp. 25-62. ISSN 2064-5007
- [2] Tóth Katalin, Folmeg Márta, Sebestyén Lilla és Fűzi Beatrix (2023). Ki mit visz át a túlsó partra? Oktatók alkalmazkodásának vizsgálata egy felsőoktatási intézmény példáján keresztül. Iskolakultúra, 33(3), 16–34. <https://doi.org/10.14232/iskkult.2023.3.16>
- [3] Thinh Duong Van és András Medve (2016). A mentorrendszer aktualitása a felsőoktatásban = Relevance of mentor system in higher education. TAYLOR, 8(3), 151–158.

- [4] Siti Hajar Halili (2019). Technological advancements in education 4.0. The Online Journal of Distance Education and e-Learning, January 2019 Volume 7, Issue 1, 63-59
- [5] M. Pintér Tibor, Bodnár Éva, Dósa Katalin, Dorner Helga, Lénárt Krisztina, Lengyelne Molnár Tünde, Gorana Mistic, Ollé János, Margary Ta Rymarenko, Vörös Zoltán, Dringó-Horváth Ida (2021). Oktatásinformatikai helyzetkép a magyarországi felsőoktatásban. Új Pedagógiai Szemle 2021 03-04 szám, 54-74, ISSN 1788-2400
- [6] Haleem Abid, Javaid Mohd, Qadri Mohd Asim and Suman Rajim (2022). Understanding the role of digital technologies in education: A review. Sustainable Operations and Computers, 3, 275-285. <https://doi.org/10.1016/j.susoc.2022.05.004>
- [7] Stohl Róbert (2021). „Így neveld a sárkányodat!” – A Z generáció képzési és tanulási szokásairól. Honvédségi Szemle: A magyar honvédség központi folyóirata, 149 (2). pp. 116-127. ISSN 2060-1506
- [8] Schnackenberg Heidi Lee, Johnson Christine (2019). Preparing the Higher Education Space for Gen Z. IGI Global, ISBN 1522577645, 9781522577645, 253
- [9] Nikoletta Tolner, András Dávid, Bertalan Beszédes (2018). Examination of digital circuits with simulation and measurement. In: Gábor Tamás Orosz (szerk.) AIS 2018 - 13th International Symposium on Applied Informatics and Related Areas, Székesfehérvár, Magyarország : Óbudai Egyetem, Alba Regia Műszaki Kar, pp. 36-41. , 6 p.
- [10] Bertalan Beszédes, Károly Széll, György Györök (2021). Redundant Photo-Voltaic Power Cell in a Highly Reliable System. ELECTRONICS (SWITZ) 10: 11 p. 1253, 20 p.
- [11] György Györök, Bertalan Beszédes (2017). Fault-tolerant Software Solutions in Microcontroller Based Systems. In: Gábor Tamás Orosz (szerk.) AIS 2017 - 12th International Symposium on Applied Informatics and Related Areas organized in the frame of Hungarian Science Festival 2017 by Óbuda University: Proceedings Székesfehérvár, Magyarország: Óbudai Egyetem, 204 p. pp. 7-12. , 6 p.
- [12] Bertalan Beszédes (2019). Reliable Presence and Intrusion Detection with Collaborative Sensor Modules in Electronic Property Protection Systems. In: IEEE (szerk.) 2019 Ieee 17th World Symposium on Applied Machine Intelligence and Informatics (SAMi 2019). Herlany, Szlovákia : IEEE pp. 354-360. , 7 p.

Augmented Reality in High School Literature: Enhancing Engagement and Evaluation

Majnár Csaba
Székesfehérvári SzC Széchenyi István
Secondary Technical School
Székesfehérvár, Hungary
majnarcsaba12@gmail.com

Rádli Ferenc Gábor
Székesfehérvári SzC Széchenyi István
Secondary Technical School
Székesfehérvár, Hungary
ferencgradli@gmail.com

Gaye Ediboglu Bartos
Alba Regia Technical Faculty
Obuda University
Székesfehérvár, Hungary
gaye.ediboglu@uni-obuda.hu

Abstract— As technology advances, the traditional use of printed textbooks is evolving into digital platforms to create a more interactive learning experience. This study aims to enhance the initial version of the Augmented Reality (AR) application previously developed by the authors. The improvements include adding more content and refining the application's evaluation process. The proposed AR application is designed for high school literature coursebooks, utilizing the Unity game engine and Vuforia Engine technology. This application overlays digital content onto physical textbooks, thereby enhancing the learning process. Specifically tailored for high school students, it enables them to access additional information, 3D models, and animations related to their textbook content. Furthermore, this research focuses on enriching the app with additional content and enhancing the evaluation process through several methods, including motivation and satisfaction surveys, content integration assessment, technical performance evaluation, qualitative analysis, and a comparison with traditional methods. The results indicate that the AR app developed in this research effectively enhances student engagement and motivation. However, it may have room for improvement in content integration within the field of literature. Consequently, the incorporation of AR technology into high school education holds great promise for enhancing the quality of education and preparing students for the digital age.

Keywords—augmented reality, AR, unity game engine, vuforia engine, high school education, interactive learning, digital textbooks, traditional methods comparison, educational technology

I. INTRODUCTION

Augmented Reality (AR) refers to a technology that adds digitally created content into a user's real-world perception. Its application spans a variety of sectors, including education, entertainment, and healthcare. In the realm of education, AR has proven to enhance learning outcomes by boosting engagement and interactivity [1]. Entertainment predominantly employs AR to craft immersive gaming experiences [2]. Within healthcare, AR has found utility in aiding medical training and enhancing patient outcomes [3]. Additionally, AR has displayed effectiveness in improving user performance in tasks like navigation, assembly, and maintenance [4]. Furthermore, AR has been leveraged in marketing to create interactive and captivating advertisements [5]. Despite its benefits, AR adoption presents challenges such as cost, technical constraints, and the absence of standardized development platforms [6].

In recent years, the utilization of augmented reality (AR) technology in educational contexts has gained significant

traction to enrich students' learning experiences [7]. By incorporating AR, traditional instructional methods can evolve into more interactive and engaging learning environments. The domain of literature education has also recognized the potential advantages of AR technology in enhancing students' comprehension and appreciation of literary works [8]. This paper presents a research study investigating the use of AR in high school literature textbooks. The study seeks to explore how AR enhances students' engagement, motivation, and comprehension of literary texts.

In this study, a pre-existing AR application designed for 10th-grade literature textbooks, aiming to improve students' motivation, engagement, and support the learning process, was enhanced. The enhancements involved augmenting the application with additional content, technological upgrades, and a more thorough evaluation. The application was created using the Unity game engine and Vuforia Engine technology, synergistically allowing the integration of digital content with physical textbooks. The research encompassed the development of the app with four distinct triggers: images, maps, short videos, and 3D models. Additionally, the study evaluated the app's effectiveness through both user and teacher assessments. The subsequent section offers a detailed account of the developed AR application.

II. DEVELOPMENT OF THE APPLICATION

In this section, details about the technologies and the content used to develop the app are explained together with how the app works.

A. Programs Used

Unity serves as a robust and widely embraced game engine and development platform, enabling developers to craft interactive 2D and 3D content across a range of devices including Desktop operating systems, gaming consoles, mobile devices, and virtual reality headsets (VR).

On the other hand, Vuforia Engine represents an augmented reality (AR) solution, affording developers a variety of tools and capabilities to construct AR applications made for mobile devices, tablets, and smart glasses. Through Vuforia Engine, developers can seamlessly integrate virtual elements into the physical world, encompassing interactive 3D models, animations, and interactive user interface components.

By utilizing these two, Unity and Vuforia Engine form a potent partnership for the creation of state-of-the-art AR

applications. Developers can harness the strengths of both platforms to craft engaging and immersive AR experiences characterized by high-quality graphics, dynamic animations, realistic physics, and interactive features. Additionally, they can tap into advanced AR functionalities like image and object recognition.

B. The Textbook Used

The book integrated into our application is "Színes Irodalom," a literature textbook utilized in Hungarian high schools for 10th-grade students, published by Oktatási Hivatal (The Hungarian Board of Education). This literary resource summarizes a wide range of literary topics, both classical and contemporary literary works, literary movements, genres, international literature, the art of literary analysis, composing literary critiques, and the intricate connection between literature and society.

C. The Application

Our application was created with the Unity engine and the Vuforia AR module. It is available to android devices above version 8.1 (Oreo) and API level 27. The app works with a 10th grade literature textbook, which is a high school textbook used nationwide in Hungary as mentioned in the previous section. Currently with the improvements, the app can recognize 10 images from the textbook (the details of the target images and triggers can be seen in the Table 1 below and samples of target images can be found in Fig. 1), and lets the user interact with those pictures in different forms namely images, 3D models and videos. It should be noted that the app asks for permission for the camera of the device. This is necessary for Vuforia to begin scanning the pictures.

After starting the app, hovering over the target images we can trigger the specific content that belongs to that target image. A photo of the app being used can be found in the Fig. 2 below. Ten target images are represented in Table 1 below together with their specific triggers. The details of the triggers are explained in the paragraph after the table.

TABLE 1 DETAILS OF THE IMAGES AND TRIGGERS

Image ID	Page number	Description of trigger
1	231	Short video from the movie called Bánk Bán (1987) (Bánk Bán n.d.)
2	242	3D model of the New York Metropolitan Museum (New York Metropolitan Museum n.d.)
3	62	Short video from the movie called Romeo and Juliet (1996) (Romeo and Juliet n.d.)
4	94	Map of Hungary with Szigetvár pinpointed
5	250	Map of the United Kingdom with Chawton pinpointed
6	262	Map of Russia with Joskar-Ola pinpointed
7	335	Jókai Mór's flat from the outside
8	344	Short video from the Hungarian movie 'Aranyember'
9	258	3D model of the Notre Dam
10	83	Image of the Asam church in München

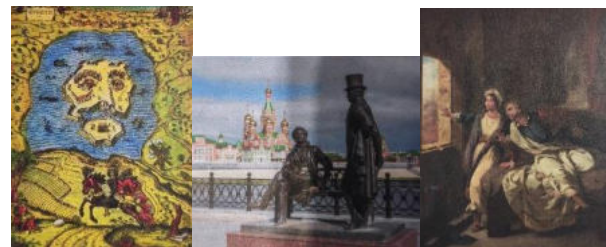


Fig. 1 Samples of the target images

The first target is on page 62, if we hover our camera above the picture with the description "Claire Danes és Leonardo Dicaprio a dráma 1996-os filmvázlatában (rendező Baz Luhrman)" a video about the movie "Romeo + Juliet 1996" appears placed above the picture. On page 94, the image titled "Orosz István grafikája" triggers a map of Hungary with Szigetvár pinpointed on the map. This is because the picture is about Szigeti Veszedelem written by Miklós Zrínyi. On page 231, the image from the movie Bank Ban triggers the scene of the film where the image is from. The painting of Eugéne Delacroix on page 242 shows a 3D model of the New York Metropolitan Museum of Art above the image. The painting is stored in this museum. On page 250, the image of the Jane Austin memorial house in Chawton triggers a map of the United Kingdom with Chawton pinpointed on it. The photo of the statue of Puskin and Anyegin in Joskar Ola makes the app show a map of Russia with Joskar Ola pinpointed above the picture. The target image on page 335 shows, makes the app display Jókai Mór's flat from the outside when the user hovers the device above the image of Jókai sitting inside his residence. On page 344, if we hover the device above the second picture featuring the movie 'Aranyember' the application triggers a video that shows the exact scene where the image is from. On page 258, hovering the device above the image of Notre Dame in the top left corner, the app shows a 3D model of the building. The photo of the Asam Church in München on page 83 shows the inside of the Church. If we place the camera of the device above this picture, the app displays a picture of the outside of the building.



Fig. 2 Images showing the app in use

D. Technological Improvements

The previous version of the app used the default focus system provided by Vuforia Engine. However, its functionality did not satisfy the demands of the user therefore a custom focusing was added using a C# script on Unity [9]. Fig. 3 below represents the focusing abilities of the new version. The new focus is also evaluated by the users in the next section.



Fig. 3 Image showing the focusing abilities

III. EVALUATION OF THE APP

An online survey was adopted to assess the effectiveness of our augmented reality (AR) app, designed as a supplement for a high school literature textbook. The purpose of this evaluation was to gather the perceptions of both users and teachers regarding the integration of AR technology with the existing literature textbook. The user evaluation involved 52 students, primarily 10th graders, with some 11th graders participating. Additionally, two literature teachers provided feedback on the app. This assessment took place at a high school in Székesfehérvár, Hungary, and the sample size met the minimum requirement of 30 participants, as suggested by Coakes and Steed in 2003 [10].

The questionnaire used for app evaluation was created using Google Forms and consisted of four sections: Respondents' Data, User Experience, Learning Outcomes, and Technical Functionality. It comprised a total of 16 questions, including five short-answer questions, 10 linear scale questions, with responses ranging from 1 (Strongly Disagree) to 5 (Strongly Agree) and an open-end question. The teachers' questionnaire contained 11 questions, most of which required brief responses, and its primary objective was to get an insight of the teacher's opinions and recommendations on the application. The following section will put forward the results of the user evaluation.

IV. RESULTS

This section shows the results of the online questionnaire designed for users and teachers. Overall, the outcomes of the survey suggest that students generally had a favorable response to the application. The data revealed that many users found the combination of the book and the app to be more captivating and interactive. More than 60% of the participants expressed that the app offered a distinctive and valuable learning experience. The detailed result of the questionnaire is provided in two sections below namely the results of the user evaluation and the results of the teacher evaluation.

A. USER EVALUATION

This section provides further details on the responses of students in 3 categories, user experience, learning outcomes and technical functionality.

1) User Experience

This section aims to assess the user experience while using the app. According to the survey results, over 90% of the respondents found the augmented reality (AR) features easy to use and navigate, although the remaining 10% found them somewhat challenging. Over half of the respondents felt that the inclusion of AR features made the literature books more engaging and interactive. An additional 9% did not find

the app to be engaging or interactive. Half of the users expressed their willingness to recommend the app to others, while the rest of the students were uncertain. The Fig. 4 shows the results on the user experience.

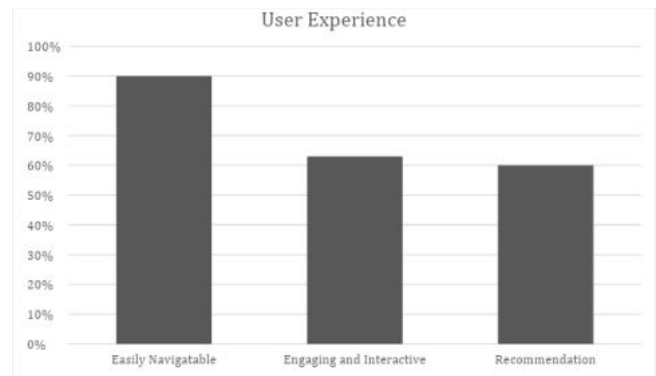


Fig. 4 Chart showing the evaluation results on user experience

2) Learning Outcomes

This section was designed to evaluate the impact of the app on actual learning. The AR features in the book app contributed to improved understanding of the settings, characters, or plot for 37% of the respondents. Increasing the number of contents may further increase the educative nature of the app. Approximately 70% of the participants believed that the experience was more unique and meaningful when compared to traditional literature books.



Fig. 5 Chart showing the evaluation results on learning outcomes

3) Technical Functionality

The ease of using the app was assessed in this section. About 45% of the respondents reported that the AR features in the app functioned smoothly without any problems, and they were satisfied with their performance and functionality. Additionally, the users found the focusing abilities of the app satisfactory.

These results underscore the significance of engaging and visually appealing features in educational applications, as well as the importance of user-friendliness.

B. TEACHER EVALUATION

The app was evaluated by two literature teachers who teach at the same high school. After using the app, the teachers were asked to fill out the questionnaire mentioned earlier. The results of the questionnaire show that the teachers provided positive feedback overall. The details of the responses are explained below.

Both teachers strongly agreed that the inclusion of 3D models, maps, and videos through AR has a potential to improve students' comprehension and visualization of the literature book content. Additionally, they believe that the app has the potential to enhance the students' understanding of literary concepts in the literature book. Similarly, both teachers find it engaging for students and they believe that the app might increase students' interest and motivation in studying the literature book. Even though, there were not teachers involved during the selection of the content, both teachers agree that the AR app aligns well with the existing curriculum and learning objectives of the 10th-grade literature book. One interesting point to mention is that one teacher did not find the app to have a potential to distract the students whereas the other thought that the app has a potential to distract the students during literature classes. In terms of encouraging students to actively participate and interact with the content of the literature book, both teachers believe that the app being more interactive than the book indicates promise in its effectiveness. Finally, both teachers indicated that they were both satisfied with the AR app and its potential to enhance the study of the literature book for 10th-grade students.

Overall, both student and teacher evaluation indicate that the app is engaging and has a great potential in increasing the interest and motivation in studying literature.

V. CONCLUSION

In our study, we introduced an upgraded version of an augmented reality (AR) app created to complement high school literature textbooks. Building on the earlier version, this enhanced app represents a significant step forward, boasting increased content and improved technology. By utilizing the Unity game engine with a customized focus, alongside the Vuforia engine, we've improved the user experience and engagement.

The augmented reality app includes a wider array of interactive elements, triggered by ten distinct target images within the textbook. These triggers activate an engaging set of interactive objects, including images, maps, short videos, and 3D models. This expansion of content ensures a more immersive interaction with the literary material, enabling students to delve deeper into the subject matter.

In terms of evaluation, we expanded our approach by not only seeking user feedback but also incorporating the expert insights of two literature teachers. 52 users interacted with the app and then shared their experiences and perspectives through an online questionnaire, covering aspects of ease of use, learning outcomes, and technical functionality. Concurrently, two experienced literature teachers assessed the app's efficacy from an educational standpoint, providing an additional layer of evaluation.

The collective feedback from both users and literature teachers has been overwhelmingly positive, emphasizing its valuable contribution to enhancing understanding and engagement with literary content. Students found the app to be intuitive, aiding their understanding of literature while making the learning process more enjoyable and captivating. However, in terms of its contribution to improve the understanding of the settings, characters, or plot in the book, the app performed poorly. On the other hand, the teachers both stated that they believed that the app has a great potential in encouraging students to actively participate and interact

with the content of the literature book. And both teachers were satisfied with the AR app and its potential to enhance the study of the literature book for 10th-grade students.

In conclusion, this augmented reality app holds promise as an evolving tool in high school literature education. Its ability to offer a more interactive and immersive learning experience has the potential to transform how students engage with and comprehend literary works. The integration of advanced technology and the inclusion of comprehensive content, coupled with a thorough evaluation process, have collectively contributed to a compelling educational resource.

Looking ahead, it is crucial to continue refining and expanding the app's capabilities, perhaps by incorporating even more diverse and interactive content triggered by additional image targets within the textbook. The insights gathered from both students and teachers will guide further enhancements, ensuring the app aligns with the needs and expectations of the educational environment. Additionally, in the next versions, it may be beneficial to work with a literature teacher while designing the content of the application thus making sure that the content is well aligned with the curriculum. This study underscores the exciting trajectory of technology's impact on education, especially within the literature and language arts domain, providing a glimpse into the promising future of augmented reality in the classroom.

VI. REFERENCES

- [1] N. Kerdprasop, N. Srisawasdi, and M. Thongmak, "The effects of augmented reality on student achievement and motivation in educational settings: A meta-analysis.," *Educational Research Review*, vol. 35, no. 3, pp. 450–458, 2020.
- [2] R. Azuma, Y. Baillet, R. Behringer, S. Feiner, S. Julier, and B. MacIntyre, "Recent advancements on augmented reality.," *IEEE Comput Graph Appl*, vol. 21, no. 6, pp. 34–47, 2001.
- [3] D. Brennan, J. McDowall, D. Wickett, and N. John, "Virtual and augmented reality in healthcare education.," *J Med Syst*, vol. 47, no. 7, pp. 1–13, 2017.
- [4] H. Zhang, Z. Zhang, L. Wang, and S. Dong, "A survey on augmented reality.," *J Vis Commun Image Represent*, vol. 55, pp. 446–462, 2018.
- [5] X. Song, J. Chen, J. Zhang, Z. Hu, and Y. Huang, "Investigating the effect of augmented reality advertising on consumer purchase intention.," *Int J Hum Comput Interact*, vol. 37, no. 11, pp. 1064–1074, 2021.
- [6] Z. Zhu, L. Zhang, X. Liang, Y. Huang, and G. Huang, "The state-of-the-art technology, applications, and research trends of augmented reality.," *Virtual Real*, vol. 22, no. 4, pp. 375–399, 2018.
- [7] M. D. Dickey, "Learning in Context: Digital Games and Young Black Men.," *Journal of the Learning Sciences*, vol. 19, no. 2, pp. 285–321, 2010.
- [8] A. M. Kamarainen, S. J. Metcalf, T. A. Grotzer, C. Dede, and J. Ravitz, "Ecologies of Learning: An Evidence-based Approach to Designing Augmented Reality Games for Learning.," *Educational Technology & Society*, vol. 16, no. 1, pp. 29–43, 2013.
- [9] "C# script for advanced focusing." [Online]. Available: <https://github.com/motilorddd/CameraFocusController/blob/main/CameraFocusController.cs>
- [10] S. Coakes and L. Steed, "SPSS analysis.," *SPSS: Analysis Without Anguish: Version 11.0 for Windows*. John Wiley, 2003.

Well-being among students in dual and traditional education

Nikoletta Tolner
Alba Regia Technical Faculty
Óbuda University
Szekesfehervar, Hungary
tolner.nikoletta@amk.uni-obuda.hu

Judit Módné Takács
Alba Regia Technical Faculty
Óbuda University
Szekesfehervar, Hungary
modne.t.judit@amk.uni-obuda.hu

József Halász
Alba Regia Technical Faculty
Óbuda University
Szekesfehervar, Hungary
halasz.jozsef@amk.uni-obuda.hu

Éva Takács
Alba Regia Technical Faculty
Óbuda University
Szekesfehervar, Hungary
takacs.eva@amk.uni-obuda.hu

Ildikó Petóné Csuka
Alba Regia Technical Faculty
Óbuda University
Szekesfehervar, Hungary
csuka.ildiko@amk.uni-obuda.hu

Tímea Bekk
Alba Regia Technical Faculty
Óbuda University
Szekesfehervar, Hungary
bekk.timea@amk.uni-obuda.hu

András Dávid
Alba Regia Technical Faculty
Óbuda University
Szekesfehervar, Hungary
david.andras@amk.uni-obuda.hu

Csaba Bráda
Alba Regia Technical Faculty
Óbuda University
Szekesfehervar, Hungary
brada.csaba@amk.uni-obuda.hu

Monika Pogatsnik
Alba Regia Technical Faculty
Óbuda University
Szekesfehervar, Hungary
pogatsnik.monika@amk.uni-obuda.hu

Abstract— *In our research, we examined the well-being of university students at the Alba Regia Technical Faculty at Óbuda University. We were interested in whether the students of the dual or traditional education felt better. The extraordinary measures of the COVID period, online learning from home, and the distance from mates and professional colleagues also caused a lot of difficulties for university students. Returning to the traditional order, attendance education, caused at least as many difficulties. During their studies, the students of the dual education program, in addition to their life as university students, are also interns at a workplace, so they are also part of an adult workplace community. Their academic success is greatly influenced by practical experience, and they also can become financially independent thanks to their dual income. In our research, we examined how these different experiences and opportunities between traditional and dual students manifest themselves in terms of indicators of well-being.*

Keywords— *well-being, university students, dual education*

I. INTRODUCTION

As university students might get involved in different kind of stressful life events like continuous and time-driven learning, midterm papers, exams on one side; local social environment, possible new living environment on the other side; and one might also include global threats like pandemics, wars, economic crises, it is not surprising that well-being is an important factor in their everyday activities and performance. An excellent review on the mental well-being of university students and academics is by Halal et al [1].

A member of today's generation of university students, Generation Z was born between 1995 and 2012, and their way of thinking and learning is strongly influenced by the fact that they have access to the internet anytime, anywhere. Research has shown [2] that they find it harder to cope with the stress of university studies than students of the previous generation. The young people of the Generation Z are very curious but less persistent. One reason may be that they grew up in front of a computer and are used to instant answers. Also, they have a lot of information to process, too

many goals and opportunities to achieve, so they find it harder to commit. If something doesn't work for them, they switch more easily.

Generation Z's sense of well-being is heavily influenced by social channels. All communication tools are available on social networks, and Generation Z uses them. The opportunities on the Internet are changing the way people interact. People are losing their sense of space and time and entering a world without borders [3]. Covid- 19 has been instrumental in encouraging this generation to spend more time online. A Latvian article also looked in part at how much their physical activity has changed and how this affects their well-being [4]. Online shopping is an element of young people's well-being as well. How much the shopping habits of this generation have changed, how they have evolved, how influencers influence today's young people and what impact social networking sites can have on them can be read in the article of the Faculty of Engineering of the University of Szeged [5].

II. ANALYSIS OF WELLBEING IN INTERNATIONAL CONTEXT

In our research first we reviewed how people are satisfied with their life in international context: in the European Union. So, we made secondary research in the international literature of subjective well-being. We are assuming that there is a close connection between the well-being of a country's population and the well-being of the country's university students. Subjective well-being was analyzed with official statistical data for the first time in 2013 [6]. It was included in the SILC data collection coordinated by Eurostat and implemented in 32 countries with a uniform methodology. The questionnaire contained 22 questions, it measured the respondents' lives and important areas of life satisfaction, the individual's sense of usefulness, the perception of the meaningfulness of life, the functionality of the personal network, the trust in people and the general sense of security. In Hungary almost 18.000 people aged 16 or older responded with subjective well-being related questionnaire questions [7].

Our article compares the values characteristic of Hungary to the international data and presents the correlations emerging from international data. The most well-known and the most cited indicator from the examination of subjective well-being is the variable measuring satisfaction with life. When filling out the questionnaire, the respondents rated the general satisfaction with life (0 = not at all satisfied, 10 = extremely satisfied). Among the countries there were neither outliers nor large-scale differences (exception of Serbia and Bulgaria with the lowest indicators). The average value was 7.1 point for the European Union as a whole. At the top of the ranking, with an average value of 8.0 point stood Denmark, Finland, Sweden, and Switzerland. The Hungarian average value was 6.2 point like the points of Cyprus, Greece and Portugal. Hungary overtook only Serbia and Bulgaria.

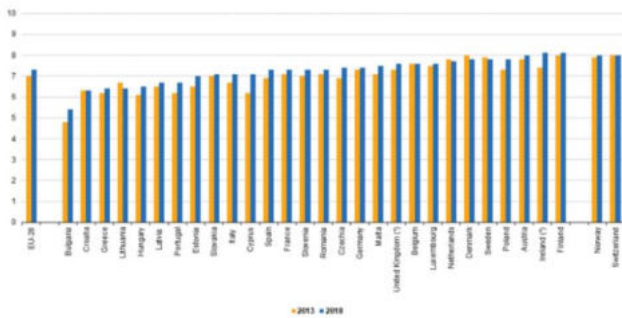


Fig. 1.: Overall life satisfaction mean rating by country, 2013 and 2018 (Source: Eurostat, 2018)

The same data collection was implemented in 2018 by Eurostat [8]. The average life satisfaction increased between 2013 and 2018 in the European Union mainly in Bulgaria, Ireland, and Cyprus. In Ireland and Finland was the highest the average life satisfaction in 2018. Satisfaction with financial situation, job and personal relationships were the most important factors for the European citizens in the life satisfaction. The average life satisfaction in Hungary, Croatia, Greece, Lithuania, Latvia, and Portugal was below the EU-28 average. It was the lowest in Bulgaria with a value of 5.4 point [8]. Life satisfaction is the highest in the Scandinavian countries while in southern and eastern countries of Europe people are generally less satisfied.

There are significant differences in age groups between the European countries. In Hungary life satisfaction decreases steadily and to a considerable extent with age. While the average value is 7.0 point for the 16-24 age group until in the 65-74 age group it is only 5.9 point. So, the average life satisfaction of university students in Hungary - who belong to this age group - is much higher than the retired people, and also higher than the older active workers. In countries with a high average life satisfaction value, there is no significant difference in life satisfaction according to age, or the older age group (65-74) is more satisfied with life than younger people. Looking at Europe as a whole, in Denmark among the 65-74 years old people was measured the highest life satisfaction with 8.6 points.

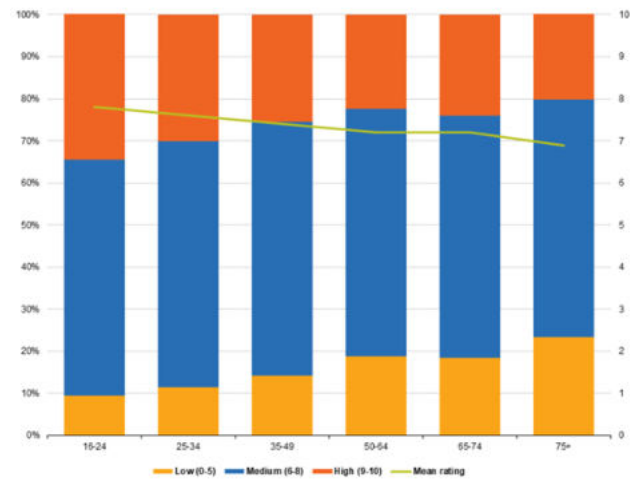


Fig. 2.: Well-being by age group (Source: Eurostat, 2018)

Material well-being can be seen as a pre-requisite for subjective well-being. This is also supported by the results of life satisfaction examined in terms of income. One of the examination methods of material differences in the society is income per capita sorting the population into five groups (fifths=quintiles) which have equal number of elements. In those countries where there is a big difference between the bottom and top income quintiles in life satisfaction, the national average value is low. The difference in the life satisfaction of the two extreme income fifths in Hungary is significant, the difference was 2.1 points in 2013 and 1.5 points in 2018.

	First quintile	Second quintile	Third quintile	Fourth quintile	Fifth quintile
EU-28	6.6	7.1	7.3	7.6	7.8
Belgium	6.7	7.2	7.7	7.9	8.0
Bulgaria	4.1	4.8	5.4	5.8	6.6
Czechia	6.7	7.2	7.4	7.7	8.1
Denmark	7.1	7.6	7.8	8.0	8.2
Germany	6.4	7.2	7.4	7.7	7.9
Estonia	6.2	6.7	7.1	7.3	7.6
Ireland	7.3 (p)	7.7 (p)	8.0 (p)	8.3 (p)	8.6 (p)
Greece	5.8	6.2	6.4	6.6	7.1
Spain	6.6	7.0	7.3	7.6	7.9
France	6.7	7.0	7.3	7.6	7.6
Croatia	5.0	6.0	6.5	6.8	7.4
Italy	6.5	6.9	7.1	7.2	7.5
Cyprus	6.2	6.7	7.0	7.4	7.6
Latvia	5.8	6.4	6.8	7.1	7.6
Lithuania	5.2	5.9	6.0	6.9	7.5
Luxembourg	6.7	7.3	7.6	7.9	8.0
Hungary	5.0	6.1	6.5	6.7	7.1
Malta	7.0	7.2	7.6	7.5	7.8
Netherlands	7.2	7.5	7.8	7.9	8.1
Austria	7.4	7.7	7.9	8.1	8.4
Poland	7.2	7.6	7.8	8.0	8.2
Portugal	5.6	6.2	6.6	7.1	7.6
Romania	6.6	7.0	7.2	7.5	8.1
Slovenia	6.4	7.1	7.4	7.6	8.0
Slovakia	6.1	6.7	7.1	7.2	7.5
Finland	7.7	8.0	8.1	8.3	8.5
Sweden	7.1	7.6	7.9	8.1	8.3
United Kingdom	7.0 (p)	7.3 (p)	7.4 (p)	7.8 (p)	8.0 (p)
Norway	7.3	7.7	7.9	8.0	8.1
Switzerland	7.4	7.8	8.0	8.1	8.4

Fig. 3.: Life satisfaction by country and income quantile (Source: Eurostat, 2018)

Social interactions, personal relationships play important role in the life satisfaction also. An important component of subjective well-being is that how meaningful the individual feels his life, his activities. In Hungary there are significant differences in judgement of life's meaningfulness according to the qualification. Among individuals with basic education the average of this satisfaction indicator is 6.4 point, while among those with higher education it is significantly higher: 7.8 point. We are assuming that the university students in Hungary are more satisfied with their life than other one with basic qualification.

Based on emotional and mood characteristics 58% of the Hungarian adult population reported feeling or being happy most or all the time and with this ratio it ranks 20th among the 32 countries.

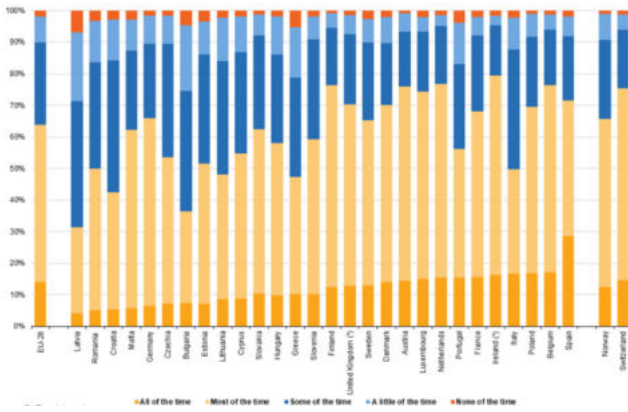


Fig. 4.: Frequency of being happy by country (Source: Eurostat, 2018)

Figure 5. shows Hungary’s relative strengths and weaknesses in well-being compared to other OECD countries [9]. Longer bar indicates better outcomes (higher wellbeing), while shorter bar indicates worse outcomes (lower well-being) – including for negative indicators, marked with a ‘*’, which have been reverse-scored. Inequalities (gaps between top and bottom, differences between groups, people falling under a deprivation threshold) are shaded with stripes.

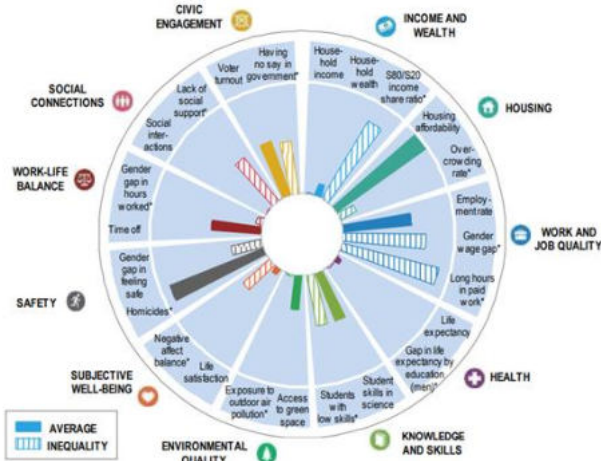


Fig. 5.: Hungary’s current well-being, 2018 or latest available year (Source: OECD, How’s Life in Hungary? 2020)

III. RESEARCH METHODS

A. INSTRUMENTS

The WHO-5 is a short 5-item questionnaire to establish psychological well-being in individuals above 18 years of age [10]. The Questionnaire is widely used, as it has been validated in more than 35 countries worldwide [11]. The above analysis consisted of more than 43000 individuals and WHO-5 Index has been suggested as an excellent measure of psychological well-being what has also been positively related to physical well-being.

The official Hungarian version of WHO-5 was used, its original publication applied 0-3 Likert scale instead of the suggested and revised 0 to five [12]. Thus, the scores were given as percentage of the possible maximum score. Additionally, 30-50 values were considered as mild risk (for additional behavioral problems), while values below 30 were calculated as severe risk (for additional behavioral problems). E.g., Krieger et al related the severity of major depression with WHO-5 Index values [13]. The Hungarian

version was validated on more than 12000 individuals, its internal consistency showed excellent properties (Cronbach $\alpha = 0.85$). The Hungarian version inversely correlated with Beck Depression Inventory Short version and the Hospital Anxiety Scale [12].

Statistical analyses were performed by STATISTICA Program Package. General Linear Model (GLM) was used to establish differences between groups (form of education, namely dual students, regular students, and corresponding students). Fisher LSD post hoc test were used, $p < 0.05$ was used to describe significant differences between groups.

B. SAMPLE

Number of respondents was 216 students. Population surveyed: students of Óbuda University (AMK Faculty). Gender distribution of respondents: 78% male and 28% female. Most of the questionnaires, 62%, were filled in by students of surveying and engineering informatics. 70% of the respondents are full-time students and 30% are part-time students. The proportion (35%-35%) of students in the surveyed full-time sample is equal between dual and traditional education. This allows it to be one of the main criteria for analysis. 1/3 of the respondents to the questionnaire live in villages, the rest live in cities. Almost half of the respondents’ parents have a university or college education as the highest level of education, only 12% have a vocational education. 81% of respondents consider the financial situation of their family to be average, with only 5% who consider their financial situation to be below average.

Almost 40% of the respondents spend between 4 and 5 hours a day online, while only a very small proportion (1%) spend up to 1 hour a day online. The time spent online by those surveyed was classified into five categories. However, when the responses were analyzed, a new category emerged. Those in the first two basic categories who spend less than three hours online each day are considered to have minimal internet usage [14], [15].

IV. RESULTS

A. Online hours and minimal internet usage

The coefficients where the relationships between the independent and dependent variables are not relevant are summarized in Figure 6. Gender, living place and background did not reveal significant differences in online hours and minimal internet usage.

Coefficients ^a						
Model		Unstandardized Coefficients		Standardized Coefficients	t	Sig.
		B	Std. Error	Beta		
1	(Constant)	3,769	,578		6,518	,000
	Female	,112	,345	,022	,324	,746
	Livingplace	,111	,163	,047	,682	,496
	Background_num	,081	,201	,028	,405	,686
a. Dependent Variable: OnlineHours						
1	(Constant)	,512	,128		3,996	,000
	Female	-,052	,076	-,046	-,676	,500
	Livingplace	-,059	,036	-,111	-1,631	,104
	Background_num	-,009	,045	-,013	-,195	,846
a. Dependent Variable: MinimalInternet						

Fig 6. Regression model coefficients between the dependent variables of time spent online and minimum time spent online and the independent variables of gender, living place and financial background. High p values were found ($p > 0.1$), indicating that the coefficients are not significant in explaining the dependent variable.

However, the form of education was associated with lower online hours in distance learning students ($F_{(2,213)}=2.85$, $p=0.06$), Fisher LSD showed significantly lower online hours in distance students comparing with regular ones ($p<0.05$) (Figure 7).

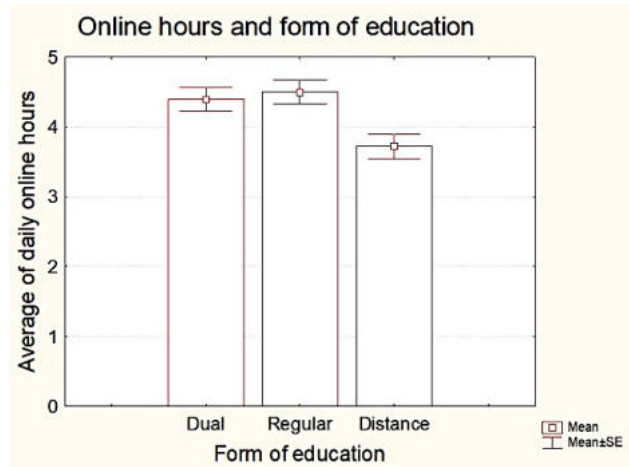


Fig 7. Means and SE of average daily online hours in students with different form of education. Significantly lower hours were present in distance students compared with regular students ($p<0.05$, Fisher LSD).

The probability of minimal internet usage was significantly different according to the form of education ($F_{(2,213)}=3.82$, $p<0.05$), Fisher LSD showed significantly higher probability of minimal internet usage in distance students comparing with regular and dual ones ($p<0.05$) (Figure 8).

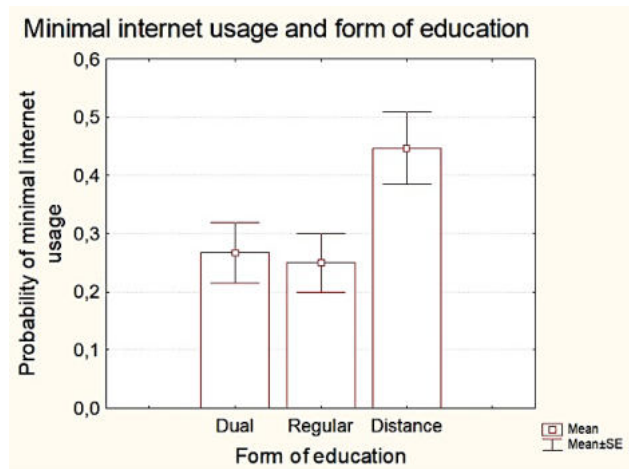


Fig 8. Means and SE of probability of minimal internet daily usage (less than 3 hours) in students with different form of education. Significantly higher probability was present in distance students compared with regular students ($p<0.05$, Fisher LSD).

B. Well-being

A histogram of WHO-5 Index results can be seen in Figure 9. The average of the 216 students was 60 ± 1.4 (mean \pm SE).

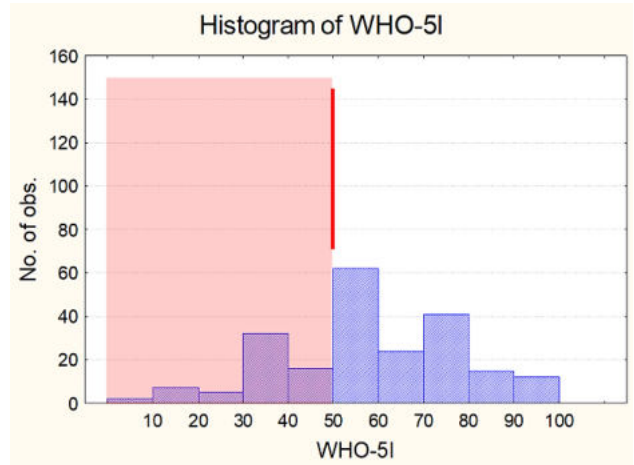


Fig 9. Histogram of WHO-5 Index in University students. Values below 50 indicate additional behavioral risk, 30-50 means mild and below 30 values severe risk for additional behavioral problems.

Neither gender nor living place modified the well-being of students can be seen in Figure 10.

Coefficients^a

Model	Unstandardized Coefficients		Standardized Coefficients		Sig.	
	B	Std. Error	Beta	t		
1	(Constant)	55,643	4,820		11,544	,000
	Female	-,267	3,270	-,006	-,082	,935
	Livingplace	1,495	1,553	,066	,963	,337

a. Dependent Variable: WHO5Index

Fig 10. Regression model coefficients between the dependent variables of WHO-5 Index values and the independent variables of gender and living place. High p values were found ($p > 0.1$), indicating that the coefficients are not significant in explaining the dependent variable.

However, the background was associated with significant differences in WHO-5 Index ($F_{(2,213)}=3.32$, $p<0.05$), Fisher LSD showed significantly higher WHO-5 Index values in well-off students compared with students with average background ($p<0.05$) (Figure 11). Interestingly, students with low financial means were like those with well-off students.

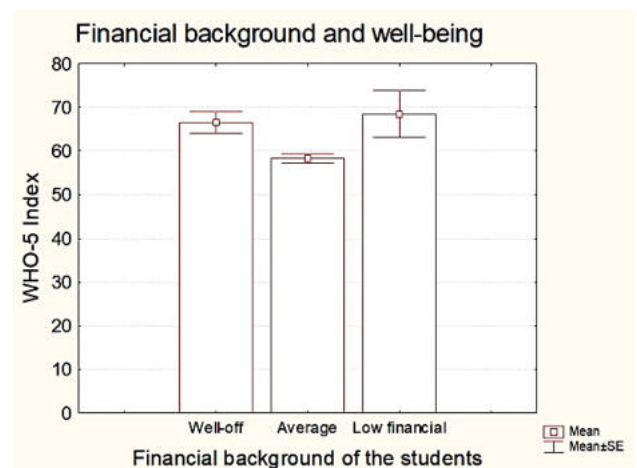


Fig 11. Means and SE of WHO-5 Index in students with different financial backgrounds. Significantly higher values were present in well-off students compared with students with average financial background ($p<0.05$, Fisher LSD).

The overall WHO-5 index did not show significant differences between students with different form of education, neither additional severe behavior risk was present. However, the probability of mild risk for additional behavioral problems showed a tendency for significant difference between groups ($F_{(2,213)}=2.67$, $p=0.07$), Fisher LSD showed significantly lower risk in dual students comparing with regular ones ($p<0.05$) (Figure 12). Corresponding students did not show significant difference from the other two groups.

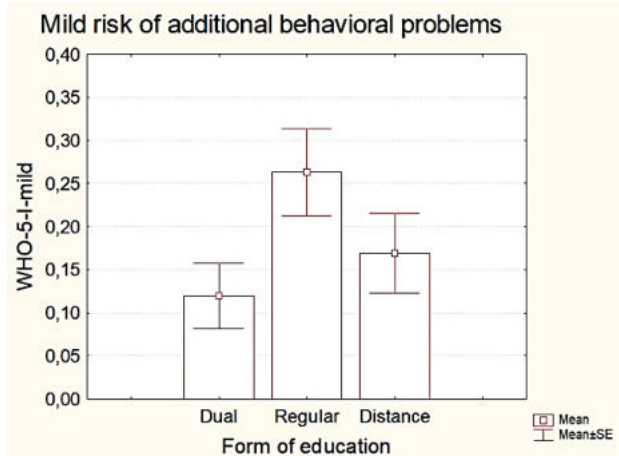


Fig 12. Means and SE of probabilities of mild additional behavioral problems (according to WHO-5 Index values between 30 and 50) in university students. A significantly lower probability was observed in dual students compared with regular students ($p<0.05$, Fisher LSD).

Looking at education patterns, it can be concluded that, because they are working, those with part time courses and dual jobs have higher material well-being and less leisure time, they are also likely to spend less time on the internet and online. It is also possible that those with higher material well-being are pursuing other types of hobbies.

V. DISCUSSION

The aim of the research was to assess the level of well-being and possible psychological difficulties of students studying at the Óbuda University, Alba Regia Technical Faculty using the WHO-5 well-being questionnaire. This validated questionnaire is used to measure levels of mental well-being and depression. During the research, the university students were asked to fill out an online questionnaire which, in addition to the WHO-5 well-being questionnaire, also asked for demographic data. The WHO-5 wellbeing questionnaire can be used as an effective tool to assess students' mental wellbeing and to identify the risk of depression in the university setting. The results of the study could be used to develop targeted interventions to improve students' psychological well-being. Fortunately, only a small portion of students at our university were in the high (severe) risk group based on the results of the WHO-5 well-being questionnaire. As our university has a long tradition of dual training, we felt it was important to compare the results of students studying in this form of training with the responses of students in traditional and correspondence courses. In most cases, there were no significant differences between the responses of students studying different forms of training, but in a few cases, we found a detectable difference.

The main findings of the present research were the following. Part time students used less internet compared to regular ones, and the probability of minimal internet usage was significantly higher in that group compared with regular and dual ones. Compared to regular students, dual students had a significantly lower risk for mild additional behavioral problems.

REFERENCES

- [1] D.H. Halat, A. Soltani, R. Dalli, L. Alsarraj and A. Malki, "Understanding and fostering mental health and well-being among university faculty: A narrative review.", *Journal of Clinical Medicine*, vol. 12, 4425, 2023.
- [2] R. Takács, et al. "Exploring coping strategies of different generations of students starting university." *Frontiers in psychology* 12 (2021): 740569.
- [3] R. Levickaite (2010) Generations x, y, z: How social networks form the concept of the world without borders (the case of Lithuania), *LIMES: Cultural Regionalistics*, 3:2, 170-183, DOI: 10.3846/limes.2010.17
- [4] I. Kravalis, K. Ciekurs, A. Ropa, I. Mavlutova, & J Hermanis, (2021). Teaching methods for Generation Z for physical activities: A stable labor market provision under the COVID-19 Pandemic. *WSEAS transactions on business and economics*, 18, 1432-1451.
- [5] C. Rimóczy, E. Kozik, (2023). Influencerek hatása a Z-generáció fogyasztási szokásaira–feltáró kutatás. *Jelenkori Társadalmi és Gazdasági Folyamatok*, 18(Különszám), 397-409.
- [6] Eurostat 2013. "Subjective well-being – statistics." <https://ec.europa.eu/eurostat/documents/1012329/1012401/2013+Module+assessment.pdf>
- [7] KSH. A szubjektív jóllét vizsgálatának eredményei nemzetközi összehasonlításban, *Statistikai Tükör*, 2015/39, KSH, 2014/2 https://www.ksh.hu/docs/hun/xftp/stattukor/jollet_nemzetkozi.pdf
- [8] Eurostat 2018. "Subjective well-being – statistics" https://ec.europa.eu/eurostat/statistics-explained/index.php?title=Subjective_well-being_-_statistics
- [9] OECD, *How's Life in Hungary? Report 2020*
- [10] WHO Regional Office for Europe, "Wellbeing measures in primary health care / The DEPCARE Project", *EUR/ICP/QCPH Report*, pp. 1–45, 1998.
- [11] P.E. Sischka, A.P. Costa, G. Steffgen and A.F. Schmidt, "The WHO-5 well-being index – validation on item response theory and the analysis of measurement invariance across 35 countries.", *Journal of Affective Disorders Reports*, vol. 1, pp. 1–14, 2020.
- [12] E. Susanszky, B., Konkoly Thege, A. Stauder and M. Kopp, "A WHO Jol-let Kerdoiv rovidített (WBI-5) magyar változatának validálása a Hungarostudy 2002 országos lakossági egészségfelmérés alapján.", *Mentalhigiene es Pszichoszomatika*, vol. 7, pp. 247–255, 2006.
- [13] T. Krieger, J. Zimmermann, S. Huffziger, B. Ubl, C. Diener et al, "Measuring depression with a well-being index: Further evidence for the validity of the WHO Well-Being Index (WHO-5) as a measure of the severity of depression", *Journal of Affective Disorders*, vol. 156, pp. 240–244, 2014.
- [14] Gy. Györök, B. Beszédes. Adaptive optocoupler degradation compensation in isolated feedback loops. In: Szakál, Anikó (szerk.) *SACI 2018 - IEEE 12th International Symposium on Applied Computational Intelligence and Informatics, Proceedings*, Temesvár, Románia. 2018, p. 604. pp. 167–171, 8440950
- [15] B. Beszédes, K. Széll, Gy. Györök. Redundant Photo-Voltaic Power Cell in a Highly Reliable System. *ELECTRONICS (SWITZ)* 10 : 11 p. 1253 , 20 p. (2021)

Motivational opportunities in higher education from a teacher's perspective

Tímea Bekk
Alba Regia Technical Faculty
Óbuda University
Székesfehérvár, Hungary
bekk.timea@amk.uni-obuda.hu

Éva Takács
Alba Regia Technical Faculty
Óbuda University
Székesfehérvár, Hungary
takacs.eva@amk.uni-obuda.hu

Péter Tarsoly
Alba Regia Technical Faculty
Óbuda University
Székesfehérvár, Hungary
tarsoly.peter@amk.uni-obuda.hu

Monika Pogatsnik
Alba Regia Technical Faculty
Óbuda University
Székesfehérvár, Hungary
pogatsnik.monika@amk.uni-obuda.hu

Abstract - In the research presented here, we investigated which methods can be used to support students' learning, to stimulate their interest and to motivate them after a difficult period of returning from online education to the face-to-face learning environment. We explored the post-Covid effects experienced by the instructors after a long period of online education in a face-to-face teaching environment. During the in-depth interviews, we also sought answers to the question: how can an instructor be motivated? Our research was conducted at the Alba Regia Faculty of Technology of Óbuda University in Székesfehérvár. The questions asked during the interviews were broadly selected, covering several topics that are necessary to enable lecturers to teach conscientiously and with sufficient motivation, in accordance with today's technology. Most teachers have tried to consider the needs of the students and to change their teaching methods. Several of them mentioned as an important aspect that their aim is to make teaching more practice-oriented, to pay attention to the theory-practice ratio, to different motivational possibilities, for example by offering a grade, tests, videos, interactive lessons.

Keywords - motivation, Covid effect, higher education, instructor perspective

I. INTRODUCTION

Motivation is an essential component of academic performance, and high levels of motivation are associated with good academic performance [1]. Highly motivated students put more effort into learning, which leads to better results [2]. High motivation can be driven by several factors. Tinto's model of student attrition [3] argues that academic integration, is a major factor in maintaining student persistence. That is, the more students feel that their intellectual needs are met at the university and the more they identify with it, the more likely students are not to drop out early [3].

The second factor in Tinto's model is social integration, i.e., students' social relationships with their fellow students and teachers. This factor is consistent with the theory of self-determination, which suggests that the need for contact is a key component of motivation [4]. Students who interact more with their peers and instructors tend to report higher satisfaction and motivation than students who have fewer social interactions identified the expectation of participation [5] [6], the desire to gain knowledge about assessment and to find out what it is about, as the primary motivation for attending university classes [7].

In the qualitative research presented in our study, we investigated which methods are suitable for helping students to learn, to

stimulate their interest and to motivate them after a difficult period. For almost a year and a half, due to the closures and the transition to online education caused by Covid, personal contact was minimal, and thus the lack of personal contact with fellow students and lecturers was a major factor in reducing student motivation. We wanted to look at another aspect of our research with students, which we had previously carried out [8], and examine the impact of post-19 Covid education on lecturers [9], [10]. How they could make students more motivated, what teaching methods they used, what they had to change compared to their teaching before Covid 19. During the in-depth interviews, we also looked for answers to the question: how can an instructor be motivated? Do they need to be motivated?

II. RESEARCH METHOD, SAMPLE, RESEARCH QUESTIONS AND HYPOTHESIS

During the in-depth interviews, the responding teachers and professors were able to express their thoughts and feelings in their own words, allowing us to gather more accurate and complex information. The in-depth interviews also allowed us to get a better understanding of the views of reclusive individuals, a great advantage over focus group discussions. Interviews lasted between 45 and 60 minutes.

An important criterion in the selection of the lecturers interviewed was to interview lecturers from all disciplines who also teach full-time. A total of 13 lecturers were interviewed, of which 4 were female and 9 were male. An important criterion for the sampling was to interview lecturers from each institute, 6 from the Institute of Engineering, 2 from the Institute of Science and Software Engineering and 5 from the Institute of Geoinformatics.

The following additional criteria were considered for the interviewed lecturers:

- lecturers who teach a basic subject and who teach a professional subject,
- age group,
- number of years in teaching,
- from all university years.

Our hypothesis was: "A motivated teacher can motivate students."

Our research questions, which we sought to answer during the interview:

1. What methods and tools do instructors use to engage students' attention during lessons, how much has this changed after the Covid period of online teaching, returning to face-to-face teaching?

2. *What is necessary for lecturers to be able to teach conscientiously and with sufficient motivation, in line with today's technology.*

During the discussions, it became clear that teachers of first year students and teacher of upper year students have different experiences. The motivations and views of the different teachers at different levels are different. A total of 15 pre-defined questions were asked, including how the instructors perceive the students, what teaching methods are used, how is accountability done, what works well or causes difficulties, and what motivates the instructor to teach?

III. PRESENTATION OF THE RESPONSES ALONG THE RESEARCH QUESTIONS

How do you see today's students?

During the interviews, we observed that several first-year teachers mentioned that students' basic skills were lacking. There is a lot of material at once and they don't have the learning techniques to process it. They try to learn in a superficial way. They prefer to learn what they can find where, they want to go deeper into what is useful and important for them.

It's hard to keep the students' attention. What they also see as a difficulty is that students are uninterested in the subject, they don't want to work in a profession, they chose the subject with parental help.

The senior colleagues divided the students into two groups. One group is made up of those who want a degree but will not necessarily work in the profession, they "need paper", and the other half are students who are very interested, want to do the assignments, enthusiastic, goal oriented.

What teaching methods do you use?

In general, you can keep young people's attention for about 20-25 minutes. It is said that during this time, the instructors try to bring the attention back using different techniques. Working in small groups is better, simulation programs can be used, tests can be taken, and the big advantage is that the results are immediately visible. YouTube videos have been used for demonstration purposes, for example in production methods, and are analyzed later. Tests are very popular with students; two types are used mainly by trainers for practice- Kahoot or Moodle test.

The idea of flexible timetabling came up. Mixing lectures and exercises. Keeping breaks on demand. It is important to emphasize the importance of the student knowing what he/she is doing and why, he/she is more willing to do it and more accepting of the task.

What kind of assessment is used?

For the trainers interviewed, it can be said that theory is taught alongside practice. During term time, the assessment is divided into two parts. In theory classes, on average, two final papers are written during the semester, divided 1/3-1/3. The ratio of theoretical and practical/computational papers varies. What can be said in general is that practical knowledge is asked first, and theory is tested by examination. The final papers are written in different ways. Some papers are written in class and others in the form of an online test.

There are also practical classes. One type is in the form of a homework assignment, depending on the subject, measuring, and counting or counting through a practical example. Students can do this at home, and there is also a practical report. Several colleagues mentioned that the assignment should also be displayed to the students with a presentation. This also develops their communication and presentation skills, so that they can present themselves properly when it comes to the final examination and thesis defense. Classic term papers, with research, are also available in several subjects. Several of them

mentioned working on daily topics that have an impact on their lives - in the form of a discussion forum. Processing case studies, making TikTok videos.

When it comes to the oral exam, teachers prefer the oral exam because, as they say, "*that's where they can help the student*". While the focus was on practical assessment during the term time, the exam is more theoretical.

In education, what do you think works well?

The following were highlighted by the trainers:

- There is a lot of material for each subject, it is easier for students to learn.
- Video recordings
- Tests
- Less theory and more practical examples
- The informal atmosphere in the classroom. Good communication between students and teachers
- Dual training
- Practice-oriented teaching
- Tradition-keeping
- Patronage system strengthens first-year classes, fewer dropouts.
- Academic student circle
- Continuous improvement
- Matlab teaching and use
- Specialized college
- Group work and presentation of results at the end
- Demonstration
- Library

What causes the most difficulties in education?

On the student side, maintaining attention is difficult. Work discipline is difficult to maintain. Students do not understand the material in class, they find it difficult to think. They can only solve the problems that are presented in class. A difficulty that has been increasing in recent years is that students cannot take notes. They think that the presentation is enough. From the teaching side, perhaps more attention should be paid to the emphasis on what is expected in a subject.

On the student side, most of today's full-time students are working while studying. They find it difficult to combine work and university. They compress their classes into a few days, they are tired, they cannot perform well.

Because our funding is capitation-based, with so many conditions and constraints, it is difficult to maintain standards. In another area, it is technical support that is a challenge, with projection difficulties for the trainers. Technical background: internet, network, outdated machinery. Lack of a server to save to.

If you encounter difficulties, how do you solve them?

Several types of difficulties emerged during the discussions. One of these is, if students do not solve the assigned tasks, how can you get them to do them. For foundation subjects, it is a common problem that they do not have a solid knowledge of their previous studies, they must repeat/re-learn the previous course material to be able to go further with the course material. Attitude is a problem on the part of the students.

When technical things get stuck, the instructor himself or student helps, or another colleague solves the problem. Here, problems with computer - projector alignment before the lecture were mentioned. Several colleagues feel that if they encounter a problem, they must solve it themselves.

Do you think the employer will provide the technical background? On a scale of 1-10, where 1 is least satisfied and 10 is completely satisfied with everything.

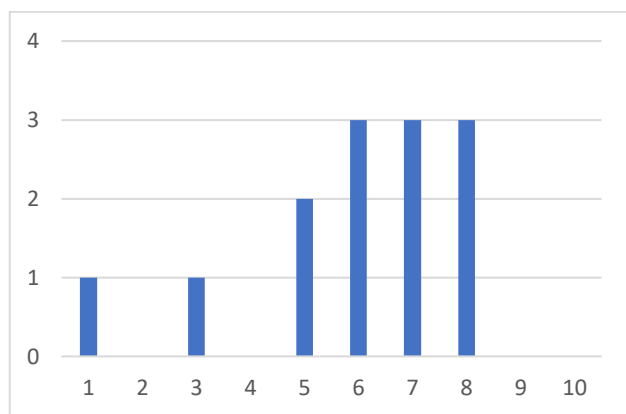


Fig. 1.: Satisfaction level of teachers

Responses ranged widely, with satisfaction scores on a scale of 1 to 10, from 1 to 8. The average satisfaction of the 13 respondents was 5.92, with a median of 6 and a standard deviation of 2.06.

Several instructors added their own words to the figure, for example, that many of the tools used are bought by the instructors so that they can use them in their teaching, thus increasing the quality of teaching.

Do you think your employer provides the necessary support for your professional development?

The number and quality of publications is an important requirement, as well as the number and quality of academic degrees. Conferences and training courses are fully supported. What has emerged as a difficulty is that there is less time for research because of the high workload. The importance of being a demonstrator student was also mentioned several times in this context.

If you had the opportunity to attend a training course on teaching methodology, would you do so?

Two thirds of respondents would like to take part in such training, but some are clearly reluctant to do so.

What motivational tools do you use to keep students interested in your teaching?

There were colleagues who said that anything extra that you do and present on your own initiative will count towards the exam or the final paper. Social media tools, Kahoot, TikTok.

Positive words of acknowledgment are important to students. If they do an assessment, they are motivated by the possibility of improvement. They like competition, for example, if there is a practical example, with given conditions, the first three groups to hand in the assignment according to the conditions will be exempted from one of the essays.

The instructors try to point out where and when they can use what they have learned in practice. Setting a goal, setting an example, if they can do something with their own hands it is always empowering for the students.

As a teacher, what would motivate you more in education?

Most of all, trainers are motivated by doing what they love. It gives them a lot of energy when students listen in class, ask questions, and have a positive attitude. Almost all interviewed teachers and professors value student feedback on their teaching work. They read it and try to change negative opinions. And positive feedback gives them wings.

Another motivating factor is the financial reward and thanks. Another motivating factor is research development. They would like to have more opportunities and time to do this.

How important do you consider theoretical and practical training to be? What do you emphasize?

According to the trainers, there are courses where the required lecture and practice are strictly adhered to, using all the time available, and there are classes where they can be more flexible in managing the two parts.

In those classes where they can be flexible with the curriculum, colleagues said that they give as much theory as necessary, most of the lessons are practical, and the rest is given up for independent study, with aids of course. If you had to show a percentage, they said 40-60% for theory and practice.

How much do students work in groups?

Groups vary, where the teacher tells who with whom should be and sometimes the students put the groups together. In pairs exercises, the instructors make sure that one good and one not so good are paired.

With these types of exercises, students can develop and strengthen cooperation, communication, team spirit, adaptability, compromise, and empathy.

How can the student keep in touch with the teacher?

Thanks to the digital technology, the trainers are very flexible with the students, they are available in any forum, such as e-mail, Teams, Messenger, personal meetings by appointment. What else has changed with the rise of the online space is that the concept of working hours has disappeared. Students now contact colleagues not only during working hours, but also at weekends and late at night. Of course, here the lecturer has a free hand and decides when to answer.

IV. MOTIVATION WORKSHOPS

Looking at both the student side and the lecturer side, we see that lecturers want to train good professionals and get them out into the labor market, they are doing their best to make this happen, and students want to get out into the world with more practical knowledge. Both sides are doing their best to achieve this, but we believe that more communication is needed to ensure that both sides achieve their goals. Two workshops are planned to achieve these goals.

A. Workshop No1. teacher student collaborative event

The participation of colleagues and students expected, where we the problems in learning and teaching is formulated in today's higher education, transform it into a task and look for solutions.

The aim is to get both students and teachers to discuss teaching methods that will help students to be more motivated, more attentive in class and more purposeful in their learning. Instructors will have the opportunity to get to know how today's students think, and if necessary, to adapt the structure of their course, keeping the important theoretical and practical content, pointing out the essential elements in a goal-oriented way. To implement the workshop, a model is planned.

Program outline:

1. Introduction - In this part, the introduction should be followed by the formulation of the objective and the focus (20 minutes)
2. Presentation - In this module, both the trainers and the students would formulate how they see the current situation. What difficulties, obstacles and good practices do they see. The students summarize the advantages and disadvantages of today's education. What is exciting in a class, what is boring? What should be changed?

3. Presentation of relevant research findings during the module (20-20 minutes).
4. Future - Would both lecturers and students articulate what they would like to achieve? Where do we want to go from the current situation? What would be the ideal education? What methods and tools could help to promote motivated learning/teaching (30 min)
5. Prioritizing, setting goals - Which of the above collections do they want to start with. Which are the most pressing ones, which will achieve small and large results? Select 2-3 items, set objectives (30 minutes)
6. Expectations and obstacles - In small groups, students and teachers discuss what expectations they have, who needs what, what questions they would like to ask each other to achieve the goals they have set. What obstacles do they see that might hinder their achievement? (30 minutes)
7. Action Plan 7 - In this section, action plans would be drawn up on what steps are needed to achieve the goal? Creation of joint groups of teachers and students from each discipline to brainstorm on innovations on a discipline-specific basis. What changes would be good? How can we get there? What would be the first step? Who would be responsible? What kind of timetable would be needed? How would barriers be addressed? (90 minutes)
8. Synthesis, summary. This is where we are now, discussing next steps, time schedule and finalizing responsibilities (30 min)
9. Closing for all participants (20 minutes)

It is recommended that at least two or three teachers from each course from each year group should be present at the workshop and 1/3 of the students from each course group in proportion to the number of courses.

The workshop should be held in the spring semester so that first-year students have an established picture of the world of higher education.

B. Workshop No2. lecturers' event

The first collaborative workshop should be followed by the second workshop, where only lecturers would participate and discuss the experiences of the previous workshop, make suggestions for teaching methods and innovations in higher education.

The first part of the workshop would be attended jointly by the trainers and would discuss the experiences of the previous workshop. They could then make suggestions on teaching methods that could be used to inspire students in class and help them to learn at home.

They would then be divided into smaller groups by subject, where they could discuss specific needs and expectations, and make innovations and suggestions, adapted to the subject. If necessary, we could propose a collection of tools that the trainers could use in their teaching, such as instruments or programs to make the teaching material more colorful and interesting.

The timing of the workshop should be planned so that as many instructors as possible can participate.

It is important not to end the process with this, but to have a follow-up in six months and a year's time, which could be in the form of another workshop or even an interview with the trainers and students, sharing experiences and measuring the results achieved.

V. CONCLUSIONS

During the discussions, we found that there is a great need for university lecturers to be recognized for their work, to get feedback not only from students but also from colleagues and management on what is working well and what they need to change.

The faculty of this study is a relatively small institution with informal and friendly atmosphere, which is exceptional in higher education and has many advantages. We believe that the teaching staff is as important as the students. During the interviews, we gained a deeper knowledge of the methods, attitudes, and opinions of the lecturers about motivation. The teachers highlighted the library, where the staff are very helpful in finding literature.

It can be concluded that the majority of instructors have tried to take into account the changing needs of students and to change their teaching methods. Several of them mentioned as an important aspect that their aim was to make teaching more practice-oriented, to pay attention to the theory-practice ratio, to different motivational possibilities, such as the offered grade, tests, videos, interactive lessons.

There is also a common perception in the world of education that young people are not hard-working and persistent enough, that they are incapable of hard work and are generally characterized as less capable than the older generation. This may be because the standards set by the older generation of teachers are no longer valid. The young generation of the 21st century is no less interested than their predecessors, but their attitudes to learning need to be recognized, and teaching thinking and methods need to be transformed, so that higher education can continue to innovate in the fast-changing world of the 21st century.

Overall, teachers who considered themselves more motivated tried to make their lessons more interesting and varied, using a much wider range of tools and methods to better motivate the digitally native young people of Generation Z to learn, as they moved from online to face-to-face education.

REFERENCES

- [1] Kusrurkar, R. A., Ten Cate, T. J., Vos, C. M. P., Westers, P., & Croiset, G. (2013). How motivation affects academic performance: a structural equation modelling analysis. *Advances in health sciences education*, 18, 57-69.
- [2] Gottfried, A.E., Marcoulides, G.A., Gottfried, A.W., & Oliver, P.H. (2013). Longitudinal pathways from math intrinsic motivation and achievement to math course accomplishments and educational attainment. *Journal of Research on Educational Effectiveness*, 6, 68–92.
- [3] Tinto, V. (1998). Colleges as communities. Taking research on student persistence seriously. *Review of Higher Education*, 21(2), 167–177.
- [4] Deci, E.L., & Ryan, R.M. (2000). The “What” and “Why” of Goal Pursuits: Human Needs and the Self-Determination of Behavior. *Psychological Inquiry*, 11, 227–268.
- [5] Wentzel, K. R. (2017). Peer relationships, motivation, and academic performance at school. In A. J. Elliot, C. S. Dweck, & D. S. Yeager (Eds.), *Handbook of competence and motivation: Theory and application* (p. 586–603). The Guilford Press
- [6] Trolian, T.L., Jach, E.A., Hanson, J.M., & Pascarella, E.T. (2016). Influencing Academic Motivation: The Effects of Student-Faculty Interaction. *Journal of College Student Development* 57, 810-826.
- [7] Vlachopoulos, P., & Jan, S. (2020). Exploring modes of lecturing as a teaching method in higher education: Student attendance, preference, and motivation. *Journal of University Teaching & Learning Practice*, 17(5), 15.
- [8] T. Bekk; M. Pogátsnik. Motivation potential in higher education after covid-19 based on personality traits. In: Petőné Csuka, Ildikó; Simon, Gyula (szerk.) AIS 2022 - 17th International Symposium on Applied Informatics and Related Areas – Proceedings Székesfehérvár, Magyarország : Óbudai Egyetem (2022) pp. 157-162. , 6 p.
- [9] B. Beszédes, K. Széll, Gy. Györök. Redundant Photo-Voltaic Power Cell in a Highly Reliable System. *ELECTRONICS (SWITZ)* 10 : 11 p. 1253 , 20 p. (2021)
- [10] Gy. Györök; B. Beszédes. Fault-tolerant Software Solutions in Microcontroller Based Systems. In: Orosz, Gábor Tamás (szerk.) AIS 2017 Proceedings Székesfehérvár, Magyarország: Óbudai Egyetem (2017) 204 p. pp. 7-12. , 6 p.

Introduction of Industrial Robotic Arms in Education Using Dobot Magician

László Gugolya*

*University Obuda AMK, Székesfehérvár, Hungary
gugolya.laszlo@uni-obuda.hu

Abstract-There is currently a narrow field of education in Hungary. At the Alba Innovár Digital Experience Centre in Székesfehérvár, Hungary, humanoid robots are used with great success. The aim of the institute is to promote career choices for young people, so the idea of including robots used in industry in the daily activities of school classes was soon raised. The first step was to find a suitable tool that could be used by as wide a range of age groups as possible. After a search, the Chinese product Dobot Magician was chosen. Thanks to its low price, this tool allows pupils to program themselves a device very similar to an industrial robot. A tender was then launched to develop a 320-hour training course focusing on the use and programming of industrial robots by alt workers. In a pilot program, 14 employees of a local multinational company were trained in the use of digital tools in a centralized environment using the Dobot Magician industrial robot trainer. After the great success of this training, robot programming was introduced in the classes of primary and secondary school students. This article gives an insight into the possibilities of Dobot Magician and its introduction into education.

I. INTRODUCTION

The Alba Innovár Digital Experience Centre in Székesfehérvár welcomes students on a daily rotation per class. This city initiative ensures that students are exposed to modern digital tools, helping them, among other things, in their career choices. The sessions will introduce 3D design, printing, Lego Robot programming, Micro:Bit, mobile devices and visual app development for humanoid robots.

In a fast-changing world, digitalization is evolving, so the activities in the Experience Centre need to follow suit. This is how the idea of incorporating industrial robots into learning sessions came about, due to their rapid expansion.

Of the tools available to me, I chose the Chinese product Dobot Magician. Its size and low price make it possible for all students to program and use a miniature version of an industrial robot.

First, we learned about the possibilities of the robot arm, and then we developed a 320-hour course aimed at the digital empowerment and development of multinational companies' employees. At the heart of this curriculum is the Dobot Magician educational industrial robot arm.

The learning material was tested and refined in a pilot course. Based on the experience gained, we also introduced robot arm programming into classroom activities.

A. The possibilities of the robotic arm

The Dobot Magician is a 4-axis robotic arm. Several accessories can be used. You can control the robot arm with a gamepad, use laser engraving, draw with a pen, use a gripper arm and a suction cup. The robot arm can also be converted into a 3D printer. These can also be extended with custom-designed end heads.



Figure 1. Dobot Magician robotic arm

Software support is extensive. Downloadable app for Android, iOS and Windows. A dedicated app for robotic arm programming, DobotStudio, is available. In addition to this, it is possible to create any external application, because the manufacturer has created a wide range of programming APIs. Within DobotStudio, the python language is preferred, but it is also possible to program the arm "outside" with a .NET library (C#, VB, C/C++), Java.



Figure 2. Drum Magician basic package

The manufacturer provides several options for the device, such as a visual kit and a conveyor. Several conveyors have been purchased for the experience centre, and the visual device control is implemented with a dedicated camera. The conveyor provides the possibility

to model more complex processes, touching on areas of collaborative robotics.



Figure 3. Conveyor set

B. Using a robotic arm with DobotStudio

The manufacturer is constantly developing this program, which allows you to gradually learn how to operate and program the robot arm.



Figure 4. DobotStudio

On the right-hand side of the program is the Operation Panel, which allows direct control of the arm, coordinate and axis control.



Figure 5. Operation Panel

Teaching & Playback

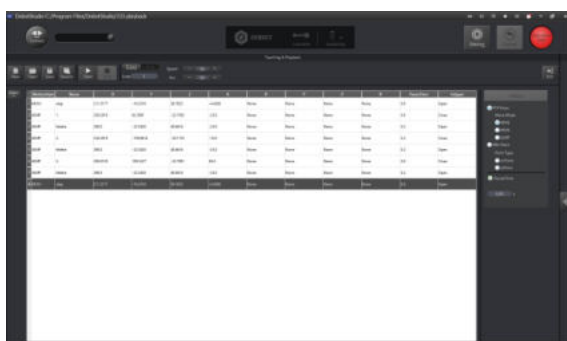


Figure 6. DobotStudio - Teaching&Playback

The first button is used to access the teach-in function. Here you can manually set the points and properties of the robot arm's path.

Blockly

In this menu you can learn how to program the robotic arm using a visual tool. The Blockly interface, which is used in many places, is completed with the commands needed to move the robot arm.

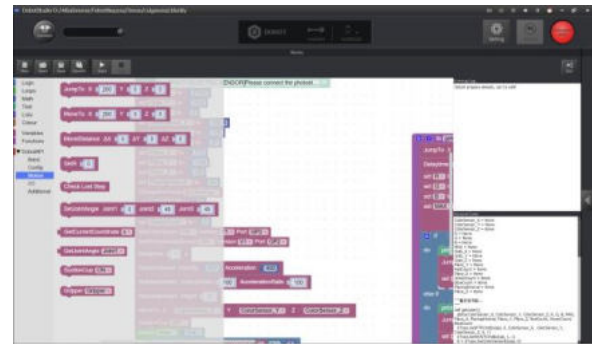


Figure 7. DobotStudio - Blockly

Python

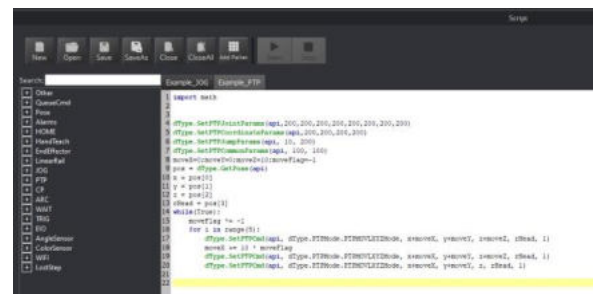


Figure 8. DobotStudio - Python

It is also possible to control the robot arm via a programming language. The left-hand side of the editor window, where the control instructions are grouped thematically, is a great help here.

Programming using an external development tool

Many external tools can be used. In our courses we used Visual Studio with C# programming language.

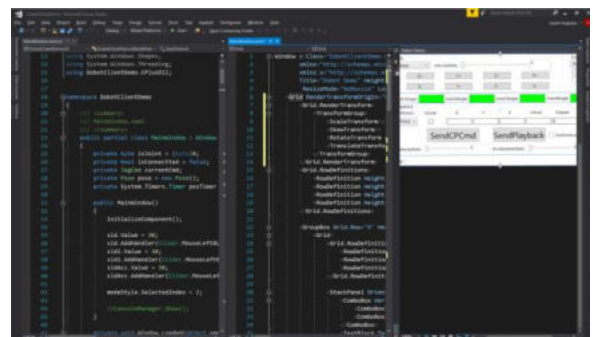


Figure 9. Visual Studio - C#

II. MATERIAL DEVELOPMENT, TESTING

A. Curriculum development

Digitalization is gaining ground in industrial manufacturing. More and more industrial robots are being used. This not only transforms engineering jobs, but also

requires a different workforce for other workers. In response to this change, a European Union project has developed a training course where companies can develop the digital competences of their own employees. Employers have realized that the only way forward is to develop and train their existing workforce. Unable to recruit a digitally skilled workforce, firms need to be involved in the digital switchover process in terms of training as well.

At the heart of the curriculum development is the industrial robotics teaching arm. The use of other digital tools is included as an additional module. For example 3D printing, mobile programming, Lego robot programming. These modules help to diversify and diversify the curriculum. Finally, there are optional modules. This was considered necessary to allow industry to choose the right block of knowledge for their employees and workplaces, according to their needs.

Table 1. - Parts of training

Basic training	
Industrial robots	
Dobot I. Teaching robotics:	
Drum structure	
Drum software	
Teaching robot movement	
Robot control with different input devices	
Drum II.- Drawing:	
Drawing with Drum	
Drawing: vector image preparation	
Drum III - Engraving	
Engraving with Drum	
Engraving: pixel image processing	
Dobot IV.:	
Basics of programming	
Drum programming: block	
Drum programming: python, C#	
3D printing	
Making simple plans	
Finished plans modification	
Create your own project	
Dobot V.:	
3D printing	
Dobot VI:	
Conveyor use	
Conveyor programming	
Total: 160 hours	

Other modules

Table 2. - Other

Additional modules
Lego robot
MIT App Inventor
Industrial simulation: v-rep
Drone programming
Micro:bit
Publication editing
Presentation creation - Prezi
Total: 80 hours

Optional modules

Table 3. - Modules

Modular training
PLC funds
PLC Advanced
HMI programming
Report management, report writing (Excel Advanced)
Report management and preparation (Excel programming)
CAD design
Pneumatics
Total: 80 hours

B. Pilot course

Almost immediately after the curriculum was developed, a local multinational company came forward to participate in such a training.

At the same time, it had to be taken into account that 8 hours a day is not the way to impart such knowledge, especially with participants who have not been in school for many years. As it is difficult to predict the composition of the group, the curriculum also needs to be flexible. The new knowledge is planned for the morning, with a focus on the robot arm. In the afternoon, practice and additional modules. This arrangement also helped the teacher's work schedule, as it allowed for more teachers to diversify the course. As a first step, 40 workers received a 2-day basic training, at the end of which a survey was conducted. As a result of this, and based on requests from employers, a group of 14 people was formed and started the 320-hour pilot course. The initial idea was that the training would be continuous, but initial discussions revealed that this was not feasible due to work schedules. Therefore, there were 2 training sessions per week at the adventure centre site.

One classroom was adapted just for this training, with each participant having their own robotic arm. A conveyor belt was provided for each pair of robots to work together, and Raspberry Pi computers were purchased to set up and test external controls.

After each major unit, the process was completed with a measurement or check. At the halfway point of the course, another milestone was added as requested by the client, further narrowing the course number to one major unit per hour. Thereafter, 12 participants continued the course.

C. Experience and results of the pilot programme

In an experiment of this kind, it is important to have a continuous dialogue and to collect feedback. Unfortunately, we were confronted with the fact that the scheduling of the workers was not as flexible as previously indicated. Thus, there were several occasions when training days had to be rescheduled due to extra work. Feedback indicated that the 320 hours of training were too long. So this was reduced to 200 hours for the next training course. There was positive feedback on the diversity of the training. They really enjoyed the mobile programming with AppInventor and the 3D design and printing was a great success. There were some very serious exam papers produced. The workers were motivated and interested throughout. They were very grateful to have the opportunity to learn again as adults and to gain new skills.

37 people participated in the basic training in 2 groups. The training covered several topics: ICT basics, internet basics, email, word processing, spreadsheets, 3D design, digital photography and image processing. At the end of each module, an independent assignment was assessed and a mixed test and a series of tasks of a summative nature were solved.

Table 4 - Results of the Digital Basic course

Title	Results
ICT basics	96%
Internet funds	96%
Email	88%
Editing	78%
Spreadsheet management	72%
3D design	69%
Photography, image processing	92%
Final test - theory	84%
Final test - exercise	76%
Total	83%

Student satisfaction feedback also showed good results. 89% of students found the training very useful. 92% of participants gained new knowledge. 84% of staff would like to continue the training.

The second part of the training was open to those who achieved good results and were supported by the company. On this basis, a group of 17 trainees was formed. This has since been reduced by 2 at the request of the employer. The training included modules on 3D design (advanced), Micro:Bit programming, mobile programming using AppInventor, Lego robot programming and vector graphics editing software (Inkspace). Of course, the robot arm (Dobot Magician) was the focus of the training, which included: instructional programming; using and programming different end heads; visual programming; python programming; designing and programming external elements.

Table 5: Results of Digital Professional Training

Title	Result
Lego programming	66%
AppInventor	73%
3D (advanced)	79%
Micro:Bit	76%

Drumstick Magician	80%
Drawing	81%
Packaging	78%
Visual programming	69%
Conveyor use	88%
Python	73%
Engraving	92%
Total:	75%

At the end of the training, the participants received a certificate from the Mayor of Székesfehérvár in the Municipal Hall.

III. INTRODUCTION OF DODOT MAGICIAN IN CLASSROOM SESSIONS

A. Study material

Based on the company courses, the first session was a 45-minute session for 13,15,17 year olds. We did not think that a Blockly-based approach was feasible in this time, or that they would encounter visual programming elements in other sessions, so we decided to go for this.

In this exercise, you have to move 4 cubes from the layout shown in the diagram. Use the "Teaching & Playback" menu item to repack!

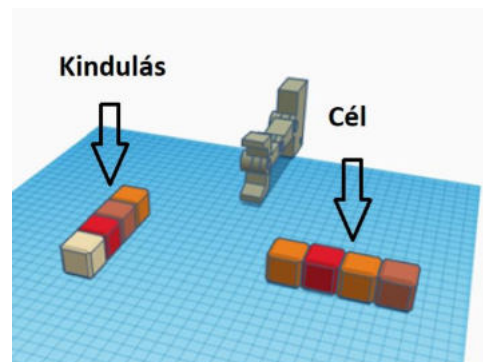


Figure 10. Tasks of classroom sessions

- Move the first frame with MOVL settings as shown in the figure!

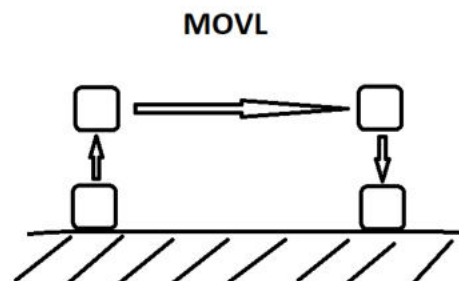


Figure 11. 2nd frame - MOVJ

- Move the second frame with MOVJ settings according to the states in the figure.

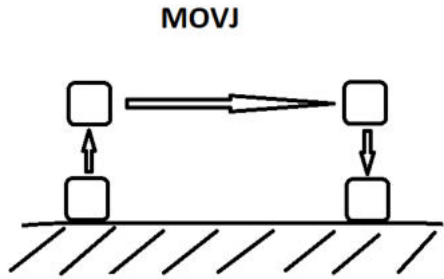


Figure 12. 2nd frame - MOVJ

- Use JUMP to move the third cube. To do this, adjust the height of the JUMP movement to 40 mm.

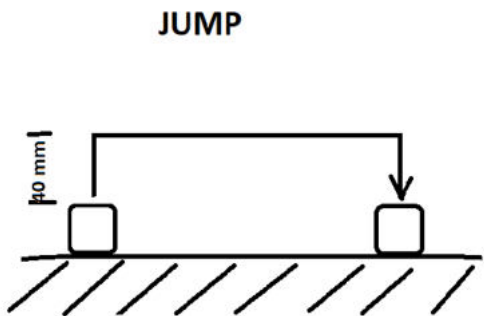


Figure 13. 3rd frame - JUMP

- Move the fourth cube around the outline.

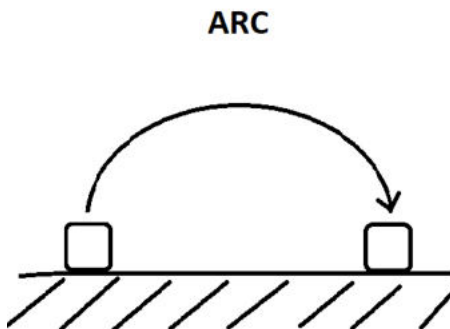


Figure 14. 4th frame - ARC

- Homework: upload your program to the robot and record (phone, tablet) a video of your program running independently. Send the finished video as an email attachment!

B. Experiences

The planned curriculum was delivered within the planned timeframe, with the younger age group not always making it to the circuits. Typically, they then preferred not to go for a break and completed the task as much as they liked it. To be honest, we were surprised by the success of the robotic arm, as we had our doubts about how the age group who had never seen such a device would react. The reception could not have been better.

After a positive reception, we started a course on programming Drum Magician the following semester. Here you can also learn about the different robot head units and visual programming.

SUMMARY

The introduction of the robotic arm has exceeded all expectations. Very successful sessions were held both in the younger age groups and in the adult courses. Building on these successes, with the support of the municipality of Székesfehérvár, we launched training courses for multinational workers in the city. The program has been a great success, which is reflected in the fact that some partners have found the content of the training useful for engineers.

We are particularly pleased that the younger age group (11-13 year olds) are also very enthusiastic about taking part in the sessions, so that they can not only learn about humanoid robots, but also meet the industrial robots of the future.

REFERENCES

- [1] Dobot Magician User Manual: <https://download.dobot.cc/product-manual/dobot-magician/pdf/V1.7.0/en/Dobot-Magician-User-Guide-V1.7.0.pdf>
- [2] DOBOT Magician V2 User Guide: <https://download.dobot.cc/product-manual/dobot-magician/v2/en/Dobot-Magician-V2-User-Guide-V1.9.0.pdf>
- [3] Dobot Magician Interface description: <https://download.dobot.cc/product-manual/dobot-magician/pdf/en/Dobot-Magician-Interface-Description-V2.pdf>

Pepper in the library

László Gugolya

OE AMK, Székesfehérvár, Hungary
gugolya.laszlo@amk.uni-obuda.hu

Abstract- Since its opening in 2017, the Alba Innovár Digital Experience Centre in Székesfehérvár has been looking for opportunities to show the potential of humanoid robots in as many places as possible. Over the years, we have been able to introduce the Pepper-type humanoid robot from Softbank Robotics to different audiences in different areas. It is the largest freely programmable humanoid robot commercially available. In the course of our activities we try to map the areas in Hungary where humanoid robots are accepted, thus helping to promote their wider acceptance and spread. 2023 was also a challenging year, with the energy crisis playing a central role. This led to the closure of institutions across the country to save money. One such institution was the Vörösmarty Mihály Library in our town, which provides library services in Fejér County. They wanted to use the good weather to create a project to attract readers when the library reopened. For this reason, we collaborated and developed an application, the first in the country, to have a humanoid robot waiting for patrons in the library and assisting with library processes (loans, recommendations, new items). This gave us the opportunity to explore a new area of how a humanoid robot appears and interacts with a traditional, everyday area, and how it affects processes.

Keywords-humanoid robot, Pepper, library, TextLib

I. INTRODUCTION

In the world of education, modern technology has long been used to aid the teaching process. Tablets, interactive whiteboards and other devices are now commonplace [1][2]. This is a natural process, as pupils grow up with them, so education has to adapt.

This process includes the emergence of humanoid robots in schools to support the educational process. Humanoid robots are also appearing in other areas of life. These include health care, where they can act as companion robots, tourism, where they can be used as information assistants, and education [3], where they can act as teaching assistants [4]. In the educational process, the presence of robots can have a stimulating effect, helping and encouraging students. It is particularly useful for language learning, since the robot is patient and often repeats the words and phrases to be learned [5]. In general, humanoid robots are a stimulating tool for learners, a better motivational tool than a conventional laptop or tablet [6][7][8]. The attitude towards learning is also much more positive, which is an important aspect in the current process [9][10][11]

Softbank's Pepper robot has been used extensively in recent years. The robot was the first in Hungary to arrive at the Alba Innovár Digital Experience Centre in Székesfehérvár in 2017. So we received many requests and

opportunities to develop and exploit its usability. One of these ideas was to use the robot to help library processes. First, a student wrote a thesis on the subject under our supervision, but unfortunately he encountered serious obstacles. We were unable to find an external library partner for the idea, and even if we did, they did not give us access to the IT system. As the thesis is time-limited, the program and the thesis documentation were implemented on a simulated library system.

Years later, thanks to a lucky coincidence, we came into contact with the Mihály Vörösmarty Library (VMK), based in Székesfehérvár. This library covers the whole Fejér County, so its IT system is also diversified and flexible to meet a wide range of needs. The energy crisis caused by the Russian-Ukrainian war led to the closure of the library. When the library reopened, the organizers saw a good opportunity to raise readers' interest by having Pepper waiting for them in the library. They also gained support for this in terms of their library system.

When designing the system, we looked at the possibility of using an existing application. Abroad, the appearance of the Pepper robot in libraries has been observed in several countries. Of course, universities are at the forefront of its development, a good example is IE University [15] in Spain, where the finished program is presented in a video¹. A good example can also be seen in the USA with Raonoke Libraries, which can also be viewed at² on YouTube. Of course, commercial companies are also open in this direction, e.g. the German company RobotLab sells the Pepper robot with library assistant software [16]. The French company Aldebaran, which makes Pepper, also has a solution for libraries. The website also describes an initiative in Germany to attract visitors to traditional libraries using Pepper. [17] These systems cannot meet the specific needs that librarians expressed during our discussions, nor can they connect to the library IT system.



¹

https://www.youtube.com/watch?v=8GVzZEGQwIw&ab_channel=IEUniversityLibrary

² <https://www.youtube.com/watch?v=xs0JSl3wsck>

II. DESCRIPTION OF ENVIRONMENT AND NEEDS

The library lending system is provided by a TextLib3 software. It can be used as a desktop application, as an Android application or as a web application. Many county, city and university libraries use this system. The developers provide the possibility for external queries, which are answered in JSON or html format [13]. In consultation with libraries and TextLib developers, requests have been developed that they would like to make interesting and helpful with the robot. The developers have given us maximum help for this, for which we are grateful.

The robot is used in two main areas, one is to share library information and news, the other is to help the process of library loans, recommendations based on previous reading and borrowing history.

III. DESIGN OF THE SYSTEM

The program is run on the robot, and communication is facilitated by the tablet on the robot. The tablet is connected to Gentoo Linux in the robot's head via a USB share. The tablet has a dedicated IP address, the Android running on it has been minimized by the manufacturer, only a browser is allowed to run, which makes available the web applications installed on the robot and other external web content.

It communicates with the library system, TextLib, using Python, a development tool developed by the manufacturer Choregraphe⁴. Information sent by TextLib is displayed through the tablet's browser.

IV. JOB SPECIFICATION

Based on preliminary discussions, the following areas have been identified to help Pepper and the program it runs.

- Access the city and library website.
- Quizzes, tests, puzzles available on the library's website with the help of the robot.
- Book recommendation based on the reader's emotions
- Recommendations for readers based on your previous loans
- Statistics on reader loans
- Search for books by different criteria
- Recommend new products by theme
- Send a message to librarians

During development, the robot was designed to be "included" as much as possible in the communication, i.e. to communicate both when requesting data and when searching for results.

V. DEVELOPMENT

As a first step in the development, a demo application was created. This was necessary because the client was not aware of the robot's capabilities and was constantly exploring them. The exact specification of the program was then

developed. There were several difficulties in the development.

The programming interface provided by the manufacturers of the humanoid robot has not performed reliably in terms of emotion recognition. Experience showed that emotion identification was almost random. The options provided by the API are also quite limited: it can recognize neutral, happy, surprised, angry, and angry emotions from the face. Based on these, it would be difficult to recommend books. We could have used an external, even cloud-based, solution to do this, but we tried to use a solution that only needed the robot and no other resources.

There were also some requests that would have required upgrades to the library system operators, but the library could not afford the extra costs.

The development possibilities are determined and strongly influenced by the system operating on the robot. The robot is running Python version 2.7 and it is not possible to develop it. This presents many difficulties both in terms of development and security. The tablet used as an output device for the robot is also not up to date, it has an old browser and therefore an old JavaScript interpreter. This part cannot be upgraded either, which is also unfortunate neither in terms of programmability nor security.

In addition to the security of the library system, the security of the robot is severely lacking. [12] This is not a problem in our case, since we basically use Pepper as an information robot.

The robot we used does not have Hungarian language support, so we had to use an external tool, Google TTS⁵. During development we insisted that the program should run on the robot. Due to many shortcomings, it could be considered to run the application on an external computer and use the robot only as an output device. We wanted to avoid this during development, we consider treating the Pepper robot as a standalone unit and adapting to any shortcomings.

To identify readers, we wanted to use the barcode on the reader ticket. This could not be fully implemented because the original robot API only has barcode reading solved and the barcode was not implemented. This has been remedied and posted on GitHub. This solution worked fine, but unfortunately it could not be implemented in a stable way due to the quality of the robot's camera and the small size of the barcode on the reader ticket. So this readout number has to be entered manually. This is not a big compromise, since the reader has to type in the password anyway.

VI. SCHEMATIC DRAWING OF THE SYSTEM USER INTERFACE

During the discussions, the structure of the program was developed. The figures also show the names of the html files used in the implementation. As the application runs on the Linux nginx⁶ web server running in the robot's head, it can be accessed remotely, as this is how the tablet's browser accesses it. Therefore, instead of using the traditional links to switch between pages, an environment variable was used to

³ <https://textlib.hu/>

⁴ <https://www.aldebaran.com/en/support/pepper-naoqi-2-9/choregraphe-setup-2510-windows>

⁵ <https://cloud.google.com/speech-to-text/>

⁶ <https://nginx.org/>

control the switching using ALMemory⁷, ensuring that the application is displayed in the same way from anywhere. Of course, this is only partially true, as different browsers can be used on desktops with the latest JavaScript engine. The same can't be said for the robot's tablet, but this solution certainly makes it easier to develop and test the application.

When you start the application, you will see the main menu, which contains the main functions.



Figure 1. - Main menu of the application

Show recommendations based on predefined areas. The areas are processed according to the ETO numbers used in library systems. The results of the search are displayed in the file etoResult.html.



Figure 2. - Recommendations

The Reader menu displays information based on the reader ID. These require a data request, code (barcode), password (inputVMKID.html, inputVMKIDPw.html) before the data is displayed. For statistics, the robot gives positive feedback, praise if the visitor has read many books.



Figure 3. - Look-up menu

Search by specific criteria: author, title, subject, publisher, anywhere.



Figure 4. - Search menu

The result of the search is displayed in tabular form in the file serachResult.html. Its content (author, title) is pronounced in Hungarian by the robot.

Vörösmarty Mihály Library menu: search for postcards, choose puzzles, quizzes and send a message to the librarians. The library's website can also be selected here.

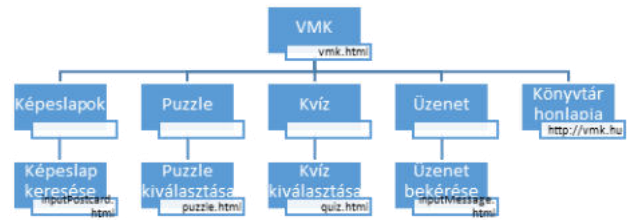


Figure 5. - The VMK menu item

Messages to the library can be displayed on a separate webpage, where you can read all the messages that readers have written. Each message is also sent to a specific email address.

New items can be displayed in the News menu within the categories (DVD/CD, book, journal, etc.) by subject (with textual names for ease of use).

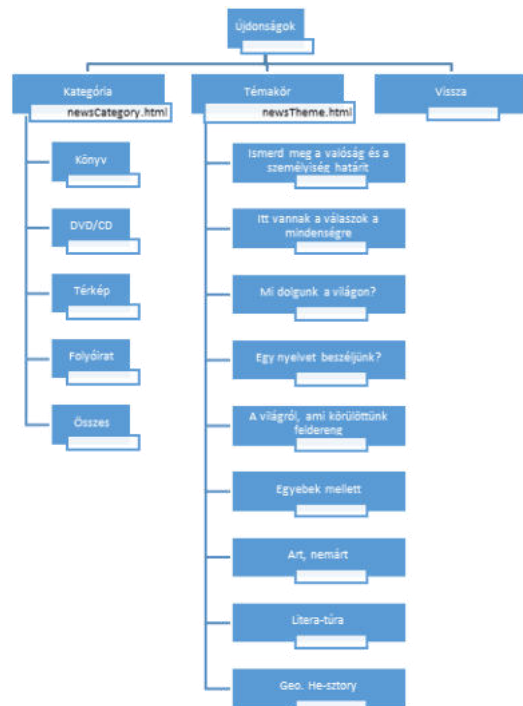


Figure 6. - What's new menu

For new items, you must enter the category and then the subject. The result of the search is displayed on the newsResult.html page.

VII. USER INTERFACE OF THE PROGRAMME

The robot also communicates via its tablet as well as speech, so it's important to design a well thought-out, modern interface that's easy to use. The design of the menus was also influenced by the ability to run a browser on the tablet. The browser supports version 1.7 of JavaScript and it is not possible to upgrade. A circular menu structure was developed in consultation with the client. The following figure shows the main menu. The others are similar. The robot also communicates via its tablet in addition to speech, so it is important to design a well thought out, modern

⁷ ALMemory documentation: <http://doc.aldebaran.com/2-5/naoqi/core/almemory-api.html?highlight=almemory>

interface that is easy to use. The design of the menus has also been influenced by the ability to run a browser on the tablet. The browser supports version 1.7 of JavaScript and it is not possible to upgrade. A circular menu structure was developed in consultation with the client. The following figure shows the main menu. The others are similar.



Figure 7. - Menu appearance

Table of search results, obtained after selecting the different search criteria, here the system returns 20 results, if you want more you have to use recursive calling.

1.	A fény harcosának kézikönyve / Coelho, Paulo (2008) (8 Példány)
2.	A fény harcosának kézikönyve / Coelho, Paulo (2013) (2 Példány)
3.	A fény harcosának kézikönyve / Coelho, Paulo (2011) (1 Példány)
4.	A győztes egyedül van / Coelho, Paulo (2009) (24 Példány)
5.	A győztes egyedül van / Coelho, Paulo (2013) (5 Példány)
6.	A győztes egyedül van / Coelho, Paulo (2015) (5 Példány)
7.	A Piedra folyó partján ültem és sírtam / Coelho, Paulo (2004) (3 Példány)
8.	A Piedra folyó partján ültem és sírtam / Coelho, Paulo ([2005]) (1 Példány)
9.	A Piedra folyó partján ültem és sírtam / Coelho, Paulo (2009, cop. 2003) (2 Példány)
10.	A Piedra folyó partján ültem és sírtam / Coelho, Paulo (2010) (2 Példány)
11.	A Piedra folyó partján ültem és sírtam / Coelho, Paulo (2012) (3 Példány)
12.	A Piedra folyó partján ültem és sírtam / Coelho, Paulo (cop. 2003) (3 Példány)
13.	A Piedra folyó partján ültem és sírtam / Coelho, Paulo (2011) (1 Példány)

Figure 8. - Search results

From the search results, you can choose the book you like and view its details.

Cím: Asimov teljes science fiction univerzuma
Szerző: [Asimov, Isaac \(1920-1992\)](#)
Közrem.: [Fencsik Flóra \(ford.\)](#)
Szerz. közl: [ford. Fencsik Flóra et al.]
Kiadás: [\[Szeged\] : Szukits, cop. 2010](#)
Sorozat: [Encyclopedia galactica alternativa/9.](#)
Eto: [820\(73\)-322.9Asimov=945.11](#)
Tárgyszó: [Amerikai angol irodalom](#) ; [Fantasztikus elbeszélés](#)
Cutter: A 88
ISBN: 978-963-497-194-8
Nyelv: magyar
Oldal: 685, [5] p.
UKazon: 201101239

Pld.	Raktár	Rakt.jelzet	Lelt.szám	Info
Központi Könyvtár : 2 kölcsönözhető; ebből 2 elvihető Foglal				
1.	Felnőtt kölcsönző	A 88	537487	Kölcsönözhető
2.	Felnőtt kölcsönző	A 88	537458	Kölcsönözhető
Zámoly : 1 kölcsönözhető; ebből 1 elvihető				
3.	Zámoly	A 88	ZAM15584	Kölcsönözhető

Figure 9. - Details of the selected book

A. Quizzes

The library wanted to use this interface to display the quizzes it had already made, which are related to local life and places of interest. These are quizzes created in Google Forms and can be completed by the robot.



Figure 10. Question from the "Towers, roofs, domes" quiz

B. Puzzle

In this module, the library has created puzzles that can be linked to the city. For example, the Ikarus bus shown in the illustration, which is linked to the local, once world-famous bus manufacturer. The puzzles were implemented using an external website⁸, so the robot displays them. Due to the size of the robot's tablet, care had to be taken not to make the number of puzzles too large, as this would result in too few elements.

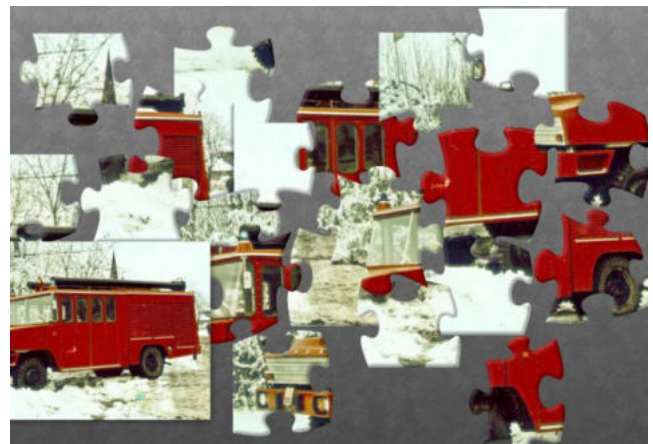


Figure 11. Puzzle - an old Ikarus bus

VIII. CHOREGRAPHE PROGRAMME

As can be seen in the figure, the program running on the robot is used to navigate between web pages and to define PythonBoxes to define the data that will be displayed in the html files and to display and pronounce their contents on the tablet using JavaScript.⁹

The Hungarian speech is provided by a robot service written in Python and run by Google. Text understanding is also implemented using another service that captures the voice in mp3 format and sends it to the Google Cloud Speech-to-text service¹⁰. This solution is already a paid service, so this was not requested by the library and the input was done via the tablet.

⁸ <https://www.jigsawplanet.com/>

⁹ Pepper Javascript API documentation: <http://doc.aldebaran.com/2-5/dev/js/index.html>

¹⁰ <https://cloud.google.com/speech-to-text/>

